UNIVERSITY OF
BIRMINGHAM

University of Birmingham Research Archive

e-theses repository

This unpublished thesis/dissertation is copyright of the author and/or third parties. The intellectual property rights of the author or third parties in respect of this work are as defined by The Copyright Designs and Patents Act 1988 or as modified by any successor legislation.

Any use made of information contained in this thesis/dissertation must be in accordance with that legislation and must be properly acknowledged. Further distribution or reproduction in any format is prohibited without the permission of the copyright holder.

Coordination Chemistry of *cis,trans*-1,3,5-Triaminocyclohexane – From Mononuclear Complexes to Supramolecular Architectures

by
Georg Peter Maria Seeber

A thesis submitted to
The University of Birmingham
for the degree of
DOCTOR OF PHILOSOPHY

School of Chemistry
The University of Birmingham
September 2003

3rd of 3 files
Section 3.5 to section 8
(Pages 94 – 262)

3.5 Closed shell TM coordination chemistry

The coordination chemistry of *trans*-tach with the closed shell d^{10}-transition metals silver(I) and zinc(II) results in the formation of coordination polymers, rather than discrete molecules as is observed with the open shell transition metals discussed in chapter 3.4. The bis*equatorial*-mono*axial* conformation of the ligand is common in these polymers, rather than the observed ring-flipped conformation found upon the coordination to open shell transition metals. The ^{1}H-NMR spectra confirms that *trans*-tach adopts a non ring-flipped conformation in solution (Figure 28), however, the signals are broadened and not all coupling constants are resolved. Additionally, a downfield shift is observed with respect to the non-protonated ligand due to the presence of lewis acidic metal ions and partial protonation in case of zinc(II) complexation.[134]

Table 12 Comparison of ^{1}H-NMR chemical shifts (δ /ppm) and spin multiplicities for **29**, **54, 55** and **56**

	$\mathbf{H_a}$	$\mathbf{2^{\bullet}H_d}$	$\mathbf{H_e}$	$\mathbf{2^{\bullet}H_b}$	$\mathbf{2^{\bullet}H_c}$	$\mathbf{H_f}$
trans-tach (**L**)	3.21	2.88	1.89	1.65	1.14	0.79
(**29**)	quint	tt	dtt	*p*dd	td	q
$\{[Ag(\mathbf{L})](NO_3)\}_n$	3.39	3.21	2.25	1.92	1.33	1.06
(**54**)	bs	t	d	d	td	q
$\{[Ag(\mathbf{L})](OTf)\}_n$	3.38	3.22	2.26	1.90	1.31	1.06
(**55**)	bs	t	d	d	td	q
$\{[Zn_2(\mathbf{L}H)Cl_4]Cl\}_n$	3.89	3.53	2.37	2.19	1.82	1.57
(**56**)	t	tt	d	d	td	q

3.5.1 Ag(I) coordination

3.5.1.1 3-D coordination network with $AgNO_3$ 54

Crystallisation of a reaction mixture of Ag(I) nitrate with *trans*-tach results in colourless crystals of **54** in moderate yield as determined by elemental analysis and multiple unit cell measurements on isolated single crystals. The structure of **54** represents a 3-dimensional coordination network with all three amino groups of *trans*-tach involved in coordinative interactions to Ag(I) ions.[212] The asymmetric unit consists of two crystallographically independent *trans*-tach ligands and two Ag(I) ions as well as two nitrate counterions. Each Ag(I) adopts a trigonal planar coordination sphere by coordinating two *equatorial* and one *axial* amino group of three different ligands (N-Ag1-N angles: 144.5, 109.8, 105.3°, Σ = 359.6° and N-Ag2-N angles: 149.3, 107.0, 103.7°, Σ = 360.0°). The two crystallographically independant Ag(I) ions have different coordination environments; two Ag1 centres coordinate to two *trans*-tach units *via* their composite four *equatorial* amino groups, forming a macrocyclic subunit by 2:2 Ag1 to *trans*-tach coordination (Figure 81, *LHS*). The Ag1…Ag1 distance is 5.3 Å in the macrocycle and each cyclic unit consists of 12 ring atoms with an inversion centre. Instead of forming macrocyclic subunits, Ag2 forms linear chains running along the crystallographic *b* axis with coordination to one of the *equatorial* amino groups of each *trans*-tach ligand (Figure 81, *RHS*). Ag2…Ag2 distances are 5.5 Å along the chain. The Ag1 macrocyclic subunits are linked to Ag2 centres *via* the remaining *trans* amino groups in *axial* position.

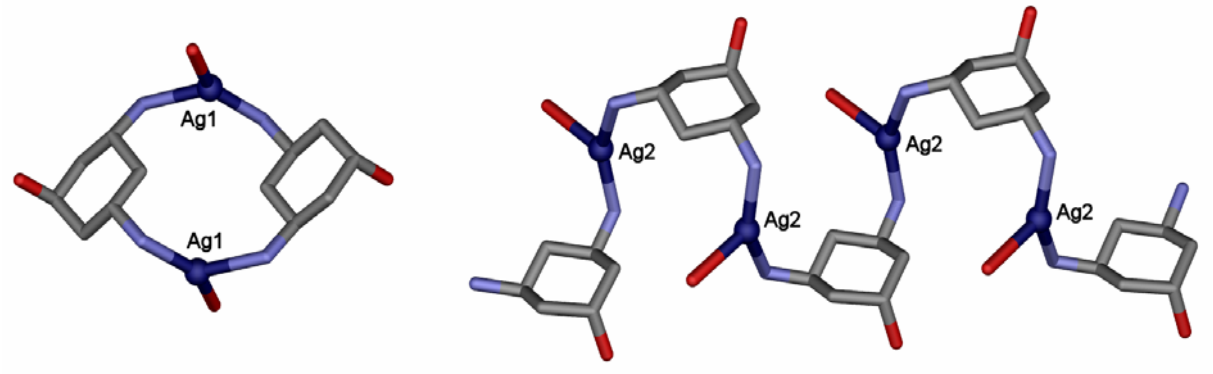


Figure 81 Ag(I) subunits of **54**. *LHS*: Ag1 coordination forms a macrocyclic subunit, Ag1…Ag1 = 5.3 Å. *RHS*: Ag2 coordination forms a linear chain along the *b* axis, Ag2…Ag2 = 5.5 Å. Ag(I) is shown as dark blue spheres, *equatorial cis* amines in light blue, *axial trans* amines in red and carbon in grey.

Both the ligand with μ_3 bridging amino groups and Ag(I) with trigonal planar coordination can be topologically abbreviated as 3-connected nodes, located at the centroid of the cyclohexane ring and the Ag(I) ions itself; this assists the further analysis of the 3-D network. Topologically, the Ag1 macrocyclic subunits represent tetragonal *closed* channel, whereas the Ag2 coordination chains represent tetragonal *helical* channels running along the crystallographic *b* axis. Upon linkage of these subunits, two more octagonal channels are formed. One of which is closed and the other helical, also running along the crystallographic *b* axis. Channels are found both along the crystallographic *b* and *a* axis (Figure 82). The nitrate counterions are located in both closed and helical octagonal channels, forming a 3-D hydrogen-bonded network with the primary amino groups (Table 13).

Table 13 3-D hydrogen-bonded network[166] (Å /°) for $\{[Ag(\mathbf{L})](NO_3)\}_n$ (**54**)

D-H ··· A	D-H	H ··· A	D ··· A	D-H ··· A
N(1) - H(1A) ··· O(1)[a]	0.90	2.20	3.078(11)	165
N(2) - H(2A) ··· O(5)[b]	0.90	2.20	3.068(17)	161
N(2) - H(2B) ··· O(5)	0.90	2.41	3.254(16)	156
N(3) - H(3A) ··· O(3)[c]	0.90	2.24	3.072(12)	154
N(3) - H(3B) ··· O(6)[c]	0.90	2.59	3.417(13)	153
N(4) - H(4A) ··· O(2)[d]	0.90	2.19	3.022(12)	153
N(4) - H(4B) ··· O(6)[e]	0.90	2.22	3.103(10)	166
N(5) - H(5A) ··· O(2)[f]	0.90	2.21	3.093(12)	168
N(5) - H(5B) ··· O(1)[a]	0.90	2.36	3.107(11)	140
N(6) - H(6A) ··· O(6)	0.90	2.22	3.116(12)	174
N(6) - H(6B) ··· O(4)[g]	0.90	2.52	3.390(14)	163

N(3) and N(6) represent the *axial* amino group nitrogen atoms and O(1)–O(6) the oxygen atoms of the nitrate counterions.

Symmetry Code: a) x,3/2-y,1/2+z; b) 1-x,-y,1-z; c) x,1/2-y,1/2+z; d) -x,1/2+y,1/2-z; e) x,1+y,z; f) -x,-1/2+y,1/2-z; g) 1-x,1/2+y,1/2-z.

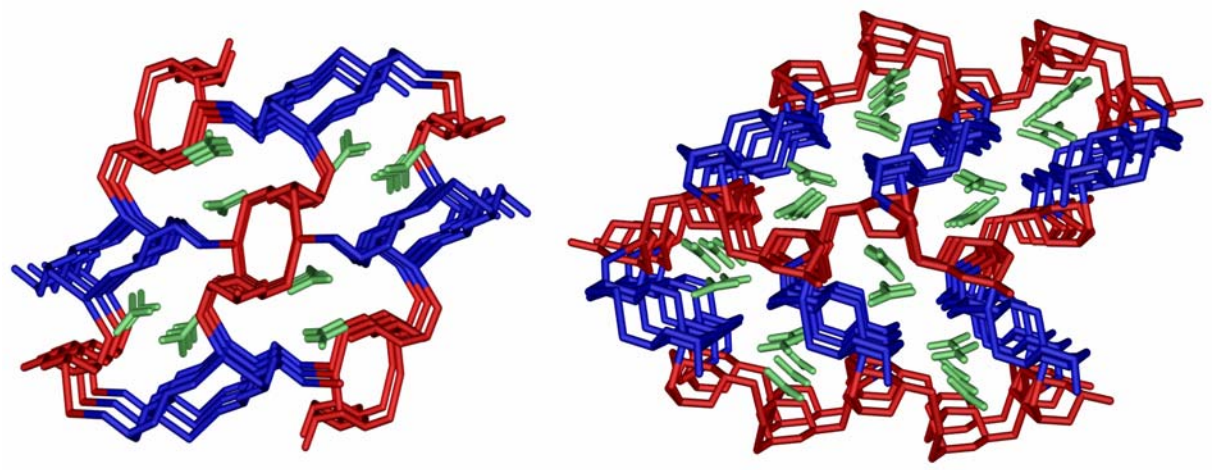


Figure 82 View along the crystallographic *b* (*LHS*) and *a* (*RHS*) axis. Arrangement of the macrocyclic Ag1 subunits (blue) along the Ag2 coordination chain (red). Nitrate counterions are represented in green.

An interesting feature observed in the structure is the presence of two crystallographically independent sets of Ag(I) ions and *trans*-tach ligands, which allows the formation of both *closed* and *helical* channels within the network. These non-uniform 3-connected nodes form the unprecedented 3-D *bi*nodal topology (4.8.10)(8.10^2) (Figure 83, *Top c*).

To understand this topology it is informative to consider the nets shown in Figure 83. Topology *a* shows a uniform 2-D (4.8^2) net,[114] in which every 3-connected node is shared by one tetragonal square and two octagons. Topology *b* demonstrates a uniform 3-D (10^3)-a net[113] which could be described as one of the 'derivatives' of the 2-D (4.8^2) net with lines broken and crosslinked to its adjacent layers (in this case *each* tetragonal square has one side broken). However, alternative arrangements of breaking and re-crosslinking may lead to other 'derivatives'. In case of **54**, breaking *half* of the tetragonal squares and subsequent crosslinking to neighbouring layers results in the new topology (Figure 83, *Top c*). The tetragonal and octagonal channels involving the broken sides are therefore individually helical (Figure 83, *Bottom*). However, the bottom of Figure 83 describes only one section of the topology of **54** with the *left* handed octagonal channel (green) and the tetragonal *right* handed channel (pink). **54** crystallises in the centrosymmetric space group $P2_1/c$, indicating the presence of a racemic mixture of enantiomeric sections of left-handed octagonal and right-handed tetragonal channels and inversion of the channel orientation to give sections of right-handed octagonal and left-handed tetragonal channels. Adjacent octagonal and tetragonal channels maintain their opposing helicity throughout the network.

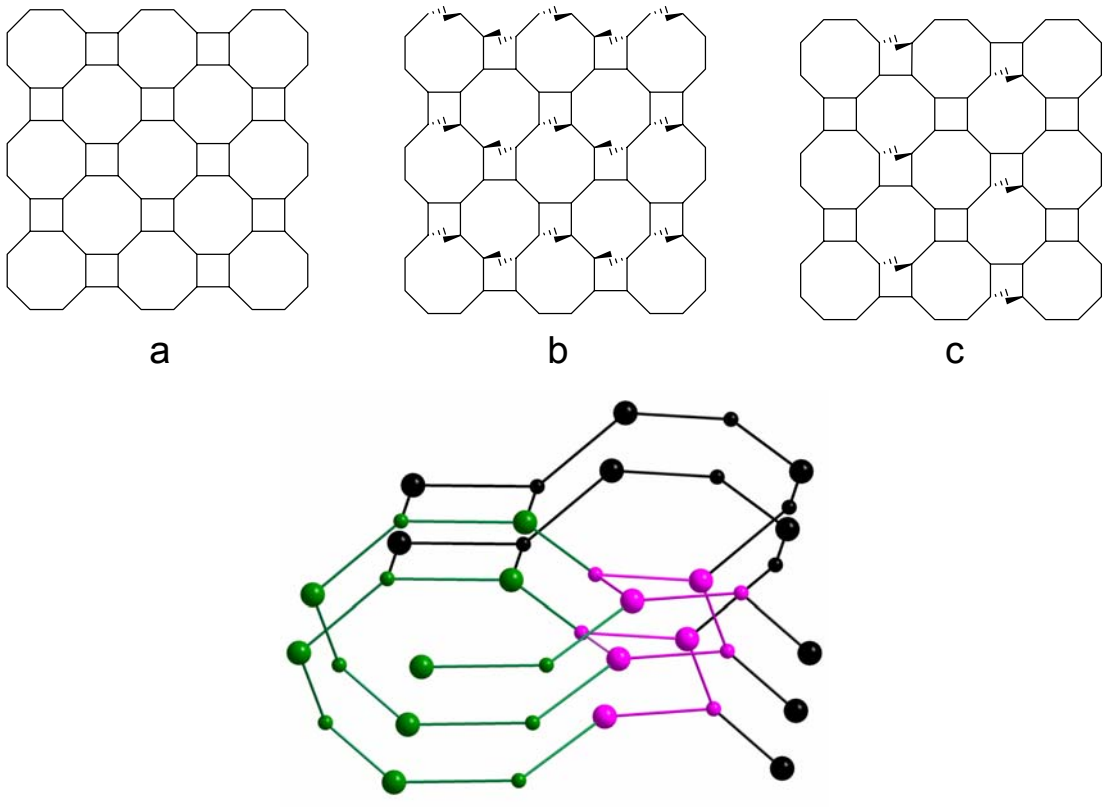


Figure 83 *Top*: Network topology of **54** is shown in *c* {(4.8.10)(8.10^2)} along with the associated topologies *a* (4.8^2) and *b* {(10^3)-a}. *Bottom*: Section of the topology of **54**. Parts of the c*losed* channels are shown in black, *helical* channels in pink and green running parallel to the crystallographic *b* axis.

It could be suggested that **54** results in a 3-D network due to the additional exocyclic *axial* amino group providing coordination out of the cyclohexane plane, in addition to the dimensions of the nitrate counterions fitting into the octagonal channels. The effect of the counterion on the resulting dimensionality of the coordination network, presumably due to size interactions, is illustrated by the exchange of the nitrate counterions to the larger triflate ions, which are too large to fit into the octagonal channels formed in **54**.

3.5.1.2 1-D coordination network with AgOTf 55

Crystallisation of a reaction mixture of Ag(I) triflate with *trans*-tach results in colourless crystals of **55** in good yield as determined by elemental analysis and multiple unit cell measurements on isolated single crystals. ^{1}H-NMR spectra confirmed the non-flipped conformation of *trans*-tach in solution (Table 12). As in the silver(I) nitrate structure

described above, all three amino groups of *trans*-tach are involved in coordinative interactions to Ag(I) ions. However, contrary to the 3-D coordination network of **54**, structure **55** results in a 1-D coordination polymer. The asymmetric unit consists of two crystallographically independent *trans*-tach ligands (L1, L2), both in the non-flipped conformation, and two Ag(I) ions (Ag1, Ag2) as well as two triflate counterions. Each Ag(I) adopts a trigonal planar coordination sphere (N-Ag1-N angles: 148.0, 114.3, 97.5°, Σ = 359.8° and N-Ag2-N angles: 148.2, 108.2, 103.2°, Σ = 359.6°) by coordinating two *equatorial* and one *axial* amino group of three different ligands. The overall structure is tube-like, formed by two chains coordinating Ag1 and Ag2 ions through the *equatorial* amino groups of the L1 and L2 (Ag…Ag distances along the chains are 8.1 Å). Both chains are linked together *via* coordination of the remaining *axial* amino groups. This arrangement leads to a staggered chain conformation of the overall tube type structure (Figure 84, *Centre*) and to the formation of two macrocyclic subunits (Figure 84, *Top*). These 2:2 subunits are formed *via* coordination of one *axial* and one *equatorial* amino group of each ligand to two Ag(I) ions. The Ag…Ag distances are 5.1 and 5.5 Å in macrocycle 1 and 2, respectively, and each cycle consists of 12 ring atoms. The space filling representation (Figure 84, *Bottom*) shows how the complementary coordination of both chains forms the overall tubular structure.

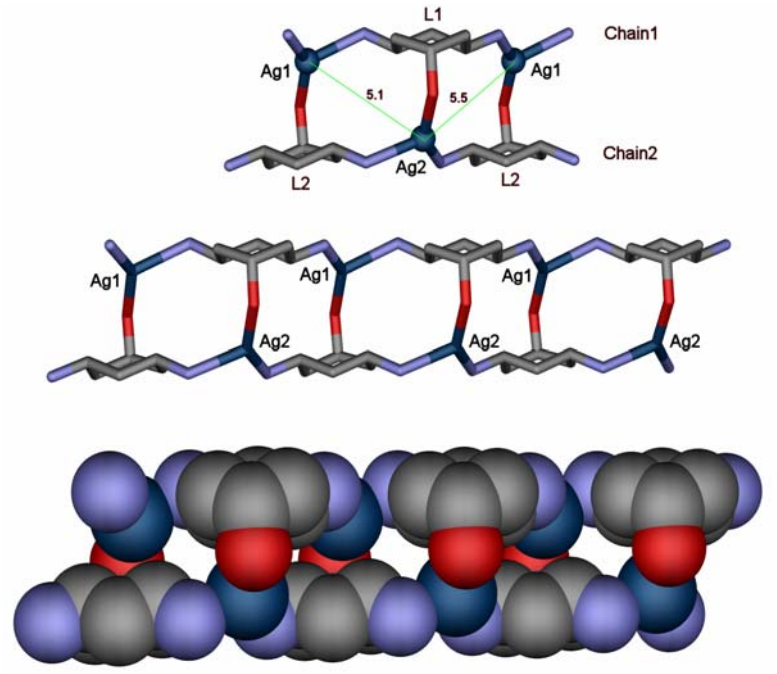


Figure 84 *Top*: Coordination of Ag(I) to *trans*-tach in a 2:2 ratio, forms the macrocyclic units in **55**; Ball and Stick (*Centre*) and space filling (*Bottom*) representation of the 1-D-coordination network. Ag(I) is shown in dark blue, *equatorial* nitrogens in light blue, *axial* nitrogens in red and carbon in grey.

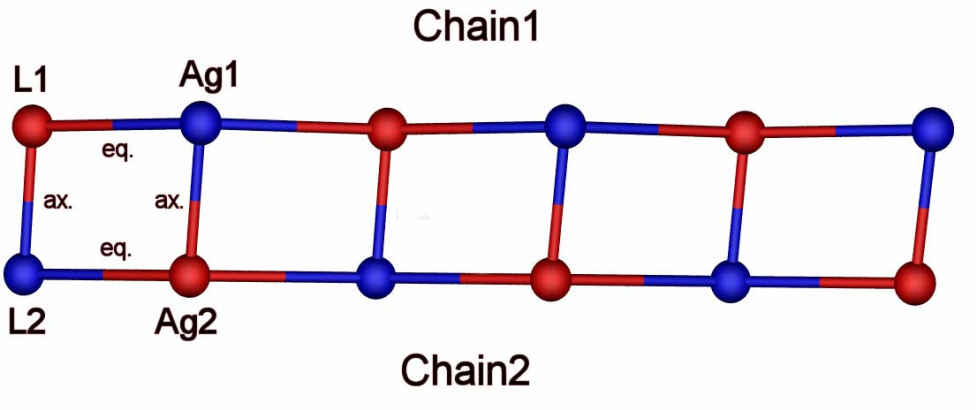


Figure 85 Network topology of **55** (4^2) with the two coordination chains formed upon coordination *via* the *equatorial* amino groups and their linkage *via* the remaining *axial* amino groups.

The topology of the structure is a uniform one dimensional (4^2) net (Figure 85). The 1-D- chains are packed in isolated layers with separations of 7.3, 10.9 and 12.4 Å and held together by a 2-D hydrogen-bonded network involving the triflate counterions (Table 14, Figure 86).

Table 14 1-D hydrogen-bonded network[166] (Å /°) for

$\{[Ag(\mathbf{L})](OTf)\}_n$ (**55**)

D-H ··· A	D-H	H ··· A	D ··· A	D-H ··· A
N(1) - H(1A) ··· O(1)[a]	0.90	2.35	3.043(7)	133
N(1) - H(1B) ··· O(1)[b]	0.90	2.20	3.055(6)	158
N(2) - H(2C) ··· O(5)[c]	0.90	2.20	3.037(7)	154
N(2) - H(2D) ··· O(5)[d]	0.90	2.33	3.216(7)	170
N(3) - H(3A) ··· O(3)[b]	0.90	2.46	3.255(7)	147
N(3) - H(3B) ··· O(6)[e]	0.90	2.31	3.170(7)	160
N(4) - H(4C) ··· O(2)[d]	0.90	2.19	2.938(6)	140
N(4) - H(4D) ··· O(6)[e]	0.90	2.14	3.021(7)	168
N(5) - H(5A) ··· O(2)[f]	0.90	2.31	3.117(8)	150
N(5) - H(5B) ··· O(1)[b]	0.90	2.32	3.199(7)	164
N(6) - H(6D) ··· O(4)[d]	0.90	2.39	3.250(7)	160

N(3) and N(6) represent the *axial* amino group nitrogen atoms and O(1)–O(6) the oxygen atoms of the triflate counterions.

Symmetry Code: a) x,y,1+z; b) -x,-1/2+y,1-z; c) x,-1+y,1+z; d) 1-x,-1/2+y,1-z; e) -x,-3/2+y,1-z; f) x,-1+y,z.

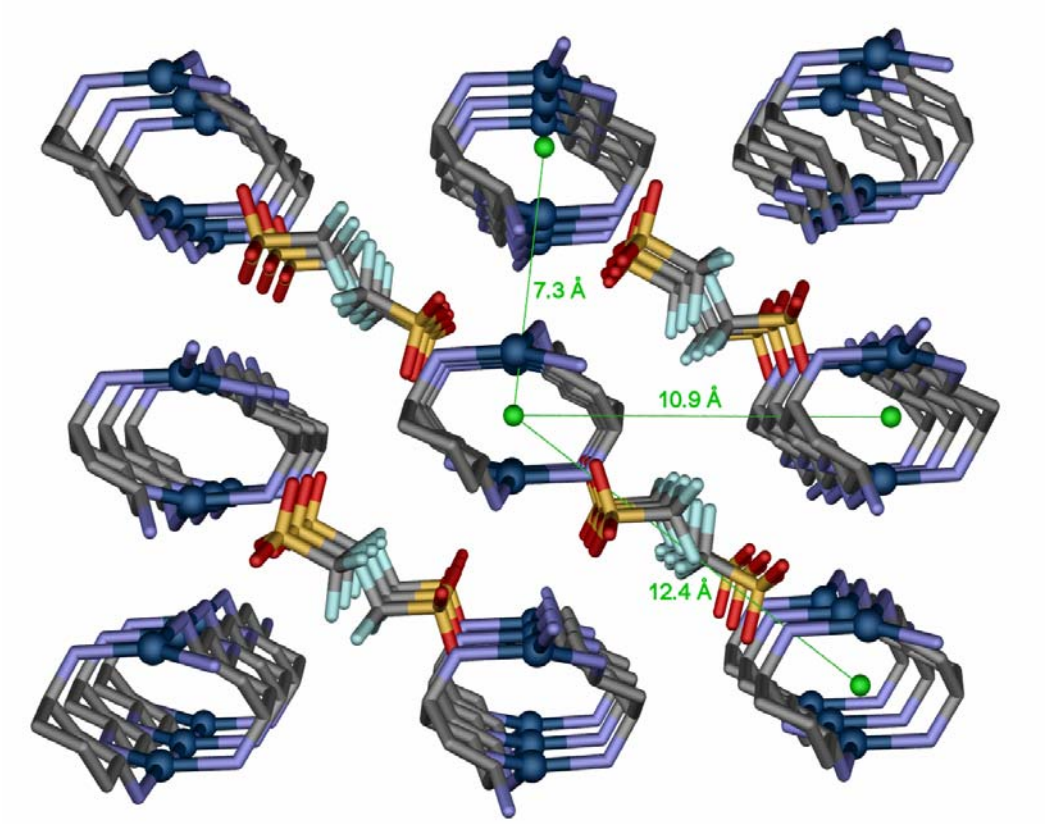


Figure 86 Layer packing of 1-D tubes of **55**. Distances between centroids, shown as green spheres, are 7.3, 10.9 and 12.4 Å. Ag(I) atoms are represented as dark blue spheres, nitrogen in light blue, sulphur in yellow, oxygen in red, fluorine in sky blue and carbon in grey.

3.5.2 Zn(II) coordination

Reactions of various zinc(II) salts, including chloride, bromide, nitrate and acetate with *trans*-tach in methanol at unadjusted pH resulted in the precipitation and isolation of white solids. These materials were insoluble in common solvents and hence no single X-ray crystal structures or NMR spectra could be obtained. However, based on the coordination behaviour of *trans*-tach with Ag(I) ions as described above it can be suggested that all three amino groups are involved in coordinative interactions; thus leading to the formation of insoluble high molecular weight coordination polymers, presumably with high dimensionality. To maintain solubility upon Zn(II) coordination, the *axial* amino groups were prevented from coordination by protonation.

3.5.2.1 1-D coordination network with $ZnCl_2$ 56

Reaction of zinc(II) chloride with *trans*-tach adjusted to pH 6.5 with hydrochloric acid results in a colourless solution from which the 1-D coordination polymer **56** crystallised. The colourless crystals obtained were of poor quality and resulted in a weak and possibly distorted data set due to twinning. The analysis of the disordered crystal structure is therefore restricted to interpretation of the coordination sphere around the heavy Zn(II) atoms without emphasis on numerical interpretation. No crystal packing or other intermolecular interactions are discussed in further detail. ^{1}H-NMR spectra of the reaction mixture shows *trans*-tach in its non-flipped conformation in solution (Table 12). This conformation is also found in the crystal structure of **56**, where both *equatorial* amino groups are involved in coordinative interactions to Zn(II) ions. The tetrahedral coordination sphere of the zinc(II) ion is completed by coordination of a terminal chloro ligand and two bridging chloro ligands towards another, identical zinc(II)-ligand unit (Figure 87). The *axial* amino group nitrogen is protonated and does not take part in coordinative interactions with Zn(II) ions. The overall structure represents a 1-dimensional zig-zag chain.

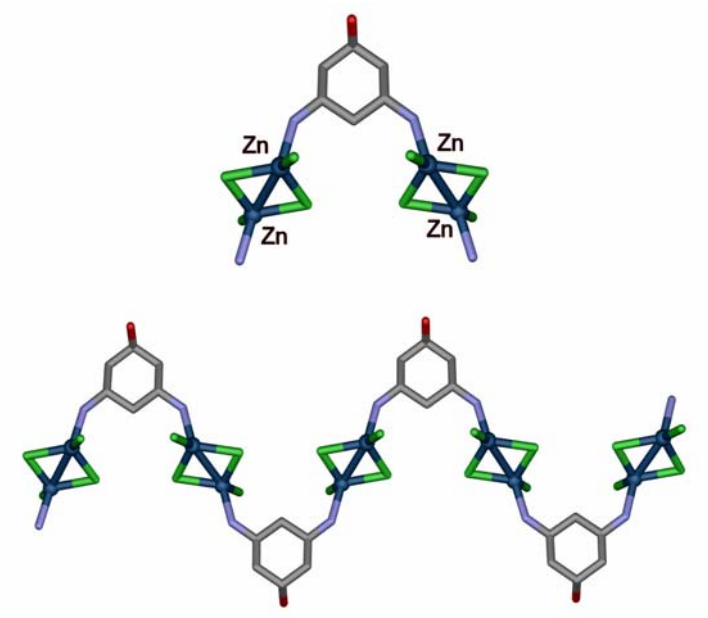


Figure 87 *Top*: Coordination environment around a single *trans*-tach ligand; Bottom: 1-D-coordination chain of **56**. Zn(II) is shown as dark blue spheres, chloride in green, *equatorial* nitrogens in light blue, *axial* nitrogens in red and carbon in grey.

3.6 Schiff base derivatives of trans-tach

Reactions of aromatic aldehydes with *trans*-tach represent efficient syntheses of extended *trans*-tach units. The aromatic Schiff bases are easily purified by extraction with organic solvents such as diethylether or dichloromethane (Figure 88). These reactions represent an inexpensive and efficient route to providing additional functionality to the parent *trans*-tach moiety, while still inheriting the *cis,trans*-geometry on the rigid cyclohexane backbone.

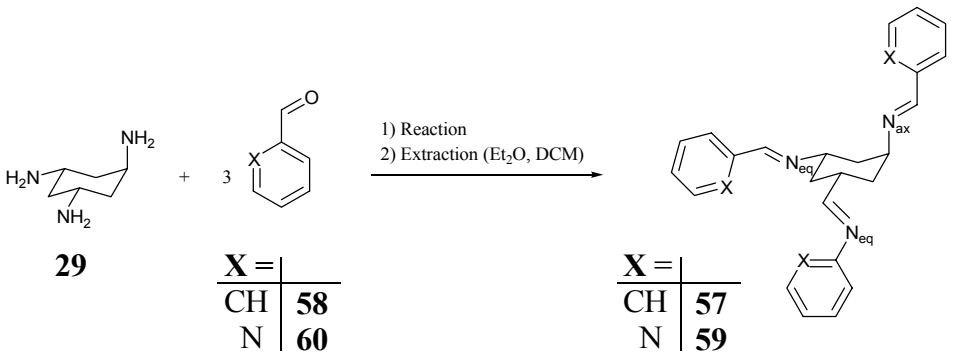


Figure 88 Reaction overview of Schiff base formation with *trans*-tach (**29**).

3.6.1 *cis,trans*-1,3,5-*tris*-Benzaldimino-cyclohexane (tbc, 57)

Reaction of *trans*-tach (**29**) with benzaldehyde (**58**) results in the formation of the Schiff base *tbc* (**57**) in moderate yield, which has been fully characterised. This compound was used as an NMR model to study the dependence of the *equatorial* and *axial* substituents on the cyclohexane ring. For NMR experiments it is important to evaluate to what extent the two different environments on the cyclohexane ring influence the substituent signals. The 2:1 ratio in which the substituents integrate is particularly informative. Furthermore, it was anticipated that the reversibility of the imine bond formation, *e.g.* acidic hydrolysis might be utilized to specifically remove substituents upon metal coordination.[151,213] However, no hydrolysis was observed upon reaction with a variety of transition metals. Instead, crystals of **57** were obtained from a reaction mixture with nickel(II) chloride (Figure 89).

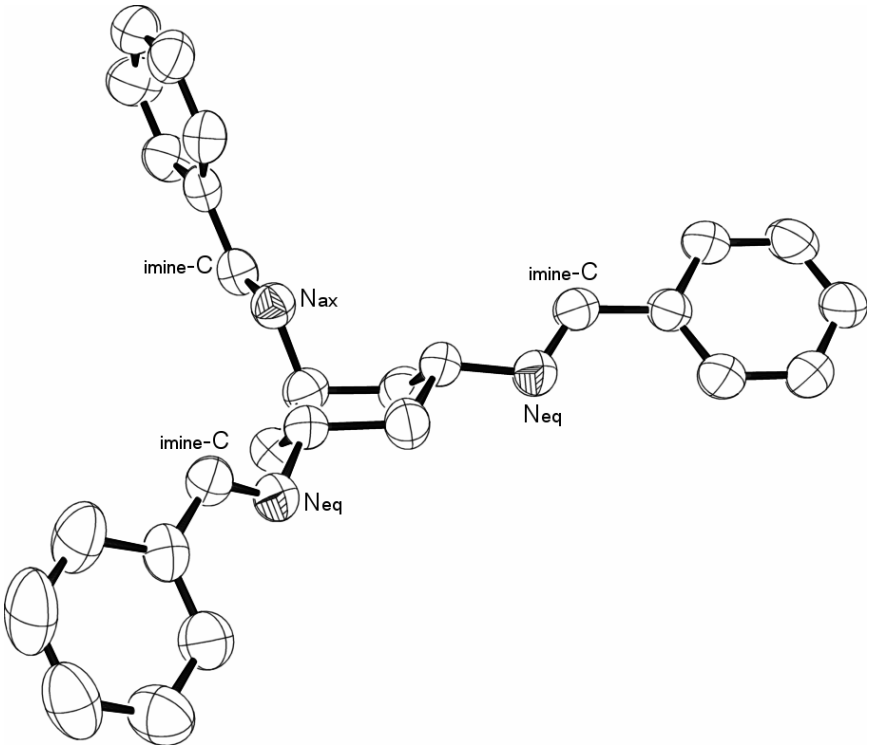


Figure 89 Ortep-3 representation of the crystal structure of tbc (**57**) at 50 % thermal ellipsoids. Hydrogen atoms are omitted. The bis*equatorial*-mono*axial* environment on the cyclohexane ring substituents can be seen clearly.

Crystal structure analysis of tbc clearly shows the cyclohexane ring in its non ring-flipped conformation, having two benzaldimino substituents in *equatorial* and one in *axial* position. The imine C=N double bonds are substituted in the sterically favoured *E* - conformation with expected bond length ($d_{C=N}$ =1.258(2) Å). It is interesting to note that the phenyl ring on the *axial* substituent is nearly perpendicular to the phenyl rings on the *equatorial* substituents with an angle of 82.7(1)° between the aromatic planes. The *equatorial* phenyl substituents are twisted by 28.4(1)° from coplanarity. This leads to an interesting packing motif, with two molecules of **57** forming a dimer through π-π stacking between *axial* phenyl substituents ($d_{\pi\text{-}\pi}$ = 3.6 Å)[214-216] and CH-π interactions between *equatorial* phenyl substituents ($d_{H\text{-}\pi}$ = 3.0 Å)[217,218] of each molecule (Figure 90, *Top*).

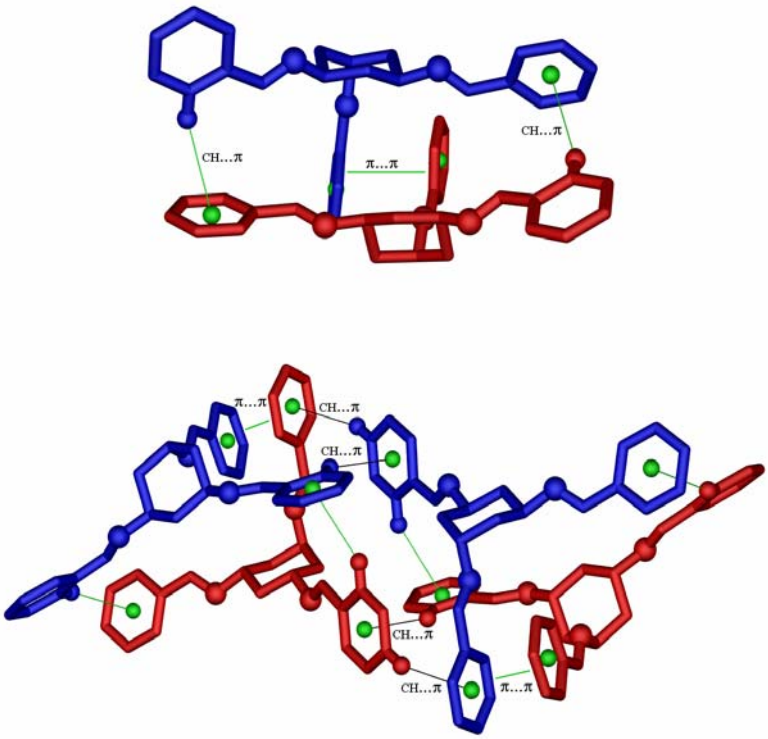


Figure 90 *Top*: Dimer of **57** involved in π- π stacking (3.6 Å) and CH-π (3.0 Å) interactions indicated by green lines; *Bottom*: CH-π interactions between two *equatorial* (2.8 Å) and *equatorial* to *axial* (3.0 Å) phenyl groups indicated by black lines, forming a chain of dimers along the crystallographic *c* axis. The green spheres represent the centres of the aromatic phenyl rings.

These dimers are connected to chains running along the crystallographic *c* axis *via* additional CH-π interactions between the two *equatorial* ($d_{H\text{-}\pi}$ = 2.8 Å) and *equatorial-axial* ($d_{H\text{-}\pi}$ = 3.0 Å) phenyl groups (Figure 90, *Bottom*). These chains form layers along the *b* axis which are in turn hexagonally arranged along the *c* axis (Figure 91).

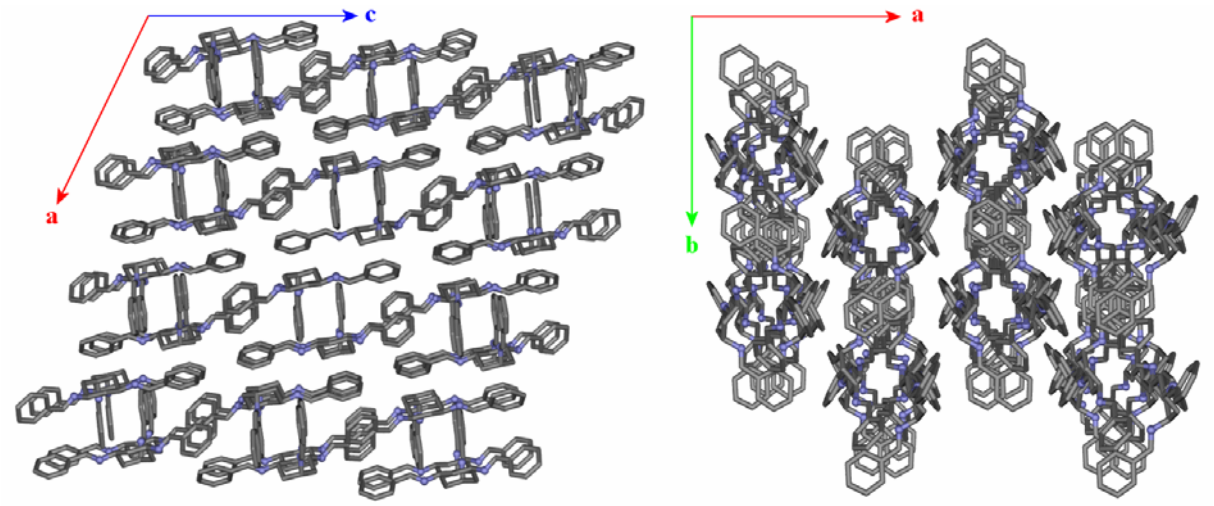


Figure 91 *LHS*: View along the crystallographic *b* axis showing a layer of chains formed upon dimer interactions; *RHS*: View along the crystallographic *c* axis showing the hexagonal arrangement of layers.

3.6.1.1 Spectroscopy of tbc

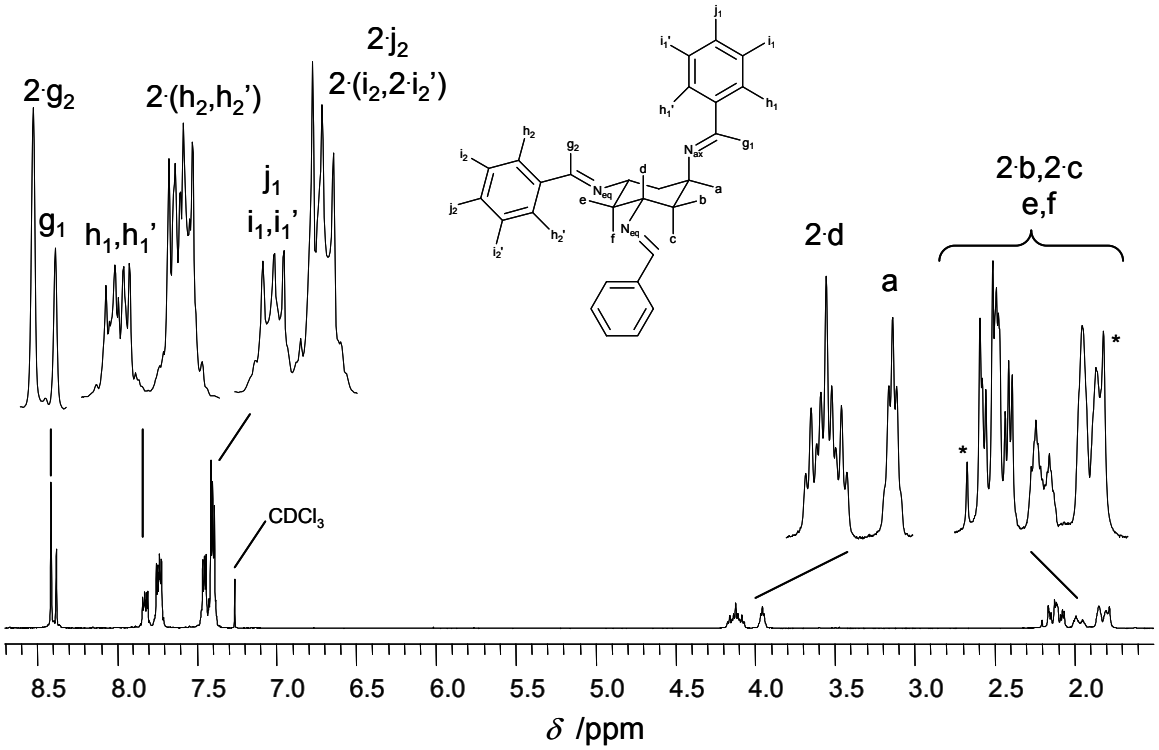


Figure 92 ^{1}H-NMR (300 MHz, $CDCl_3$) of **57**. *) indicates slight impurities.

The ^{1}H-NMR spectrum of **57** shows signals both in the aliphatic and the aromatic region. The aliphatic resonances show similar spin multiplicities for the methine protons as observed in

the non-flipped conformation of *trans*-tach. The signals for the H_d (δ = 4.11 ppm) and H_a (δ = 3.95 ppm) methine protons are resolved showing a triplet of triplet and a triplet splitting in the ratio of 2:1, respectively (Figure 28), whereas the resonances of the remaining methylene protons are not resolved and signal overlap does not allow exact assignments. In the aromatic region, the lowest field signals correspond to the imine protons H_{g2} (δ = 8.41 ppm) and H_{g1} (δ = 8.38 ppm) which both appear as singlets in a ratio of 2:1, clearly indicating the difference in *equatorial* and *axial* environments on the cyclohexane ring substituents. These different environments are also observed in the phenyl ring signals. Each phenyl group represents an AA'BB'C spin system or, to be consistent with the nomenclature used here; hh'ii'j. The multiplicities of the signals are not resolved, however the resonances split into two groups of hh' and ii'j signals for each phenyl ring, integrating 2:3. Furthermore, the resonances can be distinguished between the *equatorial* and *axial* substituents by their overall 2:1 integration (Figure 92). The relative shifts, as well as the appearance of two groups of signals for each phenyl ring, are in accordance with calculated values based on substructure analysis for chemical shift determination, implemented within the program ChemNMR Pro[219]

3.6.2 *cis,trans*-1,3,5-*tris*-(Pyridine-2-carboxaldimino)-cyclohexane (ttop, 59)

Reaction of *trans*-tach (**29**) with pyridine-2-carboxaldehyde (**60**) yields the ligand ttop (**59**) in good yield, which has been fully characterised. This ligand provides six nitrogen donor atoms in three sets of bidentate moieties in its non-flipped conformation. However, in its ring-flipped conformation, both *axial* bidentate donor sets can potentially coordinate to the same metal centre, providing a tetradentate chelating moiety[220-223] while maintaining the *equatorial* bidentate site (Figure 93).

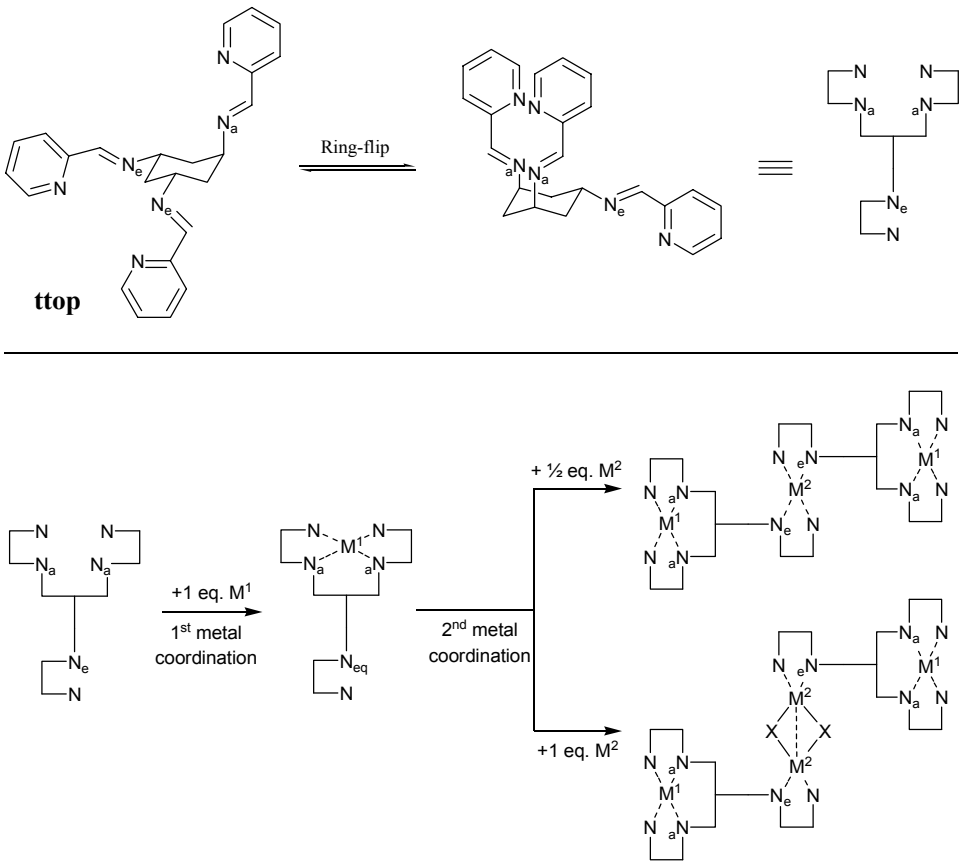


Figure 93 *Top*: Six nitrogen donor coordination of ttop (**59**); 3x2-chelating sites (*left*); 1x4 and 1x2 chelating sites (*right*) upon ring-flip. *Bottom*: Overview of potential metal coordination; stepwise coordination to the tetradentate (1st metal coordination) and bidentate (2nd metal coordination) coordination sites with different metal to ligand stoichiometries.

It is anticipated that ttop coordinates metal ions with both tetradentate and bidentate chelating moieties upon ring-flip. Furthermore, the stability difference of tetradentate to bidentate coordination ensures that metal coordination occurs in two successive steps, potentially leading to heteronuclear complexes (Figure 93, *Bottom*) with applicable electrochemical and magnetic properties.[223-226] Potential metal ions for the first metal coordination in the tetradentate binding site include Cu(II),[224,227,228] Zn(II),[222,227] Fe(II),[222] Co(II),[227] Mn(II),[229] Ni(II),[230] etc. The variety for the second metal coordination is even greater since the bidentate chelating moiety in *equatorial* position is not as sterically restrained as the tetradentate pocket. Furthermore, control over the stoichiometry and reaction conditions of the second metal coordination should principally allow the formation of complexes with different metal to ligand ratios (Figure 93, *Bottom*).

3.6.2.1 Spectroscopy of ttop

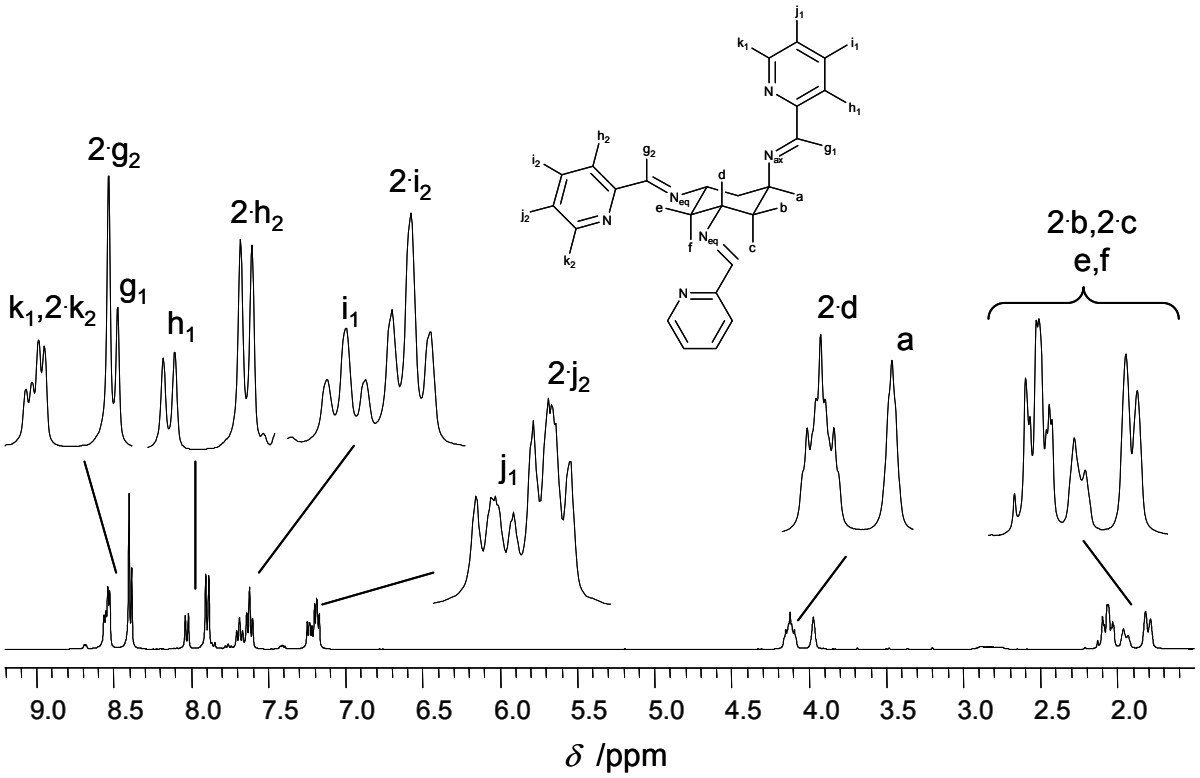


Figure 94 ^{1}H-NMR (400 MHz, $CDCl_3$) of ttop (**59**).

The ^{1}H-NMR spectrum of ttop (**59**) in deuterated chloroform on a 400 MHz spectrometer resolves 14 out of the 16 different proton environments. The non-resolved signals include the lowest field shifted protons H_k and an overlap of H_b or H_c with H_e or H_f in the aliphatic region. However, the non ring-flipped conformation of the cyclohexane ring is confirmed by the methine protons H_d and H_a. Both signals are resolved and the *axial* protons H_d (δ = 4.11 ppm, 2H) show a pseudo-triplet splitting due to a large *trans-axial* coupling to H_c and H_f (^{3}J = 11.3 Hz). Contrary to this, H_a (δ = 3.97 ppm, 1H) results in a broad singlet due to its *equatorial* position on the cyclohexane ring. The remaining methylene protons are not resolved and signal overlap does not allow exact assignment. All aromatic signals are resolved and assigned due to their 2:1 integration associated with relative positions on *equatorial* or *axial* substituents, with exception of the H_k signals, which are identified by their low field chemical shifts due to their *ortho*-position to the pyridyl-nitrogen. The imine protons H_{g2} (δ = 8.30 ppm) and H_{g1} (δ = 8.29 ppm) are identified as singlets in the ratio 2:1. The remaining pyridyl ring protons H_h, H_i and H_j are assigned in accordance with calculated

values based on substructure analysis for chemical shift determination, implemented within the program ChemNMR Pro.[219]

3.6.2.2 ^{1}H-NMR-titration of ttop with $ZnCl_2$

Contrary to the ^{1}H-NMR spectrum of ttop recorded in $CDCl_3$ on a 400 MHz spectrometer, the spectrum recorded in deuterated methanol on a 300 MHz spectrometer resolves 11 out of the overall 16 resonances. Most importantly, only one signal in the aromatic region is resolved into *equatorial* / *axial* substituents. Upon complexation with zinc(II) chloride, the spectrum broadens and 9 out of 10 low field signals become resolved. Spectra were recorded before the addition (*Lower*-black), with 0.5 equivalents (*Centre*-red) and 1.0 equivalents (*Upper*-blue) of $ZnCl_2$.[231] These spectra follow the complexation of zinc(II) by ttop. Of particular interest are the changes in resonances highlighted with arrows.

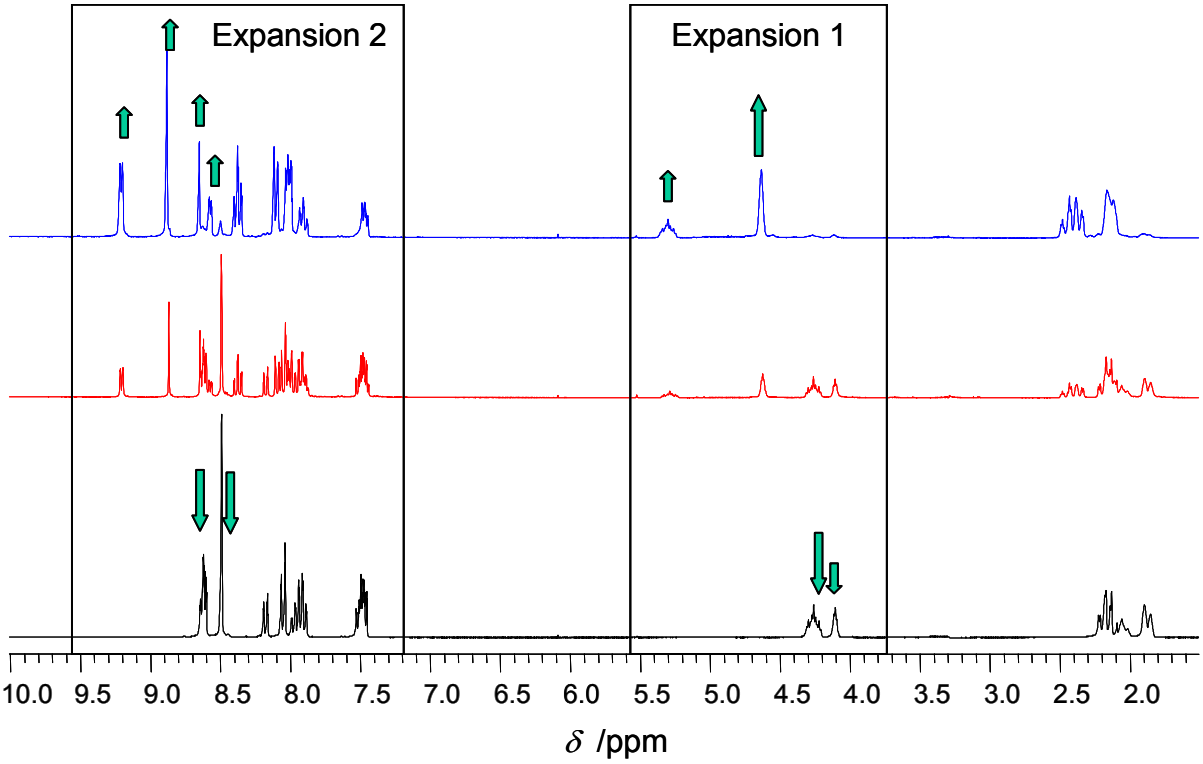


Figure 95 ^{1}H-NMR (300 MHz, CD_3OD) titration experiment of ttop (**59**) and zinc(II) chloride, solvent signals are removed for clarity. *Lower*-black: ttop, *Centre*-red: ttop + 0.5 $ZnCl_2$, *Upper*-blue: ttop + 1.0 $ZnCl_2$.

Expansion 1 (Figure 96) shows the aliphatic methine protons H_d and H_a. Before addition of zinc(II) ions, the lower field signal corresponds to H_d (δ = 4.25 ppm, 2H), showing a triplet of

triplet splitting (^3J = 11.4, 4.0 Hz) with a large *trans-axial* coupling, confirming its *axial* position on the cyclohexane ring. In contrast to this, H_a (δ = 4.10 ppm, 1H) shows only a triplet splitting with a small coupling constant ^3J = 2.9 Hz, therefore being in *equatorial* position. Upon complexation with zinc(II) chloride, both signals decrease while two new peaks rise at lower field. These new peaks observed in the spectrum upon addition of 1.0 equivalent of $ZnCl_2$ exhibit an inverted multiplicity as the triplet of triplets signal at lower field now integrates to one proton corresponding to H_a (δ = 5.30 ppm, 1H) exhibiting a large *trans-axial* coupling constant (^3J = 12.0, 4.4 Hz). This suggests a ring-flip of the cyclohexane ring upon complexation. In agreement with this, the resonance for the now *equatorial* methine protons H_d (δ = 4.63 ppm, 2H) appears as a broad singlet, integrating to two protons. The change in ratio upon integration for both pairs of signals exhibiting identical multiplicities is in agreement with the ring-flip of the cyclohexane ring. Thus, the ^{1}H-NMR spectra observed upon titration are comparable to the spectra obtained upon palladium(II) coordination (see Chapter 3.4.3).

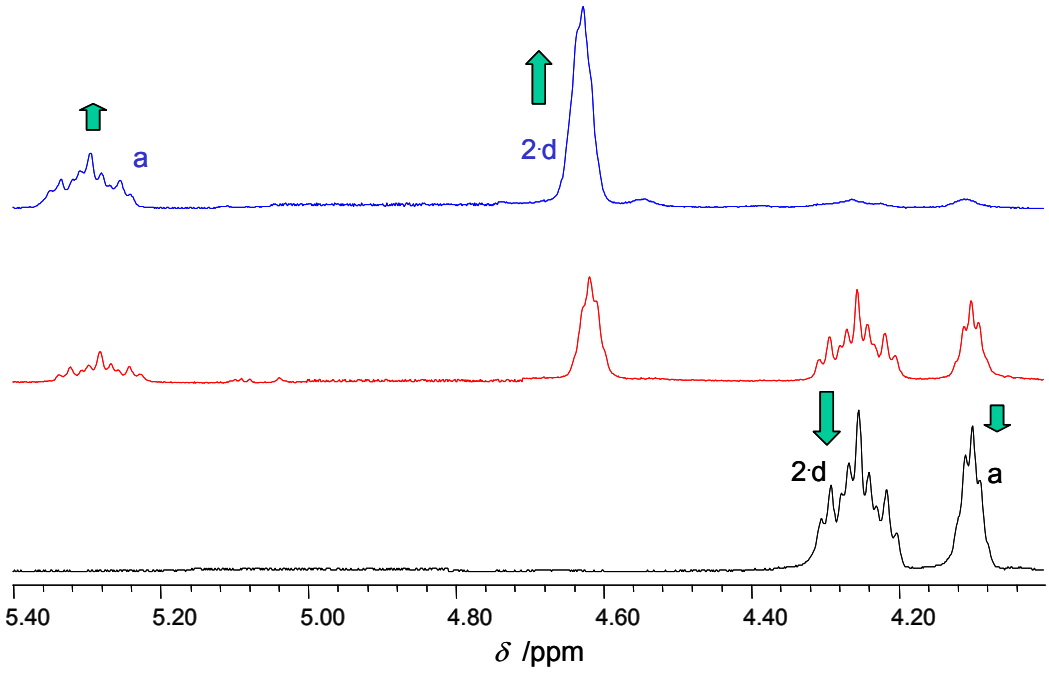


Figure 96 Expansion 1, aliphatic ^{1}H-NMR methine protons of Figure 95, *Lower*-black: ttop, *Centre*-red: ttop + 0.5 $ZnCl_2$, *Upper*-blue: ttop + 1.0 $ZnCl_2$.

The ring-flipped ttop provides a favourable tetradentate chelation site for metal ions. Expansion 2 shows the aromatic region of Figure 95, allowing a closer interpretation of the coordination environment of the zinc(II) ion. Two sets of proton signals are of particular

interest, H_k and H_g. Coordination is expected to have the greatest influence on the chemical shifts of these protons as both sets are closest to the coordinating nitrogen atoms. Indeed, the signals for H_k split into two pairs of signals H_{k2} and H_{k1} which integrate 2:1 according to the ratio of *axial* / *equatorial* substituents upon ring-flip. Furthermore, the signals for H_{k2} on the *axial* substituents become the most deshielded (δ = 9.21 ppm) due to their proximity to the coordinating pyridyl nitrogen atoms. The singlet (δ = 8.48 ppm) for the imine protons H_g, which integrates to three protons, splits into two separate singlets for H_{g2} (δ = 8.88 ppm) and H_{g1} (δ = 8.64 ppm) at lower field, integrating in a ratio of 2:1, confirming the above assignment.

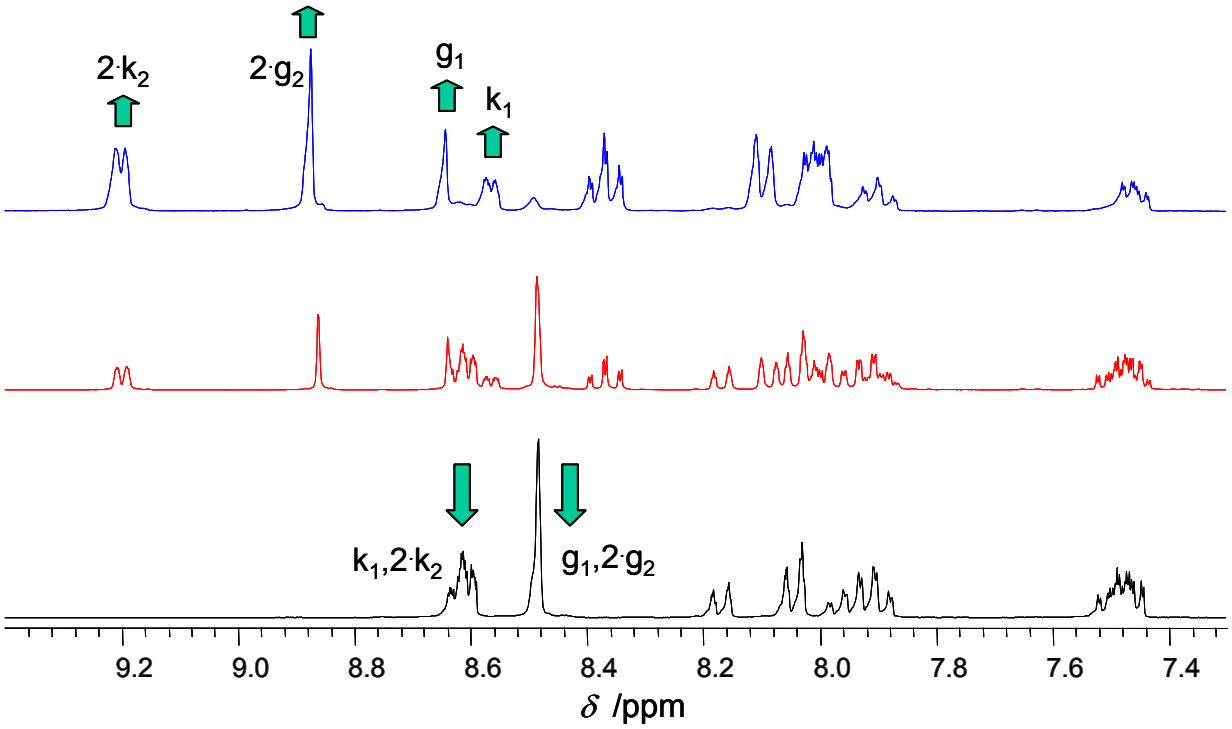


Figure 97 Expansion 2, aromatic ^{1}H-NMR region of Figure 95, *Lower*-black: ttop, *Centre*-red: ttop + 0.5 $ZnCl_2$, *Upper*-blue: ttop + 1.0 $ZnCl_2$.

To summarise the above, one equivalent of zinc(II) chloride is coordinated by the tetradentate chelating moiety formed upon ring-flip of ttop, leaving the *equatorial* bidentate coordination site uncomplexed. This coordination mode represents the anticipated coordination of one equivalent of metal ions as described in Figure 93 (1st metal coordination).

3.6.2.3 Complexation of ttop with one equivalent of $CuCl_2$ 61

Reaction of ttop with one equivalent of copper(II) chloride yields the mononuclear complex **61** in good yield, which has been fully characterised. The imine double bond is substituted in the sterically favoured *E*-conformation. The copper(II) ion is coordinated within the tetradentate chelating moiety present upon ring-flip of the cyclohexane ring (Figure 98). The Cu…N distances are 2.019(2) and 2.000(3) Å for the imine-groups and 2.035(3) and 2.101(2) Å for the pyridyl-nitrogens and lie within expected ranges.[227,228] The copper(II) ion deviates 0.376(1) Å from the tetragonal nitrogen coordination plane. The tetragonal pyramidal ($\tau = 0.27$)[167] coordination is completed by a chloro ligand, which points towards the centre of the cyclohexane ring. The Cu…Cl distance of 2.4175(8) Å lies in the longer range reported for this type of complexes.[232-234] As with the chloro ligand, the copper(II) ion is orientated towards the centre of the molecule with an interplanar angle Θ of 169.0°, placing the copper(II) at the edge of the cyclohexane ring. This large angle Θ might be explained due to the additional coordination of the two pyridyl nitrogens 'pulling' the Cu(II) towards the edge of the ring. The bidentate chelating moiety is not involved in coordinative interactions and the pyridyl ring, with its nitrogen pointing towards the chloro ligand, is orientated nearly perpendicular to the two *axial* pyridine rings with an angle of 85.4(1)°. The two *axial* pyridine rings are twisted by 22.4(2)° from co-planarity.

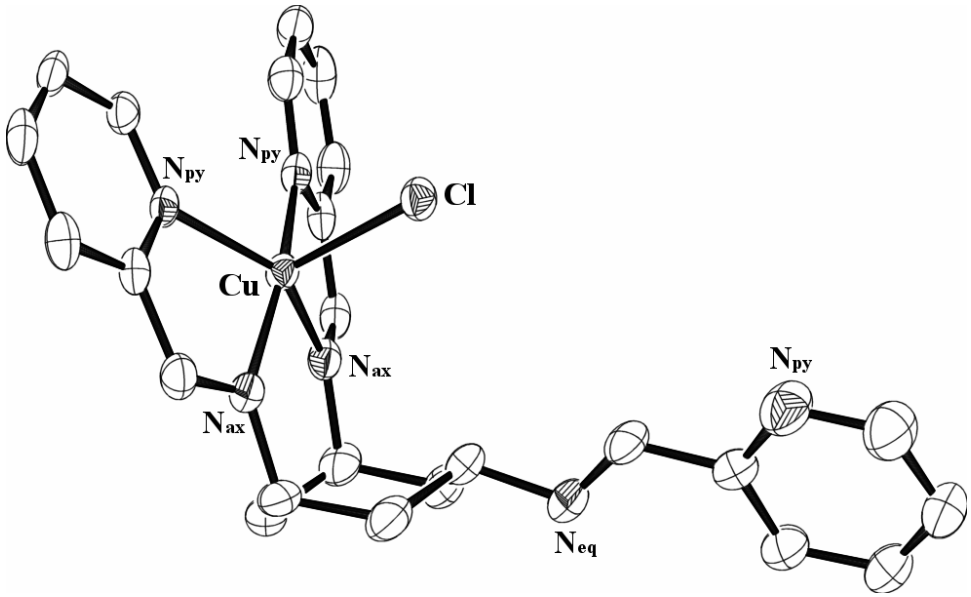


Figure 98 Ortep-3 representation of **61** with 50 % thermal ellipsoids.

3.6.2.4 Complexation of ttop (59) with two equivalents of $CuCl_2$ 62

Surprisingly, reaction of both 1.5 equivalents and 2 equivalents of copper(II) chloride with ttop results in the formation of the 2:1 metal to ligand complex **62**. This complex was characterised by elemental analysis, IR and single X-ray crystallography. No solution data allowing unambiguous identification has been thus far obtained and such studies as EPR spectroscopy and electrochemistry are yet to be carried out. Both coordination sites are complexed to copper(II) ions in a tetragonal pyramidal fashion; the tetradentate pocket coordinates Cu1 by its four nitrogen atoms available upon ring-flip of the cyclohexane ring ($d_{Cu1\ldots Nimine}$ = 1.996(6) and 2.004(6) Å, $d_{Cu1\ldots Npyridyl}$ = 2.036(6) and 2.069(5) Å). The coordination sphere of Cu1 is completed by a chloro ligand which is, contrary to complex **61**, pointing away from the cyclohexane ring ($d_{Cu1\ldots Cl3}$ = 2.427(2) Å). The *equatorial* bidentate coordination site ligates Cu2 with its two nitrogen atoms ($d_{Cu2\ldots Nimine}$ = 2.046(6) Å, $d_{Cu2\ldots Npyridyl}$ = 2.045(6) Å), in addition to a terminal ($d_{Cu2\ldots Cl2}$ = 2.256(2) Å) and two bridging ($d_{Cu2\ldots Cl1,Cl1*}$ = 2.2836(18) and 2.651(2) Å) chloro ligands. Cu1 deviates from its tetragonal coordination plane by 0.313(3) Å, whereas Cu2 only deviates by 0.191(2) Å. This is reflected in the structural parameter τ (0.20 and 0.17 for Cu1 and Cu2 respectively) being smaller for less deviation from the ideal tetragonal pyramidal coordination. Both *axial* pyridine rings are twisted by 23.8(4)° from co-planarity, whereas the *equatorial* pyridine ring is twisted by 72.2(2)° with respect to both *axial* aromatic systems. The Cu2…Cu2* distance in the dimeric complex lies with 3.497 Å within the range of μ_2-chloro bridged copper(II) dimers.[225,226,235]

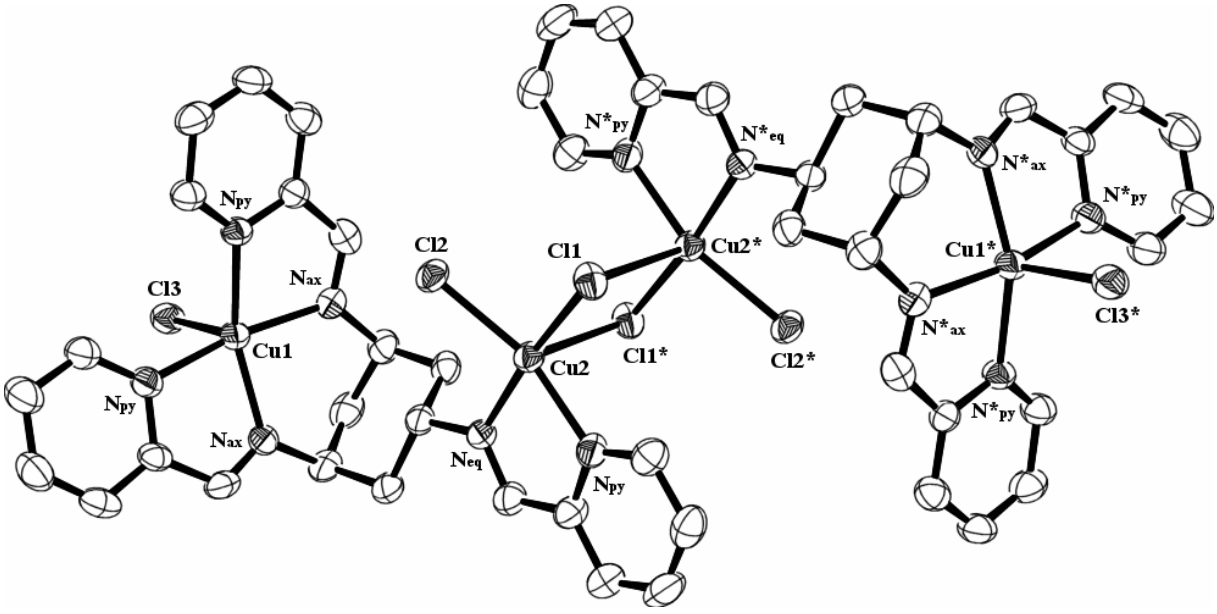


Figure 99 Ortep-3 representation of dimeric **62** with 50 % thermal ellipsoids.

Solid state comparison of the 1:1 complex **61** (Figure 100, red) and 2:1 complex **62** (Figure 100, blue) shows the difference in the coordination for the first equivalent of copper(II) ions within the tetradentate pocket utilized in both structures. Whereas the chloro ligand is oriented towards the cyclohexane ring in **61**, in **62** it is oriented away from the ring. This is due to coordination by the *equatorial* bidentate moiety to a second equivalent copper(II) in **62**; the substituent rotates into a favourable position to coordinate *via* the bidentate site, resulting in a bite angle for the nitrogen chelation of approximately 90°. This rotation is represented by a change in the torsion angle χ = 59.0° observed in **62** compared to χ = 164.6° in **61** (Figure 100, *RHS*). The bidentate chelation locates the copper(II) ion above the cyclohexane ring plane with one of its chloro ligands pointing towards the centre of the ring. This prevents the chloro ligand on Cu1 from pointing towards the centre of the cyclohexane ring as observed in **61**. This steric hindrance forces the tetradentate chelated copper(II) ion and its chloro ligand in **62** to point away from the cyclohexane ring (Figure 100, *LHS*). This geometrical restriction is further illustrated by the largest interplanar angle Θ = 193.1° for Cu1. As this angle is larger than 180°, the coordinated metal is placed furthest away from the centre of the cyclohexane ring.

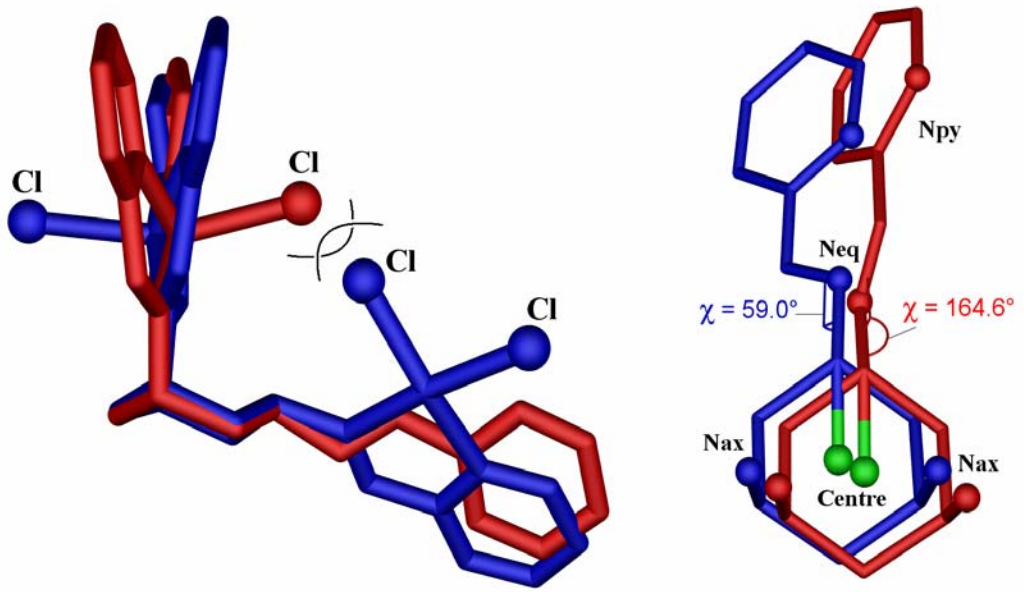


Figure 100 Comparison of **61** (red) and **62** (blue). *LHS*: The overlay of the crystal structures shows the steric hindrance of the tetradentate binding pocket with the bidentate chelation site preventing both chloro ligands pointing towards the cyclohexane ring. *RHS*: Torsion angle χ for the *equatorial* substituents in both complexes are shown. Nitrogen atoms are shown as spheres. Green spheres represent the centres of the cyclohexane rings. The *axial* substituents as well as the copper(II) and chloride ions are omitted for clarity.

4 CONCLUSIONS AND FURTHER WORK

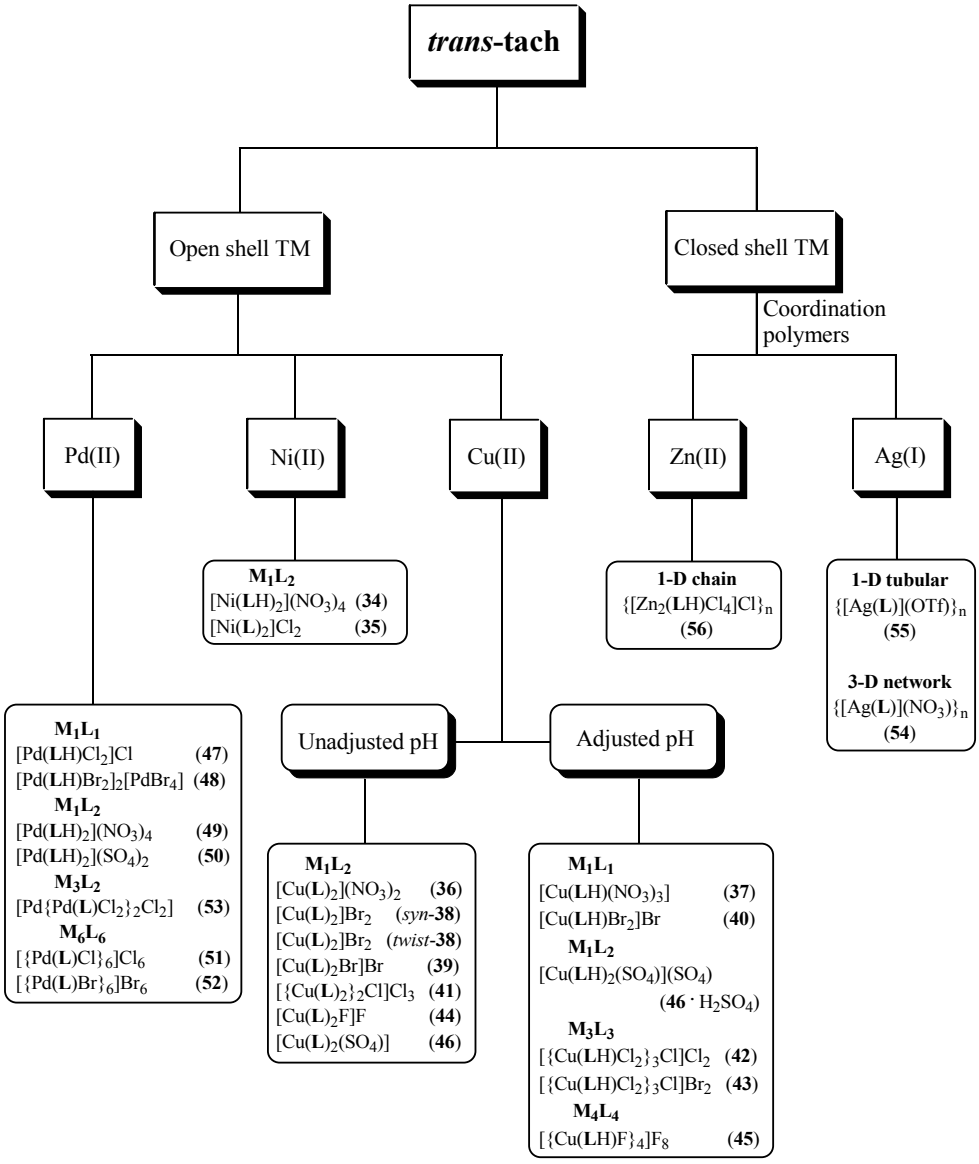


Figure 101 Overview of the crystallographically characterised transition-metal complexes of *trans*-tach (**L**). The abbreviation M_xL_y indicates the nuclearity (x) and the number of *trans*-tach ligands (y) within each complex.

In conclusion, the coordination behaviour of the rigid, aliphatic triamino ligand *cis,trans*-1,3,5-triaminocyclohexane (*trans*-tach) has been investigated (Figure 101). This has been shown to be a versatile ligand that can be understood conceptually as a rigid building block with three primary amino groups (with two types of non-interacting binding sites) available for coordination by the formation and characterisation of several new coordination

complexes. It is interesting to note that, depending on the conformation of the rigid cyclohexane backbone, the ligand can provide either a *tris*-monodentate or a bidentate-monodentate coordination motif. In the latter case, the ligand's potential as a supramolecular building block is realized as it has two non-equivalent, non-interacting binding sites, which can be utilized in the formation of large architectures. Furthermore, it is possible to distinguish between the two conformations by virtue of the characteristics of the coordinated metal.

4.1 Coordination networks

With closed shell transition metals the *trans*-tach ligand is, without exception, in the most energetically stable bis*equatorial*-mono*axial* chair conformation. In this conformation, *trans*-tach is able to act as a μ_3 bridging ligand that leads to the formation of coordination polymers. In the case of silver(I) nitrate, *trans*-tach coordination is shown to form a three-dimensional network with unprecedented topology comprising helical channels (**54**). The effect of larger counterions such as triflate is illustrated by the formation of a one-dimensional tubular structure (**55**). Protonation of the pendant amino residue and complexation of the remaining *equatorial* amino groups to zinc(II) chloride forms a one-dimensional zig-zag chain (**56**). Further studies will include exploiting the *cis*/*trans* geometry of *trans*-tach by extending the coordination sites away from the backbone in order to enlarge the channels observed in both the three-dimensional network and in the one-dimensional tubular structure.

4.2 Supramolecular architectures

Investigation into the coordination behaviour of the ligand with open shell transition metals leads primarily to discrete mono- or diligand complexes upon conformational change to the bis*axial*-mono*equatorial* binding motif. Several diligand species have been characterized, including elucidation of the [Ni(*trans*-tach)$_2$](NO$_3$)$_2$ (**34**) structure, which has been used as a method of separating the *cis* and *trans* isomers since 1968. Both *syn* and *anti* diligand arrangements with respect to the non-coordinating monodentate amino groups are observed upon reaction with Cu(NO$_3$)$_2$ (**36**), CuCl$_2$ (**41**), CuBr$_2$ (*syn*-**38**, *twist*-**38**, **39**), CuF$_2$ (**44**) and CuSO$_4$ (**46**). Protonation of these complexes forms an interesting variety of secondary

structures. Both $Cu(NO_3)_2$ (**37**) and $CuBr_2$ (**40**) diligand species fragment to form monoligand, mononuclear species upon protonation with HNO_3 and HBr, respectively.

Protonation of $CuCl_2$ and $CuBr_2$ diligand complexes with HCl, on the other hand, also results in fragmentation to monoligand units but effects the formation of trinuclear arrays (**42** and **43**). These structures make use of a trigonal planar μ_3-chloro ligand, around which three mononuclear [Cu(*trans*-tachH)Cl_2] units assemble (Figure 102, *Left*). These are the first structures reported in which trigonal planar μ_3-chloro coordination to open shell transition metals is observed. Furthermore, hydrogen-bonded interactions aggregate the trinuclear copper(II) units into 1-D chains. Protonation of the CuF_2 complex leads to the self-assembly of the first known copper fluoro cubane (**45**). Each cubane is constructed from four monoligand copper fluoro units, resulting in a discrete tetranuclear structure. These units form a three-dimensional nanoporous cubic network due to hydrogen-bonded interactions between the protonated pendant amino residues and the fluoride counterions that are incorporated within the network structure, leaving 11 Å voids in all three dimensions (Figure 102, *Centre*). Contrary to the above complexes, protonation of the $CuSO_4$ complex maintains the *syn* diligand arrangement around the copper centre with the pendant amino groups protonated (**46** • H_2SO_4). These protonated amines form strong hydrogen-bonded interactions resulting in a three-dimensional array, comprising one-dimensional channels of 15 Å diameter with the sulphate counterions incorporated into the network structure (Figure 102, *Right*).

The three supramolecular architectures formed upon hydrogen-bonded interactions in complexes (**42**, **43**), **45** and **46** • H_2SO_4 (Figure 102) can be analysed by gradually building up the nanoporous network structures from elementary building units (**45** and **46** • H_2SO_4, 'Bottom up' construction). This is illustrated by increasing the complexity upon assembly of the networks (Figure 102, *Centre* and *Right*). The hexagonal architecture formed by **42** and **43** can be analysed by separating the building units from the network ('Top down' approach, Figure 102, *Left*). Initial studies have shown all three networks to exhibit interesting magnetic properties. Further work will extend the magnetic and electrochemical analyses on these systems. The main focus in this thesis has been laid on the investigation of the solid state structures obtained upon reaction with transition metal salts. Further work will include solution state studies, particularly with respect to speciation of complexes with labile transition metal ions.

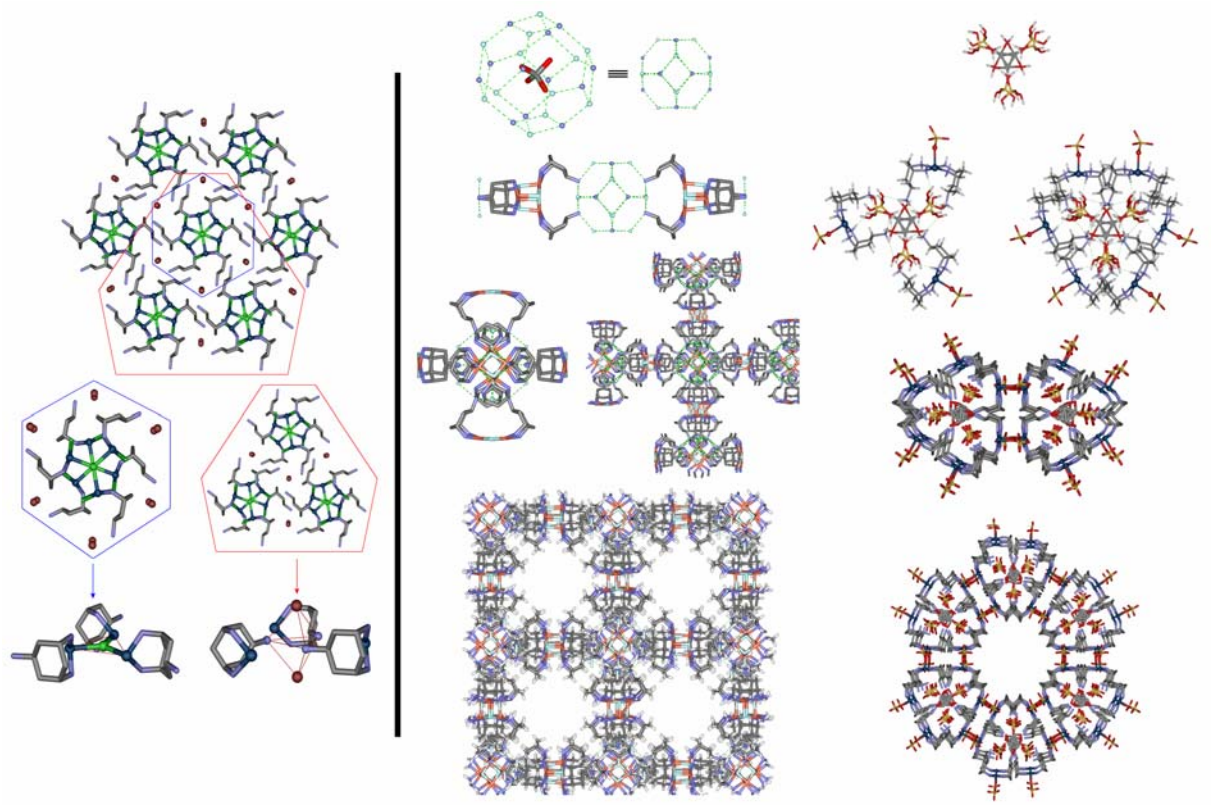


Figure 102 An overview of hydrogen-bonded supramolecular architectures is shown. *Left*: 'Top down' approach of the network formed by **42** and **43**. *Centre*: 'Bottom up' construction of the three-dimensional nanoporous network formed by **45**. *Right*: 'Bottom up' construction of the one-dimensional nanoporous network formed by (**46** · H_2SO_4).

4.3 Building block approach

In contrast to the labile open shell transition metals, palladium(II) coordination exhibits kinetic inertness and a preference for square planar coordination geometry. Reaction of *trans*-tach and palladium(II) chloride forms the fundamental mononuclear building block **47** that is amenable for use in the formation of a number of secondary structures by virtue of versatile coordination around the palladium(II) centre. All possible coordination motifs have been realised ('Tail' representing the mono*equatorial* monodentate, 'Head' the bis*axial* bidentate, coordination sites). Under a variety of reaction conditions, **47** acts as a building block to facilitate the formation of the different coordination motifs (Figure 103). Strongly alkaline conditions lead to the removal of the chloro ligands and to the formation of the mononuclear 'Head to Head' complex **49**. High temperature crystallisation in the presence of

tetrachloropalladate ions from the mother liquor facilitates the formation of the trinuclear 'Tail to Tail' complex **53**. Removal of the tetrachloropalladate ions from the mother liquor by ion exchange and subsequent neutralisation forms the 'Head to Tail' coordination observed in the hexanuclear metallamacrocycle **51**.[164]

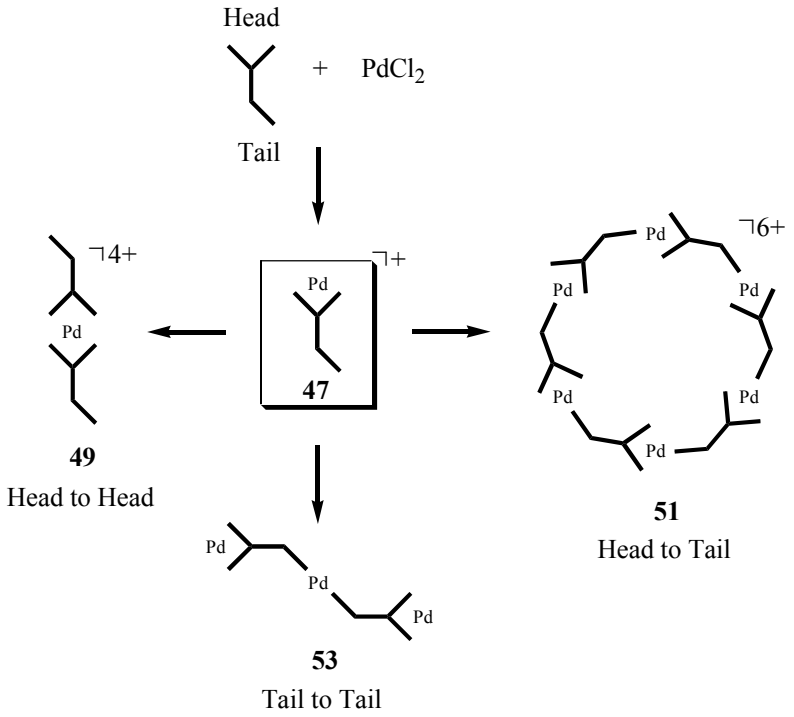


Figure 103 Reaction of *trans*-tach with palladium(II) chloride results in complex **47** which can further react to form 'Head to Head' complex **49**, 'Head to Tail' complex **51** or 'Tail to Tail' complex **53**. The Pd(II) centres are square planar and the remaining coordination sites are occupied by chloro ligands.

In addition to the variety of complexes based on **47**, the corresponding di*bromo* complex **48** is proven to act as an identical building block in the formation of the hexanuclear 'Head to Tail' complex **52**. The use of *trans*-tach in self-assembly processes will be further studied and expanded to other inert metal ions such as platinum(II).

4.4 Schiff base derivatives of trans-tach

Further to complexation investigations of the simple building block *trans*-tach, studies have been made into broadening the use of its *cis/trans* geometry by designing ligands which extend the coordination vectors away from the rigid backbone. Reaction of *trans*-tach with aromatic aldehydes allows such extension by Schiff base formation, as exemplified by

reaction with pyridine-2-carboxaldehyde in the formation of ttop (**59**). A tetradentate coordination pocket is formed upon ring-flip to the bis*axial*-mono*equatorial* conformation, providing a stable coordination environment in which suitable metals can reside. This is illustrated in this work by the binding of copper(II) (**61** and **62**) and zinc(II) (^{1}H-NMR titration) ions. The presence of the *trans* bidentate binding site allows the coupling of two chelate-coordinated complexes by interaction of the metals residing in these sites *via* μ_2 bridging chloro ligands. Further work will include the synthesis of a variety of Schiff base ligands based on *trans*-tach that can form heterometallic complexes, in order to investigate their magnetic and electrochemical properties.

4.5 Analogues of trans-tach

Future work will investigate the possibility of extending the influence of the *cis*/*trans* geometry to other systems. Based on a rigid cyclohexane backbone with three donor groups in *cis*,*trans*-1,3,5 position, a variety of homoleptic and heteroleptic ligands can be formed. Due to functional differences, it is anticipated that distinction between the *cis*- and *trans*- binding sites will be possible. Combination of the four donor atoms N, O, S and P, for example, leads to a library of ligands with different binding properties (Figure 104). Considering that the all-amino variation, *trans*-tach, has proven to be extremely versatile in its use as a supramolecular building block, this library represents great potential for the formation of supramolecular architectures.

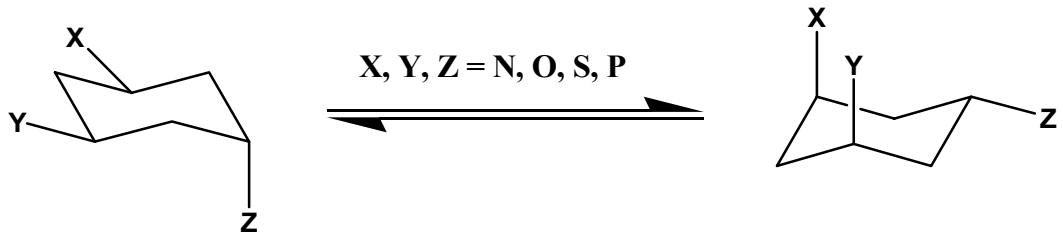


Figure 104 Combinations of the four donor atoms N, O, S and P on *cis,trans*-1,3,5 trisubstituted cyclohexane ring systems leads to a library of ligands with different binding properties: X=Y=Z, X=Y≠Z, X≠Y=Z, X≠Y≠Z.

In summary, a variety of interesting and novel structures have been formed from *cis,trans*-1,3,5-triaminocyclohexane. The simplicity of the ligand system combined with the complexity of the resulting architectures illustrate the potential of *trans*-tach as a new building block in organometallic, supramolecular chemistry.

5 EXPERIMENTAL

5.1 Materials

Gases and liquid ammonia were supplied by *B.O.C. Ltd.* and were of commercial grade and used without further purification. Solvents for synthesis (AR grade) were supplied by *Fisher Chemicals* and *Riedel-de Haen* and were also used without further purification. Reactions in water were conducted using HPLC grade water. Deuterated solvents were obtained from *Aldrich Chemical Company Ltd.* and *Avocado Research Supply*. All other reagents were supplied by *Aldrich Chemical Company Ltd.*, *Fisher Chemicals*, *Lancaster Chemicals Ltd.* or *BDH Laboratory supplies* and used without further purification.

5.2 Instrumentation

When required, syntheses were carried out using standard Schlenk line techniques under nitrogen (oxygen free, dried over calcium chloride). The following instruments were used for all analytical and spectroscopic measurements:

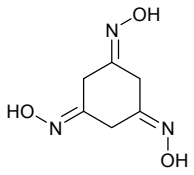
Kugelrohr distillation:	Büchi Glass Oven B-580; the cited temperature was recorded using the internal thermo element.
Melting point:	Electrothermal IA 9000 digital melting point apparatus. The given temperatures are uncorrected.
pH measurements:	Hanna Instruments HI 9025C microcomputer pH meter (HI 1230 pH electrode, HI 7669/2W temperature probe).
Elemental analysis:	EA 1110 CHNS, CE-440 Elemental Analyser and University of North London laboratory.
Mass spectrometry:	Kratos Kompact MALDI III; (ES) LCT Micromass TOF; (LSIMS) Micromass Zabspec; (CI / EI) Micromass Prospec; values in % to basis peak, assignment of main isotope of each element.
FT-IR spectroscopy:	Shimadzu FTIR-8300 Fourier Transform Infrared Spectrophotometer and Jasco FTIR-410 spectrometer using a *Golden Gate* setting for solid material; wave numbers (ν) in cm^{-1}; intensities denoted as (vs = very strong, s = strong,

	m = medium, w = weak, b = broad).
UV-Vis spectroscopy:	Shimadzu UV-3101PC UV-VIS-NIR Scanning Spectrophotometer (wavelength (λ) in nm, molar absorption coefficient (ε) $M^{-1} \cdot cm^{-1}$).
NMR spectroscopy:	Bruker DRX-500 (500 MHz ^{1}H, 125 MHz ^{13}C); DPX-400, Avance-400 (400 MHz ^{1}H, 100 MHz ^{13}C); AC-300, AV-300 (300 MHz ^{1}H, 75 MHz ^{13}C).
Single X-ray crystallography:	Bruker SMART AXS (Cu-K_α), Rigaku R-axis (Mo-K_α) and Nonius Kappa-CCD (Mo-K_α) diffractometer.
PXRD	Siemens D5000 Kristalloflex diffractometer.

Simulations of powder XRD spectra from single crystal X-ray data were performed using the program suite Powdercell.[236] All NMR spectra were recorded at room temperature unless otherwise stated. Chemical shifts are reported using the δ-scale, referenced to the residual solvent protons in the deuterated solvent for ^{1}H- and ^{13}C-NMR. The coupling constants (J) are reported in Hz as absolute values. Characterisation of spin multiplicities: s = singlet, d = doublet, t = triplet, q = quartet, quint = quintet, m = multiplet, b = broad, *p* = pseudo.

5.3 Synthesis

5.3.1 1,3,5-Cyclohexanetrionetrioxime (chtt, 31)

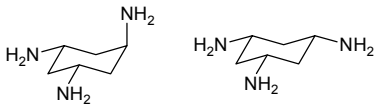


31

1,3,5-Trihydroxybenzene (anhydrous phloroglucinol, **32**, 18.58 g, 0.15 mol) and anhydrous potassium carbonate (58.37 g, 0.42 mol) were dissolved in water (450 ml) and heated gently until full dissolution. During heating, the solution turned from light violet to brown. The flask was then covered with aluminium foil and hydroxylamine hydrochloride (54.34 g, 0.78 mol) was added to the solution and stirring in the dark was continued for 4 hours. After this time a grey powder precipitated, which was filtered off (D3 sinter funnel) and washed with water

(400 ml) then acetone (200 ml) until the filtrate ran colourless. Drying in air over night yielded **31** as a grey powder.[157] Discolouration to a dark brown solid was observed over a period of a few days, and the product was therefore stored for a maximum of two days under nitrogen at 4 °C, and covered with aluminium foil prior to storage. Yield 16.85 g (0.10 mol, 66%). M.p. 135-136°C, 150 °C explosive decomposition! IR (Golden Gate) ν /cm^{-1} 3500-2500(s), 1670(s), 1470(s), 1420(s), 1380(s), 1120(s), 1000(s), 960(s), 940(s), 850(s), 820(s), 700(s), 620(s), 520(s).

5.3.2 1,3,5-Triaminocyclohexane (tach, 29 and 30)



29 **30**

In a three-necked, 5 l flask equipped with a cold finger (cooled with dry ice-acetone), overhead stirrer and ammonia inlet, chtt (**31,** 12.0 g, 0.07 mol) was dissolved in liquid ammonia (800 ml). Absolute ethanol (90 ml) was added to the ammonia solution followed by thinly sliced sodium (29.3 g, 1.28 mol), during which the vessel was continuously cooled in a dry ice-acetone bath (-78°C). After addition, the sodium dissolved, turning the ammonia solution from pale yellow to a deep blue colour. The reaction was initiated by lowering the cooling bath. The resulting exothermic reaction was continuously monitored and controlled by re-applying the bath and continuously stirring (caution!). When the reaction had started, vigorous bubbling occurred and after 15 minutes the blue ammonia solution turned white. Additional liquid ammonia (200 ml) was added to redissolve the material that had accumulated at the top of the flask. Water (25 ml) was added cautiously to the ammonia solution after 10 minutes and stirred for another 5 minutes. The mixture was filtered through a buechner funnel using suction filtration, followed by gravity filtration to remove all solids. The ammonia of the filtrate was reduced by evaporation at room temperature, yielding a dry brownish residue. This residue was made strongly alkaline with sodium hydroxide (7 g) and extracted with ether (800 ml) for 3 hours.

In parallel all solids from the filtrations were combined and washed thoroughly with ether (800 ml) in the presence of sodium hydroxide (5 g). The filtrate from subsequent suction filtration was stirred with sodium hydroxide (7 g) for 3 hours.

Both mixtures were then filtered again and the colourless filtrates combined. Reduction of the ether solution *in vacuo* afforded a crude brown oil containing both tach-isomers (**29** and **30**), which was taken up in methanol (20 ml). The subsequent isolation of the *trans*-tach was achieved using two different synthetic procedures:

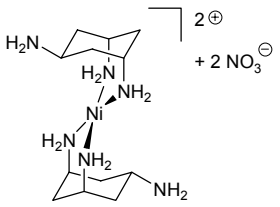
1) A standard solution of nickel(II) nitrate (9 g in 250 ml methanol) was added dropwise over a period of 2 hours. During the addition, a pink precipitate formed and was filtered off, washed with ethanol and ether and dried in air to give the Ni-*bis*(*cis*-tach)nitrate complex (**33**). Further addition of nickel(II) nitrate solution led to an orange precipitate of crude Ni-*bis*(*trans*-tach)nitrate (**34**) which was also washed with ethanol and ether and dried in air.

Yield: 2.973 g (6.74 mmol, 19 %), Ni-*bis*(*cis*-tach)nitrate (**33**)
4.487 g (10.17 mmol, 29 %), Ni-*bis*(*trans*-tach)nitrate (**34**)
48 %, Total

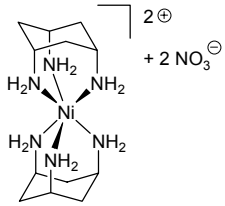
2) In this second procedure, *cis*-tach was isolated by the formation of the Ni-*bis*(*cis*-tach)nitrate (**33**) as described above. However, after all **33** had precipitated, only a small addition of nickel(II)nitrate was used to initiate precipitation of the Ni-*bis*(*trans*-tach)nitrate (**34**). Cooling overnight, followed by removal of any precipitation of **34**, and reduction of the mother liquor yielded the remaining uncomplexed *trans*-tach (**29**). Purification was achieved by kugelrohr distillation (131 °C, 1 mbar).

Yield: 3.195 g (7.24 mmol, 20 %), Ni-*bis*(*cis*-tach)nitrate (**33**)
0.355 g (0.80 mmol, 2 %), Ni-*bis*(*trans*-tach)nitrate (**34**)
2.340 g (18.11 mmol, 25 %), *trans*-tach (**29**)
47 %, Total

5.3.2.1 Isolation of cis- and trans- tach isomers from its nickel(II) complexes 34 and 33

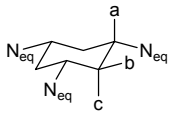


34

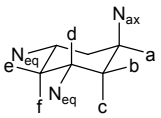


33

The pink Ni-*bis*(*cis*-tach)nitrate (**33,** 2.12 g, 4.81 mmol) and the orange Ni-*bis*(*trans*-tach)nitrate (**34,** 1.87 g, 4.24 mmol) were treated with concentrated hydrochloric acid (100 ml) to decompose the metal complexes. After dissolving and stirring for half an hour, ethanol (250 ml) was added and both *trans*-tach • 3 HCl and *cis*-tach • 3 HCl precipitated as white solids from their corresponding solutions. The solids were filtered off, washed with ethanol (100 ml) and ether (100 ml) and dried in air to give **29** and **30** as *tris*-hydrochloride salts. Analysis of



30 • 3 HCl: Yield 2.18 g (9.16 mmol, 96 %). M.p. >300 °C (sublimation). ^{1}H-NMR (300 MHz, D_2O) δ /ppm 3.41 (tt, 3H, *J* 12.2, 3.5 Hz; $\underline{H}_a$), 2.38 (dt, 3H, *J* 12.2, 3.5 Hz; $\underline{H}_b$), 1.55 (q, 3H, *J* 12.2 Hz; $\underline{H}_c$). ^{13}C-NMR (75 MHz, D_2O) δ /ppm 48.02 (3x$\underline{C}H_2$), 35.12 (3x$\underline{C}$H). IR (Golden Gate) ν /cm^{-1} 3000(s), 2050(s), 1600(m), 1480(s), 1400(s), 1390(m), 1210(s), 1000(w), 887(w).



Analysis of **29** • 3 HCl: Yield 1.94 g (8.14 mmol, 96 %). M.p. 180 °C, 1 mbar (sublimation). ^{1}H-NMR (300 MHz, D_2O) δ /ppm 4.00 (t, 1H, *J* 3.3 Hz, $\underline{H}_a$), 3.65 (tt, 2H, *J* 12.3, 3.0 Hz; $\underline{H}_d$), 2.45 (dt, 1H, *J* 12.3, 3.0 Hz; $\underline{H}_e$), 2.30 (dd, 2H, *J* 12.3, 3.0 Hz; $\underline{H}_b$), 1.90 (td, 2H, *J* 12.3, 3.3 Hz; $\underline{H}_c$), 1.65 (q, 1H, *J* 12.3 Hz; $\underline{H}_f$). ^{13}C-NMR (125 MHz, D_2O) δ /ppm 48.06 ($\underline{C}H_a$), 46.62 ($\underline{C}H_{e,f}$), 45.80 (2x$\underline{C}H_d$), 42.59 (2x$\underline{C}H_{b,c}$). IR (Golden Gate) ν /cm^{-1} 2870(s), 2781(s), 2550(m), 1605(m), 1520(m), 1408(m), 1331(w), 1204(w), 1006(w), 994(w), 910(w), 883(w),

660(w). Elemental analysis for $C_6H_{18}Cl_3N_3$, found (expected) %: C 29.97 (30.20), H 7.70 (7.60), N 17.19 (17.61).

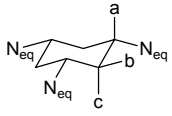
Two different approaches were adopted to isolate the amines in their deprotonated forms from the corresponding *tris*-hydrochloride salts **29** • 3 HCl and **30** • 3 HCl:

1) *Ion exchange resin (2 cm x 22 cm):* A strongly basic *Dowex 1-X8* (20-50 mesh) column was prepared by washing with water (800 ml), activating the column with 4M sodium hydroxide solution (800 ml, T < 40°C) and washing again with water until eluent is neutral (ca. 800 ml). The *tris*-hydrochloride salt (**29** • 3 HCl or **30** • 3 HCl) was then dissolved in water (3 ml) by ultrasonication and sorbed onto the ion exchange column. The column was eluted with water until the eluent became alkaline, at which point the collection started until the pH of the eluent became neutral again (ca. 250 ml water). The water was removed under reduced pressure and the resulting solid (**30**) / oil (**29**) taken up in methanol and filtered. The solvent was then removed *in vacuo* and the *cis*-tach (**30**) sublimed at a pressure of 10^{-2} mbar and a temperature of 70 °C onto a cold finger cooled to –78°C. The product was then removed as a white crystalline solid. The *trans*-tach (**29**) was distilled *in vacuo* in a kugelrohr distillation apparatus at a pressure of 10^{-1} mbar at 131 °C, resulting in colourless viscous oil.

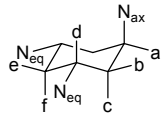
Yield: *cis*-tach (**30**), **51 %**
trans-tach (**29**), **62 %**

2) *Sodium hydroxide in methanol:* The *tris*-hydrochloride salt (**29** • 3 HCl or **30** • 3 HCl) was suspended in methanol and a methanolic solution containing four equivalents of sodium hydroxide was added. The solutions were stirred until full dissolution and filtered. The methanol was removed *in vacuo* resulting in a slightly pink solid. Following the isolation procedures above, the *cis*-tach (**30**) was sublimed and the *trans*-tach (**29**) was distilled.

Yield: *cis*-tach (**30**), **92 %**
trans-tach (**29**), **96 %**

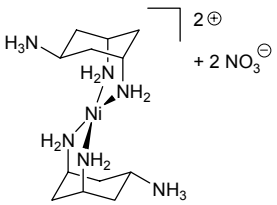


Analysis of **30**: M.p. 70 °C, 10^{-2} mbar (sublimation). ^{1}H-NMR (300 MHz, D_2O) δ /ppm 2.66 (tt, 3H, *J* 11.4, 3.5 Hz; $\underline{H}_a$), 1.86 (dt, 3H, *J* 11.4, 3.5 Hz; $\underline{H}_b$), 0.80 (q, 3H, *J* 11.4 Hz; $\underline{H}_c$). ^{13}C-NMR (75 MHz, D_2O) δ /ppm 45.82 (3x$\underline{C}H_2$), 41.40 (3x$\underline{C}H$). IR (Golden Gate) ν /cm^{-1} 3277(bm), 3190(bm), 2920(s), 2853(s), 1597(s), 1460(s), 1373(m), 1146(s), 974(w), 856(w), 671(bm). MS (CI) *m/z* 130 (M^++1).



Analysis of **29**: B.p. 131 °C, 1 mbar. ^{1}H-NMR (300 MHz, D_2O) δ /ppm 3.21 (quint, 1H, *J* 3.2 Hz, $\underline{H}_a$), 2.88 (tt, 2H, *J* 11.8, 3.7 Hz; $\underline{H}_d$), 1.89 (dtt, 1H, *J* 11.8, 3.7, 2.2 Hz; $\underline{H}_e$), 1.65 (*p*dd, 2H, *J* 11.8, 3.7, 3.2, 2.2 Hz; $\underline{H}_b$), 1.14 (td, 2H, *J* 11.8, 3.2 Hz; $\underline{H}_c$), 0.79 (q, 1H, *J* 11.8 Hz; $\underline{H}_f$). ^{13}C-NMR (75 MHz, D_2O) δ /ppm 48.26 ($\underline{C}H_{e,f}$), 46.86 ($\underline{C}H_a$), 45.97 ($\underline{C}H_{b,c}$), 42.84 ($\underline{C}H_d$). IR (Golden Gate) ν /cm^{-1} 3344(bm), 3279(bm), 3190(bm), 2924(s), 2851(s), 1589(s), 1458(m), 1377(m), 1339(w), 1269(w), 1030(w), 953(w). MS (CI) *m/z* 130 (M^++1). Elemental analysis for $C_6H_{15}N_3$ • 0.6 CH_3OH, found (expected) %: C 52.88 (53.41), H 11.86 (11.82), N 28.26 (28.31).

5.3.3 [*anti-bis*(*cis,trans*-1,3,5-Triaminocyclohexane-κ^2-N,N')-nickel(II)] dinitrate (34)

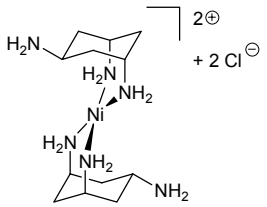


34

A methanolic solution (3 ml) of nickel(II) nitrate hexahydrate (48 mg, 0.17 mmol) was added to a solution of *trans*-tach (**29**, 40 mg, 0.31 mmol) in methanol (2 ml) giving an instant colour change from colourless to orange. Upon stirring, an orange precipitate of **34** was formed. Filtration and subsequent washing with ether yielded **34** as an orange powder. Crystallisation of the filtrate by slow evaporation of the solvent resulted in orange crystals of its *bis*-protonated form **34** • 2 HNO_3 suitable for X-ray analysis. Yield 4 mg (0.01 mmol, 5 %) crystals, 48 mg (0.11 mmol, 64 %) amorphous solid. M.p. 220 °C (dec.). IR (Golden Gate)

ν /cm^{-1} 3248-3116(bw), 2928(w), 1605(w), 1323(vs), 1207(s), 1130(s), 926(s), 883(s), 825(s), 760(m). UV/Vis (MeOH) $\lambda(\varepsilon)$ /nm(M^{-1}·cm^{-1}) 207 (30164), 466 (54). MS (ES-TOF+) *m/z* (%) 560 (31, $[Ni_2(tach)_2(NO_3)_3]^+$), 533 (11), 249 (100, $[Ni(tach)(NO_3)]^+$). Elemental analysis for $C_{12}H_{30}N_8NiO_6$, found (expected) %: C 32.89 (32.67), H 6.87 (6.86), N 25.31 (25.40).

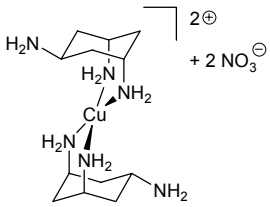
5.3.4 [*anti-bis*(*cis,trans*-1,3,5-Triaminocyclohexane-κ^2-N,N')-nickel(II)] dichloride (35)



35

A methanolic solution (10 ml) of nickel(II) chloride hexahydrate (69 mg, 0.29 mmol) was added to a solution of *trans*-tach (**29,** 75 mg, 0.58 mmol) in methanol (15 ml) giving an instant colour change from colourless to orange. Reducing the volume to 5 ml and crystallisation by slow diffusion of ether resulted in orange crystals of **35** suitable for single crystal X-ray analysis. Removal of crystals and addition of ether (10 ml) precipitated amorphous orange powder of **35**, which was filtered off and dried in air. Yield 10 mg (0.03 mmol, 9 %) crystals, 74 mg (0.19 mmol, 66 %) amorphous solid. M.p. 220 °C (dec.). IR (Golden Gate) ν /cm^{-1} 3414-3341(bm), 3155-3074(bs), 2924(s), 1570(s), 1458(s), 1369(s), 1219(s), 1191(s), 1119(s), 1069(s), 937(s), 764(s), 733(s). UV/Vis (MeOH) $\lambda(\varepsilon)$ /nm (M^{-1}·cm^{-1}) 228 (2976), 282 (497), 466 (50). MS (FAB, NOBA matrix) *m/z* (%) 353 (72, $[Ni(tach)_2Cl]^+$).

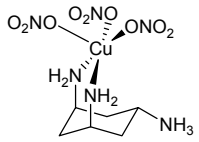
5.3.5 [*anti-bis*(*cis,trans*-1,3,5-Triaminocyclohexane-κ^2-N,N')-copper(II)] dinitrate (36)



36

A methanolic solution (10 ml) of copper(II) nitrate trihydrate (46 mg, 0.19 mmol) was added to a solution of *trans*-tach (**29,** 43.93 mg, 0.34 mmol) in methanol (10 ml) giving an instant colour change from colourless to dark violet. After stirring over night and reducing the volume by half, a violet, amorphous precipitate of **36** was formed. Filtration yielded **36** as a violet powder. Crystallisation of the filtrate by slow diffusion of ether resulted in red crystals of **36** • 0.5 HNO_3 suitable for single crystal X-ray analysis. Yield 5 mg (0.01 mmol, 5 %) crystals, 32 mg (0.07 mmol, 38 %) amorphous solid. M.p. 120 °C (dec.). IR (Golden Gate) ν /cm^{-1} 3240(s), 3140(s), 2927(w), 1601(s), 1335(vs), 1184(bs), 1061(s), 918(s), 825(m), 682(bs). UV/Vis (MeOH) $\lambda(\varepsilon)$ /nm ($M^{-1}\cdot cm^{-1}$) 243 (4827, shoulder), 330 (1317, minimum), 355 (1752), 551 (102). MS (ES-TOF+) m/z (%) 570 (10, $[Cu_2(tach)_2(NO_3)_3]^+$), 508 (30, $[Cu_2(tach)_2(NO_3)_2]^+$), 444 (52, $[Cu(tach)_2(NO_3)_2]^+$), 254 (100, $[Cu(tach)(NO_3)]^+$). Elemental analysis for $C_{12}H_{30}N_8CuO_6$ • 2 H_2O, found (expected) %: C 29.69 (29.90), H 6.83 (7.11), N 23.28 (23.25).

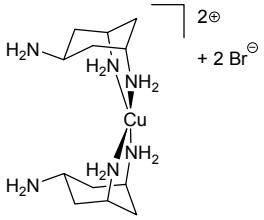
5.3.6 [*tris*-Nitrato-(*cis,trans*-1,3,5-triaminocyclohexane-κ^2-N,N')-copper(II)] (37)



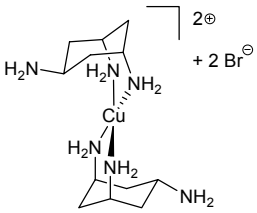
37

A methanolic solution (3 ml) of copper(II) nitrate trihydrate (79 mg, 0.33 mmol) was added to a solution of *trans*-tach (**29,** 83 mg, 0.64 mmol) in methanol (30 ml) previously adjusted to pH 6.5 with 2M nitric acid, giving an instant colour change from colourless to light blue. Reducing the volume to 3 ml and crystallisation by diffusion of ether resulted in dark blue crystals of **37** suitable for single crystal X-ray analysis. Yield 44 mg (0.12 mmol, 35 %). IR (Golden Gate) ν /cm^{-1} 3287(w), 3236(m), 3152(w), 2890(w), 1674(m), 1589(m), 1454(s), 1404(s), 1362(s), 1304(vs), 1277(vs), 1218(m), 1200(m), 1165(s), 1134(w), 1083(w), 1022(s), 926(m), 895(m), 810(m), 740(w), 714(w), 679(m), 648(m), 606(w), 575(m). MS (ES-TOF+): *m/z* (%) $[M]^+$ not observed, 570 (30, $[Cu_2(tach)_2(NO_3)_3]^+$), 254 (100, $[Cu(tach)(NO_3)]^+$).

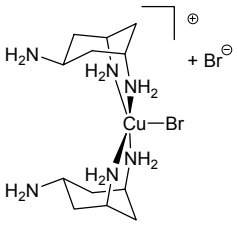
5.3.7 [*syn-bis*(*cis,trans*-1,3,5-Triaminocyclohexane-κ^2-N,N')-copper(II)] dibromide (*syn*-38), [*bis*(*cis,trans*-1,3,5-triaminocyclohexane-κ^2-N,N')-copper(II)] dibromide (*twist*-38) and [bromo-*syn*-*bis*(*cis,trans*-1,3,5-triaminocyclohexane-κ^2-N,N')-copper(II)] bromide (39)



***syn*-38**



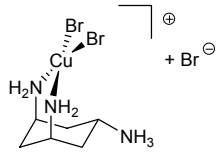
***twist*-38**



39

A methanolic solution (3 ml) of copper(II) bromide (48 mg, 0.22 mmol) was added to a solution of *trans*-tach (**29**, 56 mg, 0.54 mmol) in methanol (20 ml) giving an instant colour change from colourless to dark violet. Reducing the volume to 2 ml and filtration through cotton wool resulted in a dark violet filtrate. Crystallisation by *diffusion* of ether resulted in violet crystals of *syn*-**38** and **39** suitable for single crystal X-ray diffraction. However, crystallisation by *layering* ether results in the formation of very unstable dark blue crystals of *twist*-**38** (suitable for single crystal X-ray analysis), which form after one hour of crystallisation, but redissolve within another 2-3 hours and could not be isolated. Violet crystals of *syn*-**38** and **39** were formed over night under these crystallisation conditions. Both *syn*-**38** and **39** were isolated as inseparable crystalline material in a 1:1 ratio as estimated by multiple unit cell measurements. Yield (*syn*-**38** and **39**) 66 mg (0.14 mmol, 62 %). M.p. 200°C (dec.). IR (Golden Gate) ν /cm^{-1} 3425(m), 3198(m), 3109(m), 2920(m), 1597(s), 1578(s), 1528(w), 1458(s), 1396(m), 1346(s), 1177(m), 1157(vs), 1110(s), 1065(s), 1045(m), 918(vs), 880(m), 775(s), 760(s), 698(s), 664(s), 629(s), 601(s). MS (ES-TOF+): m/z (%) $[M]^+$ not observed, 625 (100, $[Cu_2(tach)_2Br_3]^+$), 563 (10), 482 (61, $[Cu(tach)_2Br_2]^+$), 463 (30, $[Cu_2(tach)_2Br]^+$), 402 (41, $[Cu(tach)_2Br]^+$), 334 (29, $[Cu_2(tach)Br]^+$), 273 (86, $[Cu(tach)Br]^+$), 209 (11), 191 (11, $[Cu(tach)]^+$).

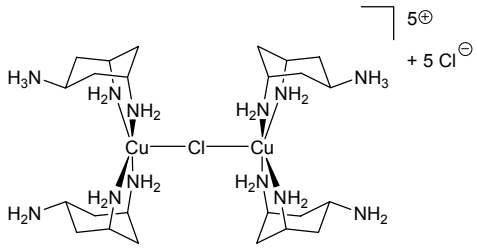
5.3.8 [Dibromo-(*cis,trans*-1,3,5-triaminocyclohexane-κ^2-N,N')-copper(II)] bromide (40)



40

A methanolic solution (3 ml) of copper(II) bromide (117 mg, 0.52 mmol) was added to a solution of *trans*-tach (**29,** 130 mg, 1.03 mmol) in methanol (30 ml) previously adjusted to pH 6.5 with 2M hydrobromic acid, giving an instant colour change from colourless through blue to green after half an hour. Upon stirring, **40** precipitated as a green solid. Dissolution in methanol and crystallisation by layering with ethanol resulted in dark green crystals of **40** suitable for single crystal X-ray analysis. The identity of amorphous and crystalline **40** was established by powder X-ray diffraction and comparison to the simulated powder XRD spectrum of crystalline **40**.[236] Yield 152 mg (0.35 mmol, 67 %). IR (Golden Gate) ν /cm^{-1} 3521(w), 3352(w), 3248(m), 3153(m), 3109(m), 3028(m), 2912(m), 1597(m), 1562(s), 1501(s), 1385(w), 1335(m), 1290(m), 1255(m), 1169(vs), 1130(s), 1103(s), 1042(s), 1006(m), 984(m), 914(vs), 895(s), 876(m), 779(s), 751(m), 679(s), 637(s). MS (ES-TOF+): *m/z* (%) $[M]^+$ not observed, 625 (40, $[Cu_2(tach)_2Br_3]^+$), 482 (8, $[Cu(tach)_2Br_2]^+$), 273 (100, $[Cu(tach)Br]^+$). Elemental analysis for $C_6H_{16}Br_3CuN_3$, found (expected) %: C 16.95 (16.62), H 3.86 (3.72), N 9.63 (9.69).

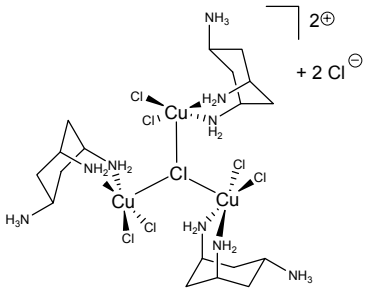
5.3.9 [(μ$_2$-Chloro)-di-{*syn-bis*(*cis,trans*-1,3,5-triaminocyclohexane-κ^2-N,N')-copper(II)}] trichloride dihydrochloride (41 · 2 HCl)



41 · 2 HCl

A methanolic solution (15 ml) of copper(II) chloride anhydrous (58 mg, 0.43 mmol) was added to a solution of *trans*-tach (**29,** 110 mg, 0.85 mmol) in methanol (25 ml) giving an instant colour change from colourless to dark blue. Reducing the volume to 2 ml and crystallisation by diffusion of ether yielded dark blue crystals of **41** • 2 HCl suitable for single crystal X-ray analysis. Amorphous material was obtained by addition of ether (10 ml) and filtration. Yield 14 mg (0.02 mmol, 10 %) crystals, 54 mg (0.08 mmol, 37 %) amorphous solid. M.p. 195 °C (dec.). IR (Golden Gate) ν /cm^{-1} 3217(s), 3116(s), 2920(m), 1609(s), 1558(s), 1458(s), 1346(s), 1165(s), 1119(m), 918(s). UV/Vis (MeOH) $\lambda(\varepsilon)$ /nm (M^{-1}·cm^{-1}) 247 (3235), 301 (1822, shoulder), 328 (1070, minimum), 355 (1518), 352 (442), 571 (106). MS (ES-TOF+) *m/z* (%) 491 (100, $[Cu_2(tach)_2Cl_3]^+$), 419 (5, $[Cu_2(tach)_2Cl\text{-}2H]^+$), 356 (8, $[Cu(tach)_2Cl]^+$), 290 (32, $[Cu_2(tach)Cl\text{-}2H]^+$), 227 (33, $[Cu(tach)Cl]^+$). Elemental analysis for $C_{24}H_{60}Cl_4Cu_2N_{12}$ • 2 HCl • H_2O, found (expected) %: C 33.36 (32.88), H 8.09 (7.36), N 18.88 (19.17).

5.3.10 [(μ$_3$-Chloro)-*tris*{dichloro-(*cis,trans*-1,3,5-triaminocyclohexane-κ^2-N,N')-copper(II)}] dichloride (42)



42

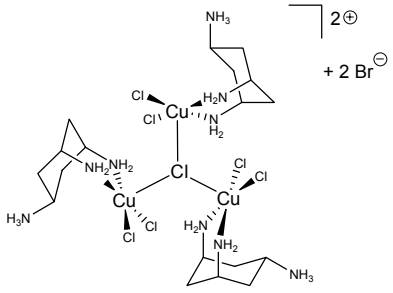
a) A methanolic solution (5 ml) of copper(II) chloride anhydrous (66 mg, 0.49 mmol) was added to a solution of *trans*-tach (**29**, 62 mg, 0.48 mmol) in methanol (30ml) previously adjusted to pH 6.5 using 2M hydrochloric acid, giving an instant colour change from colourless to light blue. The mixture was stirred for three hours and the light blue precipitate of **42** was collected by filtration.

b) Crystals suitable for single crystal X-ray analysis were grown from reaction of copper(II) chloride anhydrous and *trans*-tach (1 : 2 stoichiometric ratio) in otherwise identical reaction

conditions as described above (Note: 0.2M HCl was used to adjust the pH to 6.5). Reducing the volume to 2 ml and crystallisation by diffusion of acetone yielded **42** as light blue crystals.

The identity of the powder material obtained from a) and the crystalline material was established by powder X-ray diffraction of the microcrystalline solid and simulation of the powder XRD spectrum from the single crystal X-ray data.[236] Yield 46 mg (0.05 mmol, 32 %). IR (Golden Gate) ν /cm^{-1} 3287(m), 3225(m), 3152(m), 3128(m), 3036(m), 2939(m), 2835 (bm), 1597(vs), 1555(w), 1528(vs), 1458(vs), 1408(w), 1358(m), 1342(s), 1319(w), 1285(w), 1169(vs), 1123(vs), 1076(m), 1045(s), 1015(m), 910(vs), 891(s), 783(w), 756(w), 687(vs), 613(w), 571(w). MS (ES-TOF+): *m/z* (%) $[M]^+$ not observed, 227 (25%, $[Cu(tach)Cl]^+$), 290 (8, $[Cu_2(tach)Cl]^+$), 356 (10, $[Cu(tach)_2Cl]^+$), 491 (100, $[Cu_2(tach)_2Cl_3]^+$). Elemental analysis for $C_{18}H_{48}Cl_9Cu_3N_9$, found (expected) %: C 24.09 (24.01), H 5.39 (5.37), N 13.83 (14.00).

5.3.11 [(μ$_3$-Chloro)-*tris*{dichloro-(*cis,trans*-1,3,5-triaminocyclohexane-κ^2-N,N')-copper(II)}] dibromide (43)



43

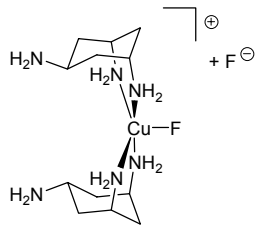
a) A methanolic solution (5 ml) of copper(II) bromide (106 mg, 0.48 mmol) was added to a solution of *trans*-tach (**29**, 61 mg, 0.47 mmol) in methanol (30 ml) previously adjusted to pH 6.5 using 2M hydrochloric acid, giving an instant colour change to turquoise blue. The mixture was stirred for three hours and the resulting turquoise precipitation of **43** was collected.

b) Crystals suitable for single crystal X-ray analysis were grown from reaction of 0.5 equivalents of copper(II) bromide to *trans*-tach in otherwise identical reaction conditions as

described above (Note: 0.2M HCl was used to adjust the pH to 6.5). Reducing the volume to 2 ml and crystallisation by diffusion of acetone yielded **43** as turquoise crystals.

The identity of the powder material obtained from a) and the crystalline material was established by powder X-ray diffraction of the microcrystalline solid and simulation of the powder XRD spectrum from the single crystal X-ray data.[236] Yield 58 mg (0.06 mmol, 37 %). IR (Golden Gate) ν /cm^{-1} 3283(m), 3221(m), 3148(m), 3113(m), 3017(m), 2932(m), 2889(bm), 1589(vs), 1555(w), 1516(vs), 1458(vs), 1404(w), 1358(m), 1339(s), 1319(w), 1281(w), 1165(vs), 1123(vs), 1069(m), 1045(s), 1007(m), 910(vs), 891(s), 779(w), 756(w), 683(vs), 610(w), 563(w). MS (ES-TOF+): *m/z* (%) $[M]^+$ not observed, 227 (12, $[Cu(tach)Cl]^+$), 273 (45, $[Cu(tach)Br]^+$), 491 (61, $[Cu_2(tach)_2Cl_3]^+$), 535 (100, $[Cu_2(tach)_2Cl_2Br]^+$), 581 (49, $[Cu_2(tach)_2ClBr_2]^+$), 625 (10, $[Cu_2(tach)_2Br_3]^+$). Elemental analysis for $C_{18}H_{48}Br_2Cl_7Cu_3N_9$, found (expected) %: C 21.92 (21.85), H 4.86 (4.89), N 12.64 (12.74).

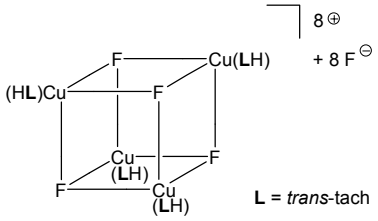
5.3.12 [Fluoro-*syn*-*bis*(*cis*,*trans*-1,3,5-triaminocyclohexane-κ^2-N,N')-copper(II)] fluoride (44)



44

Solid copper(II) fluoride hydrate (29 mg, 0.29 mmol) was added to a solution of *trans*-tach (**29,** 73 mg, 0.57 mmol) in methanol (15 ml). Dissolution of the solid copper(II) fluoride by ultrasonication resulted in a colour change from colourless to violet. Additional stirring over night and reducing the volume to 4 ml resulted in a dark violet solution. Crystallisation by slow diffusion of ether resulted in violet crystals of **44** suitable for single crystal X-ray analysis. Yield 23 mg (0.07 mmol, 24 %). IR (Golden Gate) ν /cm^{-1} 3071(s), 2932(s), 2758(s), 2530(m), 1639(m), 1593(s), 1574(s), 1462(w), 1389(w), 1207(m), 1150(w), 1111(w), 1045(w), 926(s), 876(s), 698(vs). Elemental analysis for $C_{12}H_{30}CuF_2N_6$, found (expected) %: C 39.87 (40.04), H 8.25 (8.40), N 23.21 (23.35).

5.3.13 [*tetrakis*{(μ$_3$-Fluoro)-(*cis,trans*-1,3,5-Triaminocyclohexane-κ^2-N,N')-copper(II)}] octafluoride (45)

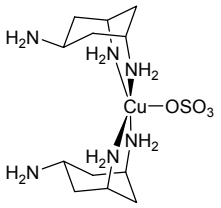


45

Caution: The toxic hydrofluoric acid (HF) is to be treated with great care. All reactions with HF were conducted in plastic vessels.

Copper(II) fluoride hydrate (29 mg, 0.29 mmol) was added to a solution of *trans*-tach (**29**, 56 mg, 0.44 mmol) in methanol (20ml) previously adjusted to pH 7.7 using 2M hydrofluoric acid. The solution gradually became violet upon stirring as the copper(II) fluoride dissolved. Continued stirring over night and reducing the volume to 4 ml resulted in an intense dark violet solution. Filtration through cotton wool and crystallisation by diffusion of ether yielded **45** as royal blue crystals embedded in white 'crusty' amorphous material. Isolation of the crystalline material was achieved by continuous cleansing of the combined crystallisation samples by ultrasonication in ether. Removal of the ether suspension resulted in royal blue crystalline material. Yield 28 mg (0.03 mmol, 39 %). IR (Golden Gate) ν /cm^{-1} 3071(s), 2932(s), 2758(s), 2530(m), 1639(m), 1593(s), 1574(s), 1462(w), 1389(w), 1207(m), 1150(w), 1111(w), 1045(w), 926(s), 876(s), 698(vs). MS (ES-TOF+): *m/z* (%) $[M]^+$ not observed, 441 (40, $[Cu_2(tach)_2F_3]^+$), 401 (100), 381 (30), 290 (25). Elemental analysis for $C_{24}H_{64}Cu_4F_{12}N_{12}$, found (expected) %: C 28.65 (28.74), H 6.56 (6.43), N 16.62 (16.76).

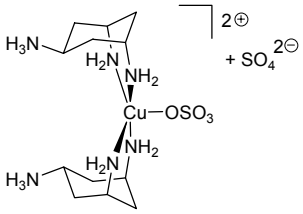
5.3.14 [Sulphato-*syn-bis*(*cis,trans*-1,3,5-triaminocyclohexane-κ^2-N,N')-copper(II)] (46)



46

Solid copper(II) sulphate hexahydrate (78 mg, 0.31 mmol) was added to a solution of *trans*-tach (**29,** 80 mg, 0.35 mmol) in methanol (20 ml) giving an instant colour change from colourless to dark violet. After stirring for two hours, the volume was reduced to 1.5 ml. Crystallisation by diffusion of ether resulted in violet crystals of **46** suitable for single crystal X-ray analysis. Yield 40 mg (0.10 mmol, 55 %). IR (Golden Gate) ν /cm^{-1} 2925(m), 2901(m), 2852(m), 1595(s), 1452(m), 1369(m), 1352(m), 1284(w), 1271(w), 1242(w), 1203(w), 1182(w), 1072(bvs), 958(m), 918(s), 899(m), 779(m), 756(w), 710(bs). MS (ES-TOF+): *m/z* (%) 418 (10, $[Cu(tach)_2SO_4]^+$), 404 (85), 391 (100), 376 (35), 360 (28). Elemental analysis for $C_{12}H_{30}CuN_6O_4S \cdot 0.1\ H_2SO_4$, found (expected) %: C 33.97 (33.69), H 7.31 (7.12), N 18.88 (19.64), S 7.97 (8.24).

5.3.15 [Sulphato-*syn-bis*(*cis,trans*-1,3,5-triaminocyclohexane-κ^2-N,N')-copper(II)] sulphate (46 · H_2SO_4)

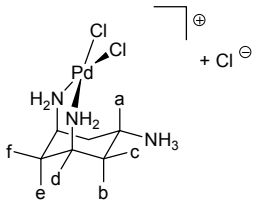


46 · H_2SO_4

A methanolic solution (3 ml) of copper(II) sulphate hexahydrate (90 mg, 0.36 mmol) was added to a solution of *trans*-tach (**29,** 87 mg, 0.68 mmol) in methanol (30 ml) giving an instant colour change from colourless to dark violet. The pH of the solution was adjusted to pH 8.8 with three drops of 2M sulphuric acid. After each drop, a precipitate was formed that

redissolved for the first two drops but remained as a suspension after the third. The reaction mixture was stirred for one and a half hours, the violet precipitate filtered off and the volume reduced the volume to ca. 2 ml. Filtration through cotton wool and microfibre filter paper was repeated until the filtrate ran clear. Crystallisation by diffusion of ether resulted in violet crystals of **46** • H_2SO_4 suitable for single crystal X-ray analysis. Yield 37 mg (0.07 mmol, 21 %). IR (Golden Gate) ν /cm^{-1} 3212(m), 3112(m), 2916(m), 1593(s), 1456(w), 1367(m), 1178(m), 1049(bvs), 920(s), 764(w), 711(bw). MS (ES-TOF+): *m/z* (%) 529 (10), 528 (40), 418 (12, $[Cu(tach)_2SO_4]^+$), 391 (15), 377 (18), 360 (100), 338 (25), 329 (10), 289 (8, $[Cu(tach)SO_4]^+$). Elemental analysis for $C_{12}H_{32}CuN_6O_8S_2$ • (H_2O) • (CH_3OH), found (expected) %: C 27.64 (27.58), H 6.76 (6.77), N 14.76 (14.84).

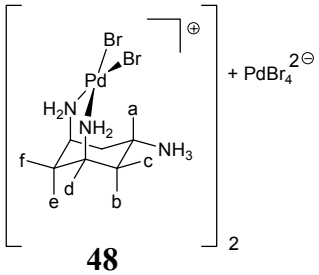
5.3.16 [Dichloro-(*cis,trans*-1,3,5-triaminocyclohexane-κ^2-N,N')-palladium(II)] chloride (47)



47

Solid palladium(II) chloride (164 mg, 0.93 mmol) was added to a solution of *trans*-tach *tris*-hydrochloride salt (**29** • 3 HCl, 199 mg, 0.83 mmol) in water (200 ml), and the resulting yellow solution refluxed for 2 days. Hot filtration resulted in an intense orange filtrate, which was concentrated to 20 ml. After a period of 1-2 days at ambient temperature, **47** crystallises as orange crystals suitable for single crystal X-ray analysis. Yield 282 mg (0.82 mmol, 71 %). COSY90, HSQC, DEPT135 and NOE experiments were measured to assign the NMR signals. ^{1}H-NMR (300 MHz, D_2O) δ /ppm 6.22 (t, 1H, *J* 13.4 Hz, $\underline{H}_a$), 4.27 (bs, N$\underline{H}_2$), 2.98 (bs, 2H, $\underline{H}_d$), 2.22 (d, 2H, *J* 13.4 Hz, $\underline{H}_c$), 2.02 (d, 1H, *J* 15.3 Hz, $\underline{H}_e$), 1.75 (td, 2H, *J* 13.4, 3.2 Hz, $\underline{H}_b$), 1.60 (d, 1H, *J* 15.3 Hz, $\underline{H}_f$). ^{13}C-NMR (75 MHz, D_2O) δ /ppm 43.96 (2x$\underline{C}H_d$), 43.53 ($\underline{C}H_a$), 34.14 (2x$\underline{C}H_{b,c}$), 33.82 ($\underline{C}H_{e,f}$). IR (Golden Gate) ν /cm^{-1} 3368(w), 3209(s), 3117(vs), 2935(s), 1585(s), 1485(s),1358(m), 1342(s), 1184(vs), 1153(vs), 1045(m), 926(s), 880(m), 718(m), 640(s), 579(s). Elemental analysis for $C_6H_{16}Cl_3N_3Pd$ • H_2O, found (expected) %: C 19.67 (19.96), H 5.02 (5.03), N 11.68 (11.64).

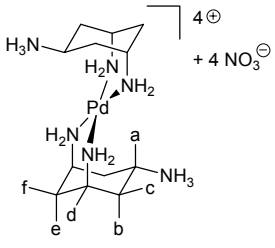
5.3.17 *bis*[Dibromo-(*cis,trans*-1,3,5-triaminocyclohexane-κ^2-N,N')-palladium(II)] tetrabromopalladate (48)



48

Solid palladium(II) bromide (201 mg, 0.76 mmol) was added to a solution of *trans*-tach *tris*-hydrobromide salt (**29** • 3 HBr, 294 mg, 0.79 mmol) in water (25 ml) and the resulting yellow solution was refluxed over night. Hot filtration resulted in an intense orange solution from which **48** crystallised as reddish, brown crystals over night. No ^{13}C-NMR spectrum was obtained due to the low solubility of crystalline **48** in D_2O. Yield 185 mg (0.15 mmol, 40 %). ^{1}H-NMR (300 MHz, D_2O) δ /ppm 6.20 (pt, 1H, *J* 13.4 Hz, $\underline{H}_a$), 3.06 (bs, 2H, $\underline{H}_d$), 2.20 (d, 2H, *J* 13.4 Hz, $\underline{H}_c$), 2.06 (d, 1H, *J* 15.6 Hz, $\underline{H}_e$), 1.76 (td, 2H, *J* 13.4, 4.0 Hz, $\underline{H}_b$), 1.65 (bd, 1H, *J* 15.6 Hz, $\underline{H}_f$). IR (Golden Gate) ν /cm^{-1} 3434(w), 3180(s), 3099(s), 2894(m), 1560(vs), 1461(vs), 1344(s), 1227(m), 1134(vs), 1041(m), 939(m), 883(s). Elemental analysis for $C_{12}H_{32}Br_8N_6Pd_3$, found (expected) %: C 11.65 (11.82), H 2.63 (2.65), N 6.75 (6.89).

5.3.18 [*anti-bis*(*cis,trans*-1,3,5-Triaminocyclohexane-κ^2-N,N')-palladium(II)] tetranitrate (49)



49

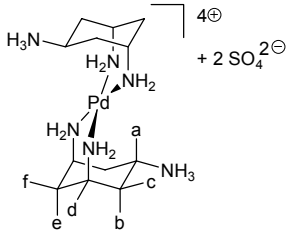
a) Mother liquor (5 ml) of **47** (21 mg, 0.06 mmol) was sorbed onto a strongly alkaline ion exchange resin (1.5 cm x 10 cm, *Dowex 1x8-50*, 20-50 mesh, charged as described in 5.3.2.1;

eluted with ca. 150 ml water). The alkaline eluent was concentrated to 10 ml and neutralised with nitric acid. Crystallisation by slow evaporation of solvent resulted in yellow crystals of **49**, suitable for single crystal X-ray analysis. Yield 16 mg (0.026 mmol, 74 %).

b) A solution of *trans*-tach (**29**, 93 mg, 0.72 mmol) in water (30 ml) was acidified with 2M nitric acid to pH 8.55 (starting pH 11.50). Palladium(II) nitrate hydrate (97 mg, 0.42 mmol) in water (2 ml) was added to the amine solution and refluxed over night. Hot filtration resulted in a pale yellow filtrate, from which **49** crystallised as yellow blocks. Yield 46 mg (0.08 mmol, 21 %).

Analytical data: M.p. 150°C (dec.). ^{1}H-NMR (300 MHz, D_2O) δ /ppm 5.38 (tt, 1H, *J* 13.2, 4.6 Hz, $\underline{H}_a$), 3.16 (bs, 2H, $\underline{H}_d$), 2.16 (bd, 2H, *J* 14.3, $\underline{H}_c$), 1.95 (dt, 1H, *J* 15.4, 4.1 Hz, $\underline{H}_e$), 1.82-1.60 (m, 3H, $\underline{H}_{b,f}$). ^{13}C-NMR (75 MHz, D_2O) δ /ppm 44.49 (2x$\underline{C}H_d$), 43.38 ($\underline{C}H_a$), 34.30 (2x$\underline{C}H_{b,c}$), 33.98 ($\underline{C}H_{e,f}$). IR (Golden Gate) ν /cm^{-1} 3209(s), 3117(vs), 2928(s), 1601(s), 1481(s), 1269(s), 1141(vs), 999(s), 821(s). MS (CI) *m/z* 363 (69, $[Pd(tach)_2\text{-}H]^+$), 234 (100, $[Pd(tach)\text{-}H]^+$), 217 (25, $[Pd(tach)\text{-}NH_3]^+$). Elemental analysis for $C_{12}H_{32}N_{10}O_{12}Pd$, found (expected) %: C 23.29 (23.45), H 5.22 (5.25), N 22.66 (22.80).

5.3.19 [*anti-bis*(*cis,trans*-1,3,5-Triaminocyclohexane-κ^2-N,N')-palladium(II)] *bis*-sulphate (50)

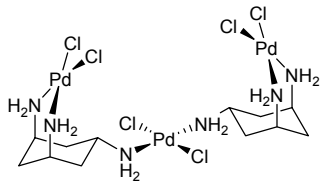


50

To a solution of *trans*-tach (**29**, 72 mg, 0.56 mmol) in water (20 ml), palladium(II) sulphate (59 mg, 0.29 mmol) was added as a solid and stirred for two hours at room temperature, then refluxed over night. Hot filtration resulted in a pale yellow filtrate, which was concentrated to 3 ml. **50** crystallised as pale yellow crystals at ambient temperature over a period of two weeks. Yield 29 mg (0.05 mmol, 35 %). ^{1}H-NMR (300 MHz, D_2O) δ /ppm 5.36 (tt, 1H, *J* 12.7, 4.4 Hz, $\underline{H}_a$), 3.12 (bs, 2H, $\underline{H}_d$), 2.12 (bd, 2H, *J* 13.7 Hz, $\underline{H}_c$), 1.89 (dt, 1H, *J* 15.6,

4.0 Hz, $\underline{H}_e$), 1.70-1.52 (m, 3H, $\underline{H}_{b,f}$). ^{13}C-NMR (75 MHz, D_2O) δ /ppm 42.65 (2x$\underline{C}H_d$), 40.74 ($\underline{C}H_a$), 33.46 (2x$\underline{C}H_{b,c}$), 32.02 ($\underline{C}H_{e,f}$). IR (Golden Gate) ν /cm^{-1} 3405(bm), 3064(m), 2902(m), 1618(s), 1525(s), 1450(s), 1354(m), 1063(vs), 750(m). Elemental analysis for $C_{12}H_{32}N_6O_8PdS_2$, found (expected) %: C 25.60 (25.78), H 5.72 (5.77), N 14.92 (15.03).

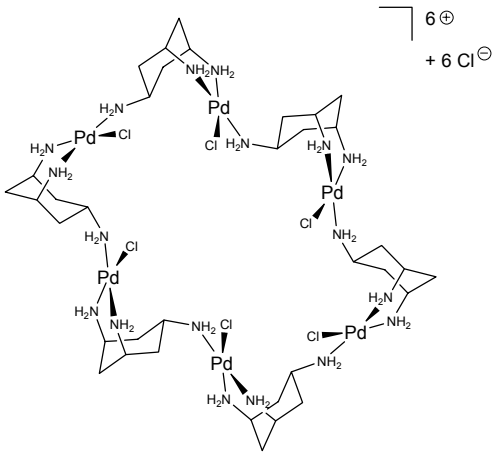
5.3.20 [*bis*{Dichloro-μ$_2$-(*cis,trans*-1,3,5-triaminocyclohexane-κ^3-N,N',N'')-palladium(II)}-*trans*-{dichloro-palladium(II)}] (53)



53

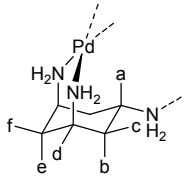
Mother liquor (2ml) of **47** (20 mg, 0.06 mmol) was heated at 80 °C for 7 days. After this time a small number of orange crystals of **53** grew that were suitable for single crystal X-ray analysis. No NMR spectra were obtained due to the insolubility of **53** in common solvents. Yield 4 mg (0.01 mmol, 26 %). IR (Golden Gate) ν /cm^{-1} 3371(w), 3190(s), 3117(vs), 3228(w), 1701(w), 1570(s), 1512(m), 1362(s), 1339(m), 1223(w), 1184(s), 1153(s), 1049(m), 930(m), 883(w), 718(s). Elemental analysis for $C_{12}H_{30}Cl_6N_6Pd_3$, found (expected) %: C 18.16 (18.24), H 3.98 (3.83), N 10.93 (10.63).

5.3.21 *cyclo*[*hexakis*{Chloro-μ$_2$-(*cis,trans*-1,3,5-triaminocyclohexane-κ^3-N,N',N'')-palladium(II)}] hexachloride (51)



51

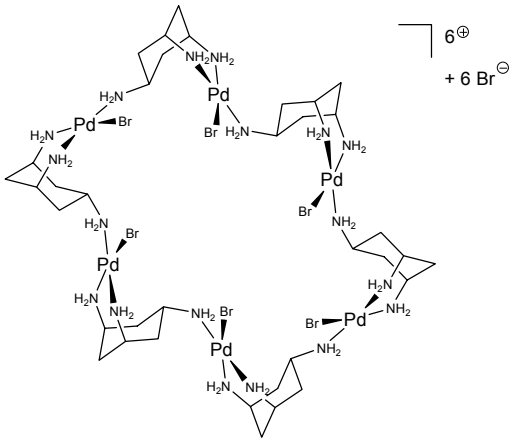
Solid palladium(II) chloride (377 mg, 2.13 mmol) was added to a solution of *trans*-tach *tris*-hydrochloride salt (**29** • 3 HCl, 424 mg, 1.78 mmol) in water (200 ml), and the resulting yellow solution refluxed over night. Hot filtration resulted in an intense orange filtrate, which was concentrated to 60 ml. The filtrate was sorbed onto an ion exchange resin in its chloride form (2 cm x 24 cm, *Dowex 1x8-50*, 20-50 mesh, charged as follows: washing with water (500 ml), activating the column with concentrated sodium chloride solution (800 ml) and washing again with water (700 ml)). The column was eluted with water until the eluent became yellow and the pH acidic, at which point the collection started until the eluent became colourless and neutral again (after ca. 400 ml water). Neutralisation of the pale yellow solution with sodium hydroxide (eluent pH 1.96) was followed by pH adjustment over a period of 5 days at 50 °C. Reducing the volume to ca. 80 ml and addition of methanol (300 ml) upon stirring produces a fine yellow precipitate. Stirring over night and collection of the precipitate by suction filtration (D3-sinter) resulted in **51** as a yellow powder. Crystals suitable for single crystal X-ray diffraction were obtained by slow diffusion of methanol into a small sample of neutralised mother liquor. Yield 354 mg (0.19 mmol, 65 %). Decomposition at 90 °C in solution (H_2O). IR (Golden Gate) ν /cm^{-1} 3379(b), 3206(vs), 3128(vs), 2924(m), 2855(w), 1582(vs), 1454(m), 1435(m), 1361(s), 1285(w), 1269(w), 1223(m), 1138(bs), 1111(s), 1084(m), 1053(s), 1030(m), 930(s), 883(m), 750(bs), 625(bs), 560(bvs). MS: No molecular ion peak corresponding to **51** was found despite employing a variety of techniques including CI, EI, FAB, MALDI and ES-TOF. However, each technique gave rise to different peaks that were attributed to the decomposition / re-speciation of the cluster. Elemental analysis for $[C_6H_{15}Cl_2N_3Pd]_6$ • 6 H_2O, found (expected) %: C 22.05 (22.20), H 5.41 (5.28), N 12.84 (12.95).



This *trans*-tach unit represents all three chemically different units in the ring structure by adding the number (1, 2 or 3) to the corresponding unit. ^{1}H-NMR spectra were recorded at 25 and 65 °C and gave identical spectra. However, at 90 °C the complex appeared to decompose into mono- and multinuclear fragments. COSY90, HSQC and DEPT135 experiments were measured to assist the assignment of the signals. ^{1}H-NMR (500 MHz, D_2O) δ /ppm 6.21 (ptt,

1H, *J* 12.7, 4.5 Hz, $\underline{H}_{a1}$), 5.45 (ptt, 1H, *J* 12.7, 4.5 Hz, $\underline{H}_{a2}$), 5.35 (ptt, 1H, *J* 12.7, 4.5 Hz, $\underline{H}_{a3}$), 4.52 (bs, $N\underline{H}_2$), 4.19 (bs, $N\underline{H}_2$), 3.25-2.92 (m, 9$\underline{H}$), 2.65 (bd, 1H, *J* 13.4 Hz, $\underline{H}_{b2}$), 2.11-1.89 (m, 5$\underline{H}$), 1.71-1.39 (m, 9H). ^{13}C-NMR (125 MHz, D_2O) δ /ppm 46.91 ($\underline{C}H_{a3}$), 46.79 ($\underline{C}H_{a2}$), 46.66 ($\underline{C}H_{a1}$), (45.88, 45.39 (two), 44.93, 44.54, 44.27, 6x$\underline{C}H_{d,d'}$), 38.83 ($\underline{C}H_{b2,c2}$), (38.73 (two), 38.10 (two), 37.93 (two), 33.93, 33.88, 8x$\underline{C}H_2$).

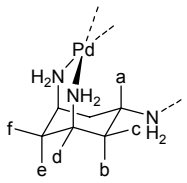
5.3.22 *cyclo*[*hexakis*{Bromo-μ_2-(*cis*,*trans*-1,3,5-triaminocyclohexane-κ^3-N,N',N'')-palladium(II)}] hexabromide (52)



52

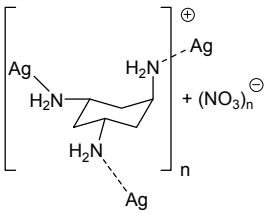
To a solution of *trans*-tach *tris*-hydrobromide salt (**29** • 3 HBr, 211 mg, 0.57 mmol) in water (300 ml), palladium(II) bromide (402 mg, 1.51 mmol) was added as a solid and the resulting solution refluxed for 9 days. Hot filtration resulted in an intense red filtrate, which was concentrated to 60 ml. The filtrate was sorbed onto an ion exchange resin in its bromide form (2 cm x 24 cm, *Dowex 1x8-50*, 20-50 mesh, charged as follows: washing with water (500 ml), activating the column with sodium bromide solution (800 ml) and washing again with water (700 ml)). The column was then eluted with water until the eluent became yellow and the pH acidic, at which point the collection started until the eluent became colourless and neutral again (after ca. 400 ml water). Neutralisation of the pale yellow solution with sodium hydroxide (eluent pH 2.95) was followed by pH adjustment over a period of 5 days at 50 °C. Reducing the volume to dryness resulted in an amorphous yellow solid of **52**. Dissolution in water (ca. 15 ml) at 55 °C, filtration and crystallisation over a period of 3 days resulted in **52** as yellow crystals suitable for single crystal X-ray diffraction. Yield: 176 mg (0.07 mmol, 78 %) amorphous solid; 50 mg (0.02 mmol, 22 %) crystalline material. IR (Golden Gate) ν /cm^{-1}

3410(m), 3186(s), 3089(vs), 2924(m), 1576(vs), 1448(w), 1435(w), 1362(s), 1292(w), 1215(m) 1149(m), 1109(m), 1080(w), 1057(s), 1026(m), 928(m), 881(w), 739(bw). Elemental analysis for $[C_6H_{15}Br_2N_3Pd]_6 \cdot 7\ H_2O$, found (expected) %: C 13.94 (13.82), H 5.20 (5.60), N 7.78 (8.06).



This *trans*-tach unit represents all three chemically different units in the ring structure by adding the number (1, 2 or 3) to the corresponding unit. ^{1}H-NMR spectra were recorded at 25 and 65 °C and gave identical spectra. COSY90 and DEPT135 experiments assisted the assignment of the NMR signals. ^{1}H-NMR (400 MHz, D_2O) δ /ppm 6.34 (pt, 1H, *J* 12.7 Hz, $\underline{H}_{a1}$), 5.25 (m, 2H, $\underline{H}_{a2,a3}$), 4.34 (bs, N$\underline{H}_2$), 4.00 (bs, N$\underline{H}_2$), 3.28-2.65 (m, 9$\underline{H}$), 2.66 (bd, 1H, *J* 13.4 Hz, $\underline{H}_{b2}$), 2.08-1.86 (m, 5$\underline{H}$), 1.70-1.34 (m, 9$\underline{H}$). ^{13}C-NMR (100 MHz, D_2O) δ /ppm (45.39, 44.85, 44.66, 43.84, 43.40, 43.16, 42.66, 42.10, 9x$\underline{C}$H), (36.99, 36.90, 36.79, 36.16, 36.00, 35.71, 31.75, 31.62, 9x$\underline{C}H_2$).

5.3.23 *poly*{[μ_3-(*cis,trans*-1,3,5-Triaminocyclohexane-κ^3-N,N',N'')-silver(I)] nitrate} (54)

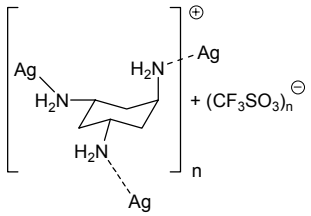


54

Silver(I) nitrate (31 mg, 0.18 mmol) in water (1.5 ml) was added dropwise to a solution of *trans*-tach (**29**, 42 mg, 0.32 mmol) in methanol (10 ml). The solution was stirred over night in the dark and crystallisation by diffusion of ether resulted in crystals of **54**, suitable for single crystal X-ray analysis. Yield: 5 mg (0.02 mmol, 33 %). ^{1}H-NMR (300 MHz, D_2O) δ /ppm 3.39 (bs, 1H, $\underline{H}_a$), 3.21 (t, 2H, *J* 12.0 Hz, $\underline{H}_d$), 2.25 (d, 1H, *J* 12.0 Hz, $\underline{H}_e$), 1.92 (d, 2H, *J* 12.0 Hz, $\underline{H}_b$), 1.33 (td, 2H, *J* 12.0, 3.5 Hz, $\underline{H}_c$), 1.06 (q, 1H, *J* 12.0 Hz, $\underline{H}_f$). ^{13}C-NMR (75 MHz, D_2O) δ /ppm 49.41 ($\underline{C}H_a$), 48.78 ($\underline{C}H_{e,f}$), 47.33 ($\underline{C}H_d$), 43.29 ($\underline{C}H_{b,c}$).

IR (Golden Gate) ν /cm^{-1} 3294(w), 3252(w), 3167(w), 2904(w), 1601(w), 1315(vs), 1180(m), 1130(m), 1114(m), 1038(s), 1003(s), 980(m), 845(w), 826(m), 698(w), 590(s), 551(m), 513(s). Elemental analysis for $[C_6H_{15}AgN_4O_3)]_n$, found (expected) %: C 24.01 (24.10), H 4.95 (5.06), N 18.93 (18.73).

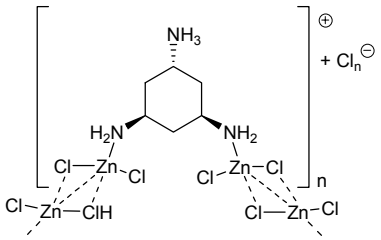
5.3.24 *catena-poly*{[μ_3-(*cis*,*trans*-1,3,5-Triaminocyclohexane-κ^3-N,N',N'')-silver(I)] trifluoromethanesulphonate} (55)



55

A methanolic solution (1.5 ml) of silver(I) triflate (88 mg, 0.34 mmol) was added dropwise to a solution of *trans*-tach (**29**, 82 mg, 0.63 mmol) in methanol (10 ml). A white precipitate was formed upon stirring, which was removed by filtration. Crystallisation by diffusion of ether resulted in colourless crystals of **55**, suitable for single crystal X-ray analysis. Yield: 74 mg (0.19 mmol, 56 %). ^{1}H-NMR (300 MHz, D_2O) δ /ppm 3.38 (bs, 1H, $\underline{H}_a$), 3.22 (t, 2H, J 8.6 Hz, $\underline{H}_d$), 2.26 (d, 1H, J 8.6 Hz, $\underline{H}_e$), 1.90 (d, 2H, J 9.6 Hz, $\underline{H}_b$), 1.31 (td, 2H, J 9.6, 2.2 Hz, $\underline{H}_c$), 1.06 (q, 1H, J 8.6 Hz, $\underline{H}_f$). IR (Golden Gate) ν /cm^{-1} 3336(m), 3275(m), 2900(w), 2856(w), 1595(m), 1458(w), 1356(w), 1269(s), 1248(vs), 1228(s), 1176(m), 1153(s), 1111(w), 1030(s), 989(m), 953(m), 922(w), 901(w), 874(w), 843(m), 808(m), 760(m), 737(w), 698(w), 636(vs). Elemental analysis for $[C_7H_{15}AgF_3N_3O_3S)]_n$, found (expected) %: C 21.52 (21.77), H 3.63 (3.92), N 10.60 (10.88).

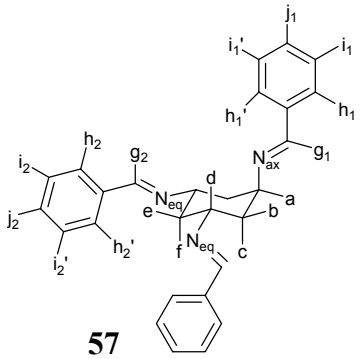
5.3.25 *catena-poly*{[Dichloro-*bis*(μ_2-chloro)-μ_2-(*cis,trans*-1,3,5-triaminocyclohexane-κ^2-N,N')-di-zinc(II)] chloride} (56)



56

An aqueous solution (2 ml) of zinc(II) chloride (31 mg, 0.23 mmol) was added to a solution of *trans*-tach (**29**, 58 mg, 0.45 mmol) in water (60ml) previously adjusted to pH 6.5 with 2M hydrochloric acid. The mixture was stirred for three hours and reduced in volume to 2 ml. Crystallisation by diffusion of methanol resulted predominantly in white amorphous precipitate. However, a few colourless crystals of **56** suitable for single crystal X-ray analysis were also obtained. Yield: 15 mg (0.03 mmol, 30%). ^{1}H-NMR (300 MHz, D_2O) δ /ppm 3.89 (t, 1H, *J* 4.0 Hz, $\underline{H}_a$), 3.53 (tt, 2H, *J* 12.0, 4.0 Hz, $\underline{H}_d$), 2.37 (d, 1H, *J* 12.0 Hz, $\underline{H}_e$), 2.19 (d, 2H, *J* 12.0 Hz, $\underline{H}_b$), 1.82 (td, 2H, *J* 12.0, 4.0 Hz, $\underline{H}_c$), 1.57 (q, 1H, *J* 12.0 Hz, $\underline{H}_f$). IR (Golden Gate) ν /cm^{-1} 3198(s), 3094(s), 2862(s), 1597(s), 1562(s), 1501(s), 1482(vs), 1404(m), 1373(w), 1280(w), 1192(s), 1099(m), 1065(m), 1026(m), 988 (w), 957(m), 895(w), 868(w), 845(w), 698(m), 660(m), 540(s). Elemental analysis for $[C_6H_{16}Cl_5N_3Zn_2)]_n$, found (expected) %: C 16.01 (16.44), H 3.62 (3.68), N 9.21 (9.59).

5.3.26 *cis,trans*-1,3,5-*tris*-Benzaldimino-cyclohexane (tbc, 57)

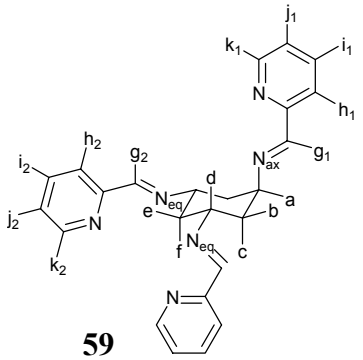


57

A solution of *trans*-tach (**29** • 3 HCl, 487 mg, 2.04 mmol) and sodium hydroxide (263 mg, 6.58 mmol) in water (15 ml) was stirred for 15 minutes. Benzaldehyde (**58**, 706 mg, 6.65

mmol) was added and the resulting mixture was ultrasonicated for 4 hours. Ether extraction (3 x 60 ml), drying of the combined organic layers ($MgSO_4$) and removal of solvent *in vacuo* resulted in an oily residue (2 ml), from which analytically pure **57** crystallised over night. Addition of hexane (20 ml) and vacuum filtration yielded **57** as a crystalline white solid. Crystals of **57**, suitable for single crystal X-ray analysis, were obtained from a reaction mixture with nickel(II) chloride. Yield: 453 mg (1.15 mmol, 56 %). M.p. 156 °C. ^{1}H-NMR (300 MHz, $CDCl_3$) δ /ppm 8.41 (s, 2H, $\underline{H}_{g2}$), 8.38 (s, 1H, $\underline{H}_{g1}$), 7.82 (AA' part of AA'BB'C spin system 1, 2H, $\underline{H}_{h1,}$ $\underline{H}_{h1'}$), 7.73 (AA' part of AA'BB'C spin system 2, 4H, $\underline{H}_{h2,}$ $\underline{H}_{h2'}$), 7.45 (BB'C part of AA'BB'C spin system 1, 3H, $\underline{H}_{i1,}$ $\underline{H}_{j1,}$ $\underline{H}_{j1'}$), 7.40 (BB'C part of AA'BB'C spin system 2, 6H, $\underline{H}_{i2,}$ $\underline{H}_{j2,}$ $\underline{H}_{j2'}$), 4.11 (tt, 2H, *J* 11.2, 3.5 Hz, $\underline{H}_d$), 3.95 (t, 1H, *J* 2.8 Hz, $\underline{H}_a$), 2.10 (m, 3H, 2•$\underline{H}_b$ or 2•$\underline{H}_c$ and $\underline{H}_e$ or $\underline{H}_f$), 1.96 (bd, 1H, *J* 11.7 Hz, $\underline{H}_{f,}$ or $\underline{H}_e$), 1.82 (bd, 2H, *J* 11.7 Hz, 2•$\underline{H}_c$ or 2•$\underline{H}_b$). ^{13}C-NMR (75 MHz, $CDCl_3$) δ /ppm 159.74 (2x$\underline{C}H_{g2}$), 158.84 ($\underline{C}H_{g1}$), 136.56 (3x$\underline{C}_{ipso}$), 130.48 (3x$\underline{C}H_{j1,j2}$), 128.59 (6x$\underline{C}H_{i1,i1',i2,i2'}$), 128.14 (6x$\underline{C}H_{h1,h1',h2,h2'}$), 65.39 (2x$\underline{C}H_d$ or $\underline{C}H_a$), 63.58 ($\underline{C}H_a$ or 2x$\underline{C}H_d$), 41.91 ($\underline{C}H_{e,f}$), 40.63 (2x$\underline{C}H_{b,c}$). IR (Golden Gate) ν /cm^{-1} 3063(w), 3032(w), 2932(m), 2862(m), 1636(s), 1582(m), 1450(w), 1381(s), 1296(m), 1211(m), 1134(w), 1065(m), 1026(m), 972(w), 849(m), 756(vs), 687(s). MS (EI+): *m/z* 393 (39, M^+). Elemental analysis for $C_{27}H_{27}N_3$, found (expected) %: C 82.51 (82.41), H 7.14 (6.92), N 10.67 (10.68).

5.3.27 *cis,trans*-1,3,5-*tris*(Pyridine-2-carboxaldimino)-cyclohexane (ttop, 59)

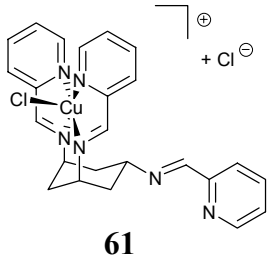


59

A methanolic solution (2 ml) of pyridine-2-carboxaldehyde (**60**, 302 mg, 3.66 mmol) was added to a solution of *trans*-tach (**29**, 154 mg, 1.19 mmol) and triethylamine (60 mg, 0.59 mmol) in methanol (30 ml). The mixture was refluxed under nitrogen over night and the

volume reduced to 5 ml. Extraction with dichloromethane (3 x 20 ml), drying of the combined organic layers ($MgSO_4$) and removal of solvent *in vacuo* yielded **59** as a light brown solid. Yield: 385 mg (0.97 mmol, 82 %). M.p. 75 °C. ^{1}H-NMR (400 MHz, $CDCl_3$) δ /ppm 8.56 (A part of ABCD spin system 1, 1H, *J* 4.5 Hz, $\underline{H}_{k1}$), 8.53 (A part of ABCD spin system 2, 2H, *J* 4.5 Hz, $\underline{H}_{k2}$), 8.40 (s, 2H, $\underline{H}_{g2}$), 8.38 (s, 1H, $\underline{H}_{g1}$), 8.02 (B part of ABCD spin system 1, 1H, *J* 8.0 Hz, $\underline{H}_{h1}$), 7.90 (B part of ABCD spin system 2, 2H, *J* 8.0 Hz, $\underline{H}_{h2}$), 7.68 (C part of ABCD spin system 1, 1H, *J* 8.0, 7.5 Hz, $\underline{H}_{i1}$), 7.62 (C part of ABCD spin system 2, 2H, *J* 8.0, 7.5 Hz, $\underline{H}_{i2}$), 7.23 (D part of ABCD spin system 1, 1H, *J* 6.5, 6.0 Hz, $\underline{H}_{j1}$), 7.12 (D part of ABCD spin system 2, 2H, *J* 6.5, 6.0 Hz, $\underline{H}_{j2}$), 4.11 (pt, 2H, *J* 11.3 Hz, $\underline{H}_{d}$), 3.97 (bs, 1H, $\underline{H}_{a}$), 2.07 (m, 3H, 2$^{\bullet}\underline{H}_{b}$ or 2$^{\bullet}\underline{H}_{c}$ and $\underline{H}_{e}$ or $\underline{H}_{f}$), 1.95 (bd, 1H, *J* 12.5 Hz, $\underline{H}_{f}$ or $\underline{H}_{e}$), 1.80 (bd, 2H, *J* 12.5 Hz, 2$^{\bullet}\underline{H}_{c}$ or 2$^{\bullet}\underline{H}_{b}$). ^{13}C-NMR (75 MHz, $CDCl_3$) δ /ppm 159.16 (2x$\underline{C}H_{g2}$), 158.83 ($\underline{C}H_{g1}$), 153.38 ($\underline{C}_{ipso1}$), 153.33 (2x$\underline{C}_{ipso2}$), 147.95 (2x$\underline{C}H_{k2}$), 147.84 ($\underline{C}H_{k1}$), 135.00 (3x$\underline{C}H_{i1,i2}$), 123.20 ($\underline{C}H_{j1}$), 123.10 (2x$\underline{C}H_{j2}$), 119.99 (2x$\underline{C}H_{h2}$), 119.75 ($\underline{C}H_{h1}$) 63.48 ($\underline{C}H_{a}$), 61.68 (2x$\underline{C}H_{d}$), 39.90 ($\underline{C}H_{e,f}$), 38.68 (2x$\underline{C}H_{b,c}$). IR (Golden Gate) ν /cm^{-1} 3059(w), 2928(m), 2858(m), 1643(s), 1585(s), 1566(s), 1466(s), 1435(s), 1373(m), 1319(w), 1288(w), 1227(w), 1134(m), 1080(m), 1042(m), 1018(w), 991(s), 972(s), 860(s), 772(vs), 741(s), 664(m), 650(m), 617(s), 662(m), 517(s). MS (ES+): *m/z* 419 ([M+Na]$^+$). Elemental analysis for $C_{24}H_{24}N_6$, found (expected) %: C 72.53 (72.70), H 6.31 (6.10), N 20.90 (21.20).

5.3.28 [Chloro-(*cis,trans*-1,3,5-*tris*(pyridine-2-carboxaldimino)-cyclohexane-κ^4-N^1,N^2,N^3,N^4)-copper(II)] chloride (61)

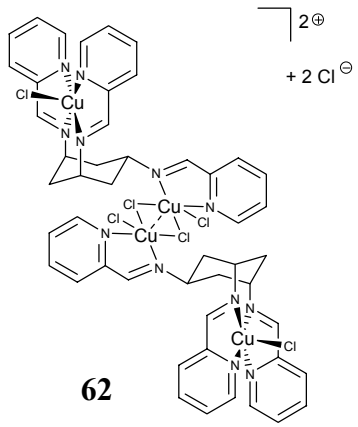


61

A methanolic solution (5 ml) of copper(II) chloride anhydrous (27 mg, 0.20 mmol) was added to a solution of ttop (**59**, 88 mg, 0.22 mmol) in methanol (15 ml). The colour changed immediately from colourless to dark green. The solution was stirred for one hour and reduced in volume to ca. 10 ml. Crystallisation by diffusion of ether resulted in green crystals of **61**. Yield: 88 mg (0.17 mmol, 85 %). IR (Golden Gate) ν /cm^{-1} 3359(bs), 3201(w), 3072(w),

3032(w), 1682(w), 1637(s), 1599(vs), 1570(m), 1516(w), 1473(w), 1441(m), 1396(m), 1338(w), 1303(m), 1273(w), 1225(m), 1200(w), 1159(m), 1132(s), 1068(w), 1047(w), 1016(m), 1001(w), 926(w), 862(m), 771(vs), 642(m). MS (ES+): *m/z* 494 [100, $[M]^+$). Elemental analysis for $C_{24}H_{24}Cl_2CuN_6$, found (expected) %: C 53.18 (54.29), H 4.63 (4.56), N 15.54 (15.83).

5.3.29 [*bis*{Dichloro-(μ_2-chloro)-μ_2-(*cis,trans*-1,3,5-*tris*(pyridine-2-carboxaldimino)-cyclohexane-κ^6-N^1,N^2,N^3,N^4,N^5,N^6)-di-copper(II)}] dichloride (62)



62

A methanolic solution (3 ml) of copper(II) chloride anhydrous (24 mg, 0.18 mmol) was added to a solution of ttop (**59**, 37 mg, 0.09 mmol) in methanol (20 ml). The colour changed immediately from colourless to dark green. The solution was stirred for three hours and reduced in volume to ca. 3 ml. Crystallisation by diffusion of ether resulted in dark green crystals of **62**. Yield: 66 mg (0.05 mmol, 55 %). IR (Golden Gate) ν /cm^{-1} 3435(m), 2037(m), 2951(m), 2925(m), 1643(s), 1597(vs), 1567(m), 1479(m), 1444(s), 1398(w), 1381(w), 1323(w), 1302(s), 1269(w), 1227(s), 1159(w), 1132(s), 1105(m), 1049(m), 1014(m), 980(s), 935(w), 881(m), 768(vs), 742(m), 696(w), 642(s). Elemental analysis for $C_{24}H_{24}Cl_4Cu_2N_6$, found (expected) %: C 42.45 (43.32), H 3.58 (3.64), N 12.51 (12.63).

6 CRYSTALLOGRAPHY

Thirty two structures are presented in this thesis. Due to the large amount of tabulated data such as atom coordinates, anisotropic displacement parameters and hydrogen atom coordinates, only tables with bond length and angles are given in this section. For additional data, the reader is referred to the supplementary data which are deposited with this thesis and can be obtained from the University of Birmingham. Structures were solved by Patterson or Direct methods with SHELXS-97[237] or SIR-92[238] using WinGX[239] routines. Refinement was accomplished by full matrix least-squares on F^2 with SHELXL-97. All non-hydrogen atoms were refined anisotropically except otherwise stated. Hydrogen atoms were placed using standard geometrical criteria and refined using a riding model. All data manipulation and presentation were performed using WinGX. Details of interest about the structure refinements are given in the tables.

The following parameters are given in the information for each structure and were calculated as follows:

Goodness-of-fit (GooF) = $\{\Sigma[w(F_o^2 - F_c^2)^2] / (n-p)\}^{1/2}$
Weighting scheme $w = [\sigma^2(F_o^2) + (A*P)^2 + B*P]^{-1}$
$P = [\max(I_{obs},0) + 2F_c^2] / 3$
p = number of parameters, n = number of data. Weighting scheme parameters A and B given for each structure.

R-factors: $R1 = \Sigma||F_o| - |F_c|| / \Sigma|F_o|$ and $wR2 = \{\Sigma[w(F_o^2 - F_c^2)^2] / \{\Sigma[w(F_o^2)^2]\}^{1/2}$
$R(int) = \Sigma|F_o^2 - F_o^2(mean)| / \Sigma[(F_o^2)]$ where both summations involve reflections for which more than one symmetry equivalent is averaged.

Only unique atoms in the asymmetric unit are numbered in the Ortep-3 representations. To illustrate the coordination environment of the compounds, these asymmetric units are expanded where appropriate.

6.1 X-ray summary table

No.	Structure	Crystal System	Space Group	a, b, c /Å	α, β, γ /º	V /Å^3
29 • 3 HCl	*trans*-tach • 3 HCl	Orthorhombic	*Pnma* (62)	7.2539(2) 9.8265(3) 16.4828(6)	90 90 90	1174.90(6)
29 • 3 HBr	*trans*-tach • 3 HBr	Monoclinic	$P2_1/m$ (11)	7.3695(2) 10.6052(3) 8.6123(2)	90 109.993(1) 90	632.53(3)
29 • 3 HNO_3	*trans*-tach • 3 HNO_3	Monoclinic	$P2_1$ (4)	6.703(2) 7.766(2) 12.597(2)	90 94.06(2) 90	654.1(4)
29 • 3 $HClO_4$	*trans*-tach • 3 $HClO_4$	Monoclinic	$P2_1/c$ (14)	13.2969(4) 8.1006(3) 16.0151(7)	90 109.772(1) 90	1623.33(11)
34 • 2 HNO_3	[Ni(**L**H)$_2$](NO$_3$)$_4$	Monoclinic	$P2_1/c$ (14)	8.4878(7) 16.5680(19) 8.5640(9)	90 110.425(5) 90	1128.6(2)
35	[Ni(**L**)$_2$]Cl$_2$	Monoclinic	$P2_1/n$ (14)	7.2420(9) 13.126(2) 12.749(3)	90 102.216(11) 90	1184.4(4)
36 • 0.5 HNO_3	[Cu(**L**)$_2$](NO$_3$)$_2$ • 0.5 HNO_3	Triclinic	*P*-1 (2)	10.674(3) 12.013(3) 9.9374(18)	93.717(14) 108.110(8) 72.970(7)	1157.5(5)
37	[Cu(**L**H)(NO$_3$)$_3$]	Orthorhombic	$Pbn2_1$ (33)	9.1456(1) 16.7280(2) 10.0301(2)	90 90 90	1534.48(4)
Syn-**38**	[Cu(**L**)$_2$]Br$_2$	Orthorhombic	*Pnma* (62)	13.5262(1) 12.8552(2) 11.8161(2)	90 90 90	2054.61(5)
twist-**38**	[Cu(**L**)$_2$]Br$_2$	Monoclinic	$P2_1/c$ (14)	13.5958(13) 14.0133(17) 13.1036(10)	90 106.385(6) 90	2395.1(4)
39	[Cu(**L**)$_2$Br]Br	Orthorhombic	*Pnma* (62)	13.2522(14) 12.7055(11) 12.5588(12)	90 90 90	2114.6(4)

40	[Cu(**L**LH)Br_2]Br	Orthorhombic	*C*2*cm* (40)	8.0516(5) 14.9956(9) 9.7979(5)	90 90 90	1182.98(12)
41 • 2 HCl	[{Cu(**L**)$_2$}$_2$Cl]Cl_3 • 2HCl	Monoclinic	$P2_1/n$ (14)	8.726(2) 18.500(4) 13.341(3)	90 96.731(2) 90	2138.8(9)
42	[{Cu(**L**LH)Cl_2}$_3$Cl]Cl_2	Hexagonal	$P6_3/m$ (176)	12.680(2) 12.680(2) 12.6287(13)	90 90 120	1758.4(4)
43	[{Cu(**L**LH)Cl_2}$_3$Cl]Br_2	Hexagonal	*P* $6_3/m$ (176)	12.6961(2) 12.6961(2) 12.6511(2)	90 90 120	1766.04(5)
44	[Cu(**L**)$_2$F]F	Monoclinic	*Cc* (9)	6.9321(1) 18.9967(4) 15.4085(3)	90 95.5820(10) 90	2019.48(6)
45	[{Cu(**L**LH)F}$_4$]F_8	Cubic	*F*-43*c* (219)	37.295(4) 37.295(4) 37.295(4)	90 90 90	51872(10)
46	[Cu(**L**)$_2$(SO_4)]	Orthorhombic	$Pbc2_1$ (29)	7.4158(1) 13.4649(2) 19.5288(5)	90 90 90	1950.01(6)
46 • H_2SO_4	[Cu(**L**LH)$_2$(SO_4)](SO_4)	Trigonal	*P*-3*c*1 (165)	28.3688(3) 28.3688(3) 12.3891(2)	90 90 120	8634.80(19)
47	[Pd(**L**LH)Cl_2]Cl	Orthorhombic	$Pbc2_1$ (29)	12.4445(1) 12.2051(1) 8.3213(1)	90 90 90	1263.89(2)
48	[Pd(**L**LH)Br_2]$_2$[$PdBr_4$]	Triclinic	*P*-1 (2)	8.8314(4) 8.8782(3) 11.5103(6)	69.095(2) 76.249(2) 60.895(2)	734.35(6)
49	[Pd(**L**LH)$_2$](NO_3)$_4$	Monoclinic	$P2_1/c$ (14)	8.3934(11) 16.649(2) 8.6914(11)	90 109.419(4) 90	1145.5(2)
50	[Pd(**L**LH)$_2$](SO_4)$_2$	Monoclinic	$P2_1/n$ (14)	8.2588(2) 17.3414(4) 9.1518(2)	90 99.120(1) 90	1294.14(5)

51	[{Pd(**L**)Cl}$_6$]Cl$_6$	Monoclinic	*I*2/*a* (15)	15.5544(9) 9.6173(5) 17.1240(9)	90 90.000(4) 90	2561.6(2)
52	[{Pd(**L**)Br}$_6$]Br$_6$	Triclinic	*P*-1 (2)	11.924(2) 12.710(3) 13.929(7)	79.12(3) 68.93(3) 88.33(3)	1932.7(7)
53	[Pd{Pd(**L**)Cl$_2$}$_2$Cl$_2$]	Monoclinic	*P*2$_1$/*n* (14)	12.4054(2) 26.6675(5) 12.8312(2)	90 90.701(1) 90	4244.51(12)
54	{[Ag(**L**)](NO$_3$)}$_n$	Monoclinic	*P*2$_1$/*c* (14)	13.717(3) 8.9401(18) 16.635(3)	90 93.60(3) 90	2035.9(7)
55	{[Ag(**L**)](OTf)}$_n$	Monoclinic	*P*2$_1$ (4)	12.4287(5) 8.1038(4) 13.0208(6)	90 10313(2) 90	1258.65(10)
56	{[Zn$_2$(**L**)Cl$_4$]}$_n$	Orthothombic	*Pnma* (62)	11.5041(2) 14.3800(2) 7.8623(1)	90 90 90	1300.65(3)
57	**tbc**	Monoclinic	*I*2/*a* (15)	18.1262(2) 10.4041(1) 25.3348(4)	90 105.974(1) 90	4593.32(10)
61	[Cu(**ttop**)Cl]Cl	Triclinic	*P*-1 (2)	7.5984(3) 11.6384(4) 16.6500(5)	73.439(2) 89.473(2) 84.853(3)	1405.44(8)
62	[{Cu$_2$(**ttop**)Cl$_3$]}$_2$]Cl$_2$	Triclinic	*P*-1 (2)	9.7929(3) 12.8175(5) 13.9117(7)	88.942(2) 78.430(2) 69.323(2)	1597.91(11)

6.2 trans-tach • 3 HCl (29 • 3 HCl)

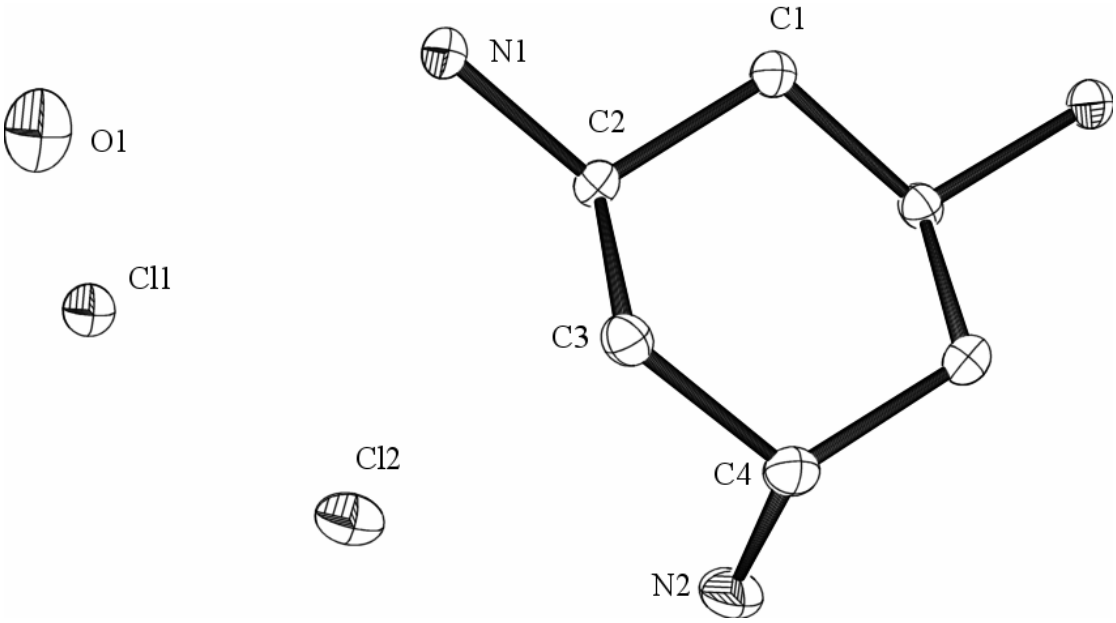
Crystallisation method	Diffusion of ethanol into water solution over 5 days.	
Empirical formula	$C_6H_{20}C_{l3}N_3O$ - ($C_6H_{18}N_3^{3+}$), 3(Cl^-), (H_2O)	
Formula weight	256.60	
Temperature	150(2) K	
Wavelength	0.71073 Å	
Crystal system	Orthorhombic	
Space group	*P n m a* (62)	
Unit cell dimensions	a = 7.2539(2) Å	α = 90°.
	b = 9.8265(3) Å	β = 90°.
	c = 16.4828(6) Å	γ = 90°.
Volume	1174.90(6) $Å^3$	
Z	4	
Density (calculated)	1.451 Mg/m^3	
Absorption coefficient	0.751 mm^{-1}	
F(000)	544	
Crystal description	Colourless plate	
Crystal size	0.32 x 0.28 x 0.2 mm^3	
Theta range for data collection	2.41 to 27.52°.	
Index ranges	0<=h<=9, 0<=k<=12, 0<=l<=21	
Reflections collected	1433	
Independent reflections	1433 [R(int) = 0.0470]	
Completeness to theta = 27.52°	99.8 %	
Absorption correction	Empirical	
Max. and min. transmission	1.029 and 0.963	
Refinement method	Full-matrix least-squares on F^2	
Data / restraints / parameters	1433 / 0 / 73	
Goodness-of-fit on F^2	1.065	
Final R indices [I>2sigma(I)]	R1 = 0.0320, wR2 = 0.0863	
R indices (all data)	R1 = 0.0383, wR2 = 0.0890	
Largest diff. peak and hole	0.594 and -0.711 e.$Å^{-3}$	
Weighting scheme parameters A and B	0.0449 and 1.0347	

Bond lengths [Å] and angles [°]

C(1)-C(2)	1.526(2)	C(2)-C(1)-C(2)#1	109.09(19)
C(1)-C(2)#1	1.526(2)	N(1)-C(2)-C(1)	109.66(13)
C(2)-N(1)	1.493(2)	N(1)-C(2)-C(3)	108.60(13)
C(2)-C(3)	1.527(2)	C(1)-C(2)-C(3)	111.73(15)
C(3)-C(4)	1.523(2)	C(4)-C(3)-C(2)	113.12(15)
C(4)-N(2)	1.516(3)	N(2)-C(4)-C(3)#1	110.79(13)
C(4)-C(3)#1	1.523(2)	N(2)-C(4)-C(3)	110.79(13)
		C(3)#1-C(4)-C(3)	111.78(19)

Symmetry transformations used to generate equivalent atoms:
#1 x,-y+1/2,z

Ortep-3 representation of *trans*-tach • 3 HCl (**29** •3 HCl): thermal ellipsoids at 50% probability, hydrogen atoms are omitted for clarity.



6.3 trans-tach • 3 HBr (29 • 3 HBr)

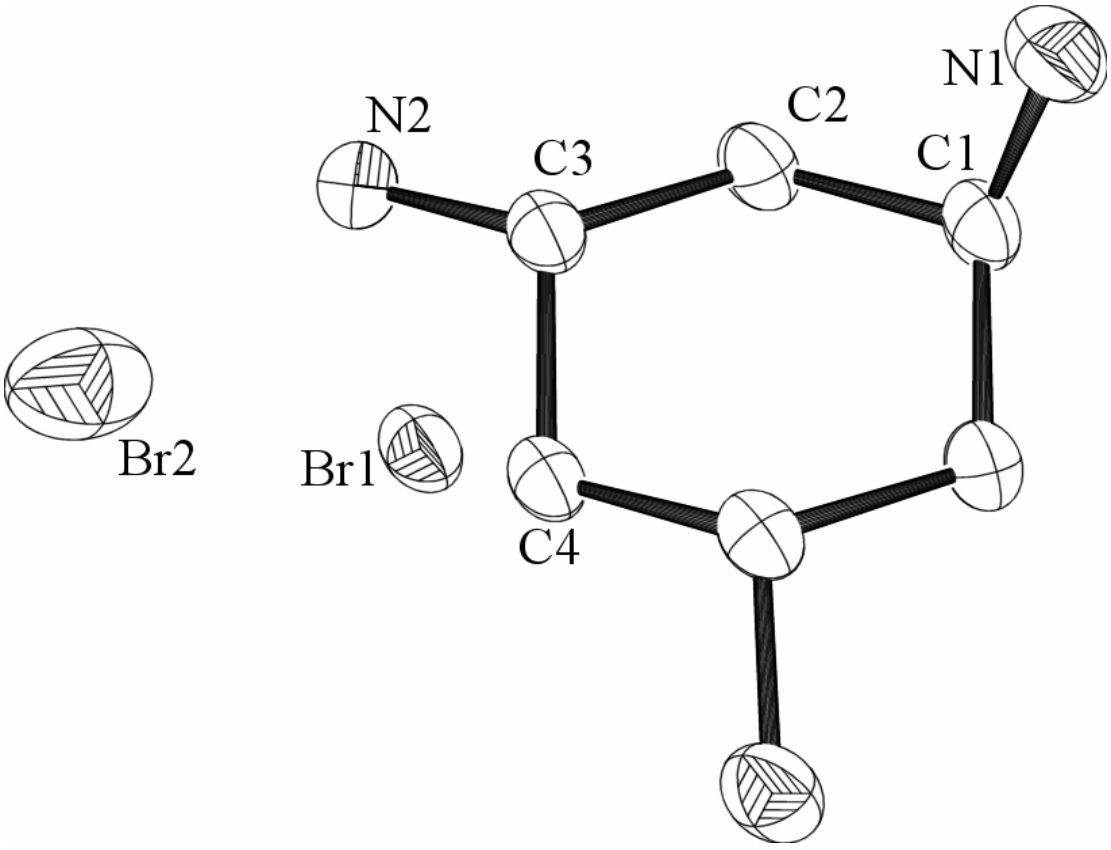
Crystallisation method	Diffusion of ethanol into water solution over 5 days.	
Empirical formula	$C_6H_{18}Br_3N_3$ - ($C_6H_{18}N_3^{3+}$), 3(Br^-)	
Formula weight	371.96	
Temperature	293(2) K	
Wavelength	1.54178 Å	
Crystal system	Monoclinic	
Space group	$P\,2_1/m$ (11)	
Unit cell dimensions	a = 7.3695(2) Å	α = 90°.
	b = 10.6052(3) Å	β = 109.993(1)°.
	c = 8.6123(2) Å	γ = 90°.
Volume	632.53(3) $Å^3$	
Z	2	
Density (calculated)	1.953 Mg/m^3	
Absorption coefficient	11.532 mm^{-1}	
F(000)	360	
Crystal description	Colourless plate	
Crystal size	0.2 x 0.14 x 0.14 mm^3	
Theta range for data collection	5.47 to 70.58°.	
Index ranges	-8<=h<=8, -11<=k<=12, -10<=l<=9	
Reflections collected	3076	
Independent reflections	1149 [R(int) = 0.0260]	
Completeness to theta = 70.58°	89.7 %	
Absorption correction	None	
Refinement method	Full-matrix least-squares on F^2	
Data / restraints / parameters	1149 / 0 / 62	
Goodness-of-fit on F^2	1.093	
Final R indices [I>2sigma(I)]	R1 = 0.0282, wR2 = 0.0727	
R indices (all data)	R1 = 0.0284, wR2 = 0.0729	
Extinction coefficient	0.0199(9)	
Largest diff. peak and hole	0.639 and -0.833 $e.Å^{-3}$	
Weighting scheme parameters A and B	0.0341 and 0.7040	

Bond lengths [Å] and angles [°]

C(1)-N(1)	1.494(6)	N(1)-C(1)-C(2)	112.0(2)
C(1)-C(2)	1.525(3)	N(1)-C(1)-C(2)#1	112.0(2)
C(1)-C(2)#1	1.525(3)	C(2)-C(1)-C(2)#1	112.1(3)
C(2)-C(3)	1.533(3)	C(1)-C(2)-C(3)	113.5(2)
C(3)-N(2)	1.489(4)	N(2)-C(3)-C(4)	109.8(2)
C(3)-C(4)	1.518(3)	N(2)-C(3)-C(2)	107.8(2)
C(4)-C(3)#1	1.518(3)	C(4)-C(3)-C(2)	111.7(2)
		C(3)-C(4)-C(3)#1	108.5(3)

Symmetry transformations used to generate equivalent atoms:
#1 x,-y+1/2,z

Ortep-3 representation of *trans*-tach • 3 HBr (**29** • 3 HBr): thermal ellipsoids at 50% probability, hydrogen atoms are omitted for clarity.



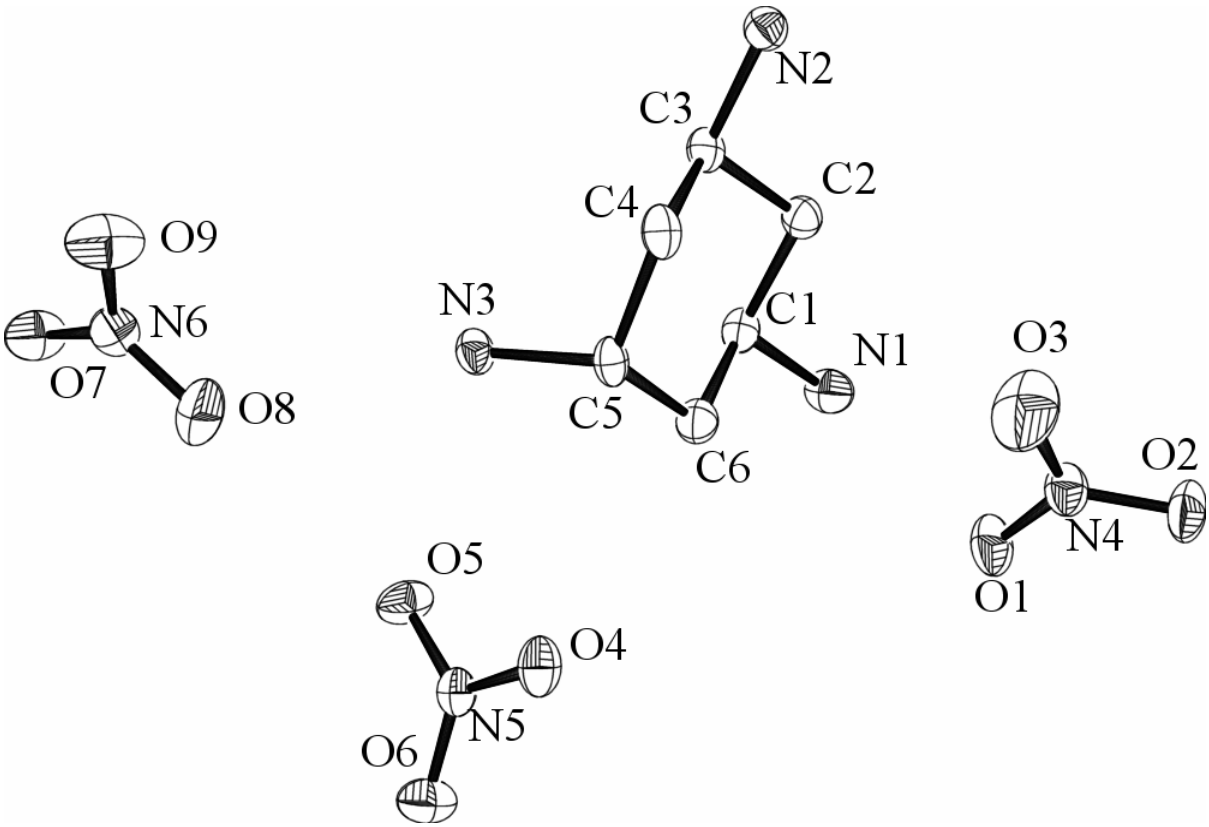
6.4 trans-tach • 3 HNO_3 (29 • 3 HNO_3)

Crystallisation method	Diffusion of ethanol into water solution over 5 days.	
Empirical formula	$C_6H_{18}N_6O_9$ - ($C_6H_{18}N_3^{3+}$), 3(NO_3^-)	
Formula weight	318.26	
Temperature	293(2) K	
Wavelength	1.54178 Å	
Crystal system	Monoclinic	
Space group	*P* 21 (4)	
Unit cell dimensions	a = 6.703(2) Å	α = 90°.
	b = 7.766(2) Å	β = 94.06(2)°.
	c = 12.597(2) Å	γ = 90°.
Volume	654.1(4) $Å^3$	
Z	2	
Density (calculated)	1.616 Mg/m^3	
Absorption coefficient	1.323 mm^{-1}	
F(000)	336	
Crystal description	Colourless plate	
Crystal size	0.2 x 0.2 x 0.1 mm^3	
Theta range for data collection	3.52 to 58.89°.	
Index ranges	-6<=h<=7, -8<=k<=8, -12<=l<=13	
Reflections collected	3065	
Independent reflections	1678 [R(int) = 0.0321]	
Completeness to theta = 58.89°	95.5 %	
Absorption correction	None	
Refinement method	Full-matrix least-squares on F^2	
Data / restraints / parameters	1678 / 1 / 190	
Goodness-of-fit on F^2	1.092	
Final R indices [I>2sigma(I)]	R1 = 0.0340, wR2 = 0.0915	
R indices (all data)	R1 = 0.0345, wR2 = 0.0921	
Absolute structure parameter	-0.2(3)	
Largest diff. peak and hole	0.212 and -0.252 $e.Å^{-3}$	
Weighting scheme parameters A and B	0.0600 and 0.0875	

Bond lengths [Å] and angles [°]

C(1)-N(1)	1.497(3)	N(5)-O(4)	1.258(3)	N(3)-C(5)-C(4)	111.40(18)
C(1)-C(2)	1.512(3)	N(5)-O(5)	1.266(3)	N(3)-C(5)-C(6)	110.49(18)
C(1)-C(6)	1.529(3)	N(6)-O(8)	1.234(3)	C(4)-C(5)-C(6)	113.83(18)
C(2)-C(3)	1.519(3)	N(6)-O(7)	1.253(3)	C(1)-C(6)-C(5)	113.4(2)
C(3)-N(2)	1.491(3)	N(6)-O(9)	1.258(3)	O(3)-N(4)-O(1)	121.8(2)
C(3)-C(4)	1.524(3)	N(1)-C(1)-C(2)	109.41(17)	O(3)-N(4)-O(2)	120.0(2)
C(4)-C(5)	1.523(3)	N(1)-C(1)-C(6)	109.19(19)	O(1)-N(4)-O(2)	118.2(2)
C(5)-N(3)	1.503(3)	C(2)-C(1)-C(6)	111.67(19)	O(6)-N(5)-O(4)	122.1(2)
C(5)-C(6)	1.531(3)	C(1)-C(2)-C(3)	108.53(17)	O(6)-N(5)-O(5)	119.64(19)
N(4)-O(3)	1.227(3)	N(2)-C(3)-C(2)	108.71(17)	O(4)-N(5)-O(5)	118.3(2)
N(4)-O(1)	1.252(3)	N(2)-C(3)-C(4)	109.61(18)	O(8)-N(6)-O(7)	121.2(2)
N(4)-O(2)	1.253(3)	C(2)-C(3)-C(4)	111.60(18)	O(8)-N(6)-O(9)	120.4(2)
N(5)-O(6)	1.231(3)	C(5)-C(4)-C(3)	112.49(18)	O(7)-N(6)-O(9)	118.4(2)

Ortep-3 representation of *trans*-tach • 3 HNO_3 (**29** • 3 HNO_3): thermal ellipsoids at 50% probability, hydrogen atoms are omitted for clarity.



6.5 trans-tach • 3 $HClO_3$ (29 • 3 $HClO_4$)

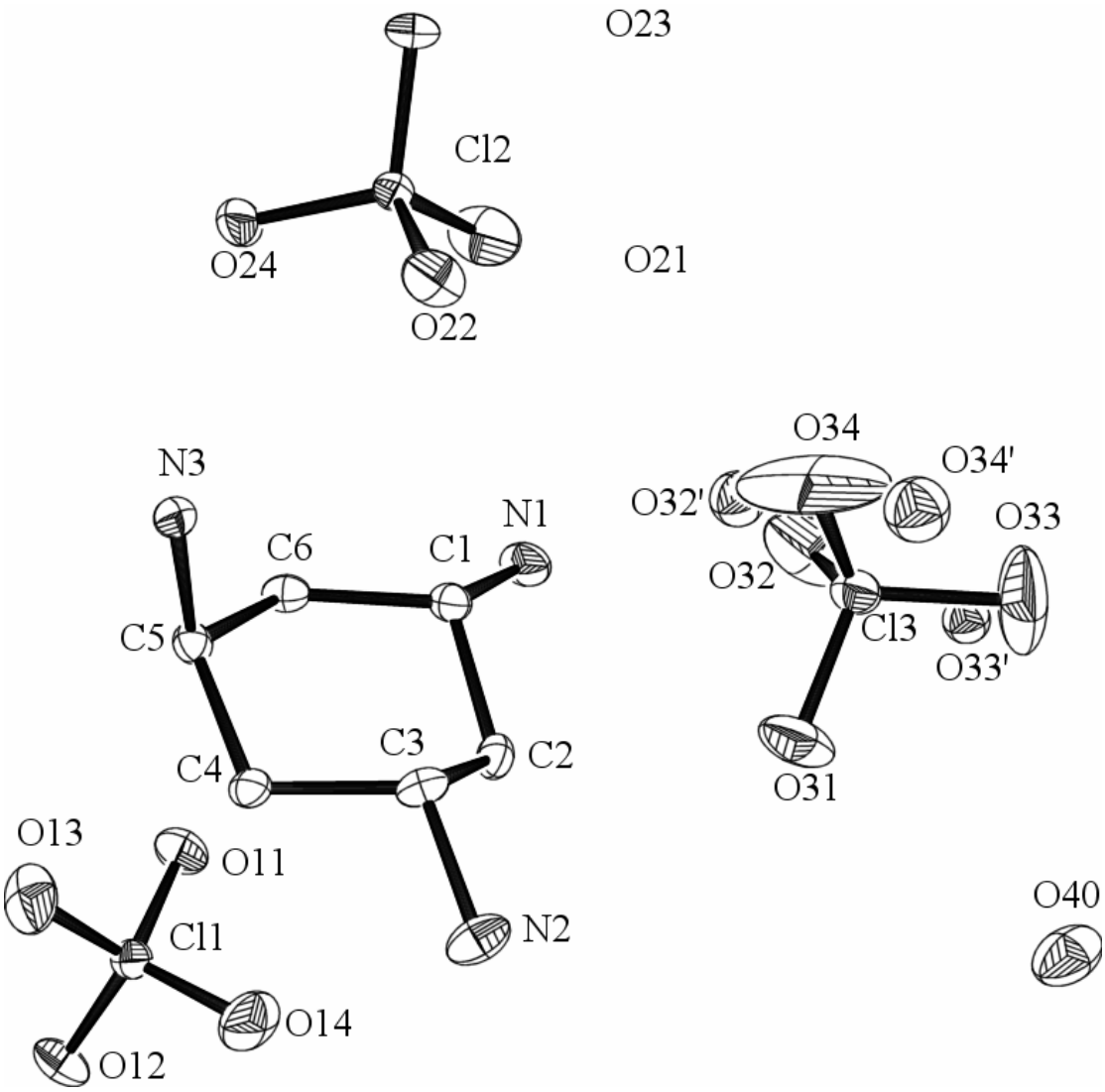
Crystallisation method	Diffusion of ether into methanol solution over 7 days.	
Empirical formula	$C_6H_{20}Cl_3N_3O_{13}$ - ($C_6H_{18}N_3^{3+}$), 3(ClO_4^-), (H_2O)	
Formula weight	448.60	
Temperature	150(2) K	
Wavelength	0.71073 Å	
Crystal system	Monoclinic	
Space group	$P\,2_1/c$ (14)	
Unit cell dimensions	a = 13.2969(4) Å	α= 90°.
	b = 8.1006(3) Å	β=109.772(1)°.
	c = 16.0151(7) Å	γ = 90°.
Volume	1623.33(11) $Å^3$	
Z	4	
Density (calculated)	1.836 Mg/m^3	
Absorption coefficient	0.640 mm^{-1}	
F(000)	928	
Crystal description	Colourless needle	
Crystal size	0.5 x 0.16 x 0.06 mm^3	
Theta range for data collection	1.63 to 27.50°.	
Index ranges	-15<=h<=14, 0<=k<=10, 0<=l<=20	
Reflections collected	10624	
Independent reflections	3363 [R(int) = 0.0000]	
Completeness to theta = 27.50°	89.9 %	
Absorption correction	Empirical	
Max.and min. transmission	1.046 and 0.965	
Refinement method	Full-matrix least-squares on F^2	
Data / restraints / parameters	3363 / 0 / 239	
Goodness-of-fit on F^2	1.053	
Final R indices [I>2sigma(I)]	R1 = 0.0577, wR2 = 0.1139	
R indices (all data)	R1 = 0.0922, wR2 = 0.1322	
Largest diff. peak and hole	0.522 and -0.487 $e.Å^{-3}$	
Weighting scheme parameters A and B	0.0305 and 6.9678	

Refinement details: Rotational disorder for the three oxygen atoms O32, O33 and O34 around the Cl3-O31 bond in the perchlorate counterion involving Cl3.

Bond lengths [Å] and angles [°]

C(5)-N(3)	1.508(5)	N(3)-C(5)-C(4)	109.7(3)	O(14)-Cl(1)-O(11)	109.1(2)
C(5)-C(4)	1.531(5)	N(3)-C(5)-C(6)	111.4(3)	O(13)-Cl(1)-O(11)	108.8(2)
C(5)-C(6)	1.532(5)	C(4)-C(5)-C(6)	114.0(3)	O(12)-Cl(1)-O(11)	108.99(19)
C(6)-C(1)	1.529(5)	C(1)-C(6)-C(5)	112.6(3)	O(21)-Cl(2)-O(23)	109.74(19)
C(1)-N(1)	1.495(5)	N(1)-C(1)-C(2)	109.8(3)	O(21)-Cl(2)-O(22)	109.6(2)
C(1)-C(2)	1.522(5)	N(1)-C(1)-C(6)	110.0(3)	O(23)-Cl(2)-O(22)	110.15(19)
C(2)-C(3)	1.523(5)	C(2)-C(1)-C(6)	110.7(3)	O(21)-Cl(2)-O(24)	109.6(2)
C(3)-N(2)	1.504(5)	C(1)-C(2)-C(3)	106.1(3)	O(23)-Cl(2)-O(24)	109.96(18)
C(3)-C(4)	1.515(5)	N(2)-C(3)-C(4)	110.2(3)	O(22)-Cl(2)-O(24)	107.81(17)
Cl(1)-O(14)	1.426(3)	N(2)-C(3)-C(2)	110.1(3)	O(34)-Cl(3)-O(31)	108.8(3)
Cl(1)-O(13)	1.440(3)	C(4)-C(3)-C(2)	111.3(3)	O(34)-Cl(3)-O(33)	110.2(5)
Cl(1)-O(12)	1.443(3)	C(3)-C(4)-C(5)	112.3(3)	O(31)-Cl(3)-O(33)	108.8(3)
Cl(1)-O(11)	1.448(3)	O(14)-Cl(1)-O(13)	110.6(2)	O(34)-Cl(3)-O(32)	112.6(4)
Cl(2)-O(21)	1.429(3)	O(14)-Cl(1)-O(12)	110.3(2)	O(31)-Cl(3)-O(32)	111.8(2)
Cl(2)-O(23)	1.436(3)	O(13)-Cl(1)-O(12)	108.98(19)	O(33)-Cl(3)-O(32)	104.5(3)
Cl(2)-O(22)	1.440(3)				
Cl(2)-O(24)	1.448(3)				
Cl(3)-O(34)	1.369(5)				
Cl(3)-O(31)	1.439(3)				
Cl(3)-O(33)	1.451(5)				
Cl(3)-O(32)	1.452(4)				

Ortep-3 representation of *trans*-tach • 3 $HClO_3$ (**29** • 3 $HClO_4$): thermal ellipsoids at 50% probability, hydrogen atoms are omitted for clarity.



6.6 [Ni(trans-tachH)$_2$)](NO$_3$)$_4$ (34 • 2 HNO$_3$)

Crystallisation method	Diffusion of ether into methanol solution over 5 days.	
Empirical formula	$C_{12}H_{32}N_{10}NiO_{12}$ - ($C_{12}H_{32}N_6Ni^{4+}$), 4(NO_3^-)	
Formula weight	567.19	
Temperature	293(2) K	
Wavelength	0.71073 A	
Crystal system	Monoclinic	
Space group	*P* $2_1/c$ (14)	
Unit cell dimensions	a = 8.4878(7) A	α = 90°.
	b = 16.5680(19) A	β = 110.425(5)°.
	c = 8.5640(9) A	γ = 90°.
Volume	1128.6(2) A^3	
Z	2	
Density (calculated)	1.669 Mg/m^3	
Absorption coefficient	0.942 mm^{-1}	
F(000)	596	
Crystal description	Orange block	
Crystal size	0.4 x 0.3 x 0.2 mm^3	
Theta range for data collection	2.84 to 25.23°.	
Index ranges	-10<=h<=10, -19<=k<=19, -10<=l<=10	
Reflections collected	6475	
Independent reflections	1933 [R(int) = 0.0225]	
Completeness to theta = 25.23°	94.6 %	
Absorption correction	SADABS, Semi-empirical	
Refinement method	Full-matrix least-squares on F^2	
Data / restraints / parameters	1933 / 0 / 160	
Goodness-of-fit on F^2	1.090	
Final R indices [I>2sigma(I)]	R1 = 0.0314, wR2 = 0.0786	
R indices (all data)	R1 = 0.0324, wR2 = 0.0793	
Largest diff. peak and hole	0.317 and -0.213 $e.A^{-3}$	
Weighting scheme parameters A and B	0.0369 and 0.6208	

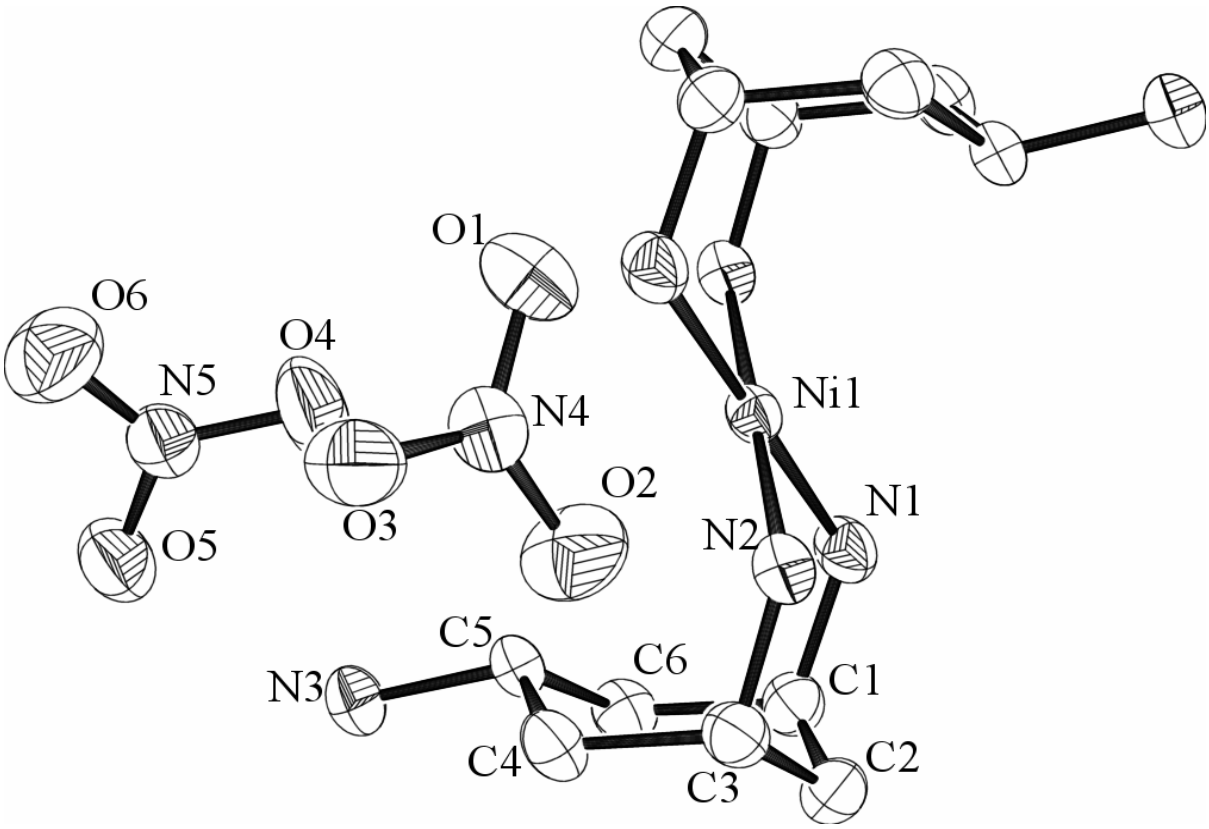
Bond lengths [Å] and angles [°]

C(1)-N(1)	1.495(2)	N(5)-O(5)	1.250(2)	C(1)-N(1)-Ni(1)	120.00(11)
C(1)-C(2)	1.515(3)	Ni(1)-N(2)#1	1.9337(16)	C(3)-N(2)-Ni(1)	119.92(12)
C(1)-C(6)	1.527(3)	Ni(1)-N(1)#1	1.9385(16)	O(1)-N(4)-O(3)	120.32(17)
C(2)-C(3)	1.521(3)			O(1)-N(4)-O(2)	121.21(17)
C(3)-N(2)	1.495(2)	N(1)-C(1)-C(2)	109.18(16)	O(3)-N(4)-O(2)	118.45(17)
C(3)-C(4)	1.523(2)	N(1)-C(1)-C(6)	111.36(16)	O(4)-N(5)-O(6)	122.7(2)
C(4)-C(5)	1.525(2)	C(2)-C(1)-C(6)	111.38(16)	O(4)-N(5)-O(5)	118.74(19)
C(5)-N(3)	1.492(2)	C(1)-C(2)-C(3)	111.38(15)	O(6)-N(5)-O(5)	118.53(18)
C(5)-C(6)	1.521(3)	N(2)-C(3)-C(2)	110.61(16)	N(2)#1-Ni(1)-N(2)	180.000(1)
N(1)-Ni(1)	1.9385(16)	N(2)-C(3)-C(4)	110.98(15)	N(2)#1-Ni(1)-N(1)	90.93(7)
N(2)-Ni(1)	1.9337(16)	C(2)-C(3)-C(4)	110.87(16)	N(2)-Ni(1)-N(1)	89.07(7)
N(4)-O(1)	1.237(2)	C(3)-C(4)-C(5)	112.45(14)	N(2)#1-Ni(1)-N(1)#1	89.07(7)
N(4)-O(3)	1.244(2)	N(3)-C(5)-C(6)	109.05(14)	N(2)-Ni(1)-N(1)#1	90.93(7)
N(4)-O(2)	1.248(2)	N(3)-C(5)-C(4)	109.25(14)	N(1)-Ni(1)-N(1)#1	180.000(1)
N(5)-O(4)	1.231(2)	C(6)-C(5)-C(4)	113.17(15)		
N(5)-O(6)	1.234(2)	C(5)-C(6)-C(1)	112.68(15)		

Symmetry transformations used to generate equivalent atoms:

#1 -x+2,-y,-z+2

Ortep-3 representation of [Ni(*trans*-tachH)$_2$)](NO$_3$)$_4$ (**34** • 2 HNO$_3$): thermal ellipsoids at 50% probability, hydrogen atoms are omitted for clarity.



6.7 [Ni(trans-tach)$_2$)]Cl$_2$ (35)

Crystallisation method	Diffusion of ether into methanol solution over 5 days.	
Empirical formula	$C_{12}H_{40}C_{l2}N_6NiO_5$ - ($C_{12}H_{30}N_6Ni^{2+}$), 2(Cl^-), 5(H_2O)	
Formula weight	478.11	
Temperature	293(2) K	
Wavelength	0.71069 Å	
Crystal system	Monoclinic	
Space group	$P\,2_1/n$ (14)	
Unit cell dimensions	a = 7.2420(9) Å	α = 90°.
	b = 13.126(2) Å	β = 102.216(11)°.
	c = 12.749(3) Å	γ = 90°.
Volume	1184.4(4) Å^3	
Z	2	
Density (calculated)	1.341 Mg/m^3	
Absorption coefficient	1.075 mm^{-1}	
F(000)	512	
Crystal description	Orange block	
Crystal size	0.5 x 0.3 x 0.2 mm^3	
Theta range for data collection	3.10 to 25.41°.	
Index ranges	-7<=h<=8, -15<=k<=15, -15<=l<=15	
Reflections collected	6843	
Independent reflections	2016 [R(int) = 0.0632]	
Completeness to theta = 25.41°	92.3 %	
Absorption correction	None	
Refinement method	Full-matrix least-squares on F^2	
Data / restraints / parameters	2016 / 0 / 125	
Goodness-of-fit on F^2	1.185	
Final R indices [I>2sigma(I)]	R1 = 0.0496, wR2 = 0.1342	
R indices (all data)	R1 = 0.0533, wR2 = 0.1431	
Extinction coefficient	0.022(5)	
Largest diff. peak and hole	0.448 and -0.685 e.Å^{-3}	
Weighting scheme parameters A and B	0.0595 and 1.7613	

Refinement details: The two protons of each pendant amino moiety were refined as a methyl group subsequently riding with two hydrogen atoms disordered over three positions.

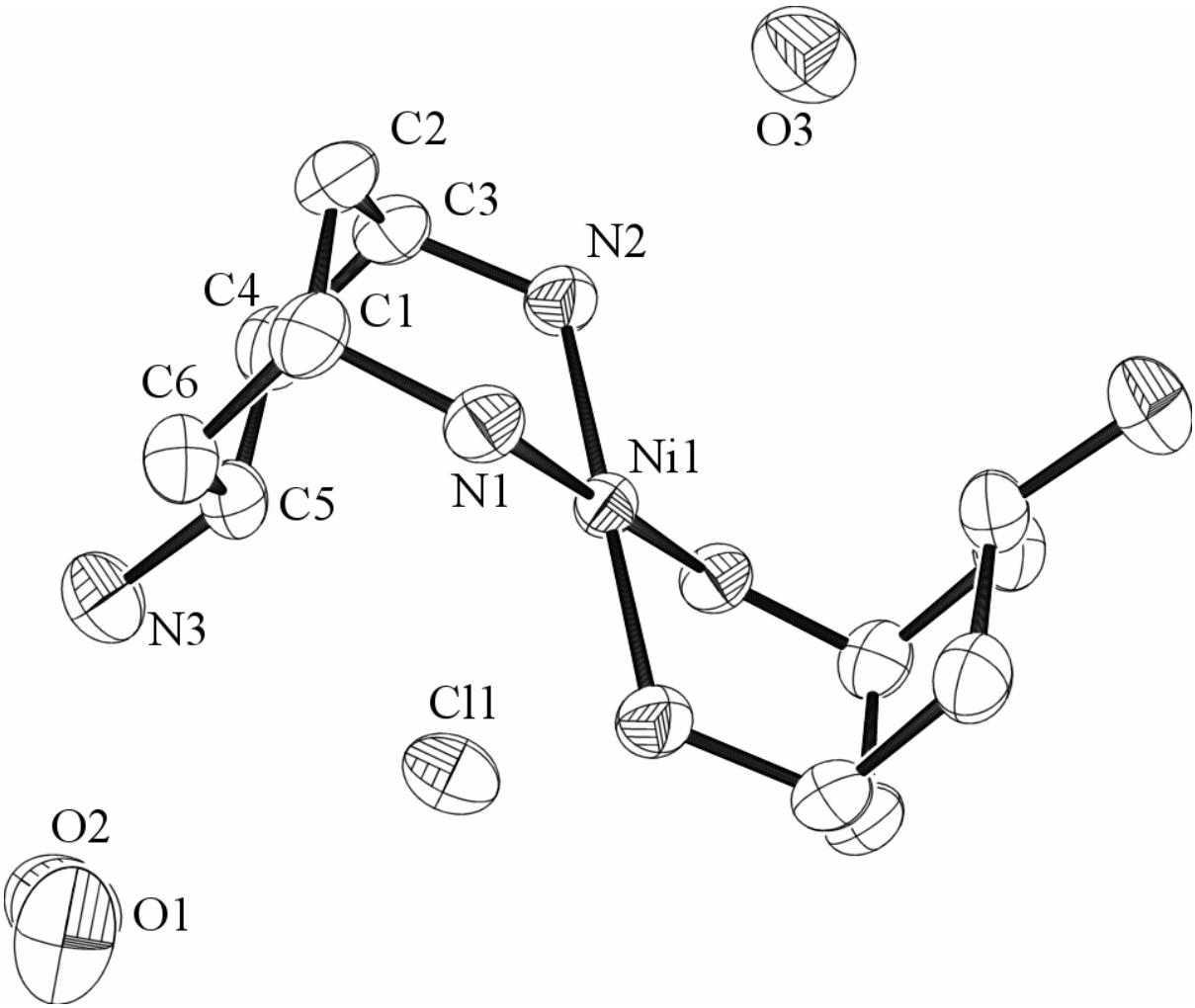
Bond lengths [Å] and angles [°]

C(1)-N(1)	1.491(5)	N(1)-C(1)-C(2)	110.0(3)	C(6)-C(5)-C(4)	112.0(3)
C(1)-C(2)	1.518(6)	N(1)-C(1)-C(6)	110.8(3)	C(5)-C(6)-C(1)	113.5(3)
C(1)-C(6)	1.535(6)	C(2)-C(1)-C(6)	110.9(4)	C(1)-N(1)-Ni(1)	119.4(2)
C(2)-C(3)	1.511(6)	C(3)-C(2)-C(1)	111.8(3)	C(3)-N(2)-Ni(1)	119.3(2)
C(3)-N(2)	1.491(5)	N(2)-C(3)-C(2)	110.1(3)	N(2)-Ni(1)-N(2)#1	180.00(10)
C(3)-C(4)	1.534(6)	N(2)-C(3)-C(4)	110.4(3)	N(2)-Ni(1)-N(1)	90.34(13)
C(4)-C(5)	1.535(6)	C(2)-C(3)-C(4)	111.6(3)	N(2)#1-Ni(1)-N(1)	89.66(13)
C(5)-N(3)	1.498(5)	C(3)-C(4)-C(5)	113.2(3)	N(2)-Ni(1)-N(1)#1	89.66(13)
C(5)-C(6)	1.509(6)	N(3)-C(5)-C(6)	109.5(3)	N(2)#1-Ni(1)-N(1)#1	90.34(13)
N(1)-Ni(1)	1.945(3)	N(3)-C(5)-C(4)	112.0(4)	N(1)-Ni(1)-N(1)#1	180.000(1)
N(2)-Ni(1)	1.935(3)				
Ni(1)-N(2)#1	1.935(3)				
Ni(1)-N(1)#1	1.945(3)				

Symmetry transformations used to generate equivalent atoms:

#1 -x+2,-y,-z+1

Ortep-3 representation of [Ni(*trans*-tach)$_2$)]Cl$_2$ (**35**): thermal ellipsoids at 50% probability, hydrogen atoms are omitted for clarity.



6.8 [Cu(trans-tach)$_2$](NO$_3$)$_2$ · 0.5 HNO$_3$ (36 · 0.5 HNO$_3$)

Crystallisation method	Diffusion of ether into methanol solution over 5 days.	
Empirical formula	$C_{26}H_{70}Cu_2N_{18}O_{20}$ - ($C_{12}H_{30}N_6Cu^{2+}$), ($C_{12}H_{32}N_6Cu^{4+}$), 6(NO_3^-), 2(CH_3OH)	
Formula weight	1082.08	
Temperature	293(2) K	
Wavelength	0.71069 Å	
Crystal system	Triclinic	
Space group	*P* -1 (2)	
Unit cell dimensions	a = 10.674(3) Å	α = 93.717(14)°.
	b = 12.013(3) Å	β = 108.110(8)°.
	c = 9.9374(18) Å	γ = 72.970(7)°.
Volume	1157.5(5) Å^3	
Z	1	
Density (calculated)	1.552 Mg/m^3	
Absorption coefficient	1.011 mm^{-1}	
F(000)	570	
Crystal description	Red plate	
Crystal size	0.3 x 0.2 x 0.08 mm^3	
Theta range for data collection	2.10 to 25.18°.	
Index ranges	-12<=h<=12, -14<=k<=12, -11<=l<=11	
Reflections collected	6121	
Independent reflections	3417 [R(int) = 0.0605]	
Completeness to theta = 25.18°	82.1 %	
Absorption correction	None	
Refinement method	Full-matrix least-squares on F^2	
Data / restraints / parameters	3417 / 0 / 331	
Goodness-of-fit on F^2	1.202	
Final R indices [I>2sigma(I)]	R1 = 0.0898, wR2 = 0.1685	
R indices (all data)	R1 = 0.1037, wR2 = 0.1775	
Largest diff. peak and hole	0.428 and -0.561 e.Å^{-3}	
Weighting scheme parameters A and B	0.0269 and 6.2337	

Refinement details: The asymmetric unit comprises two crystallographic independent complex units, one of which is protonated (involving Cu2) and the other is not (involving Cu1). This protonation assignment is based on refinement data. The two protons of the non-protonated pendant amino moiety were refined as a methyl group subsequently riding with two hydrogen atoms disordered over three positions. The oxygen atoms of nitrate counterion involving N9 are disordered over two positions.

Bond lengths [Å] and angles [°]

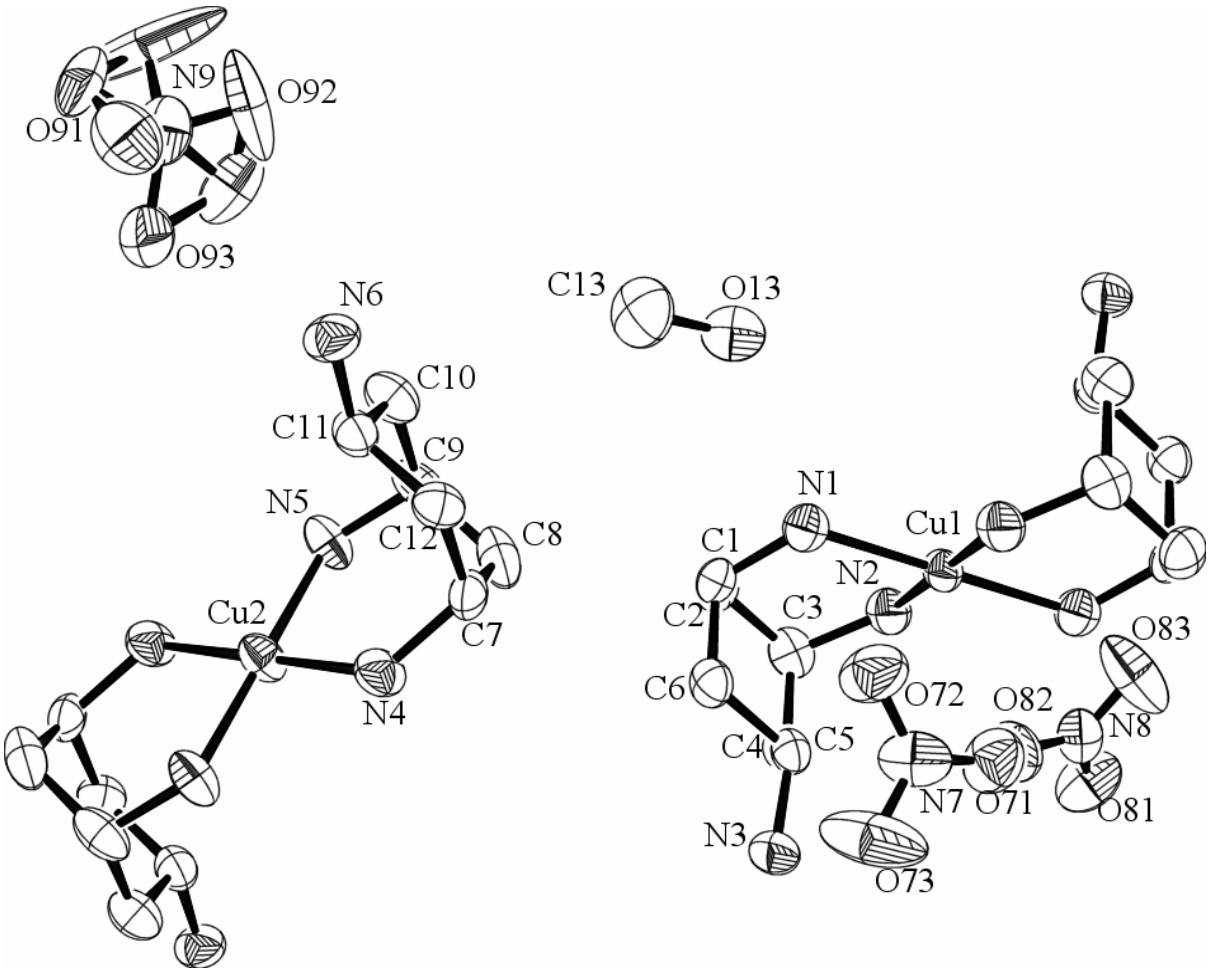
C(1)-N(1)	1.489(9)	Cu(1)-N(2)#1	2.029(6)	C(7)-N(4)-Cu(2)	124.0(5)
C(1)-C(2)	1.515(11)	Cu(2)-N(5)#2	2.015(6)	C(9)-N(5)-Cu(2)	124.2(5)
C(1)-C(6)	1.538(11)	Cu(2)-N(4)#2	2.018(6)	O(73)-N(7)-O(71)	121.5(9)
C(2)-C(3)	1.516(11)	O(91)-O(93')	1.14(3)	O(73)-N(7)-O(72)	119.4(9)
C(3)-N(2)	1.494(9)	O(91)-O(91')	1.42(2)	O(71)-N(7)-O(72)	119.0(8)
C(3)-C(4)	1.520(11)	O(91')-O(93)	1.63(2)	O(83)-N(8)-O(82)	118.6(9)
C(4)-C(5)	1.519(10)	O(92')-O(92)	1.08(2)	O(83)-N(8)-O(81)	122.1(8)
C(5)-N(3)	1.478(10)	O(92')-O(93)	1.37(3)	O(82)-N(8)-O(81)	119.3(8)
C(5)-C(6)	1.521(10)	O(92)-O(93')	1.53(3)	O(92)-N(9)-O(91)	131(2)
C(7)-C(8)	1.505(12)			O(92)-N(9)-O(92')	55.3(14)
C(7)-N(4)	1.507(9)	N(1)-C(1)-C(2)	110.8(6)	O(91)-N(9)-O(92')	158.2(17)
C(7)-C(12)	1.517(10)	N(1)-C(1)-C(6)	110.0(6)	O(92)-N(9)-O(91')	122.1(14)
C(8)-C(9)	1.537(12)	C(2)-C(1)-C(6)	110.8(6)	O(91)-N(9)-O(91')	71.7(14)
C(9)-N(5)	1.493(9)	C(1)-C(2)-C(3)	113.3(6)	O(92')-N(9)-O(91')	125.1(15)
C(9)-C(10)	1.531(11)	N(2)-C(3)-C(2)	110.1(6)	O(92)-N(9)-O(93')	79(2)
C(10)-C(11)	1.497(10)	N(2)-C(3)-C(4)	110.6(6)	O(91)-N(9)-O(93')	55.6(17)
C(11)-N(6)	1.500(9)	C(2)-C(3)-C(4)	111.5(7)	O(92')-N(9)-O(93')	116.0(17)
C(11)-C(12)	1.530(10)	C(5)-C(4)-C(3)	113.9(6)	O(91')-N(9)-O(93')	116.5(14)
C(13)-O(13)	1.429(11)	N(3)-C(5)-C(4)	109.6(6)	O(92)-N(9)-O(93)	116.5(19)
N(1)-Cu(1)	2.025(6)	N(3)-C(5)-C(6)	109.9(6)	O(91)-N(9)-O(93)	111.8(14)
N(2)-Cu(1)	2.029(6)	C(4)-C(5)-C(6)	109.8(6)	O(92')-N(9)-O(93)	64.4(14)
N(4)-Cu(2)	2.018(6)	C(5)-C(6)-C(1)	113.8(6)	O(91')-N(9)-O(93)	77.8(13)
N(5)-Cu(2)	2.015(6)	C(8)-C(7)-N(4)	110.0(6)	O(93')-N(9)-O(93)	150(2)
N(7)-O(73)	1.217(10)	C(8)-C(7)-C(12)	112.6(7)	N(1)#1-Cu(1)-N(1)	180.000(1)
N(7)-O(71)	1.249(9)	N(4)-C(7)-C(12)	111.4(6)	N(1)#1-Cu(1)-N(2)	88.7(3)
N(7)-O(72)	1.252(9)	C(7)-C(8)-C(9)	112.6(6)	N(1)-Cu(1)-N(2)	91.3(3)
N(8)-O(83)	1.228(10)	N(5)-C(9)-C(10)	112.2(7)	N(1)#1-Cu(1)-N(2)#1	91.3(3)
N(8)-O(82)	1.233(9)	N(5)-C(9)-C(8)	110.1(7)	N(1)-Cu(1)-N(2)#1	88.7(3)
N(8)-O(81)	1.274(10)	C(10)-C(9)-C(8)	111.7(7)	N(2)-Cu(1)-N(2)#1	180.000(1)
N(9)-O(92)	1.141(16)	C(11)-C(10)-C(9)	112.1(7)	N(5)-Cu(2)-N(5)#2	180.000(2)
N(9)-O(91)	1.182(16)	C(10)-C(11)-N(6)	109.6(6)	N(5)-Cu(2)-N(4)#2	85.6(2)
N(9)-O(92')	1.194(17)	C(10)-C(11)-C(12)	111.5(6)	N(5)#2-Cu(2)-N(4)#2	94.4(2)
N(9)-O(91')	1.240(15)	N(6)-C(11)-C(12)	110.4(6)	N(5)-Cu(2)-N(4)	94.4(2)
N(9)-O(93')	1.250(19)	C(7)-C(12)-C(11)	112.4(6)	N(5)#2-Cu(2)-N(4)	85.6(2)
N(9)-O(93)	1.359(18)	C(1)-N(1)-Cu(1)	121.3(5)	N(4)#2-Cu(2)-N(4)	180.000(1)
Cu(1)-N(1)#1	2.025(6)	C(3)-N(2)-Cu(1)	121.1(5)	O(93')-O(91)-N(9)	65.2(14)
O(93')-O(91)-O(91')	111(2)	O(92)-O(92')-O(93)	120(2)	N(9)-O(93)-O(91')	47.9(8)
N(9)-O(91)-O(91')	56.0(11)	N(9)-O(92')-O(93)	63.6(13)	O(92')-O(93)-O(91')	91.6(12)

N(9)-O(91')-O(91)	52.3(9)	O(92')-O(92)-N(9)	64.9(13)	O(91)-O(93')-N(9)	59.2(15)
N(9)-O(91')-O(93)	54.3(11)	O(92')-O(92)-O(93')	104(2)	O(91)-O(93')-O(92)	104.2(18)
O(91)-O(91')-O(93)	86.9(13)	N(9)-O(92)-O(93')	53.5(15)	N(9)-O(93')-O(92)	47.2(11)
O(92)-O(92')-N(9)	59.9(14)	N(9)-O(93)-O(92')	51.9(10)		

Symmetry transformations used to generate equivalent atoms:

#1 -x+1,-y+1,-z+1 #2 -x+2,-y+2,-z+2

Ortep-3 representation of [Cu(*trans*-tach)$_2$](NO$_3$)$_2$ • 0.5 HNO$_3$ (**36** • 0.5 HNO$_3$): thermal ellipsoids at 50% probability, hydrogen atoms are omitted for clarity.



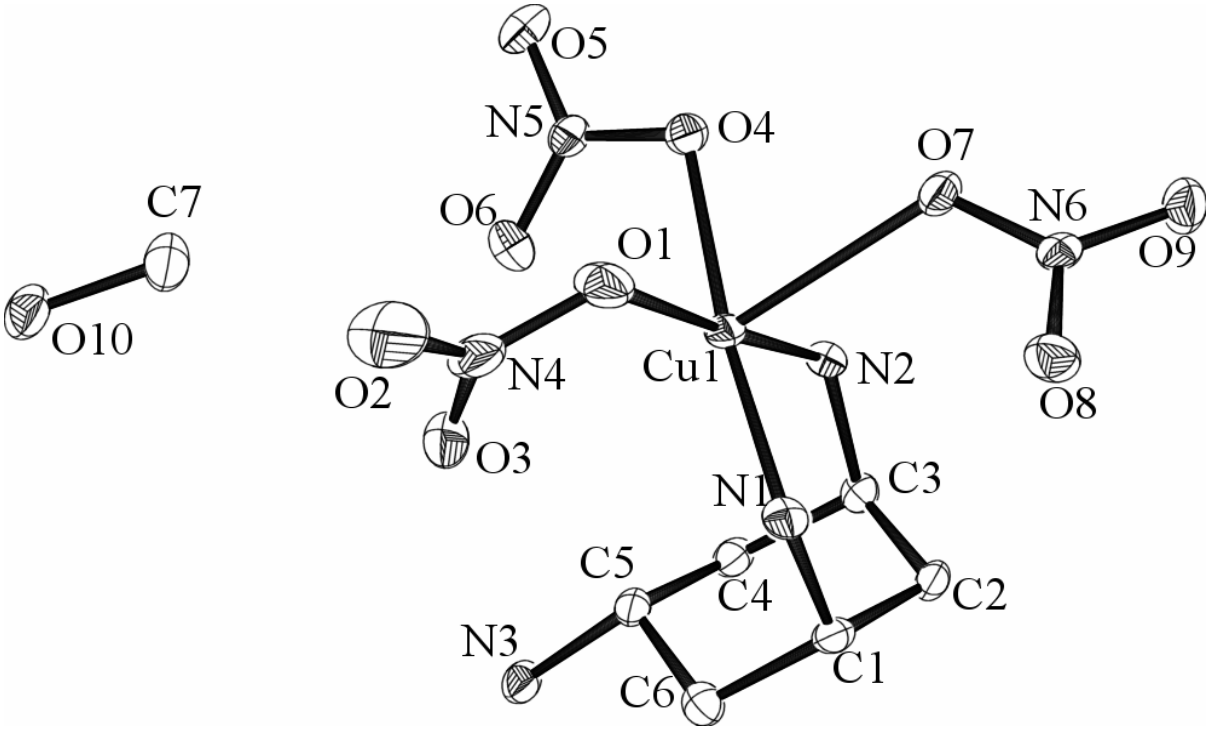
6.9 *[Cu(trans-tachH)(NO$_3$)$_3$] (37)*

Crystallisation method	Diffusion of acetone into methanol / water solution over 5 days.	
Empirical formula	$C_7H_{20}CuN_6O_{10}$ – ($C_6H_{16}N_6CuO_9$), (CH_3OH)	
Formula weight	411.83	
Temperature	150(2) K	
Wavelength	1.54178 Å	
Crystal system	Orthorhombic	
Space group	*P b n* 2_1 (33)	
Unit cell dimensions	a = 9.14560(10) Å	α = 90°.
	b = 16.7280(2) Å	β = 90°.
	c = 10.0301(2) Å	γ = 90°.
Volume	1534.48(4) Å^3	
Z	4	
Density (calculated)	1.783 Mg/m^3	
Absorption coefficient	2.656 mm^{-1}	
F(000)	852	
Crystal description	Blue blocks	
Crystal size	0.24 x 0.2 x 0.2 mm^3	
Theta range for data collection	6.89 to 70.59°.	
Index ranges	-11<=h<=10, -19<=k<=17, -10<=l<=12	
Reflections collected	6032	
Independent reflections	2412 [R(int) = 0.0289]	
Completeness to theta = 70.59°	93.4 %	
Absorption correction	None	
Refinement method	Full-matrix least-squares on F^2	
Data / restraints / parameters	2412 / 1 / 217	
Goodness-of-fit on F^2	1.104	
Final R indices [I>2sigma(I)]	R1 = 0.0360, wR2 = 0.0979	
R indices (all data)	R1 = 0.0362, wR2 = 0.0981	
Absolute structure parameter	0.00	
Largest diff. peak and hole	0.466 and -0.989 e.Å^{-3}	
Weighting scheme parameters A and B	0.0619 and 0.9033	

Bond lengths [Å] and angles [°]

C(1)-N(1)	1.496(4)	N(6)-O(8)	1.253(4)	C(3)-N(2)-Cu(1)	122.5(2)
C(1)-C(2)	1.520(5)	N(6)-O(7)	1.259(3)	O(2)-N(4)-O(3)	123.2(3)
C(1)-C(6)	1.528(4)	O(1)-Cu(1)	1.991(3)	O(2)-N(4)-O(1)	118.1(3)
C(2)-C(3)	1.527(5)	O(4)-Cu(1)	2.032(3)	O(3)-N(4)-O(1)	118.7(3)
C(3)-N(2)	1.492(4)			O(5)-N(5)-O(6)	123.4(3)
C(3)-C(4)	1.523(4)	N(1)-C(1)-C(2)	110.7(3)	O(5)-N(5)-O(4)	118.2(3)
C(4)-C(5)	1.527(5)	N(1)-C(1)-C(6)	110.2(3)	O(6)-N(5)-O(4)	118.3(3)
C(5)-N(3)	1.493(3)	C(2)-C(1)-C(6)	110.9(3)	O(9)-N(6)-O(8)	120.2(3)
C(5)-C(6)	1.527(5)	C(1)-C(2)-C(3)	114.1(2)	O(9)-N(6)-O(7)	120.3(3)
C(7)-O(10)	1.441(4)	N(2)-C(3)-C(4)	110.9(2)	O(8)-N(6)-O(7)	119.5(3)
N(1)-Cu(1)	1.989(3)	N(2)-C(3)-C(2)	109.2(3)	N(4)-O(1)-Cu(1)	115.5(2)
N(2)-Cu(1)	1.995(3)	C(4)-C(3)-C(2)	112.0(3)	N(5)-O(4)-Cu(1)	108.1(2)
N(4)-O(2)	1.239(5)	C(3)-C(4)-C(5)	112.1(3)	N(1)-Cu(1)-O(1)	90.04(13)
N(4)-O(3)	1.239(4)	N(3)-C(5)-C(6)	107.6(3)	N(1)-Cu(1)-N(2)	94.83(10)
N(4)-O(1)	1.289(4)	N(3)-C(5)-C(4)	109.8(3)	O(1)-Cu(1)-N(2)	174.99(14)
N(5)-O(5)	1.233(4)	C(6)-C(5)-C(4)	111.9(2)	N(1)-Cu(1)-O(4)	171.22(10)
N(5)-O(6)	1.236(4)	C(5)-C(6)-C(1)	111.3(3)	O(1)-Cu(1)-O(4)	87.13(10)
N(5)-O(4)	1.291(3)	C(1)-N(1)-Cu(1)	123.2(2)	N(2)-Cu(1)-O(4)	88.22(14)
N(6)-O(9)	1.242(4)				

Ortep-3 representation of [Cu(*trans*-tachH)$(NO_3)_3$] (**37**): thermal ellipsoids at 50% probability, hydrogen atoms are omitted for clarity.



6.10 [Cu(trans-tach)$_2$]Br$_2$ (syn-38)

Crystallisation method	Diffusion of ether into methanol solution overnight.	
Empirical formula	$C_{13}H_{34}Br_2CuN_6O$ – ($C_{12}H_{30}N_6Cu^{2+}$), 2(Br^-), (CH_3OH)	
Formula weight	513.82	
Temperature	293(2) K	
Wavelength	1.54178 Å	
Crystal system	Orthorhombic	
Space group	*P n m a* (62)	
Unit cell dimensions	a = 13.52620(10) Å	α = 90°.
	b = 12.8552(2) Å	β = 90°.
	c = 11.8161(2) Å	γ = 90°.
Volume	2054.61(5) Å^3	
Z	4	
Density (calculated)	1.661 Mg/m^3	
Absorption coefficient	6.153 mm^{-1}	
F(000)	1044	
Crystal description	Violet blocks	
Crystal size	0.3 x 0.2 x 0.2 mm^3	
Theta range for data collection	4.97 to 70.65°.	
Index ranges	-16<=h<=14, -12<=k<=15, -6<=l<=14	
Reflections collected	6292	
Independent reflections	1970 [R(int) = 0.0465]	
Completeness to theta = 70.65°	95.4 %	
Absorption correction	None	
Refinement method	Full-matrix least-squares on F^2	
Data / restraints / parameters	1970 / 0 / 115	
Goodness-of-fit on F^2	1.086	
Final R indices [I>2sigma(I)]	R1 = 0.0589, wR2 = 0.1732	
R indices (all data)	R1 = 0.0645, wR2 = 0.1809	
Largest diff. peak and hole	0.636 and -1.247 e.Å^{-3}	
Weighting scheme parameters A and B	0.1253 and 1.2447	

Refinement details: The atoms Cu(1), Br(1) and Br(2) are located on special positions with half occupancy, with disorder over two positions for the bromide counterion. The oxygen atom O13 of the methanol solvent molecule is also disordered over two positions. The two protons of each pendant amine moiety were refined as a methyl group subsequently riding with two hydrogen atoms disordered over three positions.

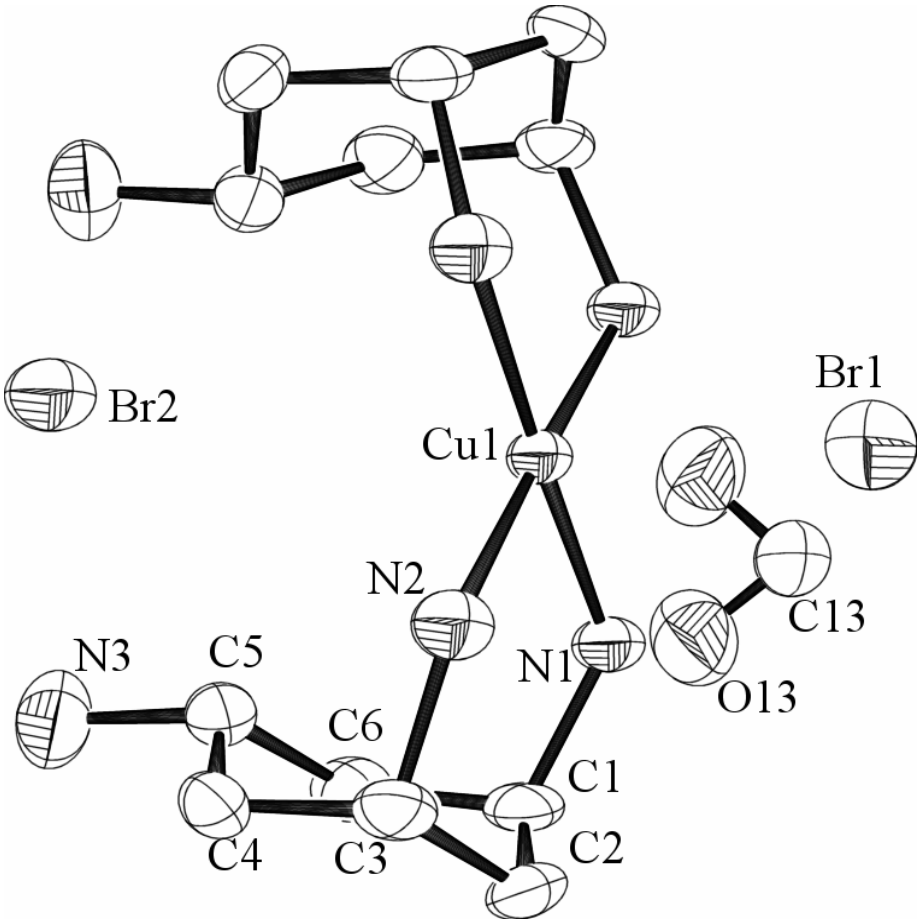
Bond lengths [Å] and angles [°]

C(1)-N(1)	1.497(5)	O(13)-O(13)#1	1.70(3)	N(3)-C(5)-C(6)	112.8(4)
C(1)-C(2)	1.507(8)	Cu(1)-N(1)#1	2.008(4)	C(4)-C(5)-C(6)	110.4(4)
C(1)-C(6)	1.525(7)	Cu(1)-N(2)#1	2.039(4)	C(1)-C(6)-C(5)	114.1(4)
C(2)-C(3)	1.529(6)			O(13)#1-C(13)-O(13)	79.6(15)
C(3)-N(2)	1.495(5)	N(1)-C(1)-C(2)	109.6(4)	C(1)-N(1)-Cu(1)	122.0(3)
C(3)-C(4)	1.517(7)	N(1)-C(1)-C(6)	111.1(4)	C(3)-N(2)-Cu(1)	124.1(3)
C(4)-C(5)	1.506(7)	C(2)-C(1)-C(6)	112.4(4)	C(13)-O(13)-O(13)#1	50.2(8)
C(5)-N(3)	1.488(6)	C(1)-C(2)-C(3)	113.3(4)	N(1)-Cu(1)-N(1)#1	87.3(2)
C(5)-C(6)	1.535(6)	N(2)-C(3)-C(4)	110.0(3)	N(1)-Cu(1)-N(2)	91.89(15)
C(13)-O(13)#1	1.329(16)	N(2)-C(3)-C(2)	110.6(3)	N(1)#1-Cu(1)-N(2)	178.36(16)
C(13)-O(13)	1.329(16)	C(4)-C(3)-C(2)	110.4(4)	N(1)-Cu(1)-N(2)#1	178.36(16)
N(1)-Cu(1)	2.008(4)	C(5)-C(4)-C(3)	113.0(3)	N(1)#1-Cu(1)-N(2)#1	91.89(15)
N(2)-Cu(1)	2.039(4)	N(3)-C(5)-C(4)	109.0(4)	N(2)-Cu(1)-N(2)#1	88.8(2)

Symmetry transformations used to generate equivalent atoms:

#1 x,-y+1/2,z

Ortep-3 representation of [Cu(*trans*-tach)$_2$]Br$_2$ (*syn*-**38**): thermal ellipsoids at 50% probability, hydrogen atoms are omitted for clarity.



6.11 [Cu(trans-tach)$_2$]Br$_2$ (twist-38)

Crystallisation method	Layer of ether on to methanolic solution within 1 hour (!). Crystals decompose within 2-3 hours of formation.	
Empirical formula	$C_{12}H_{37}Br_3CuN_6O_3$ – ($C_{12}H_{31}N_6Cu^{3+}$), 3(Br^-), 3(H_2O)	
Formula weight	616.75	
Temperature	160(2) K	
Wavelength	1.54178 Å	
Crystal system	Monoclinic	
Space group	*P* $2_1/c$ (14)	
Unit cell dimensions	a = 13.5958(13) Å	α = 90°.
	b = 14.0133(17) Å	β = 106.385(6)°.
	c = 13.1036(10) Å	γ = 90°.
Volume	2395.1(4) Å^3	
Z	4	
Density (calculated)	1.710 Mg/m^3	
Absorption coefficient	7.335 mm^{-1}	
F(000)	1236	
Crystal description	Blue plates	
Crystal size	0.2 x 0.14 x 0.06 mm^3	
Theta range for data collection	4.63 to 68.42°.	
Index ranges	-14<=h<=15, -12<=k<=15, -14<=l<=15	
Reflections collected	11991	
Independent reflections	4011 [R(int) = 0.1420]	
Completeness to theta = 68.42°	91.1 %	
Absorption correction	None	
Refinement method	Full-matrix least-squares on F^2	
Data / restraints / parameters	4011 / 0 / 217	
Goodness-of-fit on F^2	1.033	
Final R indices [I>2sigma(I)]	R1 = 0.1327, wR2 = 0.3246	
R indices (all data)	R1 = 0.1834, wR2 = 0.3657	
Largest diff. peak and hole	3.211 and -2.502 e.Å^{-3}	
Weighting scheme parameters A and B	0.1178 and 129.5854	

Refinement details: Poor crystal quality resulted in a weak dataset. The structure was refined containing three bromide counterions. Both pendant amine moieties were refined as methyl group subsequently riding. Three water molecules are disordered over four positions O1, O2, O3 and O4 each with three quarters occupancy.

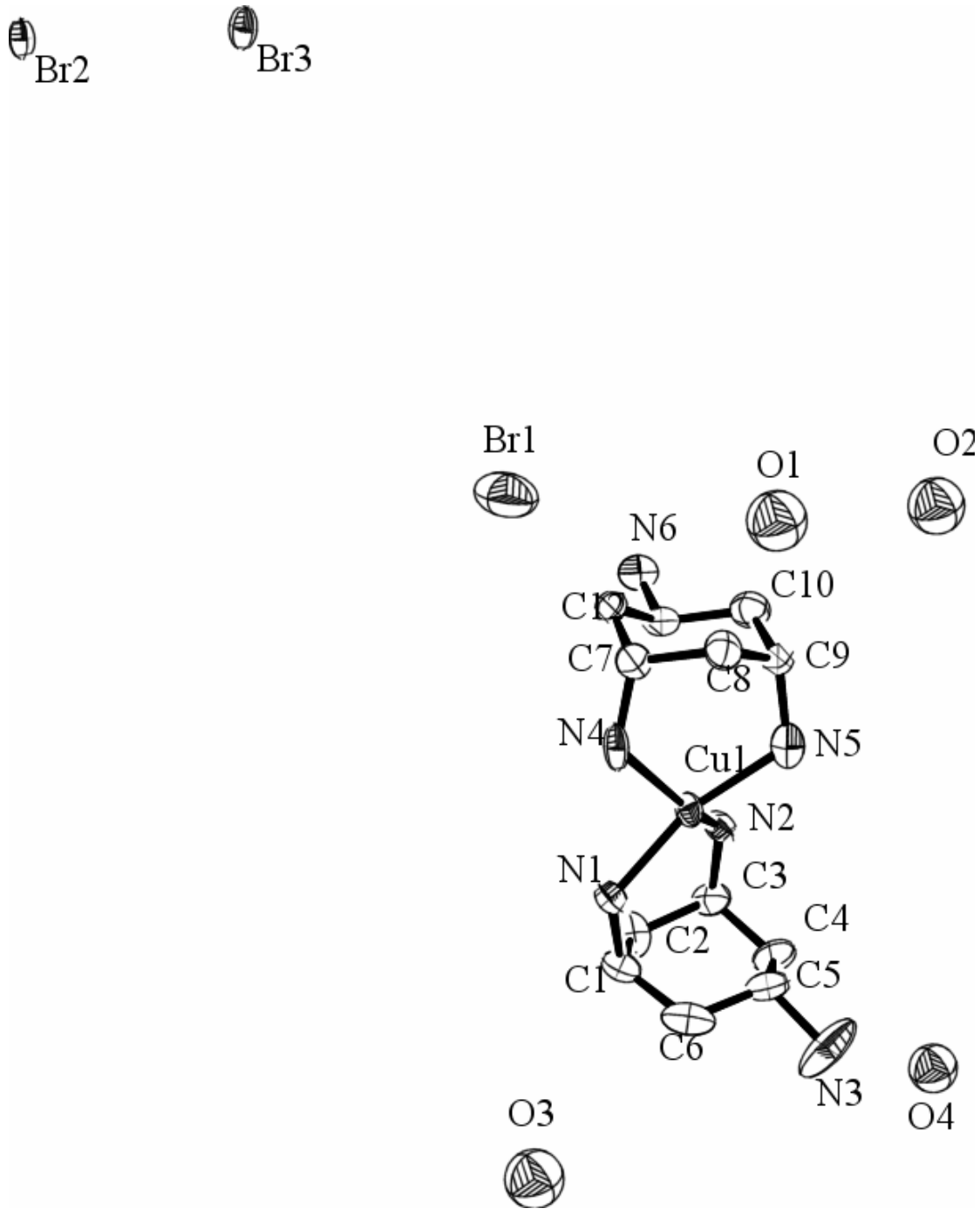
Bond lengths [Å] and angles [°]

C(1)-N(1)	1.497(17)	N(5)-Cu(1)	2.010(11)	C(8)-C(7)-C(12)	109.7(11)
C(1)-C(6)	1.51(2)	O(1)-O(3)#1	1.53(3)	C(9)-C(8)-C(7)	115.4(12)
C(1)-C(2)	1.52(2)	O(2)-O(4)#2	1.58(3)	C(8)-C(9)-N(5)	113.1(11)
C(2)-C(3)	1.54(2)	O(3)-O(1)#1	1.53(3)	C(8)-C(9)-C(10)	111.6(12)
C(3)-N(2)	1.454(16)	O(4)-O(2)#2	1.58(3)	N(5)-C(9)-C(10)	108.7(11)
C(3)-C(4)	1.51(2)			C(9)-C(10)-C(11)	112.7(11)
C(4)-C(5)	1.55(2)	N(1)-C(1)-C(6)	111.2(12)	N(6)-C(11)-C(12)	112.6(12)
C(5)-N(3)	1.48(2)	N(1)-C(1)-C(2)	108.2(11)	N(6)-C(11)-C(10)	110.8(11)
C(5)-C(6)	1.49(2)	C(6)-C(1)-C(2)	113.0(13)	C(12)-C(11)-C(10)	110.6(13)
C(7)-N(4)	1.499(17)	C(1)-C(2)-C(3)	113.4(12)	C(11)-C(12)-C(7)	112.2(12)
C(7)-C(8)	1.53(2)	N(2)-C(3)-C(4)	111.1(13)	C(1)-N(1)-Cu(1)	122.0(9)
C(7)-C(12)	1.54(2)	N(2)-C(3)-C(2)	110.7(11)	C(3)-N(2)-Cu(1)	124.8(8)
C(8)-C(9)	1.49(2)	C(4)-C(3)-C(2)	110.1(11)	C(7)-N(4)-Cu(1)	122.3(8)
C(9)-N(5)	1.521(17)	C(3)-C(4)-C(5)	111.1(12)	C(9)-N(5)-Cu(1)	118.3(8)
C(9)-C(10)	1.55(2)	N(3)-C(5)-C(6)	109.0(12)	N(1)-Cu(1)-N(5)	161.7(5)
C(10)-C(11)	1.56(2)	N(3)-C(5)-C(4)	108.0(13)	N(1)-Cu(1)-N(2)	93.0(4)
C(11)-N(6)	1.49(2)	C(6)-C(5)-C(4)	113.2(14)	N(5)-Cu(1)-N(2)	92.1(4)
C(11)-C(12)	1.49(2)	C(5)-C(6)-C(1)	114.3(12)	N(1)-Cu(1)-N(4)	89.8(4)
N(1)-Cu(1)	1.988(10)	N(4)-C(7)-C(8)	110.7(11)	N(5)-Cu(1)-N(4)	95.6(5)
N(2)-Cu(1)	2.010(12)	N(4)-C(7)-C(12)	109.3(11)	N(2)-Cu(1)-N(4)	146.4(5)
N(4)-Cu(1)	2.051(12)				

Symmetry transformations used to generate equivalent atoms:

#1 -x,-y+2,-z #2 -x,-y+2,-z+1

Ortep-3 representation of [Cu(*trans*-tach)$_2$]Br$_2$ (*twist*-**38**): thermal ellipsoids at 50% probability, hydrogen atoms are omitted for clarity.



6.12 [Cu(trans-tach)$_2$Br]Br (39)

Crystallisation method	Diffusion of ether into methanol solution overnight.	
Empirical formula	$C_{13}H_{36}Br_2CuN_6O_2$ – ($C_{12}H_{30}N_6CuBr^+$), (Br^-), (H_2O), (CH_3OH)	
Formula weight	531.84	
Temperature	270(2) K	
Wavelength	0.71069 Å	
Crystal system	Orthorhombic	
Space group	*P n m a* (62)	
Unit cell dimensions	a = 13.2522(14) Å	α = 90°.
	b = 12.7055(11) Å	β = 90°.
	c = 12.5588(12) Å	γ = 90°.
Volume	2114.6(4) Å^3	
Z	4	
Density (calculated)	1.671 Mg/m^3	
Absorption coefficient	4.830 mm^{-1}	
F(000)	1084	
Crystal description	Violet plate	
Crystal size	0.5 x 0.5 x 0.2 mm^3	
Theta range for data collection	2.23 to 25.26°.	
Index ranges	0<=h<=15, 0<=k<=14, 0<=l<=15	
Reflections collected	1928	
Independent reflections	1928 [R(int) = 0.0685]	
Completeness to theta = 25.26°	95.8 %	
Absorption correction	None	
Refinement method	Full-matrix least-squares on F^2	
Data / restraints / parameters	1928 / 0 / 121	
Goodness-of-fit on F^2	1.392	
Final R indices [I>2sigma(I)]	R1 = 0.0867, wR2 = 0.1388	
R indices (all data)	R1 = 0.0924, wR2 = 0.1404	
Largest diff. peak and hole	0.650 and -0.816 e.Å^{-3}	
Weighting scheme parameters A and B	0.0236 and 11.7101	

Refinement details: The oxygen atom O13 of the methanol solvent molecule is disordered over two positions. The two protons of each pendant amino moiety were refined as a methyl group subsequently riding with two hydrogen atoms disordered over three positions.

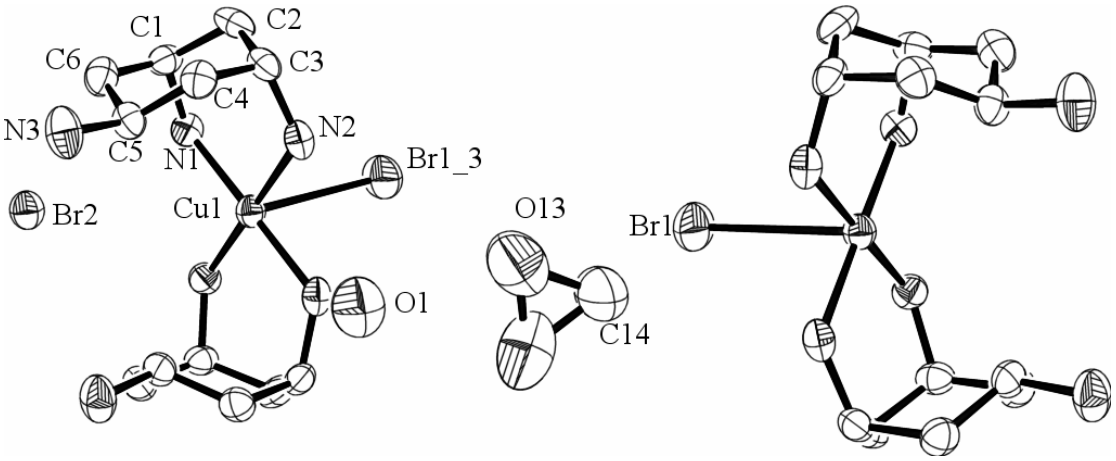
Bond lengths [Å] and angles [°]

C(1)-N(1)	1.487(9)	O(13)-O(13)#1	1.38(4)	N(3)-C(5)-C(6)	112.2(6)
C(1)-C(2)	1.523(11)	Cu(1)-N(1)#1	2.007(6)	C(4)-C(5)-C(6)	110.4(7)
C(1)-C(6)	1.524(11)	Cu(1)-N(2)#1	2.046(6)	C(1)-C(6)-C(5)	113.8(6)
C(2)-C(3)	1.520(11)			O(13)-C(14)-O(13)#1	56.3(15)
C(3)-N(2)	1.499(10)	N(1)-C(1)-C(2)	110.4(6)	C(1)-N(1)-Cu(1)	123.3(5)
C(3)-C(4)	1.518(10)	N(1)-C(1)-C(6)	110.3(6)	C(3)-N(2)-Cu(1)	124.1(5)
C(4)-C(5)	1.509(10)	C(2)-C(1)-C(6)	112.5(7)	O(13)#1-O(13)-C(14)	61.8(7)
C(5)-N(3)	1.477(9)	C(3)-C(2)-C(1)	112.7(6)	N(1)#1-Cu(1)-N(1)	87.6(3)
C(5)-C(6)	1.526(11)	N(2)-C(3)-C(4)	109.3(6)	N(1)#1-Cu(1)-N(2)	179.6(3)
C(14)-O(13)	1.47(2)	N(2)-C(3)-C(2)	110.0(6)	N(1)-Cu(1)-N(2)	92.5(2)
C(14)-O(13)#1	1.47(2)	C(4)-C(3)-C(2)	112.0(6)	N(1)#1-Cu(1)-N(2)#1	92.5(2)
N(1)-Cu(1)	2.007(6)	C(5)-C(4)-C(3)	113.6(6)	N(1)-Cu(1)-N(2)#1	179.6(3)
N(2)-Cu(1)	2.046(6)	N(3)-C(5)-C(4)	110.6(6)	N(2)-Cu(1)-N(2)#1	87.3(4)

Symmetry transformations used to generate equivalent atoms:

#1 x,-y+1/2,z

Ortep-3 representation of [Cu (*trans*-tach)$_2$Br]Br (**39**): thermal ellipsoids at 50% probability, hydrogen atoms are omitted for clarity.



6.13 [Cu(trans-tachH)Br$_2$]Br (40)

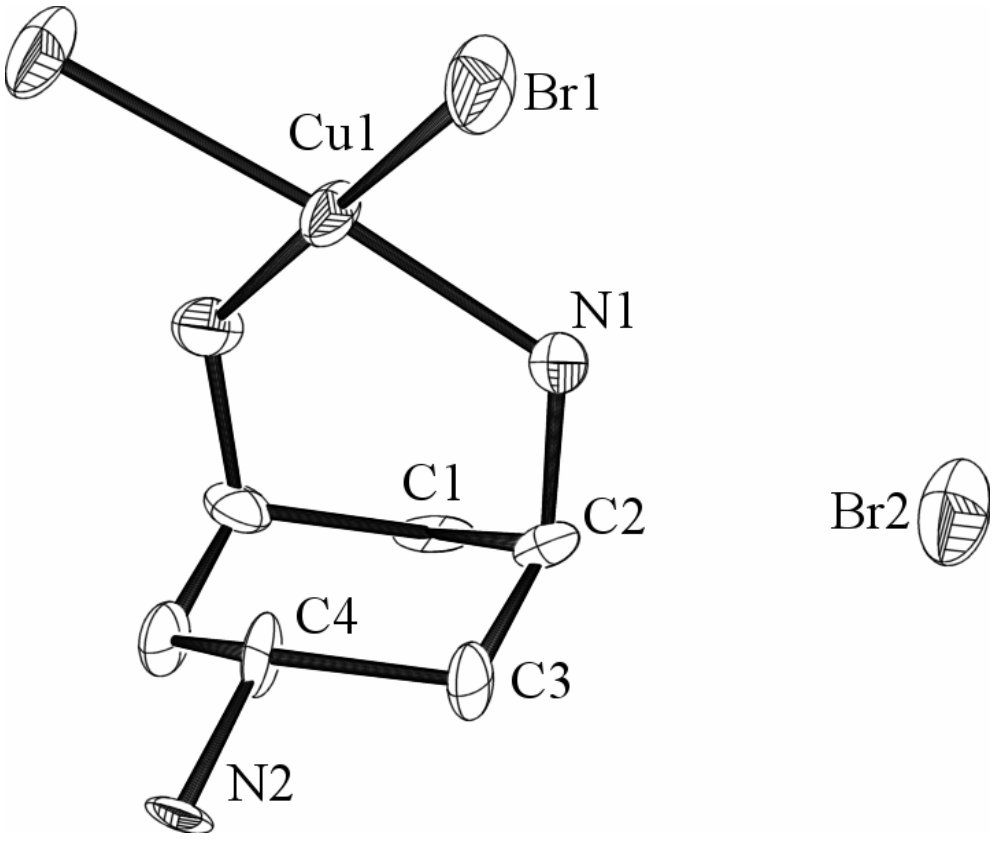
Crystallisation method	Diffusion of ether into methanol solution over 3 days.	
Empirical formula	$C_6H_{16}Br_3CuN_3$ - ($C_6H_{16}N_3CuBr_2^+$), (Br^-)	
Formula weight	433.49	
Temperature	293(2) K	
Wavelength	1.54178 Å	
Crystal system	Orthorhombic	
Space group	*C* 2 *c m* (40)	
Unit cell dimensions	a = 8.0516(5) Å	α = 90°.
	b = 14.9956(9) Å	β = 90°.
	c = 9.7979(5) Å	γ = 90°.
Volume	1182.98(12) Å^3	
Z	4	
Density (calculated)	2.434 Mg/m^3	
Absorption coefficient	14.181 mm^{-1}	
F(000)	828	
Crystal description	Green blocks	
Crystal size	0.04 x 0.04 x 0.04 mm^3	
Theta range for data collection	6.24 to 69.81°.	
Index ranges	-4<=h<=6, -11<=k<=16, -11<=l<=7	
Reflections collected	603	
Independent reflections	396 [R(int) = 0.0344]	
Completeness to theta = 69.81°	52.1 %	
Absorption correction	None	
Refinement method	Full-matrix least-squares on F^2	
Data / restraints / parameters	396 / 6 / 68	
Goodness-of-fit on F^2	1.143	
Final R indices [I>2sigma(I)]	R1 = 0.0581, wR2 = 0.1405	
R indices (all data)	R1 = 0.0586, wR2 = 0.1408	
Absolute structure parameter	0.11(14)	
Extinction coefficient	0.0028(5)	
Largest diff. peak and hole	0.941 and -1.340 e.Å^{-3}	
Weighting scheme parameters A and B	0.1158 and 0.6683	

Bond lengths [Å] and angles [°]

C(1)-C(2)#1	1.54(2)	Cu(1)-N(1)#1	2.030(15)	C(3)-C(4)-C(3)#1	109(2)
C(1)-C(2)	1.54(2)	Cu(1)-Br(1)#1	2.412(3)	N(1)-Cu(1)-N(1)#1	91.1(9)
C(2)-C(3)	1.47(3)	C(2)#1-C(1)-C(2)	114(2)	N(1)-Cu(1)-Br(1)#1	174.7(6)
C(2)-N(1)	1.49(2)	C(3)-C(2)-N(1)	113(2)	N(1)#1-Cu(1)-Br(1)#1	89.2(5)
C(3)-C(4)	1.55(2)	C(3)-C(2)-C(1)	110.3(19)	N(1)-Cu(1)-Br(1)	89.2(5)
C(4)-N(2)	1.52(4)	N(1)-C(2)-C(1)	108.3(17)	N(1)#1-Cu(1)-Br(1)	174.7(6)
C(4)-C(3)#1	1.55(2)	C(2)-C(3)-C(4)	114.8(19)	Br(1)#1-Cu(1)-Br(1)	89.97(16)
Br(1)-Cu(1)	2.412(3)	N(2)-C(4)-C(3)	111.5(17)	C(2)-N(1)-Cu(1)	122.3(12)
Cu(1)-N(1)	2.030(15)	N(2)-C(4)-C(3)#1	111.5(17)		

Symmetry transformations used to generate equivalent atoms:
#1 x,y,-z-1/2

Ortep-3 representation of [Cu(*trans*-tachH)Br_2]Br (**40**): thermal ellipsoids at 50% probability, hydrogen atoms are omitted for clarity.



6.14 [(μ_2-Cl){Cu(trans-tach)$_2$}$_2$]Cl$_3$ · 2 HCl (41 · 2 HCl)

Crystallisation method	Diffusion of ether into methanol solution over 3 days.	
Empirical formula	$C_{24}H_{72}Cl_6Cu_2N_{12}O_5$ – ($C_{24}H_{62}N_{12}Cu_2Cl^{5+}$), 5($Cl^-$), 5($H_2O$)	
Formula weight	948.72	
Temperature	293(2) K	
Wavelength	0.71073 Å	
Crystal system	Monoclinic	
Space group	*P* $2_1/n$ (14)	
Unit cell dimensions	a = 8.726(2) Å	α = 90°.
	b = 18.500(4) Å	β = 96.731(2)°.
	c = 13.341(3) Å	γ = 90°.
Volume	2138.8(9) Å^3	
Z	2	
Density (calculated)	1.473 Mg/m^3	
Absorption coefficient	1.416 mm^{-1}	
F(000)	1000	
Crystal description	Blue needles	
Crystal size	0.3 x 0.15 x 0.03 mm^3	
Theta range for data collection	1.89 to 25.40°.	
Index ranges	-10<=h<=10, -22<=k<=22, -16<=l<=16	
Reflections collected	9933	
Independent reflections	3435 [R(int) = 0.0518]	
Completeness to theta = 25.40°	87.0 %	
Absorption correction	None	
Refinement method	Full-matrix least-squares on F^2	
Data / restraints / parameters	3435 / 0 / 223	
Goodness-of-fit on F^2	1.203	
Final R indices [I>2sigma(I)]	R1 = 0.0667, wR2 = 0.1432	
R indices (all data)	R1 = 0.0726, wR2 = 0.1467	
Largest diff. peak and hole	0.384 and -0.763 e.Å^{-3}	
Weighting scheme parameters A and B	0.0454 and 6.2780	

Refinement details: The asymmetric unit contains two crystallographically independent *trans*-tach ligands, one of whose pendant amines is protonated. Refinement for both as riding methyl protons. Each pair of Cl3 / O3, Cl4 / O4 and Cl5 / O5 mixed atoms share the same positions by half occupancy, as overall 6 chloride and 5 water in the unit cell.

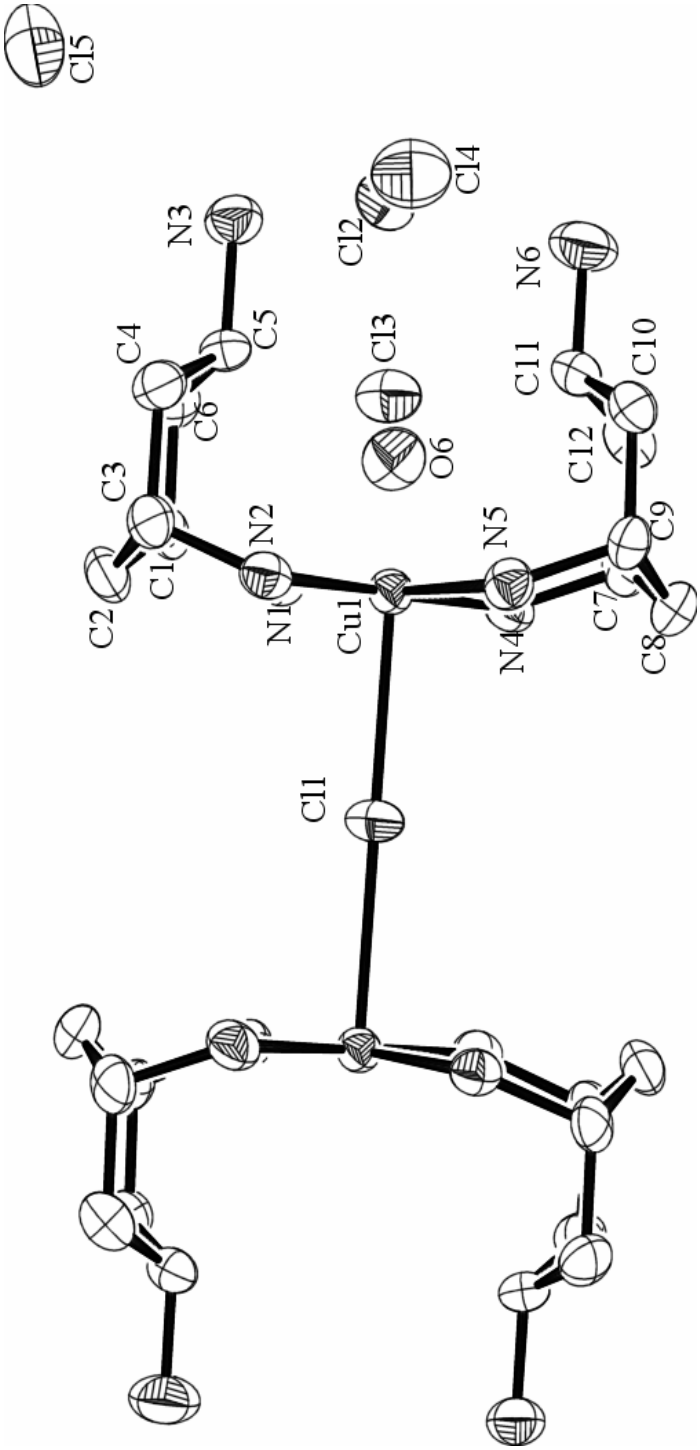
Bond lengths [Å] and angles [°]

C(1)-N(1)	1.501(6)	Cl(1)-Cu(1)#1	2.6458(7)	C(8)-C(9)-C(10)	112.6(5)
C(1)-C(6)	1.526(7)	Cl(1)-Cu(1)	2.6458(7)	C(9)-C(10)-C(11)	112.6(4)
C(1)-C(2)	1.529(7)			N(6)-C(11)-C(12)	111.9(5)
C(2)-C(3)	1.515(8)	N(1)-C(1)-C(6)	110.9(4)	N(6)-C(11)-C(10)	110.6(5)
C(3)-N(2)	1.510(7)	N(1)-C(1)-C(2)	110.2(4)	C(12)-C(11)-C(10)	109.4(5)
C(3)-C(4)	1.535(7)	C(6)-C(1)-C(2)	111.4(5)	C(11)-C(12)-C(7)	112.5(5)
C(4)-C(5)	1.529(7)	C(3)-C(2)-C(1)	113.4(4)	C(1)-N(1)-Cu(1)	124.1(3)
C(5)-N(3)	1.501(6)	N(2)-C(3)-C(2)	109.7(5)	C(3)-N(2)-Cu(1)	123.6(3)
C(5)-C(6)	1.526(7)	N(2)-C(3)-C(4)	110.3(4)	C(7)-N(4)-Cu(1)	123.1(4)
C(7)-N(4)	1.508(7)	C(2)-C(3)-C(4)	112.8(4)	C(9)-N(5)-Cu(1)	122.9(3)
C(7)-C(8)	1.528(8)	C(5)-C(4)-C(3)	111.2(4)	Cu(1)#1-Cl(1)-Cu(1)	180.00(1)
C(7)-C(12)	1.535(8)	N(3)-C(5)-C(6)	112.1(4)	N(1)-Cu(1)-N(4)	88.39(18)
C(8)-C(9)	1.509(8)	N(3)-C(5)-C(4)	110.5(4)	N(1)-Cu(1)-N(5)	174.93(17)
C(9)-N(5)	1.504(7)	C(6)-C(5)-C(4)	110.9(4)	N(4)-Cu(1)-N(5)	92.19(18)
C(9)-C(10)	1.533(7)	C(5)-C(6)-C(1)	111.9(4)	N(1)-Cu(1)-N(2)	91.92(17)
C(10)-C(11)	1.533(7)	N(4)-C(7)-C(8)	110.4(5)	N(4)-Cu(1)-N(2)	179.45(18)
C(11)-N(6)	1.478(7)	N(4)-C(7)-C(12)	109.5(5)	N(5)-Cu(1)-N(2)	87.54(17)
C(11)-C(12)	1.528(8)	C(8)-C(7)-C(12)	111.9(5)	N(1)-Cu(1)-Cl(1)	91.03(12)
N(1)-Cu(1)	2.043(4)	C(9)-C(8)-C(7)	113.5(4)	N(4)-Cu(1)-Cl(1)	88.53(13)
N(2)-Cu(1)	2.058(5)	N(5)-C(9)-C(8)	109.4(5)	N(5)-Cu(1)-Cl(1)	94.03(13)
N(4)-Cu(1)	2.047(5)	N(5)-C(9)-C(10)	110.8(4)	N(2)-Cu(1)-Cl(1)	91.02(12)
N(5)-Cu(1)	2.047(4)				

Symmetry transformations used to generate equivalent atoms:

#1 -x+2,-y+1,-z+2

Ortep-3 representation of $[(\mu_2\text{-Cl})\{Cu(\textit{trans}\text{-tach})_2\}_2]Cl_3 \bullet 2\ HCl$ (**41** • 2 HCl): thermal ellipsoids at 50% probability, hydrogen atoms are omitted for clarity.



6.15 [(μ_3-Cl){Cu(trans-tach)Cl_2}$_3$]Cl_2 (42)

Crystallisation method	Diffusion of acetone into methanol / water solution over 5 days.	
Empirical formula	$C_{18}H_{48}Cl_9Cu_3N_9$ – ($C_{18}H_{48}N_9Cu_3Cl_7^{2+}$), 2($Cl^-$)	
Formula weight	900.32	
Temperature	293(2) K	
Wavelength	0.71073 Å	
Crystal system	Hexagonal	
Space group	*P* $6_3/m$ (176)	
Unit cell dimensions	a = 12.680(2) Å	α = 90°.
	b = 12.680(2) Å	β = 90°.
	c = 12.6287(13) Å	γ = 120°.
Volume	1758.4(4) $Å^3$	
Z	2	
Density (calculated)	1.700 Mg/m^3	
Absorption coefficient	2.509 mm^{-1}	
F(000)	918	
Crystal description	Blue needles	
Crystal size	0.2 x 0.1 x 0.05 mm^3	
Theta range for data collection	1.85 to 29.41°.	
Index ranges	0<=h<=15, 0<=k<=14, 0<=l<=17	
Reflections collected	14125	
Independent reflections	1679 [R(int) = 0.0678]	
Completeness to theta = 29.41°	98.9 %	
Absorption correction	None	
Refinement method	Full-matrix least-squares on F^2	
Data / restraints / parameters	1679 / 0 / 67	
Goodness-of-fit on F^2	1.155	
Final R indices [I>2sigma(I)]	R1 = 0.0511, wR2 = 0.1104	
R indices (all data)	R1 = 0.0838, wR2 = 0.1326	
Extinction coefficient	0.0149(19)	
Largest diff. peak and hole	1.434 and -0.669 e.$Å^{-3}$	
Weighting scheme parameters A and B	0.0596 and 0.0000	

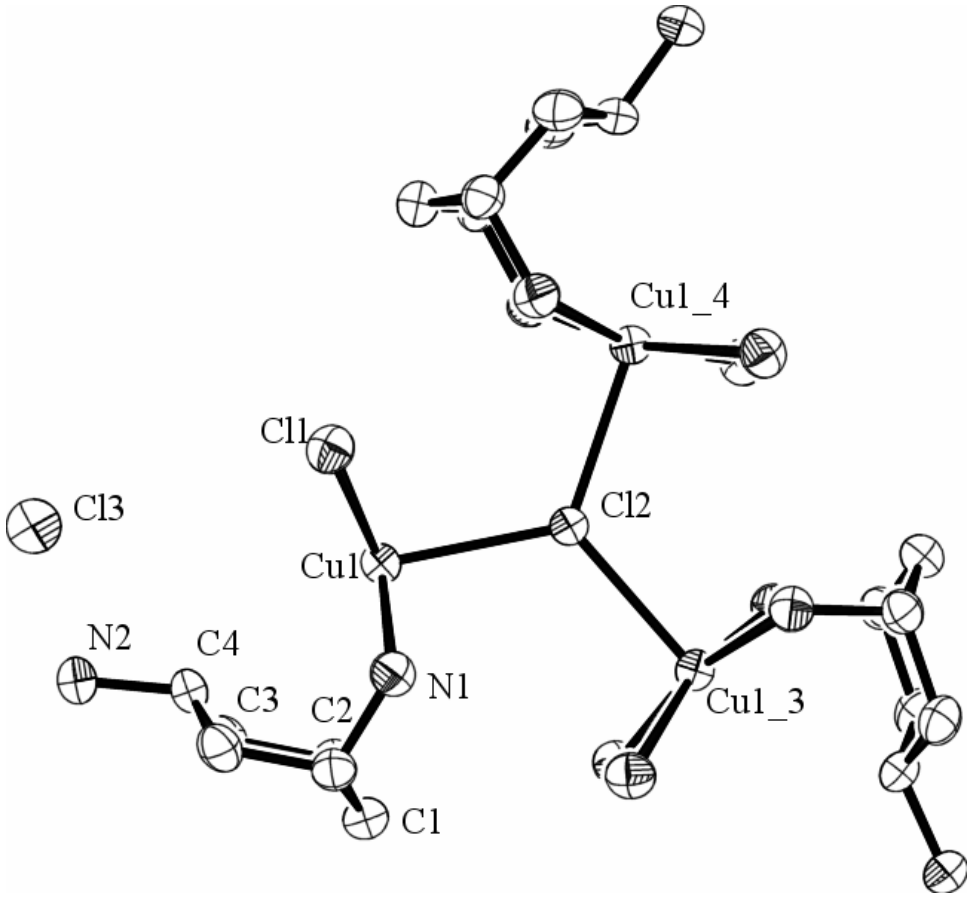
Bond lengths [Å] and angles [°]

C(1)-C(2)#1	1.515(5)	C(2)#1-C(1)-C(2)	113.1(4)	Cu(1)#3-Cl(2)-Cu(1)	120
C(1)-C(2)	1.515(5)	N(1)-C(2)-C(1)	109.6(3)	N(1)-Cu(1)-N(1)#1	88.08(18)
C(2)-N(1)	1.487(5)	N(1)-C(2)-C(3)	110.3(3)	N(1)-Cu(1)-Cl(1)	167.10(10)
C(2)-C(3)	1.521(5)	C(1)-C(2)-C(3)	111.5(4)	N(1)#1-Cu(1)-Cl(1)	89.60(9)
C(3)-C(4)	1.520(5)	C(4)-C(3)-C(2)	111.9(3)	N(1)-Cu(1)-Cl(1)#1	89.60(9)
C(4)-N(2)	1.501(7)	N(2)-C(4)-C(3)	109.6(3)	N(1)#1-Cu(1)-Cl(1)#1	167.10(10)
C(4)-C(3)#1	1.520(5)	N(2)-C(4)-C(3)#1	109.6(3)	Cl(1)-Cu(1)-Cl(1)#1	89.83(5)
N(1)-Cu(1)	2.009(3)	C(3)-C(4)-C(3)#1	113.5(5)	N(1)-Cu(1)-Cl(2)	93.79(10)
Cl(1)-Cu(1)	2.3205(10)	C(2)-N(1)-Cu(1)	120.5(2)	N(1)#1-Cu(1)-Cl(2)	93.79(10)
		Cu(1)#2-Cl(2)-			
Cl(2)-Cu(1)#2	2.5748(7)	Cu(1)#3	120	Cl(1)-Cu(1)-Cl(2)	99.03(3)
		Cu(1)#2-Cl(2)-			
Cl(2)-Cu(1)#3	2.5748(7)	Cu(1)	120	Cl(1)#1-Cu(1)-Cl(2)	99.03(3)
Cl(2)-Cu(1)	2.5748(7)				
Cu(1)-N(1)#1	2.009(3)				
Cu(1)-Cl(1)#1	2.3205(10)				

Symmetry transformations used to generate equivalent atoms:

#1 x,y,-z+3/2 #2 -x+y+2,-x+1,z #3 -y+1,x-y-1,z

Ortep-3 representation of $[(\mu_3\text{-Cl})\{Cu(\textit{trans}\text{-tach})Cl_2\}_3]Cl_2$ (**42**): thermal ellipsoids at 50% probability, hydrogen atoms are omitted for clarity.



6.16 [(μ_3-Cl){Cu(trans-tach)Cl_2}$_3$]Br_2 (43)

Crystallisation method	Diffusion of acetone into methanol / water solution over 5 days.	
Empirical formula	$C_{18}H_{48}Br_2Cl_7Cu_3N_9$ – ($C_{18}H_{48}N_9Cu_3Cl_7^{2+}$), 2($Br^-$)	
Formula weight	989.24	
Temperature	200(2) K	
Wavelength	1.54180 Å	
Crystal system	Hexagonal	
Space group	*P* $6_3/m$ (176)	
Unit cell dimensions	a = 12.6961(2) Å	α = 90°.
	b = 12.6961(2) Å	β = 90°.
	c = 12.6511(2) Å	γ = 120°.
Volume	1766.04(5) $Å^3$	
Z	2	
Density (calculated)	1.860 Mg/m^3	
Absorption coefficient	9.841 mm^{-1}	
F(000)	990	
Crystal description	Turquoise needles	
Crystal size	0.1 x 0.04 x 0.04 mm^3	
Theta range for data collection	4.02 to 70.97°.	
Index ranges	0<=h<=13, 0<=k<=12, 0<=l<=15	
Reflections collected	6507	
Independent reflections	1170 [R(int) = 0.0416]	
Completeness to theta = 70.97°	98.0 %	
Absorption correction	None	
Refinement method	Full-matrix least-squares on F^2	
Data / restraints / parameters	1170 / 0 / 66	
Goodness-of-fit on F^2	1.089	
Final R indices [I>2sigma(I)]	R1 = 0.0563, wR2 = 0.1805	
R indices (all data)	R1 = 0.0620, wR2 = 0.1858	
Largest diff. peak and hole	1.482 and -2.198 e.$Å^{-3}$	
Weighting scheme parameters A and B	0.1040 and 13.1811	

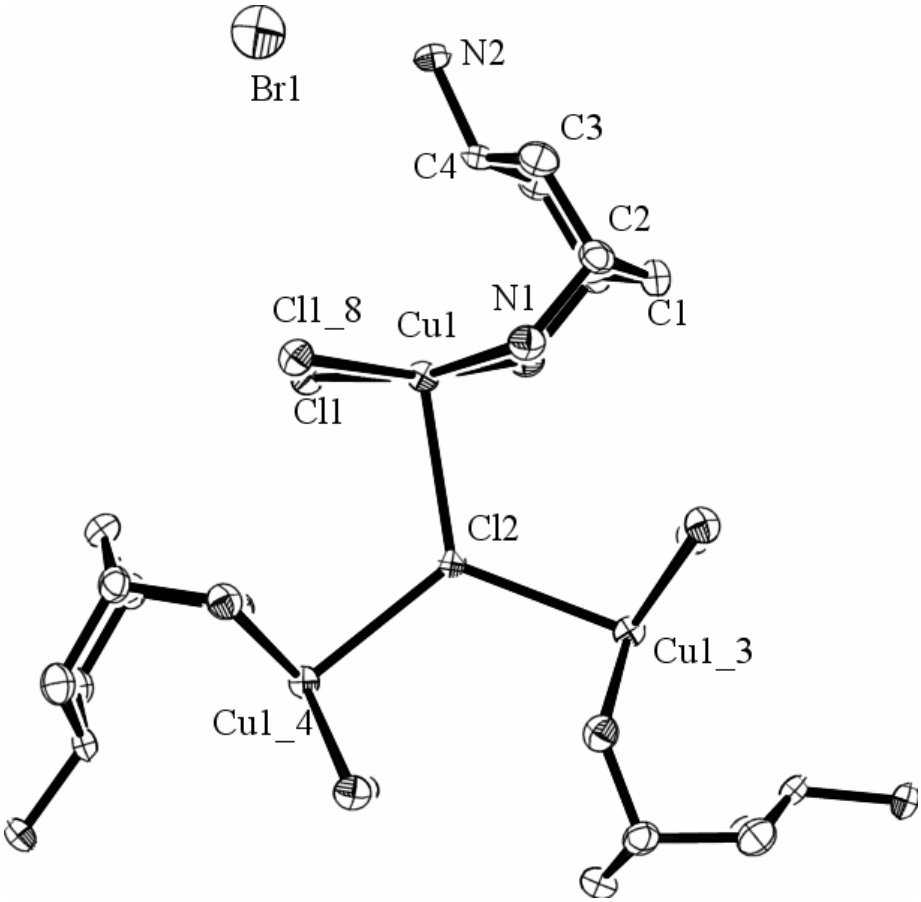
Bond lengths [Å] and angles [°]

C(1)-C(2)#1	1.524(7)	C(2)#1-C(1)-C(2)	114.0(7)	Cu(1)#3-Cl(2)-Cu(1)	120
C(1)-C(2)	1.524(7)	N(1)-C(2)-C(1)	108.8(5)	N(1)-Cu(1)-N(1)#1	87.9(3)
C(2)-N(1)	1.495(8)	N(1)-C(2)-C(3)	110.4(5)	N(1)-Cu(1)-Cl(1)	167.40(16)
C(2)-C(3)	1.525(8)	C(1)-C(2)-C(3)	110.7(6)	N(1)#1-Cu(1)-Cl(1)	89.67(15)
C(3)-C(4)	1.519(8)	C(4)-C(3)-C(2)	112.8(5)	N(1)-Cu(1)-Cl(1)#1	89.67(15)
C(4)-N(2)	1.504(10)	N(2)-C(4)-C(3)	109.8(4)	N(1)#1-Cu(1)-Cl(1)#1	167.40(16)
C(4)-C(3)#1	1.519(8)	N(2)-C(4)-C(3)#1	109.8(4)	Cl(1)-Cu(1)-Cl(1)#1	89.98(8)
N(1)-Cu(1)	2.008(5)	C(3)-C(4)-C(3)#1	113.1(7)	N(1)-Cu(1)-Cl(2)	93.32(14)
Cl(1)-Cu(1)	2.3329(15)	C(2)-N(1)-Cu(1)	121.0(4)	N(1)#1-Cu(1)-Cl(2)	93.32(14)
		Cu(1)#2-Cl(2)-			
Cl(2)-Cu(1)#2	2.5765(11)	Cu(1)#3	120	Cl(1)-Cu(1)-Cl(2)	99.17(5)
		Cu(1)#2-Cl(2)-			
Cl(2)-Cu(1)#3	2.5765(11)	Cu(1)	120	Cl(1)#1-Cu(1)-Cl(2)	99.17(5)
Cl(2)-Cu(1)	2.5765(11)				
Cu(1)-N(1)#1	2.008(5)				
Cu(1)-Cl(1)#1	2.3329(15)				

Symmetry transformations used to generate equivalent atoms:

#1 x,y,-z+3/2 #2 -x+y+2,-x+1,z #3 -y+1,x-y-1,z

Ortep-3 representation of $[(\mu_3\text{-Cl})\{Cu(\textit{trans}\text{-tachH})Cl_2\}_3]Br_2$ (**43**): thermal ellipsoids at 50% probability, hydrogen atoms are omitted for clarity.



6.17 [Cu(trans-tach)$_2$F]F (44)

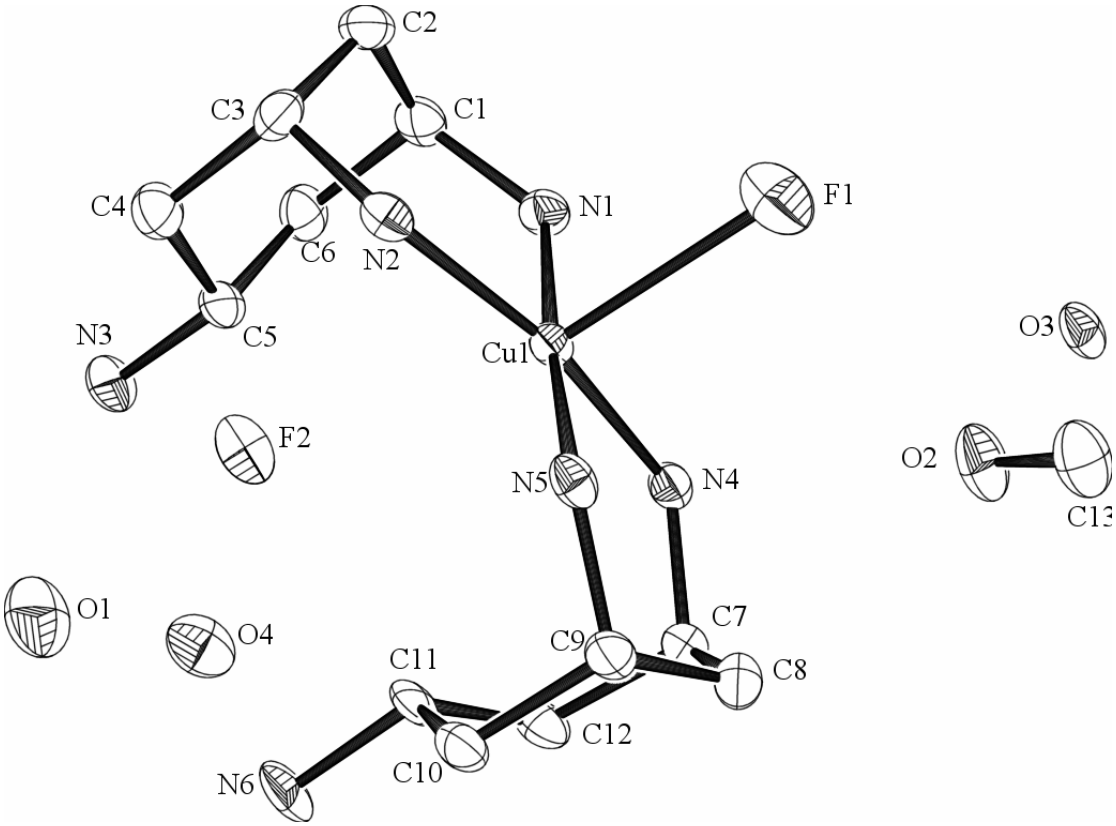
Crystallisation method	Diffusion of ether into methanol solution over 10 days.	
Empirical formula	$C_{13}H_{40}CuF_2N_6O_4$ - ($C_{12}H_{30}N_6CuF^+$), (F^-), 3(H_2O), (CH_3OH)	
Formula weight	446.05	
Temperature	211(2) K	
Wavelength	1.54178 Å	
Crystal system	Monoclinic	
Space group	*C c* (9)	
Unit cell dimensions	a = 6.93210(10) Å	α = 90°.
	b = 18.9967(4) Å	β = 95.5820(10)°.
	c = 15.4085(3) Å	γ = 90°.
Volume	2019.48(6) Å^3	
Z	4	
Density (calculated)	1.467 Mg/m^3	
Absorption coefficient	1.964 mm^{-1}	
F(000)	956	
Crystal description	Blue plates	
Crystal size	0.5 x 0.44 x 0.06 mm^3	
Theta range for data collection	4.66 to 70.45°.	
Index ranges	-8<=h<=7, -22<=k<=20, -18<=l<=13	
Reflections collected	3408	
Independent reflections	2214 [R(int) = 0.0206]	
Completeness to theta = 70.45°	91.5 %	
Absorption correction	None	
Refinement method	Full-matrix least-squares on F^2	
Data / restraints / parameters	2214 / 2 / 236	
Goodness-of-fit on F^2	1.326	
Final R indices [I>2sigma(I)]	R1 = 0.0453, wR2 = 0.1239	
R indices (all data)	R1 = 0.0455, wR2 = 0.1240	
Absolute structure parameter	0.00	
Extinction coefficient	0.0109(8)	
Largest diff. peak and hole	0.380 and -0.551 e.Å^{-3}	
Weighting scheme parameters A and B	0.0617 and 2.7083	

Refinement details: Refinement as non-protonated pendant amino moieties. The asymmetric unit contains one methanol and three water molecules.

Bond lengths [Å] and angles [°]

C(1)-N(1)	1.484(8)	N(4)-Cu(1)	2.030(5)	N(5)-C(9)-C(10)	110.6(4)
C(1)-C(2)	1.508(8)	N(5)-Cu(1)	2.027(4)	C(8)-C(9)-C(10)	110.5(4)
C(1)-C(6)	1.537(8)	F(1)-Cu(1)	2.417(4)	C(9)-C(10)-C(11)	112.5(4)
C(2)-C(3)	1.518(8)			N(6)-C(11)-C(12)	109.4(4)
C(3)-N(2)	1.501(7)	N(1)-C(1)-C(2)	110.8(5)	N(6)-C(11)-C(10)	112.2(4)
C(3)-C(4)	1.522(7)	N(1)-C(1)-C(6)	110.3(4)	C(12)-C(11)-C(10)	110.2(4)
C(4)-C(5)	1.540(8)	C(2)-C(1)-C(6)	112.0(5)	C(11)-C(12)-C(7)	113.9(4)
C(5)-N(3)	1.473(7)	C(1)-C(2)-C(3)	113.5(4)	C(1)-N(1)-Cu(1)	122.8(4)
C(5)-C(6)	1.518(8)	N(2)-C(3)-C(2)	110.3(4)	C(3)-N(2)-Cu(1)	123.3(4)
C(7)-N(4)	1.479(7)	N(2)-C(3)-C(4)	110.3(4)	C(7)-N(4)-Cu(1)	122.4(3)
C(7)-C(8)	1.518(8)	C(2)-C(3)-C(4)	112.2(5)	C(9)-N(5)-Cu(1)	123.7(3)
C(7)-C(12)	1.535(7)	C(3)-C(4)-C(5)	112.5(4)	N(5)-Cu(1)-N(4)	92.61(16)
C(8)-C(9)	1.510(8)	N(3)-C(5)-C(6)	110.9(4)	N(5)-Cu(1)-N(2)	87.7(2)
C(9)-N(5)	1.484(7)	N(3)-C(5)-C(4)	112.2(5)	N(4)-Cu(1)-N(2)	168.90(18)
C(9)-C(10)	1.532(7)	C(6)-C(5)-C(4)	110.5(4)	N(5)-Cu(1)-N(1)	175.75(19)
C(10)-C(11)	1.535(7)	C(5)-C(6)-C(1)	113.1(4)	N(4)-Cu(1)-N(1)	87.6(2)
C(11)-N(6)	1.480(6)	N(4)-C(7)-C(8)	110.8(4)	N(2)-Cu(1)-N(1)	92.91(16)
C(11)-C(12)	1.510(8)	N(4)-C(7)-C(12)	110.8(4)	N(5)-Cu(1)-F(1)	88.08(16)
C(13)-O(2)	1.413(7)	C(8)-C(7)-C(12)	111.7(4)	N(4)-Cu(1)-F(1)	93.93(16)
N(1)-Cu(1)	2.040(5)	C(9)-C(8)-C(7)	113.2(4)	N(2)-Cu(1)-F(1)	97.17(16)
N(2)-Cu(1)	2.032(5)	N(5)-C(9)-C(8)	111.6(4)	N(1)-Cu(1)-F(1)	87.67(17)

Ortep-3 representation of [Cu(*trans*-tach)$_2$F]F (**44**): thermal ellipsoids at 50% probability, hydrogen atoms are omitted for clarity.



6.18 [{Cu(trans-tachH)F}$_4$]F$_4$ (45)

Crystallisation method	Diffusion of ether into methanol / water solution overnight.	
Empirical formula	$C_{32.17}H_{127}Cu_4F_{12}N_{12}O_{23.33}$ - ($C_{24}H_{64}N_{12}Cu_4F_4^{8+}$), 8($F^-$), 8.17($CH_3OH$), 15.16($H_2O$)	
Formula weight	1537.95	
Temperature	200(2) K	
Wavelength	1.54180 Å	
Crystal system	Cubic	
Space group	*F* -4 3 *c* (219)	
Unit cell dimensions	a = 37.295(4) Å	α = 90°.
	b = 37.295(4) Å	β = 90°.
	c = 37.295(4) Å	γ = 90°.
Volume	51872(10) Å^3	
Z	24	
Density (calculated)	1.182 Mg/m^3	
Absorption coefficient	1.851 mm^{-1}	
F(000)	19552	
Crystal description	Royal blue cubes	
Crystal size	0.20 x 0.20 x 0.20 mm^3	
Theta range for data collection	2.37 to 58.90°.	
Index ranges	1<=h<=41, 0<=k<=29, -20<=l<=23	
Reflections collected	30462	
Independent reflections	3027 [R(int) = 0.0488]	
Completeness to theta = 58.90°	99.9 %	
Absorption correction	Semi-empirical from equivalents	
Max. and min. transmission	0.7085 and 0.7085	
Refinement method	Full-matrix least-squares on F^2	
Data / restraints / parameters	3027 / 0 / 193	
Goodness-of-fit on F^2	1.185	
Final R indices [I>2sigma(I)]	R1 = 0.0606, wR2 = 0.1663	
R indices (all data)	R1 = 0.0670, wR2 = 0.1801	
Absolute structure parameter	0.45(6)	
Largest diff. peak and hole	0.748 and -0.541 e.Å^{-3}	
Weighting scheme parameters A and B	0.1326 and 58.0490	

Refinement details: The fluoride counterions are identified by their short hydrogen-bonded interactions. The oxygen atoms O15A and O15B are disordered over two positions. The methanol solvent containing C7 and O1 is only partially occupied. Additionally, oxygen atom O1 is disordered over four positions and excess electron density at O1, with respect to the occupancy of the methanol carbon atom C7, is refined as water solvent.

Bond lengths [Å] and angles [°]

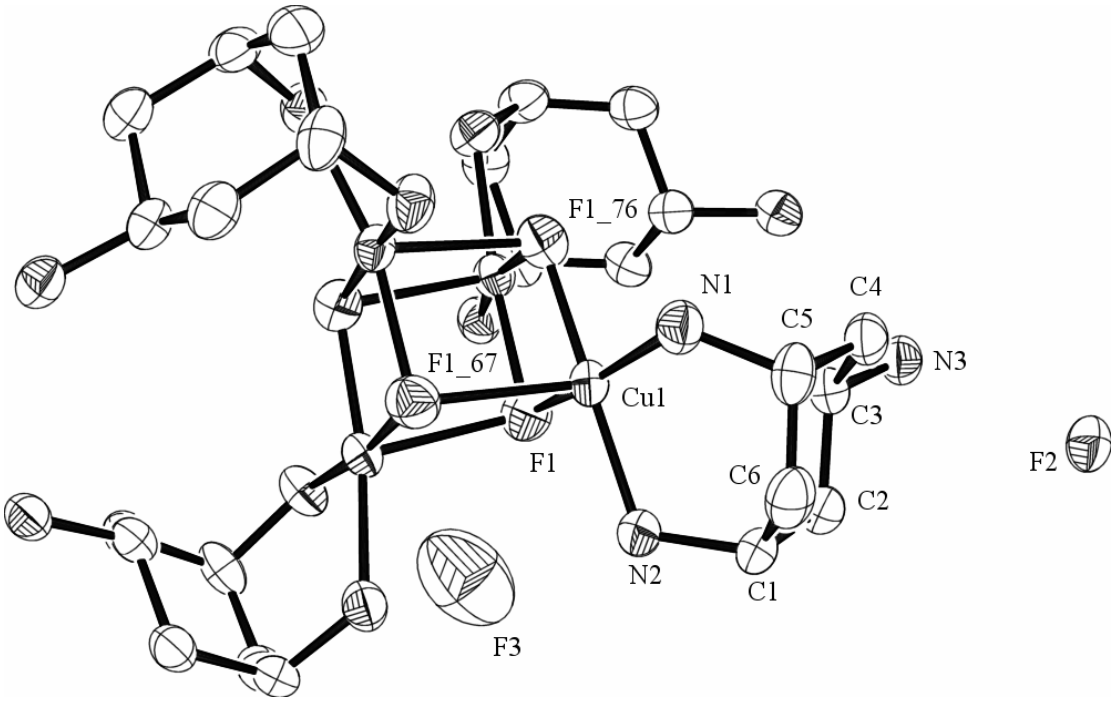
C(1)-N(2)	1.500(8)	Cu(1)-F(1)#3	1.962(4)	O(15B)-O(15A)-O(15A)#4	52(2)
C(1)-C(2)	1.515(9)	Cu(1)-F(1)#7	2.318(4)	O(15B)-O(15A)-O(15A)#5	52(2)
C(1)-C(6)	1.516(10)	Cu(1)-Cu(1)#3	2.9969(16)	O(15A)#4-O(15A)-O(15A)#5	60.000(12)
C(2)-C(3)	1.519(8)			O(15A)#5-O(15B)-O(15A)#4	75(4)
C(3)-N(3)	1.481(7)	N(2)-C(1)-C(2)	111.1(5)	O(15A)#5-O(15B)-O(15A)	75(4)
C(3)-C(4)	1.523(8)	N(2)-C(1)-C(6)	109.5(5)	O(15A)#4-O(15B)-O(15A)	75(4)
C(4)-C(5)	1.530(9)	C(2)-C(1)-C(6)	111.6(5)	Cu(1)#3-F(1)-Cu(1)	98.87(16)
C(5)-C(6)	1.486(10)	C(1)-C(2)-C(3)	113.4(5)	Cu(1)#3-F(1)-Cu(1)#6	96.27(15)
C(5)-N(1)	1.498(8)	N(3)-C(3)-C(2)	110.9(5)	Cu(1)-F(1)-Cu(1)#6	95.68(15)
C(7)-O(1)#1	1.437(15)	N(3)-C(3)-C(4)	109.1(4)	F(1)#3-Cu(1)-F(1)	80.91(16)
C(7)-O(1)	1.437(15)	C(2)-C(3)-C(4)	112.3(5)	F(1)#3-Cu(1)-N(2)	173.1(2)
C(7)-O(1)#2	1.437(15)	C(3)-C(4)-C(5)	111.4(5)	F(1)-Cu(1)-N(2)	93.07(19)
C(7)-O(1)#3	1.437(15)	C(6)-C(5)-N(1)	111.0(5)	F(1)#3-Cu(1)-N(1)	92.53(17)
C(8)-O(2)	1.428(15)	C(6)-C(5)-C(4)	110.6(5)	F(1)-Cu(1)-N(1)	167.13(18)
C(9)-O(3)	1.460(19)	N(1)-C(5)-C(4)	110.0(5)	N(2)-Cu(1)-N(1)	92.7(2)
N(1)-Cu(1)	2.007(5)	C(5)-C(6)-C(1)	114.7(5)	F(1)#3-Cu(1)-F(1)#7	83.65(15)
N(2)-Cu(1)	1.990(5)	O(1)#1-C(7)-O(1)	109.5	F(1)-Cu(1)-F(1)#7	83.19(15)
O(15A)-O(15B)	1.13(5)	O(1)#1-C(7)-O(1)#2	109.471(6)	N(2)-Cu(1)-F(1)#7	99.12(17)
O(15A)-O(15A)#4	1.38(8)	O(1)-C(7)-O(1)#2	109.471(4)	N(1)-Cu(1)-F(1)#7	107.22(17)
O(15A)-O(15A)#5	1.38(8)	O(1)#1-C(7)-O(1)#3	109.471(2)	F(1)#3-Cu(1)-Cu(1)#3	40.82(10)
O(15B)-O(15A)#5	1.13(5)	O(1)-C(7)-O(1)#3	109.471(3)	F(1)-Cu(1)-Cu(1)#3	40.30(11)
O(15B)-O(15A)#4	1.13(5)	O(1)#2-C(7)-O(1)#3	109.471(1)	N(2)-Cu(1)-Cu(1)#3	132.82(17)
F(1)-Cu(1)#3	1.962(4)	C(5)-N(1)-Cu(1)	119.7(4)	N(1)-Cu(1)-Cu(1)#3	131.37(15)
F(1)-Cu(1)	1.983(3)	C(1)-N(2)-Cu(1)	117.5(4)	F(1)#7-Cu(1)-Cu(1)#3	84.59(9)

Symmetry transformations used to generate equivalent atoms:

#1 -x+1/2,-y+1/2,z #2 -x+1/2,y,-z+1/2 #3 x,-y+1/2,-z+1/2

#4 -z+1/2,x,-y+1/2 #5 y,-z+1/2,-x+1/2 #6 -x+1,z+0,-y+1/2 #7 -x+1,-z+1/2,y+0

Ortep-3 representation of [{Cu(*trans*-tachH)F}$_4$]F$_4$ (**45**): thermal ellipsoids at 50% probability, hydrogen atoms are omitted for clarity.



6.19 [Cu(trans-tach)$_2$(SO$_4$)] (46)

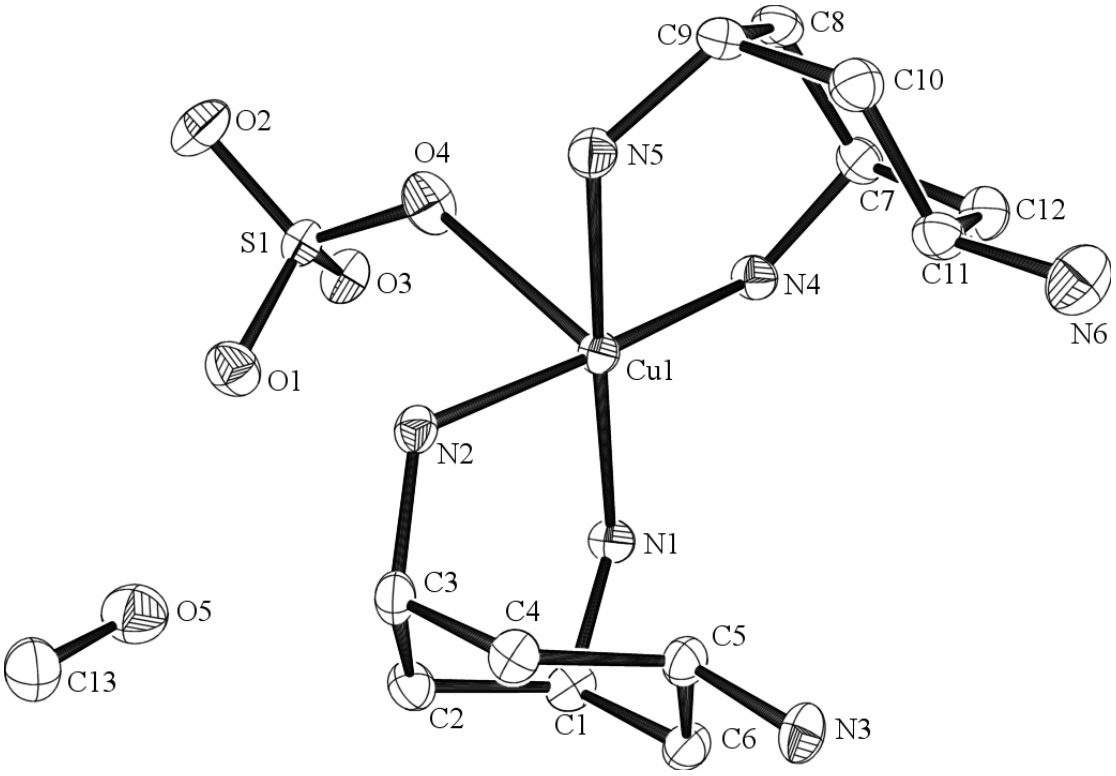
Crystallisation method	Diffusion of ether into methanol solution over 2 weeks.	
Empirical formula	$C_{13}H_{34}CuN_6O_5S$ - ($C_{12}H_{30}N_6CuSO_4$), (CH_3OH)	
Formula weight	450.06	
Temperature	150(2) K	
Wavelength	0.71073 Å	
Crystal system	Orthorhombic	
Space group	*P b c* 2_1 (29)	
Unit cell dimensions	a = 7.41580(10) Å	α = 90°.
	b = 13.4649(2) Å	β = 90°.
	c = 19.5288(5) Å	γ = 90°.
Volume	1950.01(6) Å^3	
Z	4	
Density (calculated)	1.533 Mg/m^3	
Absorption coefficient	1.264 mm^{-1}	
F(000)	956	
Crystal description	Violet blocks	
Crystal size	0.24 x 0.2 x 0.2 mm^3	
Theta range for data collection	2.09 to 30.08°.	
Index ranges	0<=h<=10, 0<=k<=18, 0<=l<=27	
Reflections collected	18286	
Independent reflections	2935 [R(int) = 0.0576]	
Completeness to theta = 30.08°	99.5 %	
Absorption correction	Empirical	
Max. and min. transmission	0.947 and 1.089	
Refinement method	Full-matrix least-squares on F^2	
Data / restraints / parameters	2935 / 1 / 247	
Goodness-of-fit on F^2	1.032	
Final R indices [I>2sigma(I)]	R1 = 0.0311, wR2 = 0.0736	
R indices (all data)	R1 = 0.0385, wR2 = 0.0759	
Absolute structure parameter	0.00	
Largest diff. peak and hole	0.389 and -0.486 e.Å^{-3}	
Weighting scheme parameters A and B	0.0434 and 0.7108	

Refinement details: The two protons of each pendant amino moiety were refined as a methyl group subsequently riding with two hydrogen atoms disordered over three positions.

Bond lengths [Å] and angles [°]

C(1)-N(1)	1.482(5)	O(3)-S(1)	1.489(2)	N(6)-C(11)-C(12)	113.5(3)
C(1)-C(2)	1.534(6)	O(4)-S(1)	1.472(3)	C(10)-C(11)-C(12)	110.2(3)
C(1)-C(6)	1.536(5)	O(4)-Cu(1)	2.439(3)	C(7)-C(12)-C(11)	114.3(3)
C(2)-C(3)	1.551(6)			C(1)-N(1)-Cu(1)	122.6(3)
C(3)-N(2)	1.492(5)	N(1)-C(1)-C(2)	110.4(3)	C(3)-N(2)-Cu(1)	122.5(2)
C(3)-C(4)	1.524(5)	N(1)-C(1)-C(6)	110.5(3)	C(7)-N(4)-Cu(1)	123.5(3)
C(4)-C(5)	1.529(6)	C(2)-C(1)-C(6)	111.7(3)	C(9)-N(5)-Cu(1)	124.0(2)
C(5)-N(3)	1.481(5)	C(1)-C(2)-C(3)	112.1(4)	S(1)-O(4)-Cu(1)	130.69(17)
C(5)-C(6)	1.533(6)	N(2)-C(3)-C(4)	111.2(3)	O(2)-S(1)-O(4)	111.44(18)
C(7)-N(4)	1.486(5)	N(2)-C(3)-C(2)	108.8(3)	O(2)-S(1)-O(1)	109.17(17)
C(7)-C(12)	1.520(6)	C(4)-C(3)-C(2)	112.1(3)	O(4)-S(1)-O(1)	109.06(17)
C(7)-C(8)	1.523(6)	C(3)-C(4)-C(5)	114.0(3)	O(2)-S(1)-O(3)	108.18(16)
C(8)-C(9)	1.524(6)	N(3)-C(5)-C(4)	109.8(3)	O(4)-S(1)-O(3)	109.10(16)
C(9)-N(5)	1.491(5)	N(3)-C(5)-C(6)	112.7(3)	O(1)-S(1)-O(3)	109.88(17)
C(9)-C(10)	1.532(6)	C(4)-C(5)-C(6)	111.4(3)	N(4)-Cu(1)-N(2)	174.55(14)
C(10)-C(11)	1.534(6)	C(5)-C(6)-C(1)	113.6(3)	N(4)-Cu(1)-N(1)	87.89(11)
C(11)-N(6)	1.477(6)	N(4)-C(7)-C(12)	111.2(3)	N(2)-Cu(1)-N(1)	91.21(13)
C(11)-C(12)	1.554(6)	N(4)-C(7)-C(8)	109.1(3)	N(4)-Cu(1)-N(5)	92.51(14)
C(13)-O(5)	1.412(7)	C(12)-C(7)-C(8)	112.8(3)	N(2)-Cu(1)-N(5)	88.69(12)
N(1)-Cu(1)	2.025(3)	C(7)-C(8)-C(9)	113.1(4)	N(1)-Cu(1)-N(5)	176.79(14)
N(2)-Cu(1)	2.020(3)	N(5)-C(9)-C(8)	110.0(3)	N(4)-Cu(1)-O(4)	88.60(12)
N(4)-Cu(1)	2.009(3)	N(5)-C(9)-C(10)	110.3(3)	N(2)-Cu(1)-O(4)	86.51(11)
N(5)-Cu(1)	2.045(3)	C(8)-C(9)-C(10)	112.3(3)	N(1)-Cu(1)-O(4)	106.70(12)
O(1)-S(1)	1.486(3)	C(9)-C(10)-C(11)	112.5(3)	N(5)-Cu(1)-O(4)	76.50(12)
O(2)-S(1)	1.462(3)	N(6)-C(11)-C(10)	109.8(3)		

Ortep-3 representation of [Cu(*trans*-tach)$_2$(SO$_4$)] (**46**): thermal ellipsoids at 50% probability, hydrogen atoms are omitted for clarity.

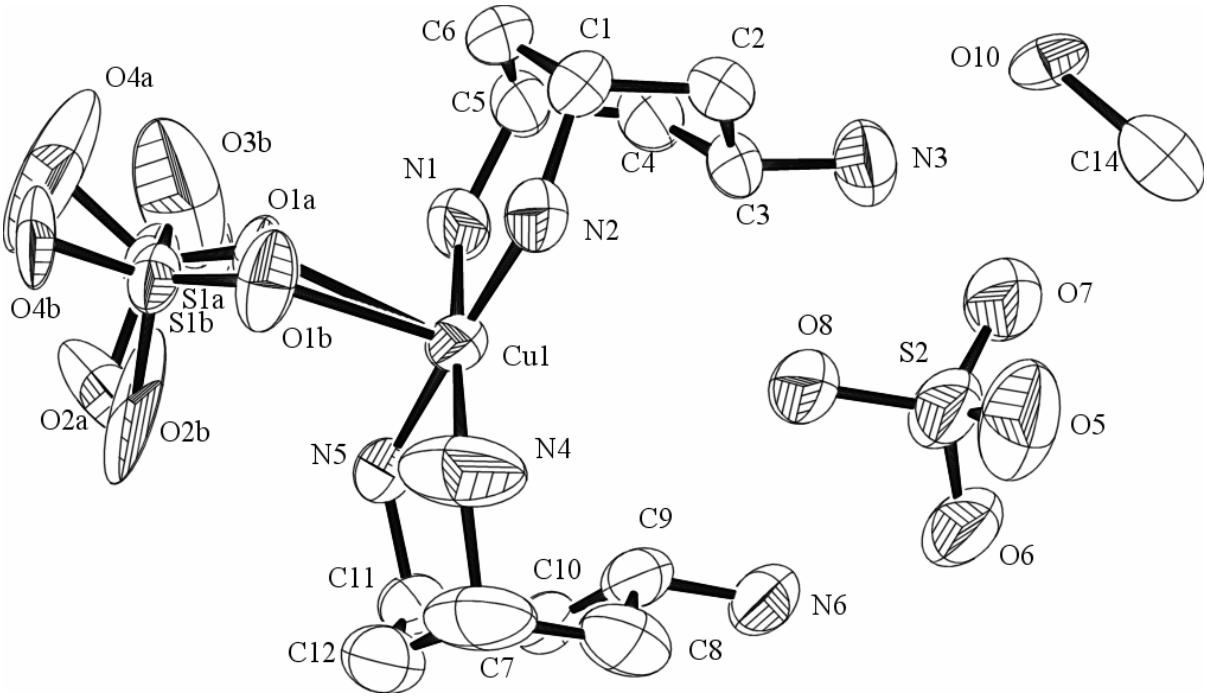


6.20 [Cu(trans-tachH)$_2$(SO$_4$)]SO$_4$ (46 · H$_2$SO$_4$)

Crystallisation method	Diffusion of ether into methanol / water solution over 2 weeks.	
Empirical formula	$C_{12.33}H_{37.50}CuN_6O_{10.42}S_2$ - ($C_{12}H_{32}N_6CuO_4S^{2+}$), ($SO_4^{2-}$), 0.33($CH_3OH$), 2.09($H_2O$)	
Formula weight	564.31	
Temperature	200(2) K	
Wavelength	1.54178 Å	
Crystal system	Trigonal	
Space group	*P* -3 *c* 1 (165)	
Unit cell dimensions	a = 28.3688(3) Å	α = 90°.
	b = 28.3688(3) Å	β = 90°.
	c = 12.3891(2) Å	γ = 120°.
Volume	8634.80(19) Å^3	
Z	12	
Density (calculated)	1.302 Mg/m^3	
Absorption coefficient	2.883 mm^{-1}	
F(000)	3574	
Crystal description	violet plates	
Crystal size	0.36 x 0.08 x 0.06 mm^3	
Theta range for data collection	1.80 to 58.96°.	
Index ranges	0<=h<=27, 0<=k<=27, 0<=l<=13	
Reflections collected	29093	
Independent reflections	4158 [R(int) = 0.1306]	
Completeness to theta = 58.96°	100.0 %	
Absorption correction	None	
Refinement method	Full-matrix least-squares on F^2	
Data / restraints / parameters	4158 / 20 / 348	
Goodness-of-fit on F^2	1.010	
Final R indices [I>2sigma(I)]	R1 = 0.0962, wR2 = 0.2741	
R indices (all data)	R1 = 0.1435, wR2 = 0.3056	
Extinction coefficient	0.00019(6)	
Largest diff. peak and hole	1.210 and -0.529 e.Å^{-3}	
Weighting scheme parameters A and B	0.1979 and 0.0000	

Refinement details: The sulphato ligand is disordered over two positions with a 60:40 ratio in occupancies for the two A and B sets. The methanol molecule is disordered over three positions and the oxygen atoms O9 and O11 are partially occupied. This results in 25.08 water molecules per unit cell considering the fully occupied oxygen atom O12.

Ortep-3 representation of [Cu(*trans*-tachH)$_2$(SO$_4$)]SO$_4$ (**46** • H$_2$SO$_4$): thermal ellipsoids at 50% probability, hydrogen atoms and water molecules are omitted for clarity.



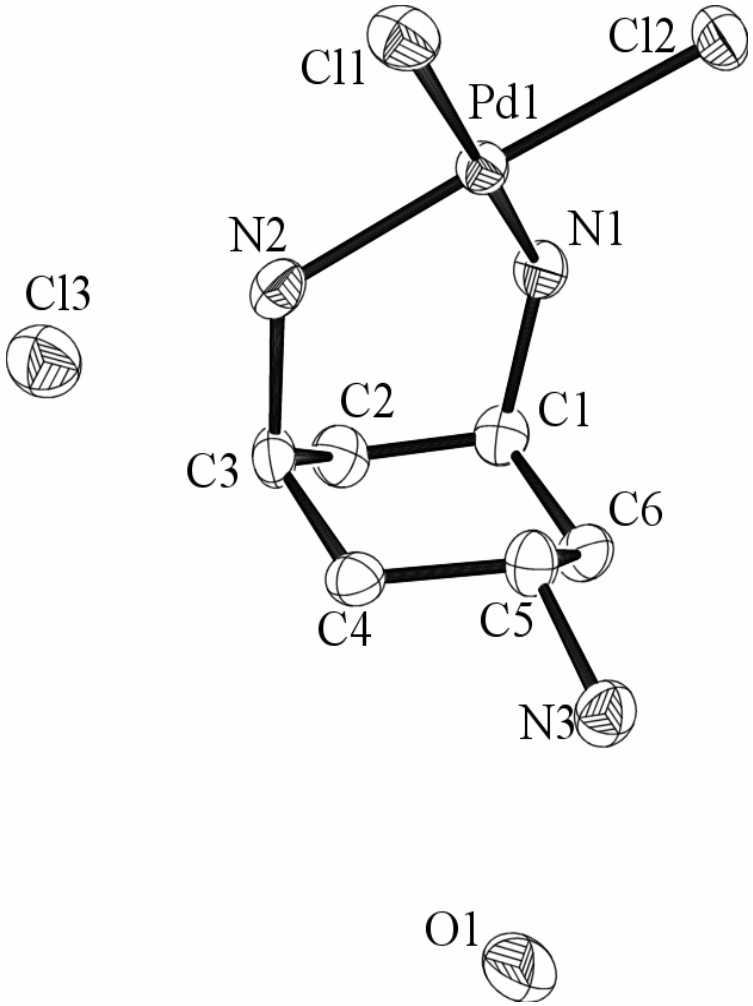
6.21 [Pd(trans-tachH)Cl_2]Cl (47)

Crystallisation method	From saturated aqueous solution over 1-2 days.	
Empirical formula	$C_6H_{18}Cl_3N_3OPd$ - ($C_6H_{16}N_3PdCl_2^+$), (Cl^-), (H_2O)	
Formula weight	360.98	
Temperature	298(2) K	
Wavelength	1.54178 Å	
Crystal system	Orthorhombic	
Space group	**P b c** 2_1 (29)	
Unit cell dimensions	a = 12.44450(10) Å	α = 90°.
	b = 12.20510(10) Å	β = 90°.
	c = 8.32130(10) Å	γ = 90°.
Volume	1263.89(2) $Å^3$	
Z	4	
Density (calculated)	1.897 Mg/m^3	
Absorption coefficient	17.500 mm^{-1}	
F(000)	720	
Crystal description	Orange needles	
Crystal size	0.15 x 0.02 x 0.02 mm^3	
Theta range for data collection	3.55 to 70.71°.	
Index ranges	-15<=h<=14, -13<=k<=14, -9<=l<=8	
Reflections collected	5508	
Independent reflections	1904 [R(int) = 0.0519]	
Completeness to theta = 70.71°	96.1 %	
Absorption correction	None	
Refinement method	Full-matrix least-squares on F^2	
Data / restraints / parameters	1904 / 4 / 134	
Goodness-of-fit on F^2	1.021	
Final R indices [I>2sigma(I)]	R1 = 0.0431, wR2 = 0.1064	
R indices (all data)	R1 = 0.0459, wR2 = 0.1082	
Absolute structure parameter	0.14(2)	
Largest diff. peak and hole	2.710 and -1.893 e.$Å^{-3}$	
Weighting scheme parameters A and B	0.0728 and 0.0000	

Bond lengths [Å] and angles [°]

C(1)-N(1)	1.508(8)	Pd(1)-N(1)	2.046(6)	N(3)-C(5)-C(6)	108.4(6)
C(1)-C(2)	1.510(10)	Pd(1)-N(2)	2.047(6)	C(4)-C(5)-C(6)	112.6(6)
C(1)-C(6)	1.526(10)	N(1)-C(1)-C(2)	109.9(5)	C(1)-C(6)-C(5)	113.6(6)
C(2)-C(3)	1.539(9)	N(1)-C(1)-C(6)	111.3(6)	N(1)-Pd(1)-N(2)	90.9(2)
C(3)-N(2)	1.485(8)	C(2)-C(1)-C(6)	112.3(6)	N(1)-Pd(1)-Cl(2)	88.18(16)
C(3)-C(4)	1.520(10)	C(1)-C(2)-C(3)	113.2(6)	N(2)-Pd(1)-Cl(2)	178.55(18)
C(4)-C(5)	1.533(10)	N(2)-C(3)-C(4)	110.9(6)	N(1)-Pd(1)-Cl(1)	178.8(2)
C(5)-N(3)	1.478(10)	N(2)-C(3)-C(2)	110.0(5)	N(2)-Pd(1)-Cl(1)	88.24(16)
C(5)-C(6)	1.540(10)	C(4)-C(3)-C(2)	112.2(5)	Cl(2)-Pd(1)-Cl(1)	92.70(6)
Cl(1)-Pd(1)	2.3232(16)	C(3)-C(4)-C(5)	114.0(6)	C(1)-N(1)-Pd(1)	119.0(4)
Cl(2)-Pd(1)	2.3142(19)	N(3)-C(5)-C(4)	109.1(6)	C(3)-N(2)-Pd(1)	119.5(4)

Ortep-3 representation of [Pd(*trans*-tachH)Cl_2]Cl (**47**): thermal ellipsoids at 50% probability, hydrogen atoms are omitted for clarity.



6.22 [Pd(trans-tachH)Br_2]$_2$[$PdBr_4$] (48)

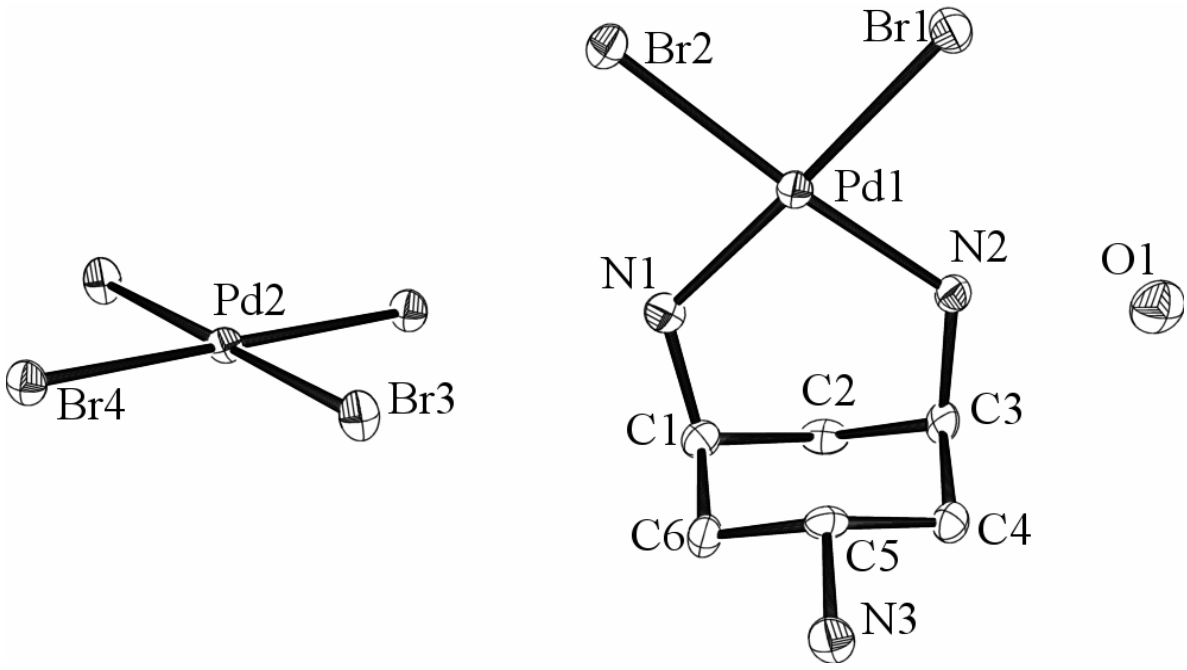
Crystallisation method	Standing of saturated aqueous solution overnight.	
Empirical formula	$C_{12}H_{36}Br_8N_6O_2Pd_3$ - 2($C_6H_{16}N_3PdBr_2^{+}$), ($PdBr_4^{2-}$), 2(H_2O)	
Formula weight	1254.95	
Temperature	150(2) K	
Wavelength	0.71073 Å	
Crystal system	Triclinic	
Space group	*P*-1 (2)	
Unit cell dimensions	a = 8.8314(4) Å	α = 69.095(2)°.
	b = 8.8782(3) Å	β = 76.249(2)°.
	c = 11.5103(6) Å	γ = 60.895(2)°.
Volume	734.35(6) $Å^3$	
Z	1	
Density (calculated)	2.838 Mg/m^3	
Absorption coefficient	12.722 mm^{-1}	
F(000)	584	
Crystal description	Red plates	
Crystal size	0.1 x 0.1 x 0.06 mm^3	
Theta range for data collection	1.90 to 27.50°.	
Index ranges	-10<=h<=11, -10<=k<=11, 0<=l<=14	
Reflections collected	18770	
Independent reflections	3371 [R(int) = 0.1237]	
Completeness to theta = 27.50°	99.7 %	
Absorption correction	Gaussian	
Max. and min. transmission	0.492 and 0.174	
Refinement method	Full-matrix least-squares on F^2	
Data / restraints / parameters	3371 / 3 / 149	
Goodness-of-fit on F^2	1.084	
Final R indices [I>2sigma(I)]	R1 = 0.0444, wR2 = 0.1155	
R indices (all data)	R1 = 0.0513, wR2 = 0.1189	
Extinction coefficient	0.0023(7)	
Largest diff. peak and hole	1.833 and -1.866 e.$Å^{-3}$	
Weighting scheme parameters A and B	0.0641 and 4.4332	

Bond lengths [Å] and angles [°]

C(1)-N(1)	1.485(9)	Pd(2)-Br(4)#1	2.4348(6)	C(1)-N(1)-Pd(1)	122.4(4)
C(1)-C(6)	1.525(9)	Pd(2)-Br(3)#1	2.4413(7)	C(3)-N(2)-Pd(1)	123.4(4)
C(1)-C(2)	1.532(9)	N(1)-C(1)-C(6)	112.0(6)	N(1)-Pd(1)-N(2)	94.7(2)
C(2)-C(3)	1.522(10)	N(1)-C(1)-C(2)	111.1(5)	N(1)-Pd(1)-Br(1)	177.59(17)
C(3)-N(2)	1.493(9)	C(6)-C(1)-C(2)	111.0(5)	N(2)-Pd(1)-Br(1)	87.64(16)
C(3)-C(4)	1.524(9)	C(3)-C(2)-C(1)	113.6(5)	N(1)-Pd(1)-Br(2)	85.73(16)
C(4)-C(5)	1.520(9)	N(2)-C(3)-C(2)	111.5(5)	N(2)-Pd(1)-Br(2)	171.06(16)
C(5)-N(3)	1.503(8)	N(2)-C(3)-C(4)	110.1(6)	Br(1)-Pd(1)-Br(2)	92.11(3)
C(5)-C(6)	1.527(9)	C(2)-C(3)-C(4)	111.8(5)	Br(4)#1-Pd(2)-Br(4)	180.00(3)
N(1)-Pd(1)	2.037(6)	C(5)-C(4)-C(3)	111.4(5)	Br(4)#1-Pd(2)-Br(3)	90.98(2)
N(2)-Pd(1)	2.061(6)	N(3)-C(5)-C(4)	108.7(5)	Br(4)-Pd(2)-Br(3)	89.02(2)
Br(1)-Pd(1)	2.4319(8)	N(3)-C(5)-C(6)	108.5(5)	Br(4)#1-Pd(2)-Br(3)#1	89.02(2)
Br(2)-Pd(1)	2.4404(8)	C(4)-C(5)-C(6)	111.8(5)	Br(4)-Pd(2)-Br(3)#1	90.98(2)
Br(3)-Pd(2)	2.4413(7)	C(1)-C(6)-C(5)	113.4(5)	Br(3)-Pd(2)-Br(3)#1	180.00(3)
Br(4)-Pd(2)	2.4348(6)				

Symmetry transformations used to generate equivalent atoms:
#1 -x,-y+1,-z+1

Ortep-3 representation of [Pd(*trans*-tachH)Br_2]$_2$[$PdBr_4$] (**48**): thermal ellipsoids at 50% probability, hydrogen atoms are omitted for clarity.



6.23 [Pd(trans-tachH)$_2$)](NO$_3$)$_4$ (49)

Crystallisation method	Evaporation of aqueous solution over 2 weeks.	
Empirical formula	$C_{12}H_{32}N_{10}O_{12}Pd$ - ($C_{12}H_{32}N_6Pd^{4+}$), 4(NO_3^-)	
Formula weight	614.88	
Temperature	298(2) K	
Wavelength	0.71069 Å	
Crystal system	Monoclinic	
Space group	$P\,2_1/c$ (14)	
Unit cell dimensions	a = 8.3934(11) Å	α = 90°.
	b = 16.649(2) Å	β = 109.419(4)°.
	c = 8.6914(11) Å	γ = 90°.
Volume	1145.5(2) Å^3	
Z	2	
Density (calculated)	1.783 Mg/m^3	
Absorption coefficient	0.891 mm^{-1}	
F(000)	632	
Crystal description	Pale yellow needles	
Crystal size	0.2 x 0.08 x 0.05 mm^3	
Theta range for data collection	2.45 to 25.47°.	
Index ranges	-10<=h<=10, -20<=k<=20, -10<=l<=10	
Reflections collected	6093	
Independent reflections	2026 [R(int) = 0.0680]	
Completeness to theta = 25.47°	95.1 %	
Absorption correction	None	
Refinement method	Full-matrix least-squares on F^2	
Data / restraints / parameters	2026 / 0 / 161	
Goodness-of-fit on F^2	1.333	
Final R indices [I>2sigma(I)]	R1 = 0.0857, wR2 = 0.1172	
R indices (all data)	R1 = 0.1043, wR2 = 0.1240	
Extinction coefficient	0.0021(8)	
Largest diff. peak and hole	0.504 and -0.807 e.Å^{-3}	
Weighting scheme parameters A and B	0.0000 and 5.1164	

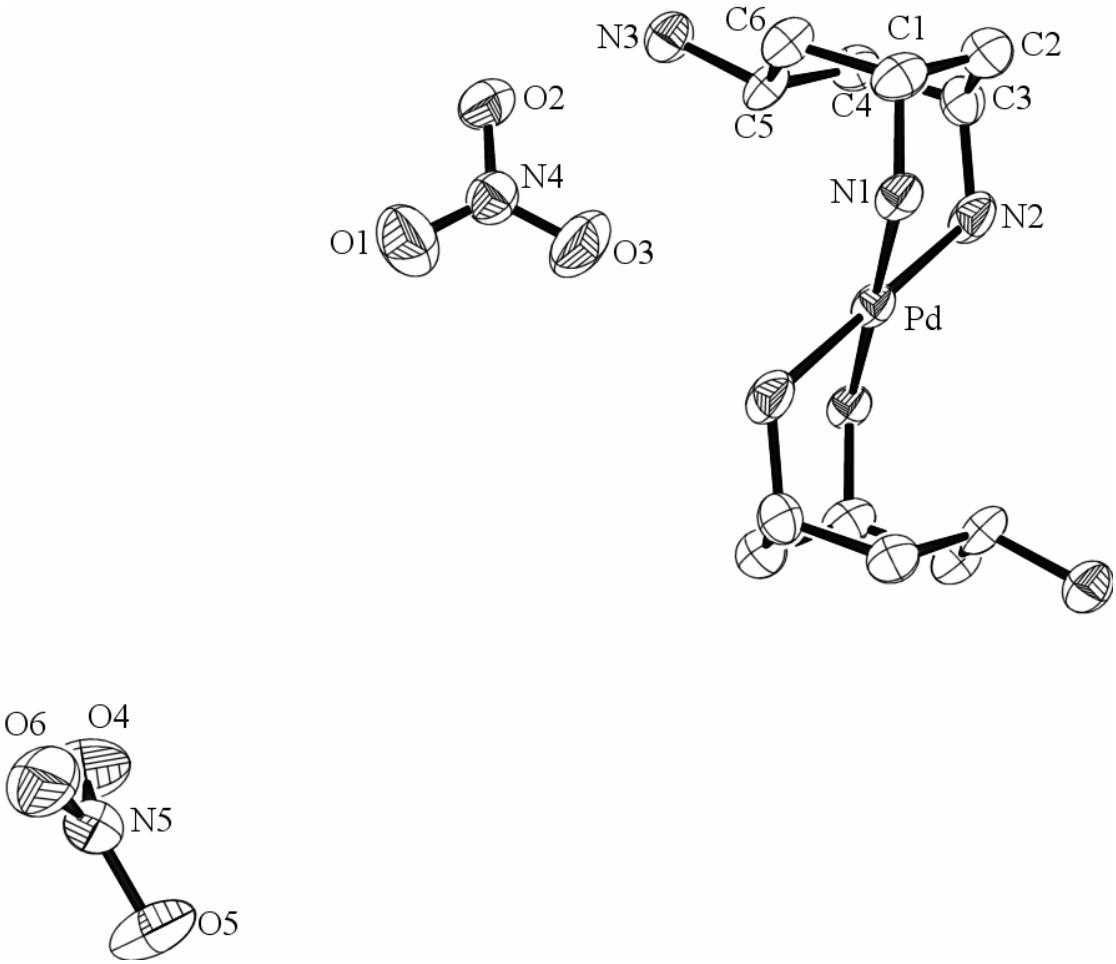
Bond lengths [Å] and angles [°]

C(1)-N(1)	1.496(9)	N(1)-C(1)-C(2)	111.0(6)	C(3)-N(2)-Pd	118.5(4)
C(1)-C(2)	1.513(10)	N(1)-C(1)-C(6)	110.7(6)	O(1)-N(4)-O(3)	122.5(8)
C(1)-C(6)	1.524(10)	C(2)-C(1)-C(6)	111.6(6)	O(1)-N(4)-O(2)	117.9(7)
C(2)-C(3)	1.522(11)	C(1)-C(2)-C(3)	113.2(7)	O(3)-N(4)-O(2)	119.6(7)
C(3)-N(2)	1.491(9)	N(2)-C(3)-C(2)	110.4(6)	O(6)-N(5)-O(5)	120.4(7)
C(3)-C(4)	1.530(10)	N(2)-C(3)-C(4)	111.2(6)	O(6)-N(5)-O(4)	120.8(7)
C(4)-C(5)	1.515(10)	C(2)-C(3)-C(4)	111.3(6)	O(5)-N(5)-O(4)	118.8(7)
C(5)-N(3)	1.496(8)	C(5)-C(4)-C(3)	113.1(6)	N(2)-Pd-N(2)#1	180.0(4)
C(5)-C(6)	1.523(10)	N(3)-C(5)-C(4)	109.4(6)	N(2)-Pd-N(1)#1	90.5(2)
N(1)-Pd	2.054(6)	N(3)-C(5)-C(6)	109.0(6)	N(2)#1-Pd-N(1)#1	89.5(2)
N(2)-Pd	2.053(6)	C(4)-C(5)-C(6)	113.5(6)	N(2)-Pd-N(1)	89.5(2)
N(4)-O(1)	1.220(8)	C(5)-C(6)-C(1)	112.9(6)	N(2)#1-Pd-N(1)	90.5(2)
N(4)-O(3)	1.220(8)	C(1)-N(1)-Pd	118.4(4)	N(1)#1-Pd-N(1)	180.0(3)
N(4)-O(2)	1.254(8)				
N(5)-O(6)	1.242(8)				
N(5)-O(5)	1.242(7)				
N(5)-O(4)	1.248(8)				
Pd-N(2)#1	2.053(6)				
Pd-N(1)#1	2.054(6)				

Symmetry transformations used to generate equivalent atoms:

#1 -x,-y,-z

Ortep-3 representation of [Pd(*trans*-tachH)$_2$)](NO$_3$)$_4$ (**49**): thermal ellipsoids at 50% probability, hydrogen atoms are omitted for clarity.



6.24 [Pd(trans-tachH)$_2$](SO$_4$)$_2$ (50)

Crystallisation method	Evaporation of aqueous solution over 2 weeks.	
Empirical formula	$C_{12}H_{44}N_6O_{14}PdS_2$ - ($C_{12}H_{32}N_6Pd^{4+}$), 2(SO_4^{2-}), 6(H_2O)	
Formula weight	667.05	
Temperature	120(2) K	
Wavelength	0.71073 Å	
Crystal system	Monoclinic	
Space group	$P\,2_1/n$ (14)	
Unit cell dimensions	a = 8.2588(2) Å	α = 90°.
	b = 17.3414(4) Å	β = 99.1200(10)°.
	c = 9.1518(2) Å	γ = 90°.
Volume	1294.14(5) Å^3	
Z	2	
Density (calculated)	1.712 Mg/m^3	
Absorption coefficient	0.952 mm^{-1}	
F(000)	696	
Crystal description	Pale yellow plates	
Crystal size	0.2 x 0.16 x 0.06 mm^3	
Theta range for data collection	2.35 to 35.05°.	
Index ranges	-13<=h<=13, 0<=k<=27, 0<=l<=14	
Reflections collected	23350	
Independent reflections	5618 [R(int) = 0.0527]	
Completeness to theta = 35.05°	98.2 %	
Absorption correction	None	
Refinement method	Full-matrix least-squares on F^2	
Data / restraints / parameters	5618 / 9 / 178	
Goodness-of-fit on F^2	1.053	
Final R indices [I>2sigma(I)]	R1 = 0.0326, wR2 = 0.0686	
R indices (all data)	R1 = 0.0495, wR2 = 0.0760	
Largest diff. peak and hole	0.712 and -1.004 e.Å^{-3}	
Weighting scheme parameters A and B	0.0279 and 1.1423	

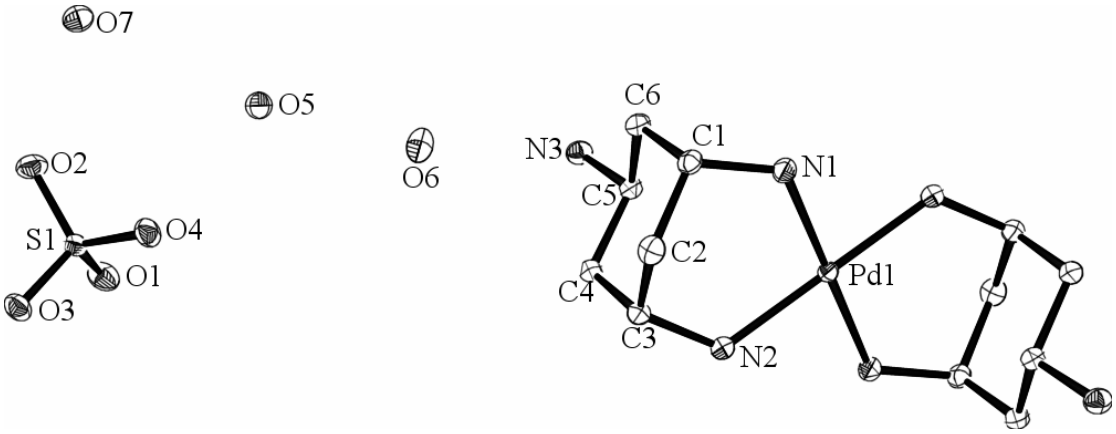
Bond lengths [Å] and angles [°]

C(1)-N(1)	1.495(2)	Pd(1)-N(2)#1	2.0550(14)	C(1)-N(1)-Pd(1)	121.91(10)
C(1)-C(2)	1.530(2)	Pd(1)-N(1)#1	2.0635(13)	C(3)-N(2)-Pd(1)	122.06(10)
C(1)-C(6)	1.531(2)	N(1)-C(1)-C(2)	111.27(12)	O(4)-S(1)-O(3)	109.59(8)
C(2)-C(3)	1.526(2)	N(1)-C(1)-C(6)	111.27(13)	O(4)-S(1)-O(2)	110.32(8)
C(3)-N(2)	1.496(2)	C(2)-C(1)-C(6)	111.45(13)	O(3)-S(1)-O(2)	109.91(8)
C(3)-C(4)	1.529(2)	C(3)-C(2)-C(1)	113.62(13)	O(4)-S(1)-O(1)	110.19(9)
C(4)-C(5)	1.528(2)	N(2)-C(3)-C(2)	111.47(13)	O(3)-S(1)-O(1)	107.69(8)
C(5)-N(3)	1.496(2)	N(2)-C(3)-C(4)	110.53(13)	O(2)-S(1)-O(1)	109.09(8)
C(5)-C(6)	1.523(2)	C(2)-C(3)-C(4)	111.41(13)	N(2)-Pd(1)-N(2)#1	180.00(10)
N(1)-Pd(1)	2.0635(13)	C(5)-C(4)-C(3)	112.25(13)	N(2)-Pd(1)-N(1)#1	85.24(5)
N(2)-Pd(1)	2.0550(14)	N(3)-C(5)-C(6)	110.19(12)	N(2)#1-Pd(1)-N(1)#1	94.76(5)
O(1)-S(1)	1.4816(14)	N(3)-C(5)-C(4)	108.83(13)	N(2)-Pd(1)-N(1)	94.76(5)
O(2)-S(1)	1.4802(13)	C(6)-C(5)-C(4)	111.01(14)	N(2)#1-Pd(1)-N(1)	85.24(5)
O(3)-S(1)	1.4790(13)	C(5)-C(6)-C(1)	111.58(12)	N(1)#1-Pd(1)-N(1)	180.00(10)
O(4)-S(1)	1.4746(13)				

Symmetry transformations used to generate equivalent atoms:

#1 -x,-y,-z

Ortep-3 representation of [Pd(*trans*-tachH)$_2$](SO$_4$)$_2$ (**50**): thermal ellipsoids at 50% probability, hydrogen atoms are omitted for clarity.



6.25 [Pd{Pd(μ$_2$-trans-tach)Cl$_2$}$_2$Cl$_2$] (53)

Crystallisation method	Evaporation of aqueous solution at 80°C over 7 days.	
Empirical formula	$C_{12}H_{30}Cl_6N_6Pd_3$	
Formula weight	790.32	
Temperature	298(2) K	
Wavelength	1.54178 Å	
Crystal system	Monoclinic	
Space group	*I* 2/*a* (15)	
Unit cell dimensions	a = 15.5544(9) Å	α = 90°.
	b = 9.6173(5) Å	β = 90.000(4)°.
	c = 17.1240(9) Å	γ = 90°.
Volume	2561.6(2) Å^3	
Z	4	
Density (calculated)	2.049 Mg/m^3	
Absorption coefficient	22.670 mm^{-1}	
F(000)	1536	
Crystal description	Orange blocks	
Crystal size	0.3 x 0.3 x 0.3 mm^3	
Theta range for data collection	5.17 to 70.69°.	
Index ranges	-16<=h<=17, -10<=k<=11, -16<=l<=20	
Reflections collected	5038	
Independent reflections	2140 [R(int) = 0.1149]	
Completeness to theta = 70.69°	86.9 %	
Refinement method	Full-matrix least-squares on F^2	
Data / restraints / parameters	2140 / 0 / 123	
Goodness-of-fit on F^2	1.036	
Final R indices [I>2sigma(I)]	R1 = 0.0863, wR2 = 0.2145	
R indices (all data)	R1 = 0.1031, wR2 = 0.2351	
Largest diff. peak and hole	1.839 and -1.688 e.Å^{-3}	
Weighting scheme parameters A and B	0.0000 and 0.0000	

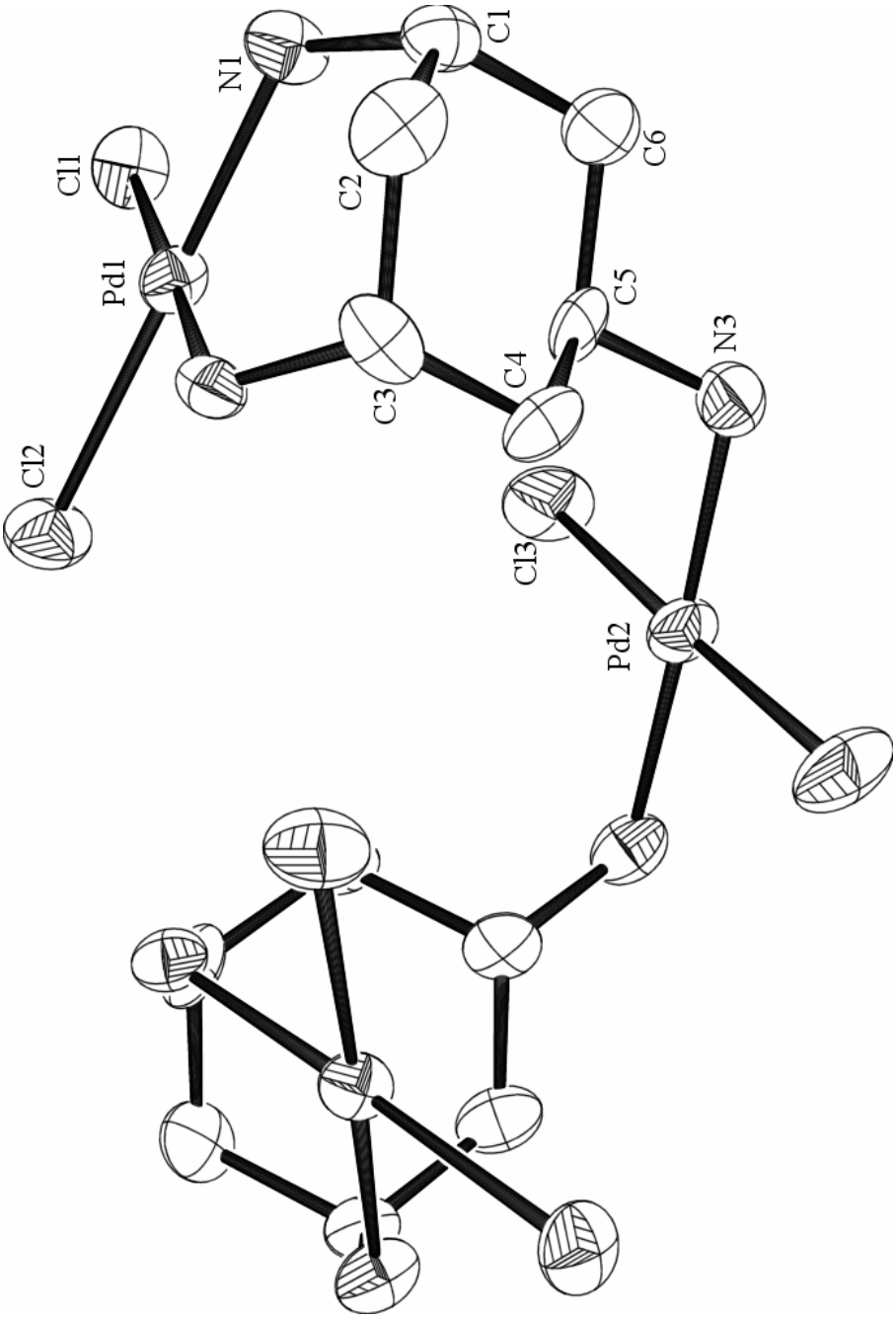
Bond lengths [Å] and angles [°]

C(1)-N(1)	1.457(16)	N(1)-C(1)-C(6)	113.7(11)	C(5)-N(3)-Pd(2)	112.3(8)
C(1)-C(6)	1.53(2)	N(1)-C(1)-C(2)	109.4(11)	N(1)-Pd(1)-N(2)	91.4(4)
C(1)-C(2)	1.551(18)	C(6)-C(1)-C(2)	110.2(10)	N(1)-Pd(1)-Cl(2)	177.7(3)
C(2)-C(3)	1.51(2)	C(3)-C(2)-C(1)	111.5(11)	N(2)-Pd(1)-Cl(2)	86.6(3)
C(3)-N(2)	1.471(16)	N(2)-C(3)-C(2)	111.2(11)	N(1)-Pd(1)-Cl(1)	88.1(3)
C(3)-C(4)	1.531(19)	N(2)-C(3)-C(4)	111.7(11)	N(2)-Pd(1)-Cl(1)	178.3(3)
C(4)-C(5)	1.544(18)	C(2)-C(3)-C(4)	113.6(11)	Cl(2)-Pd(1)-Cl(1)	93.87(13)
C(5)-N(3)	1.487(17)	C(3)-C(4)-C(5)	112.2(10)	N(3)#1-Pd(2)-N(3)	177.8(6)
C(5)-C(6)	1.526(18)	N(3)-C(5)-C(6)	111.2(11)	N(3)#1-Pd(2)-Cl(3)	89.6(3)
N(1)-Pd(1)	2.042(11)	N(3)-C(5)-C(4)	109.5(9)	N(3)-Pd(2)-Cl(3)	90.5(3)
N(2)-Pd(1)	2.061(10)	C(6)-C(5)-C(4)	109.9(12)	N(3)#1-Pd(2)-Cl(3)#1	90.5(3)
N(3)-Pd(2)	2.063(12)	C(5)-C(6)-C(1)	112.8(12)	N(3)-Pd(2)-Cl(3)#1	89.6(3)
Cl(1)-Pd(1)	2.325(3)	C(1)-N(1)-Pd(1)	121.0(8)	Cl(3)-Pd(2)-Cl(3)#1	177.3(2)
Cl(2)-Pd(1)	2.318(3)	C(3)-N(2)-Pd(1)	117.8(7)		
Cl(3)-Pd(2)	2.302(3)				
Pd(2)-N(3)#1	2.063(12)				
Pd(2)-Cl(3)#1	2.302(3)				

Symmetry transformations used to generate equivalent atoms:

#1 -x+3/2,y,-z

Ortep-3 representation of $[Pd\{Pd(\mu_2\text{-}trans\text{-}tach)Cl_2\}_2Cl_2]$ (**53**): thermal ellipsoids at 50% probability, hydrogen atoms are omitted for clarity.



6.26 cyclo[{Pd(μ$_2$-trans-tach)Cl}$_6$]Cl$_6$ (51)

Crystallisation method	Diffusion of methanol into aqueous solution over 3 days.	
Empirical formula	$C_{36}H_{113.12}Cl_{12}N_{18}O_{11.56}Pd_6$ - ($C_{36}H_{90}N_{18}Pd_6Cl_6^{6+}$), 6($Cl^-$), 11.56($H_2O$)	
Formula weight	2047.32	
Temperature	296(2) K	
Wavelength	0.71073 Å	
Crystal system	Triclinic	
Space group	*P* -1 (2)	
Unit cell dimensions	a = 11.924(2) Å	α = 79.12(3)°.
	b = 12.710(3) Å	β = 68.93(3)°.
	c = 13.929(3) Å	γ = 88.33(3)°.
Volume	1932.7(7) Å^3	
Z	1	
Density (calculated)	1.759 Mg/m^3	
Absorption coefficient	1.837 mm^{-1}	
F(000)	1028	
Crystal description	Yellow plates	
Crystal size	0.15 x 0.10 x 0.08 mm^3	
Theta range for data collection	1.60 to 29.09°.	
Index ranges	-16<=h<=16, -17<=k<=17, -19<=l<=19	
Reflections collected	15688	
Independent reflections	8782 [R(int) = 0.0439]	
Completeness to theta = 29.09°	84.7 %	
Absorption correction	None	
Refinement method	Full-matrix least-squares on F^2	
Data / restraints / parameters	8782 / 0 / 431	
Goodness-of-fit on F^2	1.151	
Final R indices [I>2sigma(I)]	R1 = 0.0613, wR2 = 0.1303	
R indices (all data)	R1 = 0.0684, wR2 = 0.1353	
Extinction coefficient	0.0056(5)	
Largest diff. peak and hole	0.724 and -0.937 e.Å^{-3}	
Weighting scheme parameters A and B	0.0311 and 8.7247	

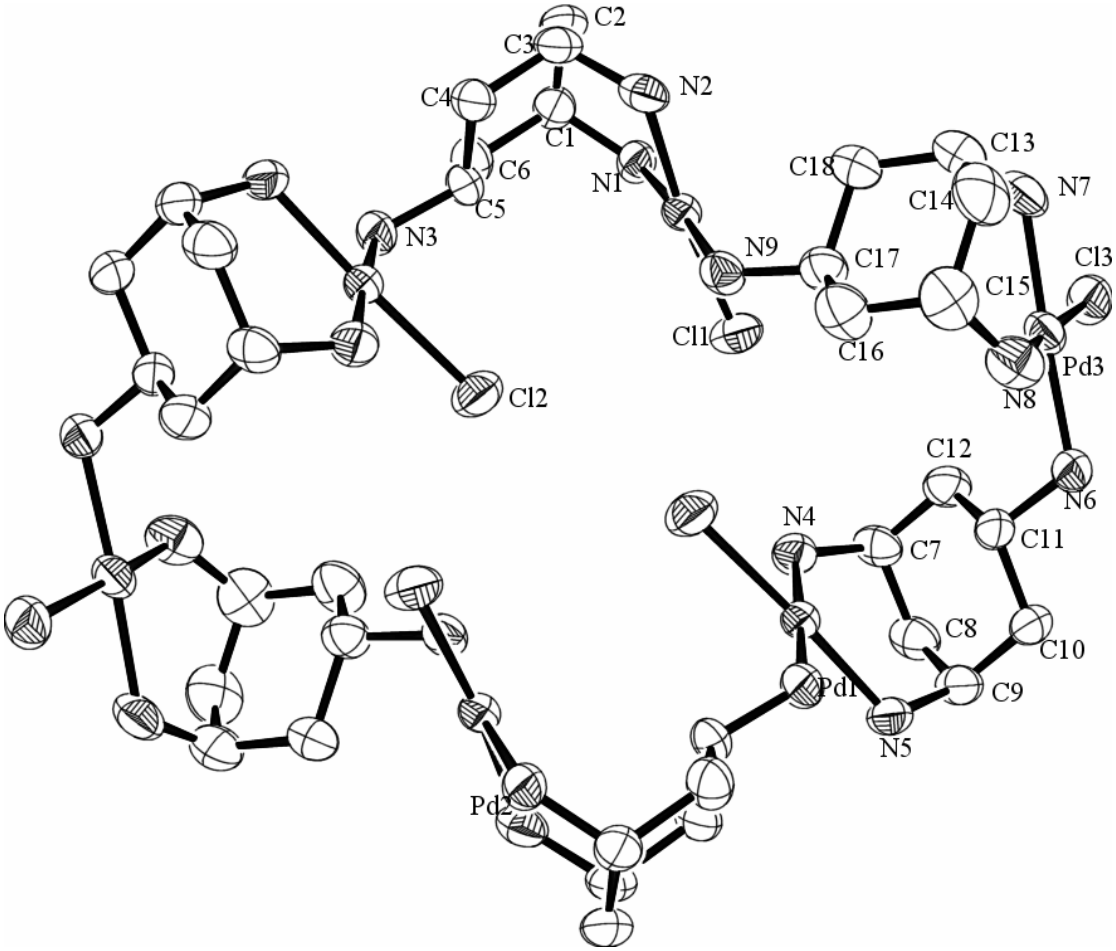
Refinement details: The three chloride counterions in the asymmetric unit are disordered over six positions Cl4, Cl5, Cl6A, Cl6B, Cl7A and Cl7B. The crystal water is disordered over nine positions with a total occupancy of 11.56 water molecules per palladium(II) ring unit.

Bond lengths [Å] and angles [°]

C(1)-N(1)	1.497(8)	Pd(2)-N(3)	2.067(5)	C(15)-C(14)-C(13)	113.1(6)
C(1)-C(6)	1.520(9)	Pd(3)-N(7)	2.034(6)	N(8)-C(15)-C(14)	110.5(8)
C(1)-C(2)	1.534(10)	Pd(3)-N(8)	2.048(6)	N(8)-C(15)-C(16)	111.5(7)
C(2)-C(3)	1.519(10)	Pd(3)-N(6)	2.063(5)	C(14)-C(15)-C(16)	112.0(7)
C(3)-N(2)	1.499(9)	N(4)-Pd(2)#1	2.060(5)	C(15)-C(16)-C(17)	114.1(6)
C(3)-C(4)	1.513(9)	N(5)-Pd(2)#1	2.056(5)	N(9)-C(17)-C(18)	109.0(5)
C(4)-C(5)	1.522(8)	O(6A)-O(6B)	1.15(3)	N(9)-C(17)-C(16)	111.2(6)
C(5)-N(3)	1.494(8)	O(7A)-O(7B)#2	1.293(8)	C(18)-C(17)-C(16)	110.2(6)
C(5)-C(6)	1.541(9)	O(7A)-O(7B)	1.293(8)	C(17)-C(18)-C(13)	113.1(6)
C(7)-N(4)	1.491(8)			N(1)-Pd(1)-N(2)	91.1(2)
C(7)-C(12)	1.520(10)	N(1)-C(1)-C(6)	112.2(5)	N(1)-Pd(1)-N(9)	175.7(2)
C(7)-C(8)	1.531(9)	N(1)-C(1)-C(2)	110.2(6)	N(2)-Pd(1)-N(9)	90.7(2)
C(8)-C(9)	1.532(11)	C(6)-C(1)-C(2)	111.7(6)	N(1)-Pd(1)-Cl(1)	88.94(15)
C(9)-N(5)	1.489(8)	C(3)-C(2)-C(1)	112.2(5)	N(2)-Pd(1)-Cl(1)	174.12(17)
C(9)-C(10)	1.523(10)	N(2)-C(3)-C(4)	110.5(5)	N(9)-Pd(1)-Cl(1)	89.71(16)
C(10)-C(11)	1.535(8)	N(2)-C(3)-C(2)	110.6(6)	N(5)#1-Pd(2)-N(4)#1	91.4(2)
C(11)-N(6)	1.488(8)	C(4)-C(3)-C(2)	112.9(6)	N(5)#1-Pd(2)-N(3)	91.4(2)
C(11)-C(12)	1.539(9)	C(3)-C(4)-C(5)	112.5(5)	N(4)#1-Pd(2)-N(3)	177.3(2)
C(13)-N(7)	1.481(10)	N(3)-C(5)-C(4)	110.0(5)	N(5)#1-Pd(2)-Cl(2)	177.00(18)
C(13)-C(14)	1.526(12)	N(3)-C(5)-C(6)	110.9(5)	N(4)#1-Pd(2)-Cl(2)	88.14(16)
C(13)-C(18)	1.533(11)	C(4)-C(5)-C(6)	111.6(5)	N(3)-Pd(2)-Cl(2)	89.14(16)
C(14)-C(15)	1.506(12)	C(1)-C(6)-C(5)	112.4(6)	N(7)-Pd(3)-N(8)	92.9(3)
C(15)-N(8)	1.493(11)	N(4)-C(7)-C(12)	111.9(5)	N(7)-Pd(3)-N(6)	176.1(2)
C(15)-C(16)	1.534(11)	N(4)-C(7)-C(8)	110.2(5)	N(8)-Pd(3)-N(6)	90.7(2)
C(16)-C(17)	1.538(9)	C(12)-C(7)-C(8)	111.9(6)	N(7)-Pd(3)-Cl(3)	86.85(19)
C(17)-N(9)	1.485(9)	C(7)-C(8)-C(9)	112.4(6)	N(8)-Pd(3)-Cl(3)	174.6(2)
C(17)-C(18)	1.528(9)	N(5)-C(9)-C(10)	110.8(6)	N(6)-Pd(3)-Cl(3)	89.37(17)
Cl(1)-Pd(1)	2.3159(17)	N(5)-C(9)-C(8)	111.2(6)	C(1)-N(1)-Pd(1)	119.3(4)
Cl(2)-Pd(2)	2.3080(18)	C(10)-C(9)-C(8)	111.8(5)	C(3)-N(2)-Pd(1)	119.7(4)
Cl(3)-Pd(3)	2.292(2)	C(9)-C(10)-C(11)	113.2(5)	C(5)-N(3)-Pd(2)	113.3(4)
Cl(6A)-Cl(6B)	1.232(17)	N(6)-C(11)-C(10)	109.7(5)	C(7)-N(4)-Pd(2)#1	118.4(4)
Cl(7A)-Cl(7B)	0.61(2)	N(6)-C(11)-C(12)	111.3(5)	C(9)-N(5)-Pd(2)#1	119.0(4)
Pd(1)-N(1)	2.052(5)	C(10)-C(11)-C(12)	110.7(6)	C(11)-N(6)-Pd(3)	118.6(4)
Pd(1)-N(2)	2.063(5)	C(7)-C(12)-C(11)	113.8(5)	C(13)-N(7)-Pd(3)	122.4(5)
Pd(1)-N(9)	2.072(5)	N(7)-C(13)-C(14)	110.5(7)	C(15)-N(8)-Pd(3)	120.8(5)
Pd(2)-N(5)#1	2.056(5)	N(7)-C(13)-C(18)	111.6(7)	C(17)-N(9)-Pd(1)	118.5(4)
Pd(2)-N(4)#1	2.060(5)	C(14)-C(13)-C(18)	111.9(7)	O(7B)#2-O(7A)-O(7B)	180.0(12)

Symmetry transformations used to generate equivalent atoms: #1 -x+1,-y+2,-z+1 #2 -x+1,-y,-z

Ortep-3 representation of *cyclo*[{Pd(μ_2-*trans*-tach)Cl}$_6$]Cl$_6$ (**51**): thermal ellipsoids at 50% probability, hydrogen atoms, chloride counterions and solvent molecules are omitted for clarity.



6.27 cyclo[{Pd(μ$_2$-trans-tach)Br}$_6$]Br$_6$ (52)

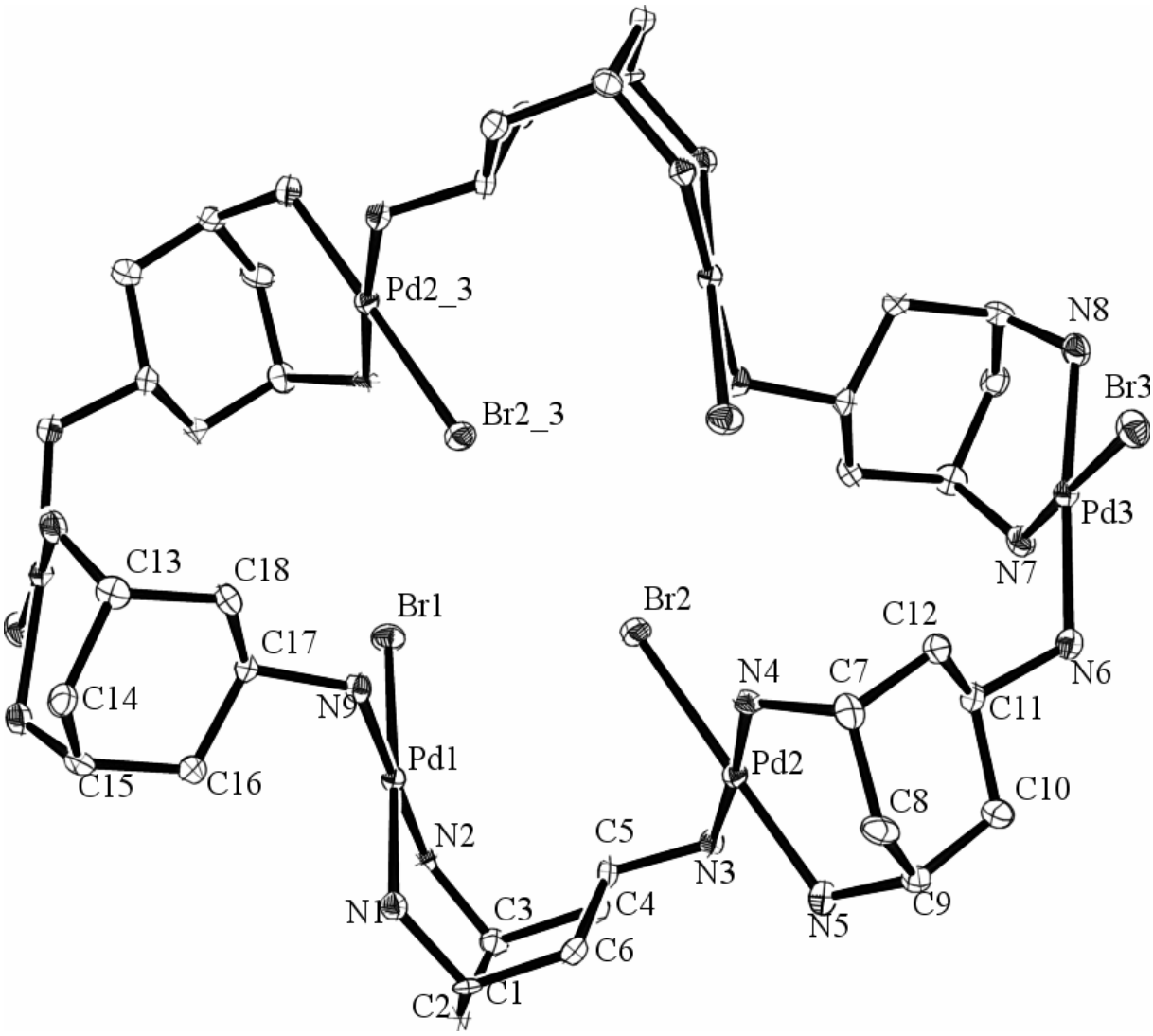
Crystallisation method	Diffusion of methanol into aqueous solution over 3 days.	
Empirical formula	$C_{36}H_{130}Br_{12}N_{18}O_{20}Pd_6$ - ($C_{36}H_{90}N_{18}Pd_6Br_6^{6+}$), 6($Br^-$), 20($H_2O$)	
Formula weight	2732.90	
Temperature	120(2) K	
Wavelength	0.71073 Å	
Crystal system	Monoclinic	
Space group	$P\,2_1/n$ (14)	
Unit cell dimensions	a = 12.4054(2) Å	α = 90°.
	b = 26.6675(5) Å	β = 90.7010(10)°.
	c = 12.8312(2) Å	γ = 90°.
Volume	4244.51(12) Å^3	
Z	2	
Density (calculated)	2.138 Mg/m^3	
Absorption coefficient	6.958 mm^{-1}	
F(000)	2656	
Crystal description	Yellow plates	
Crystal size	0.26 x 0.14 x 0.07 mm^3	
Theta range for data collection	1.53 to 26.00°.	
Index ranges	-15<=h<=15, 0<=k<=32, 0<=l<=15	
Reflections collected	26763	
Independent reflections	8317 [R(int) = 0.1146]	
Completeness to theta = 26.00°	99.7 %	
Absorption correction	Empirical	
Max. and min. transmission	1.196 and 0.759	
Refinement method	Full-matrix least-squares on F^2	
Data / restraints / parameters	8317 / 30 / 475	
Goodness-of-fit on F^2	1.130	
Final R indices [I>2sigma(I)]	R1 = 0.0391, wR2 = 0.0848	
R indices (all data)	R1 = 0.0647, wR2 = 0.0919	
Largest diff. peak and hole	0.891 and -0.913 e.Å^{-3}	
Weighting scheme parameters A and B	0.0415 and 7.1151	

Table 3. Bond lengths [Å] and angles [°] for gs320.

C(1)-N(1)	1.492(7)	N(8)-C(15)#1	1.487(7)	N(8)#1-C(15)-C(14)	110.0(5)
C(1)-C(2)	1.508(8)	N(8)-Pd(3)	2.053(5)	N(8)#1-C(15)-C(16)	111.8(5)
C(1)-C(6)	1.525(7)	N(9)-Pd(1)	2.061(5)	C(14)-C(15)-C(16)	111.6(5)
C(2)-C(3)	1.520(8)	Br(1)-Pd(1)	2.4243(7)	C(17)-C(16)-C(15)	113.7(5)
C(3)-N(2)	1.490(7)	Br(2)-Pd(2)	2.4260(7)	N(9)-C(17)-C(16)	108.1(4)
C(3)-C(4)	1.534(7)	Br(3)-Pd(3)	2.4433(7)	N(9)-C(17)-C(18)	109.7(4)
C(4)-C(5)	1.522(8)			C(16)-C(17)-C(18)	112.4(5)
C(5)-N(3)	1.485(6)	N(1)-C(1)-C(2)	111.1(4)	C(13)-C(18)-C(17)	114.2(4)
C(5)-C(6)	1.526(8)	N(1)-C(1)-C(6)	110.4(4)	C(1)-N(1)-Pd(1)	119.6(3)
C(7)-N(4)	1.497(6)	C(2)-C(1)-C(6)	111.2(4)	C(3)-N(2)-Pd(1)	120.1(3)
C(7)-C(12)	1.521(8)	C(1)-C(2)-C(3)	113.9(5)	C(5)-N(3)-Pd(2)	114.0(3)
C(7)-C(8)	1.536(8)	N(2)-C(3)-C(2)	110.6(5)	C(7)-N(4)-Pd(2)	120.5(3)
C(8)-C(9)	1.523(8)	N(2)-C(3)-C(4)	111.2(5)	C(9)-N(5)-Pd(2)	118.3(4)
C(9)-N(5)	1.503(6)	C(2)-C(3)-C(4)	110.8(4)	C(11)-N(6)-Pd(3)	121.4(3)
C(9)-C(10)	1.515(8)	C(5)-C(4)-C(3)	112.3(4)	C(13)#1-N(7)-Pd(3)	118.8(4)
C(10)-C(11)	1.538(8)	N(3)-C(5)-C(4)	111.8(4)	C(15)#1-N(8)-Pd(3)	120.4(4)
C(11)-N(6)	1.504(7)	N(3)-C(5)-C(6)	109.8(4)	C(17)-N(9)-Pd(1)	115.5(3)
C(11)-C(12)	1.526(8)	C(4)-C(5)-C(6)	111.1(5)	N(2)-Pd(1)-N(9)	177.72(19)
C(13)-N(7)#1	1.490(7)	C(1)-C(6)-C(5)	112.3(4)	N(2)-Pd(1)-N(1)	90.74(18)
C(13)-C(14)	1.519(8)	N(4)-C(7)-C(12)	110.9(4)	N(9)-Pd(1)-N(1)	91.54(18)
C(13)-C(18)	1.532(7)	N(4)-C(7)-C(8)	110.4(4)	N(2)-Pd(1)-Br(1)	89.75(13)
C(14)-C(15)	1.516(8)	C(12)-C(7)-C(8)	112.1(5)	N(9)-Pd(1)-Br(1)	87.97(13)
C(15)-N(8)#1	1.487(7)	C(9)-C(8)-C(7)	112.1(5)	N(1)-Pd(1)-Br(1)	178.23(12)
C(15)-C(16)	1.534(8)	N(5)-C(9)-C(10)	111.8(4)	N(5)-Pd(2)-N(4)	92.04(19)
C(16)-C(17)	1.529(8)	N(5)-C(9)-C(8)	109.3(4)	N(5)-Pd(2)-N(3)	90.00(18)
C(17)-N(9)	1.504(6)	C(10)-C(9)-C(8)	113.4(5)	N(4)-Pd(2)-N(3)	175.91(17)
C(17)-C(18)	1.542(8)	C(9)-C(10)-C(11)	115.3(5)	N(5)-Pd(2)-Br(2)	179.07(13)
N(1)-Pd(1)	2.078(5)	N(6)-C(11)-C(12)	108.7(4)	N(4)-Pd(2)-Br(2)	88.19(13)
N(2)-Pd(1)	2.041(5)	N(6)-C(11)-C(10)	108.2(4)	N(3)-Pd(2)-Br(2)	89.83(13)
N(3)-Pd(2)	2.057(4)	C(12)-C(11)-C(10)	111.7(5)	N(8)-Pd(3)-N(7)	89.39(19)
N(4)-Pd(2)	2.048(4)	C(7)-C(12)-C(11)	113.9(5)	N(8)-Pd(3)-N(6)	174.59(18)
N(5)-Pd(2)	2.042(5)	N(7)#1-C(13)-C(14)	109.9(4)	N(7)-Pd(3)-N(6)	89.59(19)
N(6)-Pd(3)	2.065(5)	N(7)#1-C(13)-C(18)	112.4(4)	N(8)-Pd(3)-Br(3)	88.96(14)
N(7)-C(13)#1	1.490(7)	C(14)-C(13)-C(18)	111.7(5)	N(7)-Pd(3)-Br(3)	176.81(13)
N(7)-Pd(3)	2.061(5)	C(15)-C(14)-C(13)	113.4(5)	N(6)-Pd(3)-Br(3)	91.80(13)

Symmetry transformations used to generate equivalent atoms: #1 -x+1,-y+2,-z+1

Ortep-3 representation of *cyclo*[{Pd(μ_2-*trans*-tach)Br}$_6$]Br$_6$ (**52**): thermal ellipsoids at 50% probability, hydrogen atoms, bromide counterions and solvent molecules are omitted for clarity.



6.28 poly{[Ag(μ$_3$-trans-tach)](NO$_3$)} (54)

Crystallisation method	Diffusion of ether into methanol / water solution over 2 days.	
Empirical formula	$C_6H_{15}AgN_4O_3$ - ($C_6H_{15}N_3Ag^+$), (NO_3^-)	
Formula weight	299.09	
Temperature	293(2) K	
Wavelength	1.54178 Å	
Crystal system	Monoclinic	
Space group	*P* $2_1/c$ (14)	
Unit cell dimensions	a = 13.717(3) Å	α = 90°.
	b = 8.9401(18) Å	β = 93.60(3)°.
	c = 16.635(3) Å	γ = 90°.
Volume	2035.9(7) Å^3	
Z	8	
Density (calculated)	1.952 Mg/m^3	
Absorption coefficient	15.857 mm^{-1}	
F(000)	1200	
Crystal description	Colourless plates	
Crystal size	0.2 x 0.2 x 0.04 mm^3	
Theta range for data collection	3.23 to 70.76°.	
Index ranges	-16<=h<=13, -5<=k<=10, -20<=l<=20	
Reflections collected	8413	
Independent reflections	3773 [R(int) = 0.0466]	
Completeness to theta = 70.76°	96.5 %	
Refinement method	Full-matrix least-squares on F^2	
Data / restraints / parameters	3773 / 0 / 253	
Goodness-of-fit on F^2	1.035	
Final R indices [I>2sigma(I)]	R1 = 0.0579, wR2 = 0.1542	
R indices (all data)	R1 = 0.0662, wR2 = 0.1606	
Largest diff. peak and hole	1.659 and -1.146 e.Å^{-3}	
Weighting scheme parameters A and B	0.0882 and 5.7217	

Bond lengths [Å] and angles [°]

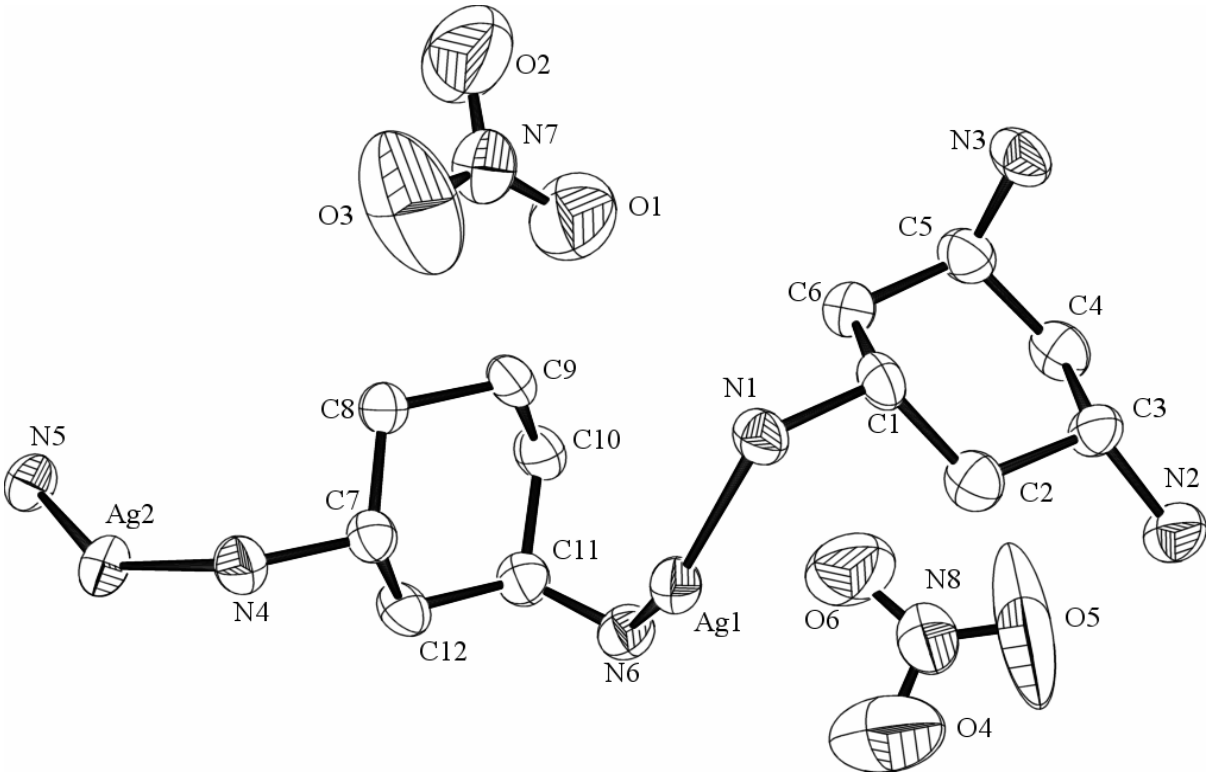
Ag(1)-N(1)	2.230(6)	C(7)-C(8)	1.508(9)	N(1)-C(1)-C(2)	109.6(5)
Ag(1)-N(6)	2.241(6)	C(7)-C(12)	1.525(9)	N(1)-C(1)-C(6)	110.9(5)
Ag(1)-N(2)#1	2.361(6)	C(8)-C(9)	1.518(9)	C(2)-C(1)-C(6)	109.6(6)
Ag(2)-N(5)	2.206(6)	C(9)-N(5)#5	1.482(8)	C(1)-C(2)-C(3)	112.3(6)
Ag(2)-N(4)	2.220(6)	C(9)-C(10)	1.514(10)	N(2)-C(3)-C(2)	108.3(6)
Ag(2)-N(3)#2	2.442(6)	C(10)-C(11)	1.527(10)	N(2)-C(3)-C(4)	112.2(6)
O(1)-N(7)	1.210(10)	C(11)-C(12)	1.539(9)	C(2)-C(3)-C(4)	110.0(6)
O(2)-N(7)	1.252(11)			C(5)-C(4)-C(3)	112.7(6)
O(3)-N(7)	1.173(11)	N(1)-Ag(1)-N(6)	144.5(2)	N(3)-C(5)-C(4)	113.0(6)
O(4)-N(8)	1.251(14)	N(1)-Ag(1)-N(2)#1	109.8(2)	N(3)-C(5)-C(6)	110.1(6)
O(5)-N(8)	1.120(12)	N(6)-Ag(1)-N(2)#1	105.3(2)	C(4)-C(5)-C(6)	110.4(6)
O(6)-N(8)	1.244(12)	N(5)-Ag(2)-N(4)	149.3(2)	C(1)-C(6)-C(5)	111.1(6)
N(1)-C(1)	1.486(8)	N(5)-Ag(2)-N(3)#2	107.0(2)	N(4)-C(7)-C(8)	110.3(5)
N(2)-C(3)	1.487(8)	N(4)-Ag(2)-N(3)#2	103.7(2)	N(4)-C(7)-C(12)	109.0(5)
N(2)-Ag(1)#1	2.361(6)	C(1)-N(1)-Ag(1)	115.9(4)	C(8)-C(7)-C(12)	110.4(6)
N(3)-C(5)	1.497(9)	C(3)-N(2)-Ag(1)#1	115.5(4)	C(7)-C(8)-C(9)	111.0(5)
N(3)-Ag(2)#3	2.442(6)	C(5)-N(3)-Ag(2)#3	120.1(4)	N(5)#5-C(9)-C(10)	110.2(5)
N(4)-C(7)	1.478(8)	C(7)-N(4)-Ag(2)	116.6(4)	N(5)#5-C(9)-C(8)	109.2(6)
N(5)-C(9)#4	1.482(8)	C(9)#4-N(5)-Ag(2)	116.3(4)	C(10)-C(9)-C(8)	111.1(5)
N(6)-C(11)	1.472(10)	C(11)-N(6)-Ag(1)	120.2(4)	C(9)-C(10)-C(11)	114.3(6)
C(1)-C(2)	1.507(10)	O(3)-N(7)-O(1)	131.9(11)	N(6)-C(11)-C(10)	111.3(6)
C(1)-C(6)	1.513(10)	O(3)-N(7)-O(2)	115.1(11)	N(6)-C(11)-C(12)	110.7(6)
C(2)-C(3)	1.527(9)	O(1)-N(7)-O(2)	113.0(9)	C(10)-C(11)-C(12)	111.8(6)
C(3)-C(4)	1.538(10)	O(5)-N(8)-O(6)	129.7(16)	C(7)-C(12)-C(11)	115.1(5)
C(4)-C(5)	1.523(10)	O(5)-N(8)-O(4)	117.0(16)		
C(5)-C(6)	1.534(10)	O(6)-N(8)-O(4)	113.0(10)		

Symmetry transformations used to generate equivalent atoms:

#1 -x+1,-y+1,-z+1 #2 x,-y+1/2,z+1/2 #3 x,-y+1/2,z-1/2

#4 -x+2,y-1/2,-z+3/2 #5 -x+2,y+1/2,-z+3/2

Ortep-3 representation of *poly*{[Ag(μ_3-*trans*-tach)](NO_3)} (**54**): thermal ellipsoids at 50% probability, hydrogen atoms are omitted for clarity.



6.29 catena-poly{[Ag(μ$_3$-trans-tach)](CF$_3$SO$_3$)} (55)

Crystallisation method	Diffusion of ether into methanol solution over 2 days.	
Empirical formula	$C_7H_{15}AgF_3N_3O_3S$ - ($C_6H_{15}N_3Ag^+$), ($CF_3SO_3^-$)	
Formula weight	386.15	
Temperature	150(2) K	
Wavelength	0.71073 Å	
Crystal system	Monoclinic	
Space group	$P\,2_1$ (4)	
Unit cell dimensions	a = 12.4287(5) Å	α = 90°.
	b = 8.1038(4) Å	β = 106.313(2)°.
	c = 13.0208(6) Å	γ = 90°.
Volume	1258.65(10) Å^3	
Z	4	
Density (calculated)	2.038 Mg/m^3	
Absorption coefficient	1.809 mm^{-1}	
F(000)	768	
Crystal description	Colourless plates	
Crystal size	0.2 x 0.2 x 0.05 mm^3	
Theta range for data collection	1.63 to 27.53°.	
Index ranges	-16<=h<=15, -10<=k<=9, 0<=l<=16	
Reflections collected	12541	
Independent reflections	5440 [R(int) = 0.0674]	
Completeness to theta = 27.53°	99.2 %	
Absorption correction	Empirical	
Transmission Tmin, Tmax	0.831, 1.119	
Refinement method	Full-matrix least-squares on F^2	
Data / restraints / parameters	5440 / 1 / 325	
Goodness-of-fit on F^2	1.033	
Final R indices [I>2sigma(I)]	R1 = 0.0373, wR2 = 0.0771	
R indices (all data)	R1 = 0.0506, wR2 = 0.0827	
Absolute structure parameter	0.47(3)	
Largest diff. peak and hole	0.625 and -0.454 e.Å^{-3}	
Weighting scheme parameters A and B	0.0215 and 3.9954	

Refinement details: Additional symmetry suggests centrosymmetric space group $P2_1/m$ (11), which is in accordance with an absolute structure parameter close to 0.5. However, solving the structure in a centrosymmetric space group proved to be difficult and refinement resulted in disorder of one silver(I) atom and one *trans*-tach ligand with unsatisfactory values for the parameters R1 and *w*R2.

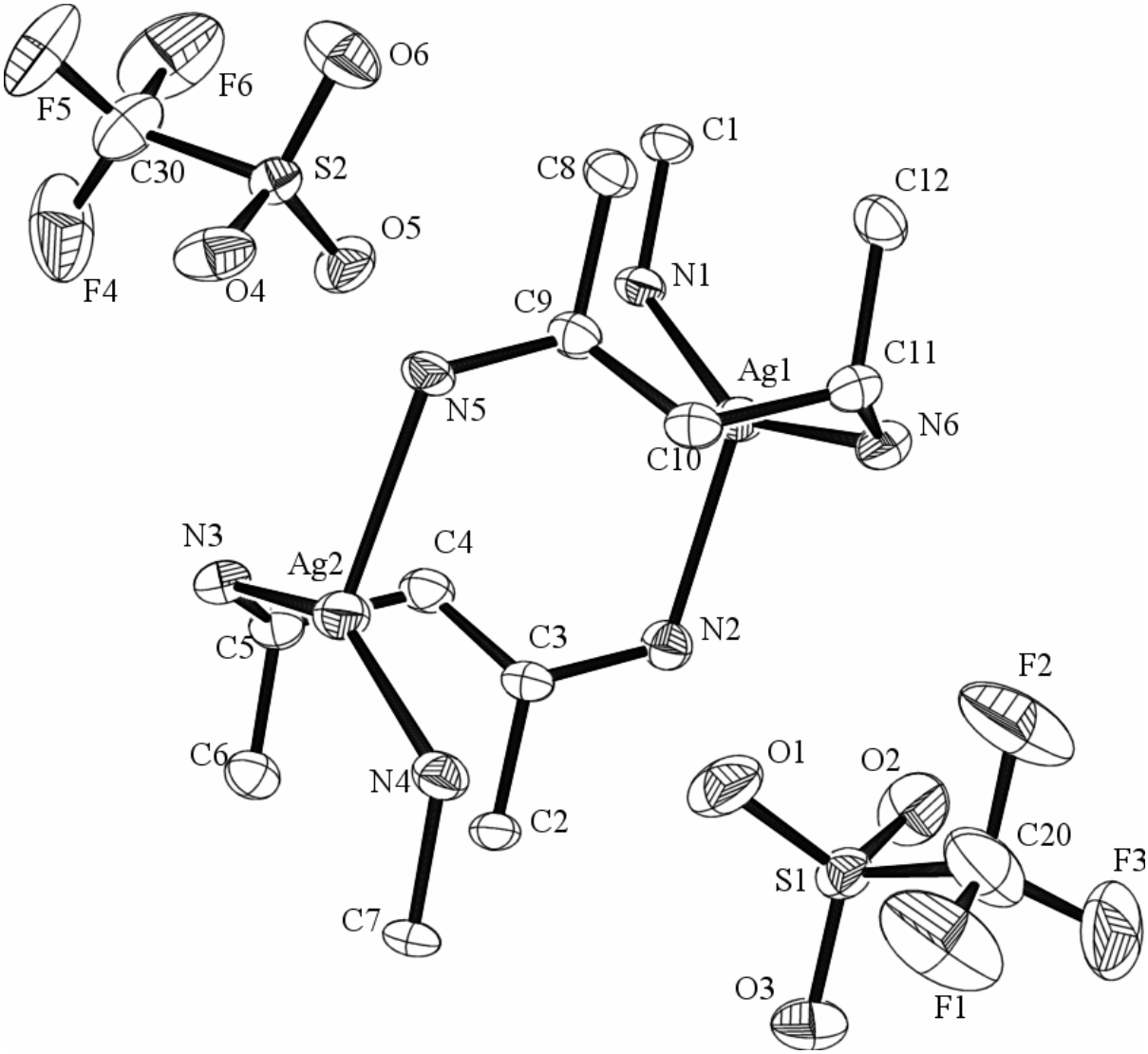
Bond lengths [Å] and angles [°]

C(3)-C(4)	1.523(8)	C(30)-F(6)	1.333(9)	N(4)-C(7)-C(12)#2	112.0(5)
C(4)-C(5)	1.530(8)	C(30)-S(2)	1.814(7)	C(8)#2-C(7)-C(12)#2	109.2(5)
C(5)-N(3)	1.504(7)	N(1)-Ag(1)	2.217(5)	C(7)#1-C(8)-C(9)	112.3(4)
C(5)-C(6)	1.525(8)	N(2)-Ag(1)	2.366(5)	N(5)-C(9)-C(8)	114.0(4)
C(6)-C(1)#2	1.522(8)	N(3)-Ag(2)	2.244(5)	N(5)-C(9)-C(10)	108.3(5)
C(7)-N(4)	1.475(6)	N(4)-Ag(2)	2.212(5)	C(8)-C(9)-C(10)	111.0(5)
C(7)-C(8)#2	1.524(8)	N(5)-Ag(2)	2.397(4)	C(9)-C(10)-C(11)	115.1(5)
C(7)-C(12)#2	1.531(8)	N(6)-Ag(1)	2.277(5)	N(6)-C(11)-C(12)	109.8(5)
C(8)-C(7)#1	1.524(8)	O(1)-S(1)	1.440(4)	N(6)-C(11)-C(10)	111.3(5)
C(8)-C(9)	1.527(7)	O(2)-S(1)	1.434(5)	C(12)-C(11)-C(10)	110.9(4)
C(9)-N(5)	1.470(7)	O(3)-S(1)	1.443(5)	C(11)-C(12)-C(7)#1	113.0(5)
C(9)-C(10)	1.530(8)	O(4)-S(2)	1.439(5)	F(3)-C(20)-F(1)	107.1(7)
C(10)-C(11)	1.537(8)	O(5)-S(2)	1.437(4)	F(3)-C(20)-F(2)	107.5(7)
C(11)-N(6)	1.500(7)	O(6)-S(2)	1.429(5)	F(1)-C(20)-F(2)	107.4(7)
C(11)-C(12)	1.532(8)			F(3)-C(20)-S(1)	112.3(6)
C(12)-C(7)#1	1.531(8)	C(4)-C(3)-C(2)	112.3(5)	F(1)-C(20)-S(1)	111.4(5)
C(20)-F(3)	1.323(10)	C(3)-C(4)-C(5)	115.0(5)	F(2)-C(20)-S(1)	110.9(5)
C(20)-F(1)	1.345(9)	N(3)-C(5)-C(6)	109.5(4)	F(4)-C(30)-F(5)	108.6(7)
C(20)-F(2)	1.349(9)	N(3)-C(5)-C(4)	110.6(5)	F(4)-C(30)-F(6)	108.3(6)
C(20)-S(1)	1.786(7)	C(6)-C(5)-C(4)	111.3(5)	F(5)-C(30)-F(6)	108.3(6)
C(30)-F(4)	1.305(9)	C(5)-C(6)-C(1)#2	112.8(5)		
C(30)-F(5)	1.330(7)	N(4)-C(7)-C(8)#2	110.6(4)		

Symmetry transformations used to generate equivalent atoms:

#1 x,y-1,z #2 x,y+1,z

Ortep-3 representation of *catena-poly*{[Ag(μ_3-*trans*-tach)](CF_3SO_3)} (**55**): thermal ellipsoids at 50% probability, hydrogen atoms are omitted for clarity.



6.30 catena-poly{[$Zn_2(\mu_2$-trans-tach)$(\mu_2$-Cl)$_2Cl_2$]} (56)

Crystallisation method	Diffusion of methanol into aqueous solution over 3 weeks.	
Empirical formula	$C_6H_{15}Cl_4N_3Zn_2$	
Formula weight	401.7	
Temperature	293(2) K	
Wavelength	1.54178 Å	
Crystal system	Orthorhombic	
Space group	*P n m a* (62)	
Unit cell dimensions	a = 11.5041(2) Å	α = 90°.
	b = 14.3800(2) Å	β = 90°.
	c = 7.86230(10) Å	γ = 90°.
Volume	1300.65(3) $Å^3$	
Z	4	
Density (calculated)	2.052 Mg/m^3	
Absorption coefficient	11.873 mm^{-1}	
F(000)	800	
Crystal description	Colourless block	
Crystal size	0.4 x 0.4 x 0.34 mm^3	
Theta range for data collection	6.15 to 70.49°.	
Index ranges	-9<=h<=14, -16<=k<=17, -8<=l<=8	
Reflections collected	4138	
Independent reflections	1215 [R(int) = 0.0263]	
Completeness to theta = 70.49°	94.1 %	
Absorption correction	None	
Refinement method	Full-matrix least-squares on F^2	
Data / restraints / parameters	1215 / 0 / 84	
Goodness-of-fit on F^2	2.984	
Final R indices [I>2sigma(I)]	R1 = 0.1916, wR2 = 0.5305	
R indices (all data)	R1 = 0.1918, wR2 = 0.5311	
Extinction coefficient	0.047(13)	
Largest diff. peak and hole	5.599 and -1.808 $e.Å^{-3}$	
Weighting scheme parameters A and B	0.2000 and 0.0000	

Refinement details: Very poor crystal quality with disorder around the heavy atom positions. The bridging chloro ligands are disordered over minimum two positions. Structure solution and refinement as non-protonated *trans*-tach ligand, even though elemental analysis and non-coordinating pendant amino group indicate protonation.

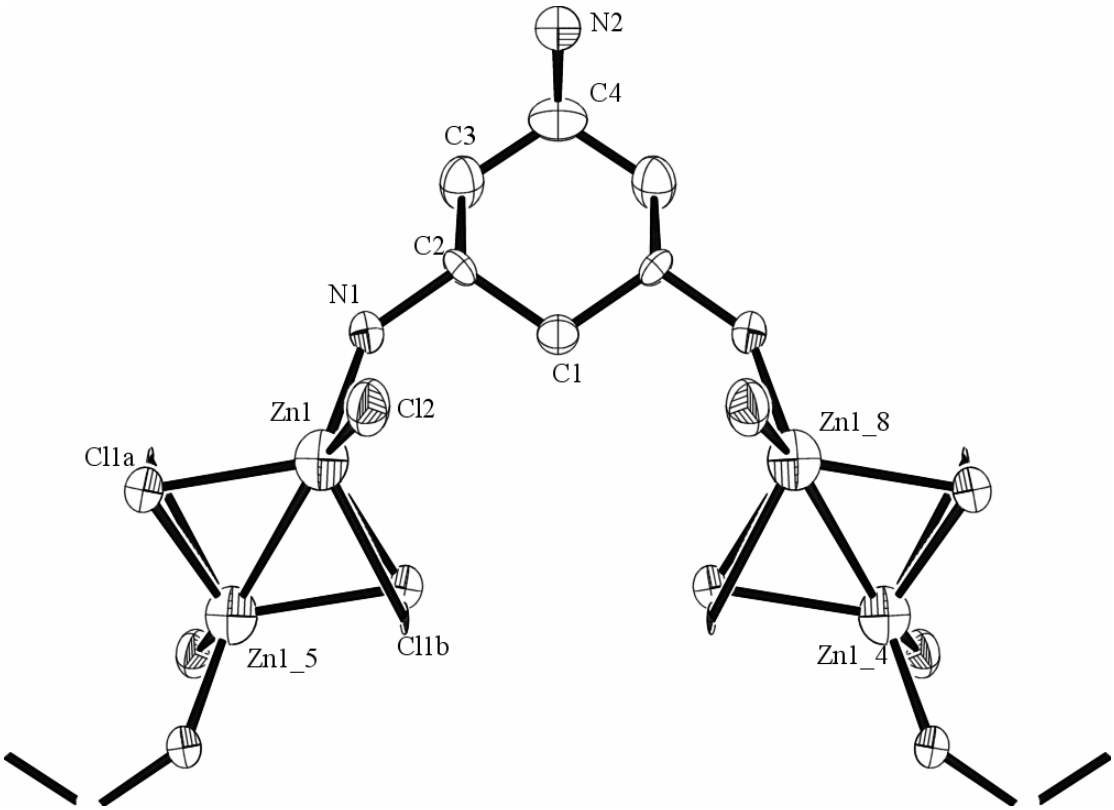
Bond lengths [Å] and angles [°]

C(1)-C(2)	1.516(12)	C(2)-C(1)-C(2)#1	110.4(11)	Cl(1A)#2-Zn(1)-Cl(2)	125.70(14)
C(1)-C(2)#1	1.516(12)	N(1)-C(2)-C(3)	111.9(10)	N(1)-Zn(1)-Cl(1B)#2	89.3(4)
				Cl(1B)-Zn(1)-	
C(2)-N(1)	1.459(11)	N(1)-C(2)-C(1)	110.3(8)	Cl(1B)#2	109.1(4)
				Cl(1A)-Zn(1)-	
C(2)-C(3)	1.477(16)	C(3)-C(2)-C(1)	111.4(9)	Cl(1B)#2	24.8(4)
				Cl(1A)#2-Zn(1)-	
C(3)-C(4)	1.491(15)	C(2)-C(3)-C(4)	113.6(10)	Cl(1B)#2	94.2(3)
C(4)-C(3)#1	1.491(15)	C(3)#1-C(4)-C(3)	113.3(14)	Cl(2)-Zn(1)-Cl(1B)#2	135.8(3)
C(4)-N(2)	1.49(2)	C(3)#1-C(4)-N(2)	114.3(9)	N(1)-Zn(1)-Zn(1)#2	115.3(4)
				Cl(1B)-Zn(1)-	
N(1)-Zn(1)	1.967(10)	C(3)-C(4)-N(2)	114.3(9)	Zn(1)#2	61.0(3)
				Cl(1A)-Zn(1)-	
Zn(1)-Cl(1B)	2.255(13)	C(2)-N(1)-Zn(1)	129.0(8)	Zn(1)#2	52.04(11)
				Cl(1A)#2-Zn(1)-	
Zn(1)-Cl(1A)	2.296(4)	N(1)-Zn(1)-Cl(1B)	123.9(5)	Zn(1)#2	51.25(10)
Zn(1)-Cl(1A)#2	2.321(4)	N(1)-Zn(1)-Cl(1A)	109.6(3)	Cl(2)-Zn(1)-Zn(1)#2	145.40(15)
				Cl(1B)#2-Zn(1)-	
Zn(1)-Cl(2)	2.382(3)	Cl(1B)-Zn(1)-Cl(1A)	106.6(3)	Zn(1)#2	48.1(3)
				Cl(1B)#2-Cl(1A)-	
Zn(1)-Cl(1B)#2	2.653(14)	N(1)-Zn(1)-Cl(1A)#2	101.3(3)	Zn(1)	95.8(6)
		Cl(1B)-Zn(1)-		Cl(1B)#2-Cl(1A)-	
Zn(1)-Zn(1)#2	2.865(4)	Cl(1A)#2	28.2(4)	Zn(1)#2	72.6(6)
		Cl(1A)-Zn(1)-		Zn(1)-Cl(1A)-	
Cl(1A)-Cl(1B)#2	1.118(17)	Cl(1A)#2	103.29(13)	Zn(1)#2	76.71(13)
				Cl(1A)#2-Cl(1B)-	
Cl(1A)-Zn(1)#2	2.321(4)	N(1)-Zn(1)-Cl(2)	99.2(3)	Zn(1)	79.1(8)
				Cl(1A)#2-Cl(1B)-	
Cl(1B)-Cl(1A)#2	1.118(17)	Cl(1B)-Zn(1)-Cl(2)	101.7(4)	Zn(1)#2	59.4(6)
				Zn(1)-Cl(1B)-	
Cl(1B)-Zn(1)#2	2.653(14)	Cl(1A)-Zn(1)-Cl(2)	115.93(14)	Zn(1)#2	70.9(4)

Symmetry transformations used to generate equivalent atoms:

#1 x,-y+1/2,z #2 -x+2,-y,-z+1

Ortep-3 representation of *catena-poly*{[$Zn_2(\mu_2$-*trans*-tach)$(\mu_2$-Cl$)_2Cl_2$]} (**56**): thermal ellipsoids at 50% probability.



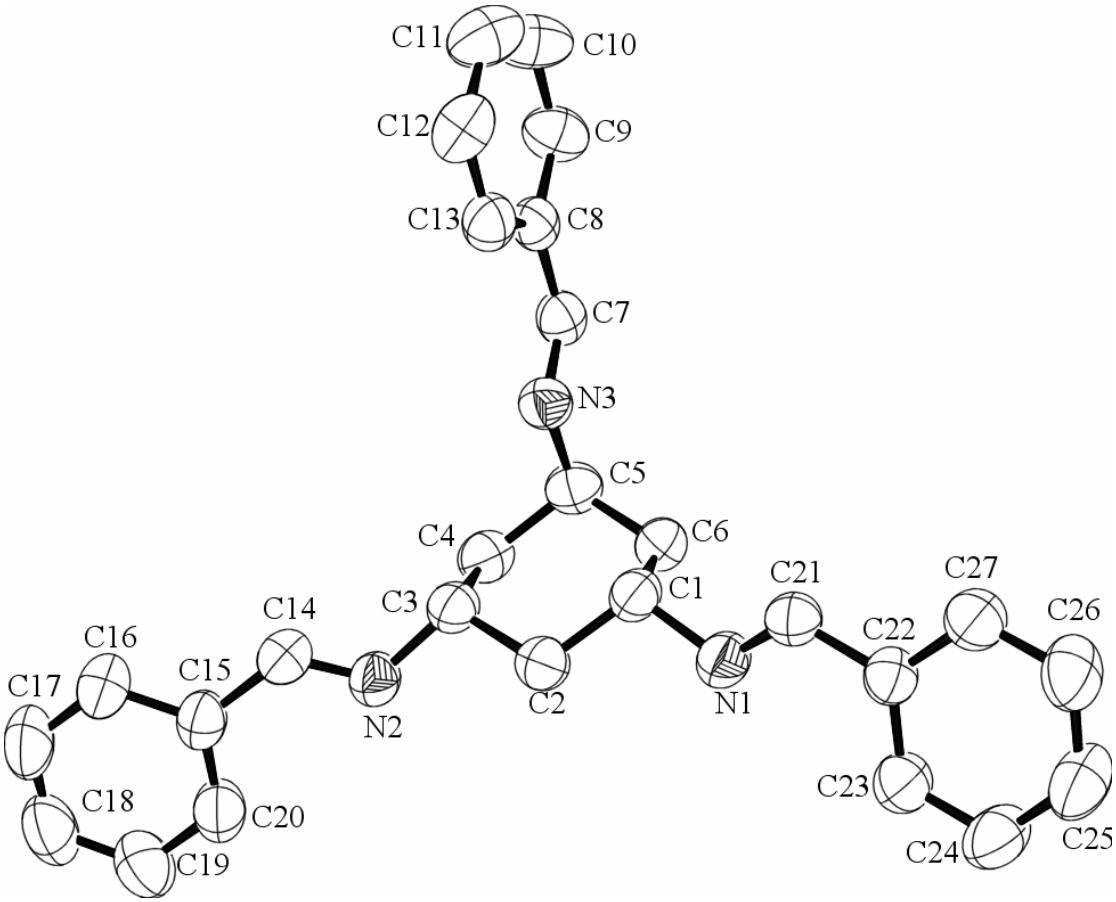
6.31 tbc (57)

Crystallisation method	Evaporation of methanol solution over 3 days.	
Empirical formula	$C_{27}H_{27}N_3$	
Formula weight	393.52	
Temperature	293(2) K	
Wavelength	1.54178 Å	
Crystal system	Monoclinic	
Space group	*I* 2/*a* (15)	
Unit cell dimensions	a = 18.1262(2) Å	α = 90°.
	b = 10.40410(10) Å	β = 105.974(1)°.
	c = 25.3348(4) Å	γ = 90°.
Volume	4593.32(10) $Å^3$	
Z	8	
Density (calculated)	1.138 Mg/m^3	
Absorption coefficient	0.516 mm^{-1}	
F(000)	1680	
Crystal description	Colourless plate	
Crystal size	0.4 x 0.3 x 0.1 mm^3	
Theta range for data collection	3.63 to 59.98°.	
Index ranges	-20<=h<=20, -9<=k<=11, -27<=l<=28	
Reflections collected	7826	
Independent reflections	3306 [R(int) = 0.0469]	
Completeness to theta = 59.98°	96.8 %	
Absorption correction	None	
Refinement method	Full-matrix least-squares on F^2	
Data / restraints / parameters	3306 / 0 / 272	
Goodness-of-fit on F^2	1.038	
Final R indices [I>2sigma(I)]	R1 = 0.0715, wR2 = 0.1784	
R indices (all data)	R1 = 0.0797, wR2 = 0.1927	
Extinction coefficient	0.0041(5)	
Largest diff. peak and hole	0.330 and -0.267 $e.Å^{-3}$	
Weighting scheme parameters A and B	0.0975 and 0.5059	

Bond lengths [Å] and angles [°]

C(1)-N(1)	1.475(2)	C(21)-C(22)	1.474(3)	C(12)-C(11)-C(10)	119.8(2)
C(1)-C(2)	1.521(3)	C(22)-C(23)	1.370(3)	C(13)-C(12)-C(11)	120.1(2)
C(1)-C(6)	1.522(3)	C(22)-C(27)	1.389(3)	C(12)-C(13)-C(8)	120.90(19)
C(2)-C(3)	1.526(3)	C(23)-C(24)	1.384(3)	N(2)-C(14)-C(15)	122.44(18)
C(3)-N(2)	1.464(2)	C(24)-C(25)	1.373(3)	C(20)-C(15)-C(16)	117.6(2)
C(3)-C(4)	1.518(3)	C(25)-C(26)	1.351(3)	C(20)-C(15)-C(14)	121.38(18)
C(4)-C(5)	1.531(3)	C(26)-C(27)	1.387(3)	C(16)-C(15)-C(14)	121.0(2)
C(5)-N(3)	1.469(3)			C(17)-C(16)-C(15)	120.5(3)
C(5)-C(6)	1.527(3)	N(1)-C(1)-C(2)	108.40(16)	C(18)-C(17)-C(16)	120.6(2)
C(7)-N(3)	1.258(2)	N(1)-C(1)-C(6)	109.24(16)	C(17)-C(18)-C(19)	120.0(2)
C(7)-C(8)	1.471(3)	C(2)-C(1)-C(6)	110.48(16)	C(18)-C(19)-C(20)	119.8(3)
C(8)-C(9)	1.378(3)	C(1)-C(2)-C(3)	112.93(16)	C(15)-C(20)-C(19)	121.4(2)
C(8)-C(13)	1.391(3)	N(2)-C(3)-C(4)	107.80(15)	N(1)-C(21)-C(22)	123.08(18)
C(9)-C(10)	1.376(3)	N(2)-C(3)-C(2)	109.58(15)	C(23)-C(22)-C(27)	118.51(18)
C(10)-C(11)	1.375(4)	C(4)-C(3)-C(2)	110.55(17)	C(23)-C(22)-C(21)	122.34(17)
C(11)-C(12)	1.372(3)	C(3)-C(4)-C(5)	112.70(15)	C(27)-C(22)-C(21)	119.14(17)
C(12)-C(13)	1.371(3)	N(3)-C(5)-C(6)	109.89(15)	C(22)-C(23)-C(24)	120.96(19)
C(14)-N(2)	1.258(2)	N(3)-C(5)-C(4)	109.08(16)	C(25)-C(24)-C(23)	119.4(2)
C(14)-C(15)	1.470(3)	C(6)-C(5)-C(4)	109.59(16)	C(26)-C(25)-C(24)	120.7(2)
C(15)-C(20)	1.373(3)	C(1)-C(6)-C(5)	112.63(16)	C(25)-C(26)-C(27)	119.9(2)
C(15)-C(16)	1.384(3)	N(3)-C(7)-C(8)	123.00(18)	C(26)-C(27)-C(22)	120.4(2)
C(16)-C(17)	1.383(4)	C(9)-C(8)-C(13)	118.25(19)	C(21)-N(1)-C(1)	117.51(17)
C(17)-C(18)	1.351(4)	C(9)-C(8)-C(7)	120.13(18)	C(14)-N(2)-C(3)	118.44(17)
C(18)-C(19)	1.360(4)	C(13)-C(8)-C(7)	121.62(17)	C(7)-N(3)-C(5)	117.98(17)
C(19)-C(20)	1.381(3)	C(10)-C(9)-C(8)	120.8(2)		
C(21)-N(1)	1.259(2)	C(11)-C(10)-C(9)	120.2(2)		

Ortep-3 representation of tbc (**57**): thermal ellipsoids at 50% probability, hydrogen atoms are omitted for clarity.



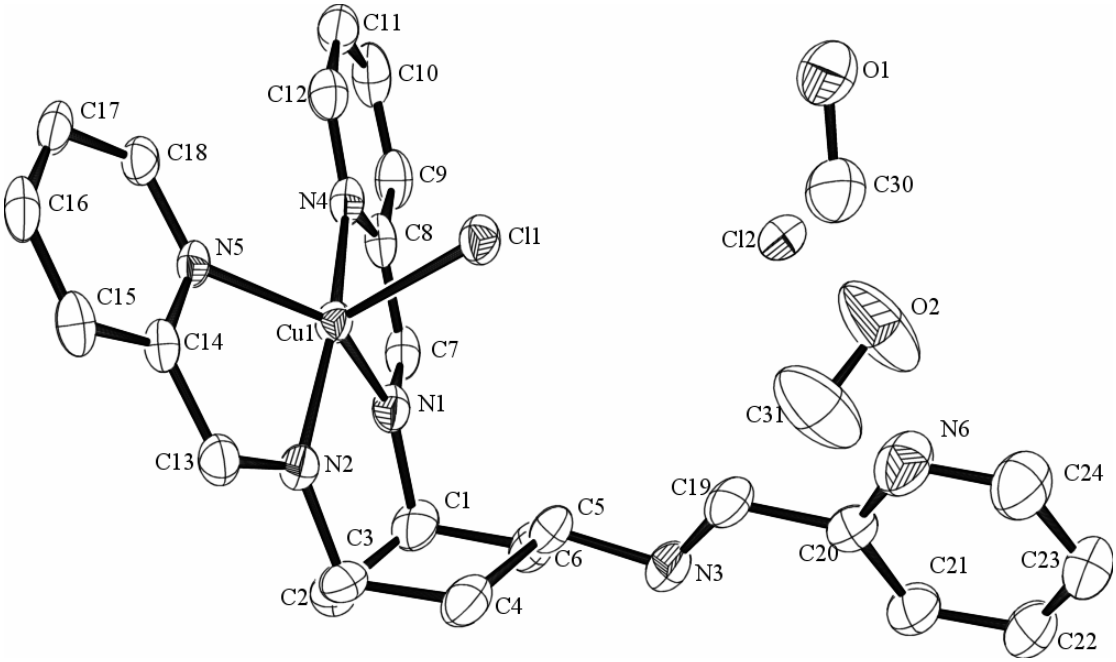
6.32 [Cu(ttop)Cl]Cl (61)

Crystallisation method	Diffusion of ether into methanol solution over 5 days.	
Empirical formula	$C_{26}H_{32}Cl_2CuN_6O_2$ - ($C_{24}H_{24}N_6CuCl^+$), (Cl^-), 2(CH_3OH)	
Formula weight	595.02	
Temperature	200(2) K	
Wavelength	1.54178 Å	
Crystal system	Triclinic	
Space group	*P* -1 (2)	
Unit cell dimensions	a = 7.5984(3) Å	α = 73.439(2)°.
	b = 11.6384(4) Å	β = 89.473(2)°.
	c = 16.6500(5) Å	γ = 84.853(3)°.
Volume	1405.44(8) $Å^3$	
Z	2	
Density (calculated)	1.406 Mg/m^3	
Absorption coefficient	3.124 mm^{-1}	
F(000)	618	
Crystal description	Green needles	
Crystal size	0.2 x 0.16 x 0.06 mm^3	
Theta range for data collection	2.77 to 60.00°.	
Index ranges	-8<=h<=8, -13<=k<=10, -18<=l<=18	
Reflections collected	6851	
Independent reflections	3936 [R(int) = 0.0339]	
Completeness to theta = 60.00°	94.1 %	
Absorption correction	None	
Refinement method	Full-matrix least-squares on F^2	
Data / restraints / parameters	3936 / 0 / 335	
Goodness-of-fit on F^2	1.052	
Final R indices [I>2sigma(I)]	R1 = 0.0436, wR2 = 0.1187	
R indices (all data)	R1 = 0.0520, wR2 = 0.1282	
Extinction coefficient	0.0016(5)	
Largest diff. peak and hole	0.565 and -0.539 $e.Å^{-3}$	
Weighting scheme parameters A and B	0.0881 and 0.0258	

Bond lengths [Å] and angles [°]

C(1)-N(1)	1.487(4)	C(31)-O(2)	1.362(7)	N(5)-C(18)-C(17)	122.9(3)
C(1)-C(2)	1.509(6)	N(1)-Cu(1)	2.019(2)	N(3)-C(19)-C(20)	122.4(3)
C(1)-C(6)	1.530(5)	N(2)-Cu(1)	2.000(3)	N(6)-C(20)-C(21)	122.0(3)
C(2)-C(3)	1.532(5)	N(4)-Cu(1)	2.035(3)	N(6)-C(20)-C(19)	114.9(3)
C(3)-N(2)	1.484(4)	N(5)-Cu(1)	2.101(2)	C(21)-C(20)-C(19)	123.1(3)
C(3)-C(4)	1.520(5)	Cl(1)-Cu(1)	2.4175(8)	C(22)-C(21)-C(20)	119.2(4)
C(4)-C(5)	1.530(5)			C(23)-C(22)-C(21)	119.4(3)
C(5)-N(3)	1.477(4)	N(1)-C(1)-C(2)	110.5(3)	C(22)-C(23)-C(24)	117.9(4)
C(5)-C(6)	1.509(5)	N(1)-C(1)-C(6)	109.0(3)	N(6)-C(24)-C(23)	124.5(4)
C(7)-N(1)	1.267(4)	C(2)-C(1)-C(6)	111.5(3)	C(7)-N(1)-C(1)	118.3(3)
C(7)-C(8)	1.452(5)	C(1)-C(2)-C(3)	112.8(3)	C(7)-N(1)-Cu(1)	113.9(2)
C(8)-N(4)	1.362(4)	N(2)-C(3)-C(4)	112.1(3)	C(1)-N(1)-Cu(1)	127.7(2)
C(8)-C(9)	1.371(5)	N(2)-C(3)-C(2)	108.3(3)	C(13)-N(2)-C(3)	118.0(3)
C(9)-C(10)	1.384(5)	C(4)-C(3)-C(2)	111.9(3)	C(13)-N(2)-Cu(1)	114.3(2)
C(10)-C(11)	1.385(5)	C(3)-C(4)-C(5)	113.5(3)	C(3)-N(2)-Cu(1)	127.3(2)
C(11)-C(12)	1.387(5)	N(3)-C(5)-C(6)	107.7(3)	C(19)-N(3)-C(5)	116.8(3)
C(12)-N(4)	1.336(4)	N(3)-C(5)-C(4)	109.3(3)	C(12)-N(4)-C(8)	117.5(3)
C(13)-N(2)	1.277(4)	C(6)-C(5)-C(4)	110.7(3)	C(12)-N(4)-Cu(1)	130.1(2)
C(13)-C(14)	1.460(5)	C(5)-C(6)-C(1)	112.9(3)	C(8)-N(4)-Cu(1)	112.4(2)
C(14)-N(5)	1.360(4)	N(1)-C(7)-C(8)	118.9(3)	C(18)-N(5)-C(14)	117.6(3)
C(14)-C(15)	1.387(4)	N(4)-C(8)-C(9)	122.7(3)	C(18)-N(5)-Cu(1)	132.2(2)
C(15)-C(16)	1.383(5)	N(4)-C(8)-C(7)	114.1(3)	C(14)-N(5)-Cu(1)	109.53(18)
C(16)-C(17)	1.372(5)	C(9)-C(8)-C(7)	123.2(3)	C(24)-N(6)-C(20)	117.0(3)
C(17)-C(18)	1.395(4)	C(8)-C(9)-C(10)	119.0(3)	N(2)-Cu(1)-N(1)	90.53(11)
C(18)-N(5)	1.335(4)	C(9)-C(10)-C(11)	119.1(3)	N(2)-Cu(1)-N(4)	166.00(11)
C(19)-N(3)	1.259(5)	C(10)-C(11)-C(12)	118.7(3)	N(1)-Cu(1)-N(4)	80.65(11)
C(19)-C(20)	1.466(5)	N(4)-C(12)-C(11)	122.9(3)	N(2)-Cu(1)-N(5)	80.90(10)
C(20)-N(6)	1.340(5)	N(2)-C(13)-C(14)	118.9(3)	N(1)-Cu(1)-N(5)	149.84(10)
C(20)-C(21)	1.384(5)	N(5)-C(14)-C(15)	122.5(3)	N(4)-Cu(1)-N(5)	101.32(10)
C(21)-C(22)	1.376(6)	N(5)-C(14)-C(13)	115.1(3)	N(2)-Cu(1)-Cl(1)	99.98(8)
C(22)-C(23)	1.360(6)	C(15)-C(14)-C(13)	122.3(3)	N(1)-Cu(1)-Cl(1)	115.42(8)
C(23)-C(24)	1.373(6)	C(16)-C(15)-C(14)	118.7(3)	N(4)-Cu(1)-Cl(1)	93.64(8)
C(24)-N(6)	1.335(5)	C(17)-C(16)-C(15)	119.3(3)	N(5)-Cu(1)-Cl(1)	94.60(7)
C(30)-O(1)	1.393(5)	C(16)-C(17)-C(18)	118.9(3)		

Ortep-3 representation of [Cu(ttop)Cl]Cl (**61**): thermal ellipsoids at 50% probability, hydrogen atoms are omitted for clarity.



6.33 [{$Cu_2(\mu_2$-ttop)$(\mu_2$-Cl)$Cl_2\}_2]Cl_2$ (62)

Crystallisation method	Diffusion of ether into methanol solution over 5 days.	
Empirical formula	$C_{26}H_{32}Cl_4Cu_2N_6O_2 – (C_{24}H_{24}N_6Cu_2Cl_3^{+}), (Cl^{-}), 2(CH_3OH)$	
Formula weight	729.46	
Temperature	150(2) K	
Wavelength	0.71073 Å	
Crystal system	Triclinic	
Space group	*P* -1 (2)	
Unit cell dimensions	a = 9.7929(3) Å	α = 88.942(2)°.
	b = 12.8175(5) Å	β = 78.430(2)°.
	c = 13.9117(7) Å	γ = 69.323(2)°.
Volume	1597.91(11) $Å^3$	
Z	2	
Density (calculated)	1.516 Mg/m^3	
Absorption coefficient	1.699 mm^{-1}	
F(000)	744	
Crystal description	Green plates	
Crystal size	0.20 x 0.20 x 0.12 mm^3	
Theta range for data collection	1.70 to 25.00°.	
Index ranges	-11<=h<=11, -15<=k<=15, 0<=l<=16	
Reflections collected	21121	
Independent reflections	5623 [R(int) = 0.0546]	
Completeness to theta = 25.00°	99.7 %	
Absorption correction	Gaussian	
Max. and min. transmission	0.8221 and 0.7275	
Refinement method	Full-matrix least-squares on F^2	
Data / restraints / parameters	5623 / 0 / 370	
Goodness-of-fit on F^2	1.119	
Final R indices [I>2sigma(I)]	R1 = 0.0659, wR2 = 0.1666	
R indices (all data)	R1 = 0.0909, wR2 = 0.1781	
Extinction coefficient	0.0023(8)	
Largest diff. peak and hole	0.91 and -0.58 $e.Å^{-3}$	
Weighting scheme parameters A and B	0.0613 and 9.625	

Refinement details: The chloride counterion is disordered over two positions Cl4 / Cl4' in the ratio 95:5. The two methanol solvent molecules are disordered over four positions with additional disordered oxygen atoms O1 and O2 over two positions.

Bond lengths [Å] and angles [°]

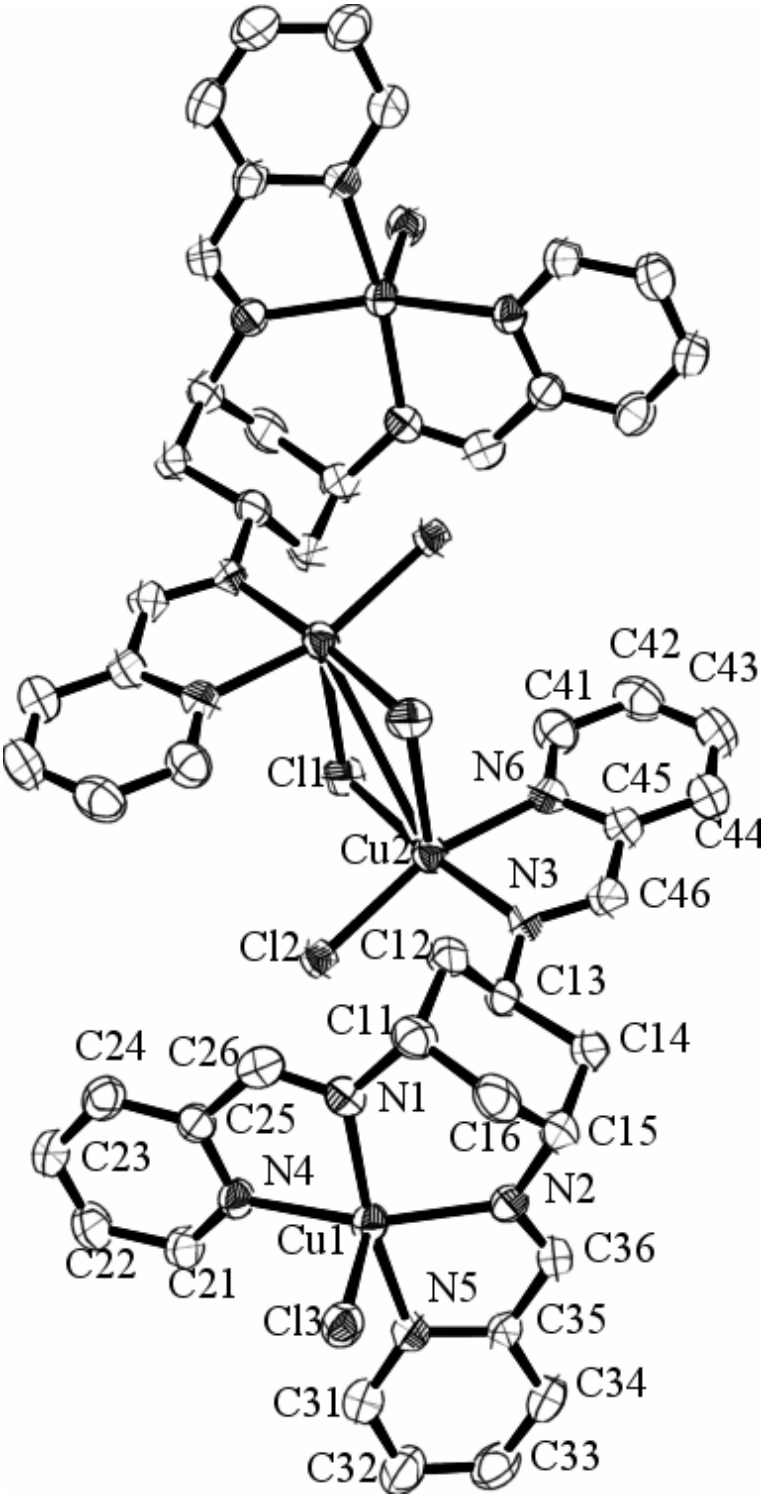
Cu(1)-N(1)	1.996(6)	C(33)-C(34)	1.346(11)	N(3)-Cu(2)-Cl(2)	93.44(16)
Cu(1)-N(2)	2.004(6)	C(34)-C(35)	1.388(10)	N(6)-Cu(2)-Cl(1)	92.85(18)
Cu(1)-N(5)	2.036(6)	C(35)-C(36)	1.481(10)	N(3)-Cu(2)-Cl(1)	172.24(17)
Cu(1)-N(4)	2.069(5)	C(41)-C(42)	1.393(11)	Cl(2)-Cu(2)-Cl(1)	92.87(7)
Cu(1)-Cl(3)	2.4273(19)	C(42)-C(43)	1.381(12)	N(6)-Cu(2)-Cl(1)#1	90.12(17)
Cu(2)-N(6)	2.045(6)	C(43)-C(44)	1.363(12)	N(3)-Cu(2)-Cl(1)#1	92.43(16)
Cu(2)-N(3)	2.046(6)	C(44)-C(45)	1.374(10)	Cl(2)-Cu(2)-Cl(1)#1	106.92(7)
Cu(2)-Cl(2)	2.2564(18)	C(45)-C(46)	1.450(10)	Cl(1)-Cu(2)-Cl(1)#1	90.06(6)
Cu(2)-Cl(1)	2.2836(18)	C(1)-O(1')	1.160(18)	Cu(2)-Cl(1)-Cu(2)#1	89.94(6)
Cu(2)-Cl(1)#1	2.6507(19)	C(1)-O(1)	1.402(17)	C(26)-N(1)-C(11)	118.9(6)
Cl(1)-Cu(2)#1	2.6507(19)	O(1)-O(1')	1.555(18)	C(26)-N(1)-Cu(1)	114.4(5)
N(1)-C(26)	1.272(9)	Cl(4)-Cl(4')	1.15(4)	C(11)-N(1)-Cu(1)	126.7(5)
N(1)-C(11)	1.478(9)	Cl(4')-O(2)	1.89(4)	C(36)-N(2)-C(15)	120.2(6)
N(2)-C(36)	1.256(9)	O(2)-O(2')	0.81(3)	C(36)-N(2)-Cu(1)	114.2(5)
N(2)-C(15)	1.484(9)	O(2)-C(2)	1.34(3)	C(15)-N(2)-Cu(1)	125.5(5)
N(3)-C(46)	1.268(9)	O(2')-C(2)	1.05(3)	C(46)-N(3)-C(13)	120.6(6)
N(3)-C(13)	1.489(9)	O(3)-C(3)	1.115(19)	C(46)-N(3)-Cu(2)	113.8(5)
N(4)-C(21)	1.338(9)	O(3)-O(3')	1.45(2)	C(13)-N(3)-Cu(2)	125.6(4)
N(4)-C(25)	1.352(9)	O(3)-C(3')	1.83(3)	C(21)-N(4)-C(25)	117.5(6)
N(5)-C(31)	1.315(9)	C(3)-C(3')	1.43(3)	C(21)-N(4)-Cu(1)	131.3(5)
N(5)-C(35)	1.359(9)	C(3)-C(3)#2	1.68(3)	C(25)-N(4)-Cu(1)	110.9(4)
N(6)-C(41)	1.322(9)	C(3)-O(3')	1.75(3)	C(31)-N(5)-C(35)	117.7(6)
N(6)-C(45)	1.354(9)	O(3')-C(3')	1.03(3)	C(31)-N(5)-Cu(1)	130.4(5)
C(11)-C(16)	1.504(10)			C(35)-N(5)-Cu(1)	111.7(5)
C(11)-C(12)	1.532(10)	N(1)-Cu(1)-N(2)	91.4(2)	C(41)-N(6)-C(45)	118.6(6)
C(12)-C(13)	1.517(10)	N(1)-Cu(1)-N(5)	167.4(2)	C(41)-N(6)-Cu(2)	128.3(5)
C(13)-C(14)	1.526(9)	N(2)-Cu(1)-N(5)	81.4(2)	C(45)-N(6)-Cu(2)	113.1(5)
C(14)-C(15)	1.537(10)	N(1)-Cu(1)-N(4)	80.8(2)	N(1)-C(11)-C(16)	110.0(6)
C(15)-C(16)	1.497(11)	N(2)-Cu(1)-N(4)	155.4(2)	N(1)-C(11)-C(12)	109.1(6)
C(21)-C(22)	1.396(10)	N(5)-Cu(1)-N(4)	101.6(2)	C(16)-C(11)-C(12)	111.6(6)
C(22)-C(23)	1.369(11)	N(1)-Cu(1)-Cl(3)	98.31(16)	C(13)-C(12)-C(11)	110.3(6)
C(23)-C(24)	1.381(11)	N(2)-Cu(1)-Cl(3)	100.92(16)	N(3)-C(13)-C(12)	109.5(5)
C(24)-C(25)	1.381(10)	N(5)-Cu(1)-Cl(3)	93.19(17)	N(3)-C(13)-C(14)	114.5(6)
C(25)-C(26)	1.471(10)	N(4)-Cu(1)-Cl(3)	103.27(16)	C(12)-C(13)-C(14)	110.3(6)
C(31)-C(32)	1.400(11)	N(6)-Cu(2)-N(3)	79.8(2)	C(13)-C(14)-C(15)	109.4(6)
C(32)-C(33)	1.374(12)	N(6)-Cu(2)-Cl(2)	162.00(17)	N(2)-C(15)-C(16)	110.7(6)
N(2)-C(15)-C(14)	108.5(6)	C(34)-C(35)-C(36)	123.6(6)	O(2)-O(2')-C(2)	91(4)
C(16)-C(15)-C(14)	112.7(6)	N(2)-C(36)-C(35)	118.4(6)	O(2')-C(2)-O(2)	37.0(18)

C(15)-C(16)-C(11)	113.5(6)	N(6)-C(41)-C(42)	122.2(8)	C(3)-O(3)-O(3')	85.1(15)
N(4)-C(21)-C(22)	122.2(7)	C(43)-C(42)-C(41)	118.7(8)	C(3)-O(3)-C(3')	51.2(13)
C(23)-C(22)-C(21)	119.4(7)	C(44)-C(43)-C(42)	119.0(7)	O(3')-O(3)-C(3')	33.9(10)
C(22)-C(23)-C(24)	119.0(7)	C(43)-C(44)-C(45)	119.6(8)	O(3)-C(3)-C(3')	91.3(17)
C(25)-C(24)-C(23)	118.6(7)	N(6)-C(45)-C(44)	121.9(7)	O(3)-C(3)-C(3)#2	144(2)
N(4)-C(25)-C(24)	123.1(6)	N(6)-C(45)-C(46)	114.3(6)	C(3')-C(3)-C(3)#2	123.8(18)
N(4)-C(25)-C(26)	114.4(6)	C(44)-C(45)-C(46)	123.8(7)	O(3)-C(3)-O(3')	55.6(12)
C(24)-C(25)-C(26)	122.5(6)	N(3)-C(46)-C(45)	119.0(7)	C(3')-C(3)-O(3')	35.8(11)
N(1)-C(26)-C(25)	118.2(6)	O(1')-C(1)-O(1)	74.1(11)	C(3)#2-C(3)-O(3')	158.9(17)
N(5)-C(31)-C(32)	123.0(7)	C(1)-O(1)-O(1')	45.8(8)	C(3')-O(3')-O(3)	94(2)
C(33)-C(32)-C(31)	117.8(8)	C(1)-O(1')-O(1)	60.1(10)	C(3')-O(3')-C(3)	54.6(18)
C(34)-C(33)-C(32)	120.6(7)	Cl(4)-Cl(4')-O(2)	152(3)	O(3)-O(3')-C(3)	39.3(9)
C(33)-C(34)-C(35)	118.6(7)	O(2')-O(2)-C(2)	52(3)	O(3')-C(3')-C(3)	90(2)
N(5)-C(35)-C(34)	122.3(7)	O(2')-O(2)-Cl(4')	138(4)	O(3')-C(3')-O(3)	52.2(17)
N(5)-C(35)-C(36)	113.9(6)	C(2)-O(2)-Cl(4')	87.9(18)	C(3)-C(3')-O(3)	37.4(9)

Symmetry transformations used to generate equivalent atoms:

#1 -x+1,-y+1,-z+1 #2 -x+1,-y,-z+1

Ortep-3 representation of $[\{Cu_2(\mu_2\text{-ttop})(\mu_2\text{-Cl})Cl_2\}_2]Cl_2$ (**62**): thermal ellipsoids at 50% probability, hydrogen atoms and solvent molecules are omitted for clarity.



7 SUPPLEMENTARY DATA

7.1 Table of Θ and χ for all complexes

A definition of the interplanar angle Θ and the torsion angle χ is given in Figure **34**.

Table 15 Overview of interplanar angle Θ and torsion angle χ for all complexes. t*rans*-Tach is abbreviated as **L**.

	Θ			χ[a)]		
Copper(II)						
$[Cu(\mathbf{L})_2](NO_3)_2 \bullet 0.5\ HNO_3$ (**36** $\bullet 0.5\ HNO_3$)	150.8	171.4		/		
$[Cu(\mathbf{L}H)(NO_3)_3]$ (**37**)		161.2		/		
$[Cu(\mathbf{L})_2]Br_2$ (*syn*-**38**)		161.9		/		
$[Cu(\mathbf{L})_2]Br_2$ (*twist*-**38**)	158.2	158.4		/		
$[Cu(\mathbf{L})_2Br]Br$ (**39**)		157.2		/		
$[Cu(\mathbf{L}H)Br_2]Br$ (**40**)		151.2		/		
$[\{Cu(\mathbf{L})_2\}_2Cl]Cl_3 \bullet 2\ HCl$ (**41** $\bullet 2\ HCl$)	159.5	161.6		/		
$[\{Cu(\mathbf{L}H)Cl_2\}_3Cl]Cl_2$ (**42**)		142.7		/		
$[\{Cu(\mathbf{L}H)Cl_2\}_3Cl]Br_2$ (**43**)		142.7		/		
$[Cu(\mathbf{L})_2F]F$ (**44**)	160.4	161.7		/		
$[\{Cu(\mathbf{L}H)F\}_4]F_8$ (**45**)		145.8		/		
$[Cu(\mathbf{L})_2(SO_4)]$ (**46**)	152.8	161.3		/		
$[Cu(\mathbf{L}H)_2(SO_4)](SO_4)$ (**46** $\bullet H_2SO_4$)	153.3	175.5		/		
Nickel(II)						
$[Ni(\mathbf{L}H)_2](NO_3)_4$ (**34** $\bullet 2\ HNO_3$)		140.4		/		
$[Ni(\mathbf{L})_2]Cl_2$ (**35**)		141.2		/		
Palladium(II)						
$[Pd(\mathbf{L}H)Cl_2]Cl$ (**47**)		146.0		/		
$[Pd(\mathbf{L}H)Br_2]_2[PdBr_4]$ (**48**)		170.8		/		
$[Pd(\mathbf{L}H)_2](NO_3)_4$ (**49**)		142.8		/		
$[Pd(\mathbf{L}H)_2](SO_4)_2$ (**50**)		165.2		/		
$[\{Pd(\mathbf{L})Cl\}_6]Cl_6$ (**51**)	148.5	147.2	159.7	123.5	116.6	112.1
$[\{Pd(\mathbf{L})Br\}_6]Br_6$ (**52**)	148.0	149.6	148.0	122.4	127.6	114.7
$[Pd\{Pd(\mathbf{L})Cl_2\}_2Cl_2]$ (**53**)		150.3			133.6	
Silver(I)						
$\{[Ag(\mathbf{L})](NO_3)\}_n$ (**54**)		/		9.4	89.1	89.3 (ax)
				5.1	11.2	0.2 (ax)
$\{[Ag(\mathbf{L})](OTf)\}_n$ (**55**)		/		116.6	129.8	17.8 (ax)
				123.2	133.7	15.0 (ax)
Schiff base ligands[b)]						
tbc (**57**)		/		151.6	162.3	172.2 (ax)
[Cu(**ttop**)Cl]Cl (**61**)		169.0			164.6	
$[\{Cu_2(\mathbf{ttop})Cl_3\}_2]Cl_2$ (**62**)		193.6			59.0	

a) The torsion angle χ describes torsions around *equatorial* C-N bonds unless otherwise stated (ax).

b) For the Schiff base derivatives of *trans*-tach, χ is defined as the torsion angle between the centre of the cyclohexane ring, the methine carbon, amino group nitrogen and the imine carbon of the organic substituent rather than the complexed metal, which would only apply for **62**.

7.2 Speciation resolution of a triprotic ligand A

The dissociation constants K_a for the triprotic ligand **A** can be described as follows:

$$H_2O + H_3A^{3+} \leftrightarrow H_3O^+ + H_2A^{2+} \Rightarrow K_{a1} = \frac{\left[H_3O^+\right]\cdot\left[H_2A^{2+}\right]}{\left[H_3A^{3+}\right]} \quad (1)$$

$$H_2O + H_2A^{2+} \leftrightarrow H_3O^+ + HA^{1+} \Rightarrow K_{a2} = \frac{\left[H_3O^+\right]\cdot\left[HA^{1+}\right]}{\left[H_2A^{2+}\right]} \quad (2)$$

$$H_2O + HA^{1+} \leftrightarrow H_3O^+ + A \Rightarrow K_{a3} = \frac{\left[H_3O^+\right]\cdot\left[A\right]}{\left[HA^{1+}\right]} \quad (3)$$

The corresponding fractional compositions α are[161]

$$\alpha_3 = \frac{\left[H_3A^{3+}\right]}{C} = \frac{\left[H_3O^+\right]^3}{\left[H_3O^+\right]^3 + K_{a1}\left[H_3O^+\right]^2 + K_{a1}K_{a2}\left[H_3O^+\right] + K_{a1}K_{a2}K_{a3}}$$

$$\alpha_2 = \frac{\left[H_2A^{2+}\right]}{C} = \frac{K_{a1}\left[H_3O^+\right]^2}{\left[H_3O^+\right]^3 + K_{a1}\left[H_3O^+\right]^2 + K_{a1}K_{a2}\left[H_3O^+\right] + K_{a1}K_{a2}K_{a3}}$$

$$\alpha_1 = \frac{\left[HA^{1+}\right]}{C} = \frac{K_{a1}K_{a2}\left[H_3O^+\right]}{\left[H_3O^+\right]^3 + K_{a1}\left[H_3O^+\right]^2 + K_{a1}K_{a2}\left[H_3O^+\right] + K_{a1}K_{a2}K_{a3}}$$

$$\alpha_0 = \frac{\left[A\right]}{C} = \frac{K_{a1}K_{a2}K_{a3}}{\left[H_3O^+\right]^3 + K_{a1}\left[H_3O^+\right]^2 + K_{a1}K_{a2}\left[H_3O^+\right] + K_{a1}K_{a2}K_{a3}}$$

C is the overall concentration of all species in solution:

$$C = [H_3\mathbf{A}^{3+}] + [H_2\mathbf{A}^{2+}] + [H\mathbf{A}^{1+}] + [\mathbf{A}].$$

The *tris*-protonated species $H_3\mathbf{A}^{3+}$ is the dominant species at lower pH since α_3 is proportional to $[H_3O^+]^3$. Similarly, with increasing pH, $[H_3\mathbf{A}^{3+}]$ tends towards zero while **A** becomes the dominent species.

The pH at intersection points of fractional compositions are identical with the pK_a values for these equilibria. This is exemplified in the equilibrium where $[H_3\mathbf{A}^{3+}] = [H_2\mathbf{A}^{2+}]$:

$$K_{a1} = \frac{\left[H_3O^+\right]\cdot\left[H_2A^{2+}\right]}{\left[H_3A^{3+}\right]}$$

taking $-\log_{10}$

$$pK_{a1} = pH - \log_{10}\left(\frac{\left[H_2A^{2+}\right]}{\left[H_3A^{3+}\right]}\right)$$

since $[H_3\mathbf{A}^{3+}] = [H_2\mathbf{A}^{2+}]$ and $\log_{10}(1) = 0$

$$pK_{a1} = pH$$

The maximum concentration of species are half-way between their adjacent pK_a values. This is exemplified by the maximum concentration for $[H_2\mathbf{A}^{2+}]$. Since $H_2\mathbf{A}^{2+}$ is the major species present in solution, the major equilibrium is the disproportionation reaction:

$$2H_2A^{2+} \leftrightarrow H_3A^{3+} + HA^{1+} \Rightarrow K = \frac{\left[H_3A^{3+}\right]\cdot\left[HA^{1+}\right]}{\left[H_2A^{2+}\right]^2}$$

To include the proton concentration $[H_3O^+]$ in the equation, the first two equilibrium equations (1) and (2) are added.

$$H_2O + H_3A^{3+} \leftrightarrow H_3O^+ + H_2A^{2+} \Rightarrow K_{a1} = \frac{\left[H_3O^+\right]\cdot\left[H_2A^{2+}\right]}{\left[H_3A^{3+}\right]} \quad (1)$$

$$H_2O + H_2A^{2+} \leftrightarrow H_3O^+ + HA^{1+} \Rightarrow K_{a2} = \frac{\left[H_3O^+\right]\cdot\left[HA^{1+}\right]}{\left[H_2A^{2+}\right]} \quad (2)$$

$$2H_2O + H_3A^{3+} \leftrightarrow 2H_3O^+ + HA^{1+} \Rightarrow \beta_{a2} = K_{a1}K_{a2} = \frac{\left[H_3O^+\right]^2\left[HA^{1+}\right]}{\left[H_3A^{3+}\right]}$$

taking $-\log_{10}$

$$p\beta_{a2} = 2pH - \log_{10}\left(\frac{[HA^{1+}]}{[H_3A^{3+}]}\right)$$

since the disproportionation reaction predicts $[H_3\mathbf{A}^{3+}] = [H\mathbf{A}^{1+}]$

$$pH = \frac{1}{2}p\beta_{a2} = \frac{1}{2}(pK_{a1} + pK_{a2})$$

7.3 Re-numbered hexanuclear ring complexes 51 and 52

Complexes **51** and **52** were renumbered from the original published scheme[164] for systematic comparison between crystallographic and NMR data: The most low field shifted NMR signals Ha, Hb and Hc in the original manuscript correspond to the methine protons on C5, C11 and C17 respectively and are referred to as Ha1, Ha2 and Ha3 in this thesis. Hd corresponds to the *axial* methylene proton on C12 (H12a) and is here referred to as Hb2.

Ring unit 1 consists of Pd1, N1-N3 and C1-C6; Ring unit 2 consists of Pd2, N4-N6 and C7-C12; Ring unit 3 consists of Pd3, N7-N9 and C13-C18. The cyclic complexes are formed by connection of each ring through the 'Tail' amino group coordinating to Pd(II) chelated by the 'Head' amino groups of an adjacent ring. Connectivity as follows: Ring1-Ring2, Ring2-Ring3, Ring3-Ring1.

Changes made in atom nomenclature to be consistent with NMR:
Pd-ring1 corresponds to NMR signal Ha1, Pd-ring2 corresponds to NMR signal Ha2, Pd-ring3 corresponds to NMR signal Ha3.

Grey shadings underline changes from published structures

NEW	Published	NEW	Published
Pd 1	Pd 2	C 1	C13
Pd 2	Pd 3	C 2	C14
Pd 3	Pd 1	C 3	C 15
Cl 1	Cl 2	C 4	C16
Cl 2	Cl 3	C 5	C17
Cl 3	Cl 1	C 6	C18
Cl 4	Cl 4	C 7	C 7
Cl 5	Cl 5	C 8	C 12
Cl 6A	Cl 6A	C 9	C 11
Cl 6B	Cl 6B	C 10	C 10
Cl 7A	Cl 7A	C 11	C 9
Cl 7B	Cl 7B	C 12	C 8
N 1	N 7	C 13	C 1
N 2	N 8	C 14	C 6
N 3	N 9	C 15	C 5
N 4	N 4	C 16	C 4
N 5	N 5	C 17	C 3
N 6	N 6	C 18	C 1
N 7	N 1	O 1	O 1
N 8	N 2	O 2	O 2
N 9	N 3	O 3	O 3
		O 4	O 4
		O 5	O 5
		O 6A	O 6A
		O 6B	O 6B
		O 7A	O 7A
		O 7B	O 7B

7.4 Correlated NMR data for complex 51

Assignment of the ^{1}H-NMR signals of **51** to their corresponding ring units through tentative correlation of their 2-D-NMR spectra:

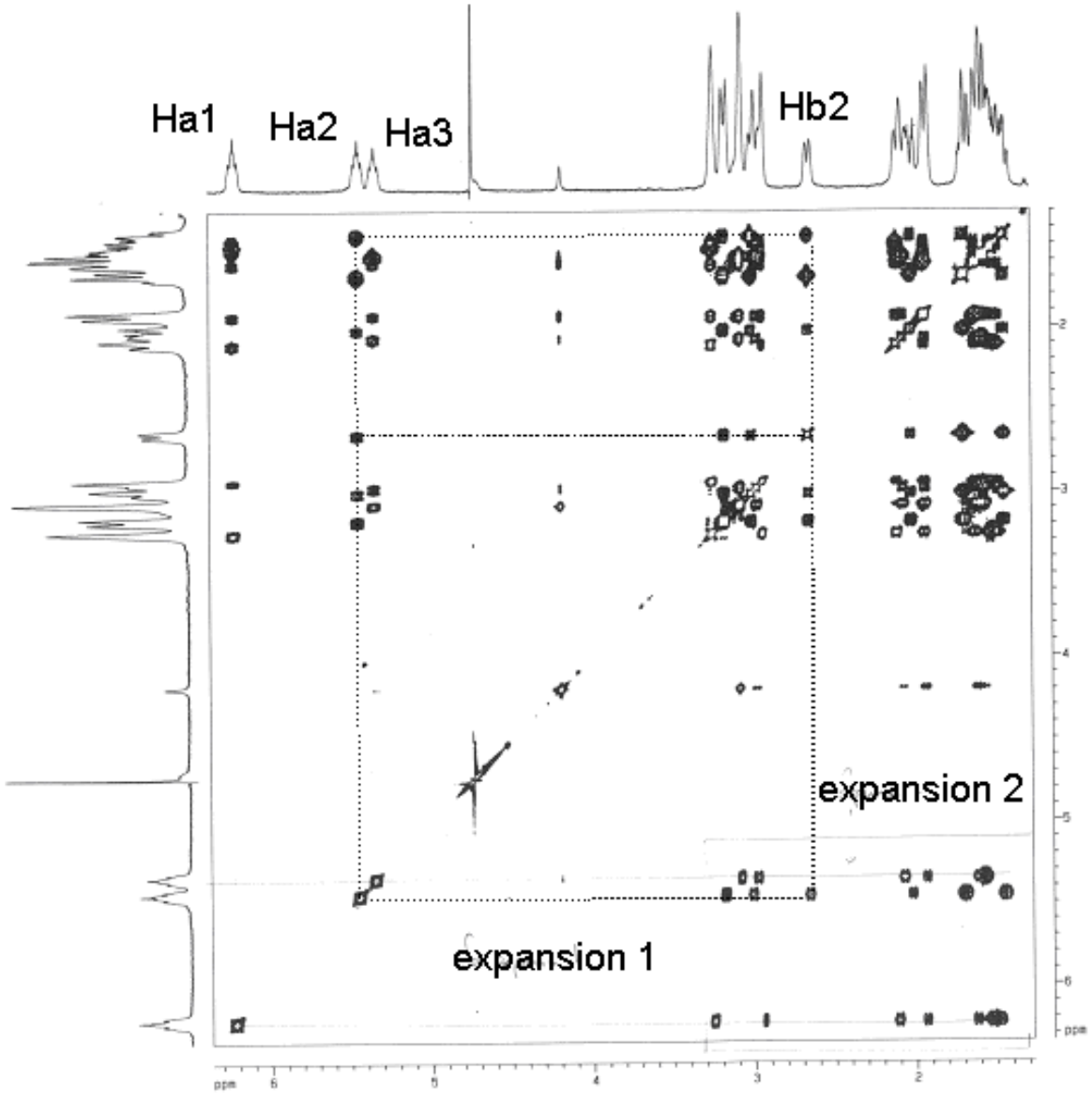


Figure 105 COSY-NMR spectrum (500 MHz, D_2O) of **51**. HOHAHA experiment with a 150 ms spin lock period and a 10 KHz spin lock field. The dotted lines show the correlation between H_{a2} and H_{b2}.

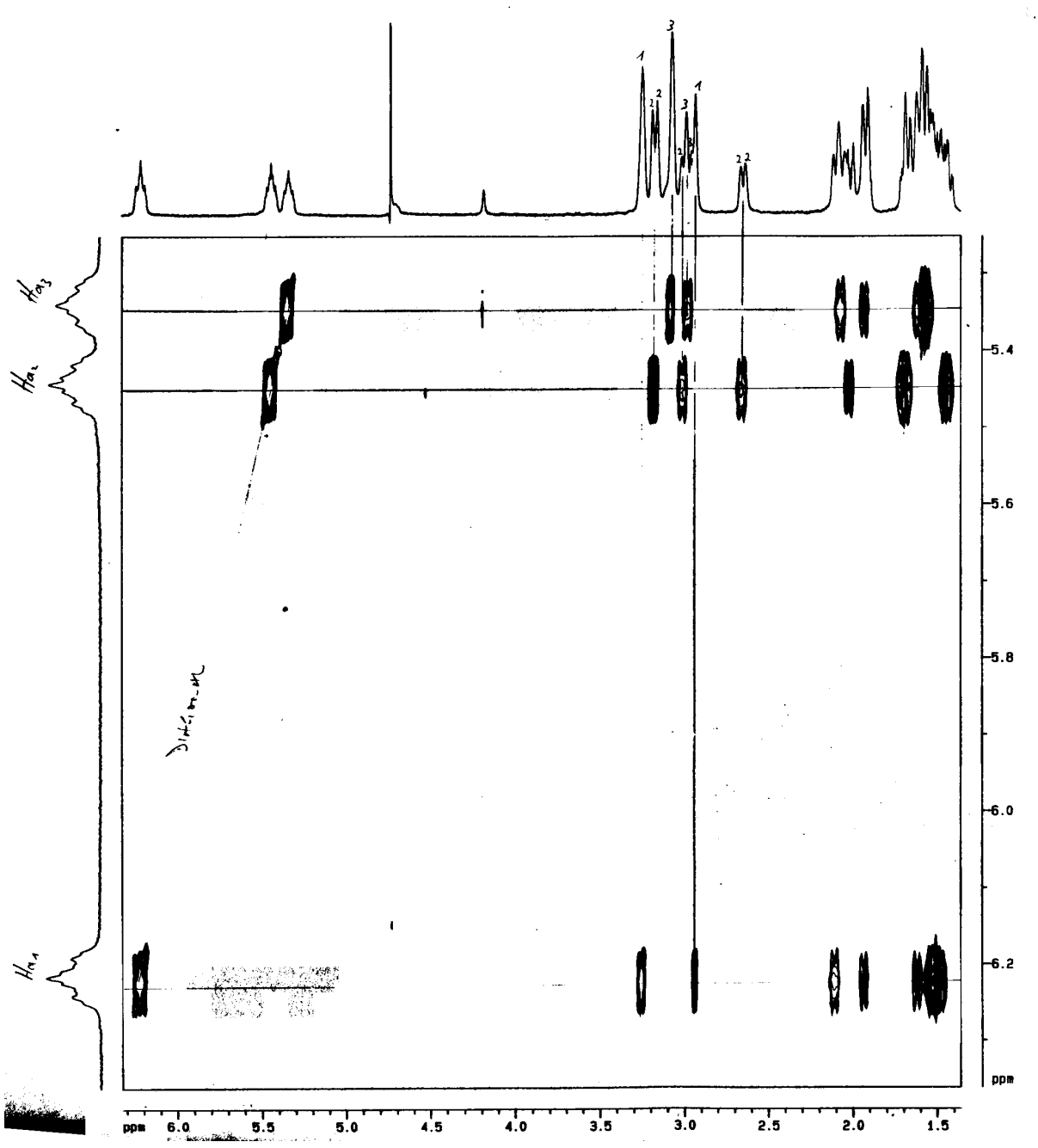


Figure 106 Expansion 1: coupling between protons H_{a2} and H_{b2}.

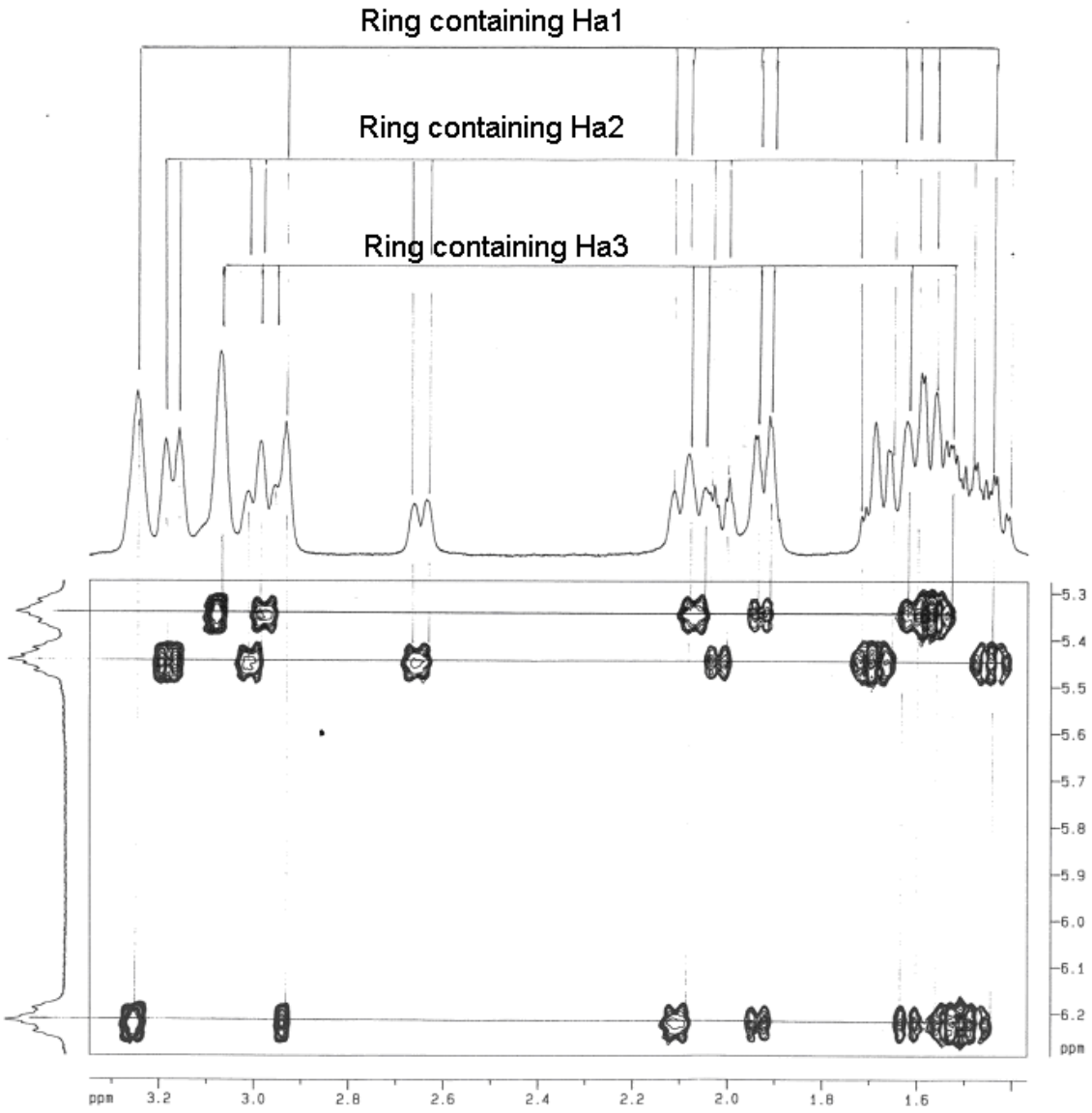


Figure 107 Expansion 2: Assignment of the three sets of ring units corresponding to H_{a1}, H_{a2} and H_{a3}.

8 REFERENCES

(1) J. M. Lehn *Supramolecular Chemistry, Concepts and Perspectives*; VCH: Weinheim, **1995**.

(2) G. M. Whitesides, J. P. Mathias, C. T. Seto *Science* **1991**, *254*, 1312.

(3) D. Philp, J. F. Stoddart *Angew. Chem., Int. Ed. Engl.* **1996**, *35*, 1155.

(4) P. Ehrlich *Studies on Immunity*; Wiley: New York, **1906**.

(5) E. Fischer *Ber. Deutsch. Chem. Ges.* **1894**, *27*, 2985.

(6) A. Werner *Zeitschr. Anorg. Chem.* **1893**, *3*, 267.

(7) J.-M. Lehn *Perspectives in Coordination Chemistry*; VCH: Weinheim, **1992**; p 447.

(8) Y. A. Ovchinnikov, V. T. Ivanov, A. M. Skrob *Membrane Active Complexones*; Elsevier: New York, **1974**.

(9) H. Brockmann, H. Geeren *Justus Liebigs Ann. Chem.* **1957**, *603*, 217.

(10) J. Beck, H. Gerlach, V. Prelog, W. Voser *Helv. Chim. Acta* **1962**, *46*, 620.

(11) M. M. Shemyakin, N. A. Aldanova, E. I. Vinogradova, M. Y. Feigina *Tetrahedron Lett.* **1963**, 1921.

(12) B. C. Pressman *Proc. Natl. Acad. Sci. U. S. A.* **1965**, *53*, 1077.

(13) B. C. Pressman, E. J. Harris, W. S. Jagger, J. H. Johnson *Proc. Natl. Acad. Sci. U. S. A.* **1967**, *58*, 1949.

(14) B. T. Kilbourn, J. D. Dunitz, L. A. R. Pioda, W. Simon *J. Mol. Biol.* **1967**, *30*, 559.

(15) C. J. Pedersen *J. Am. Chem. Soc.* **1967**, *89*, 7017.

(16) C. J. Pedersen *Angew. Chem., Int. Ed. Engl.* **1988**, *27*, 1021.

(17) B. Dietrich, J.-M. Lehn, J.-P. Sauvage *Tetrahedron Lett.* **1969**, 2855.

(18) B. Dietrich, J.-M. Lehn, J.-P. Sauvage, J. Blanzat *Tetrahedron* **1973**, *29*, 1629.

(19) B. Dietrich, J.-M. Lehn, J.-P. Sauvage *Tetrahedron* **1973**, *29*, 1647.

(20) J.-M. Lehn *Struct. Bonding* **1973**, *16*, 1.

(21) J.-M. Lehn *Pure Appl. Chem.* **1978**, *50*, 871.

(22) J. M. Lehn *Angew. Chem., Int. Ed. Engl.* **1988**, *27*, 89.

(23) J. M. Lehn *Science* **1985**, *227*, 849.

(24) I. Dance *New J. Chem.* **2003**, *27*, 1.

(25) A. Harada, J. Li, M. Kamachi *Nature* **1992**, *356*, 325.

(26) A. Harada, J. Li, M. Kamachi *Nature* **1994**, *370*, 126.

(27) J. Rebek *Angew. Chem., Int. Ed. Engl.* **1990**, *29*, 245.

(28) D. B. Amabilino, J. F. Stoddart *Chem. Rev.* **1995**, *95*, 2725.

(29) M. C. T. Fyfe, J. F. Stoddart *Acc. Chem. Res.* **1997**, *30*, 393.

(30) F. Voegtle *Supramolecular Chemistry*; John Wiley&Sons: New York, **1991**.

(31) T. Glaser, B. Hedman, K. O. Hodgson, E. I. Solomon *Acc. Chem. Res.* **2000**, *33*, 859.

(32) M. Schweiger, S. R. Seidel, A. M. Arif, P. J. Stang *Inorg. Chem.* **2002**, *41*, 2556.

(33) S. Leininger, B. Olenyuk, P. J. Stang *Chem. Rev.* **2000**, *100*, 853.

(34) D. Gatteschi, L. Pardi, A. L. Barra, A. Muller, J. Doring *Nature* **1991**, *354*, 463.

(35) R. E. P. Winpenny *J. Chem. Soc., Dalton Trans.* **2002**, 1.

(36) A. Muller, S. Q. N. Shah, H. Bogge, M. Schmidtmann *Nature* **1999**, *397*, 48.

(37) D. L. Caulder, K. N. Raymond *Acc. Chem. Res.* **1999**, *32*, 975.

(38) D. L. Caulder, K. N. Raymond *J. Chem. Soc., Dalton Trans.* **1999**, 1185.

(39) P. N. W. Baxter, J. M. Lehn, G. Baum, D. Fenske *Chem. Eur. J.* **1999**, *5*, 102.

(40) P. N. W. Baxter, J. M. Lehn, B. O. Kneisel, G. Baum, D. Fenske *Chem. Eur. J.* **1999**, *5*, 113.

(41) R. W. Saalfrank, I. Bernt, E. Uller, F. Hampel *Angew. Chem., Int. Ed.* **1997**, *36*, 2482.

(42) R. W. Saalfrank, R. Burak, S. Reihs, N. Low, F. Hampel, H. D. Stachel, J. Lentmaier, K. Peters, E. M. Peters, H. G. Vonschnering *Angew. Chem., Int. Ed.* **1995**, *34*, 993.

(43) F. A. Cotton, G. Wilkinson *Advanced Inorganic Chemistry*; John Wiley and Sons: New York, **1988**.

(44) M. Fujita *Chem. Soc. Rev.* **1998**, *27*, 417.

(45) P. M. Stricklen, E. J. Volcko, J. G. Verkade *J. Am. Chem. Soc.* **1983**, *105*, 2494.

(46) P. J. Stang, B. Olenyuk *Acc. Chem. Res.* **1997**, *30*, 502.

(47) B. Olenyuk, A. Fechtenkotter, P. J. Stang *J. Chem. Soc., Dalton Trans.* **1998**, 1707.

(48) M. Fujita, K. Ogura *Coord. Chem. Rev.* **1996**, *148*, 249.

(49) M. D. Levin, P. J. Stang *J. Am. Chem. Soc.* **2000**, *122*, 7428.

(50) T. Kusukawa, M. Fujita *Angew. Chem., Int. Ed.* **1998**, *37*, 3142.

(51) A. W. Maverick, S. C. Buckingham, Q. Yao, J. R. Bradbury, G. G. Stanley *J. Am. Chem. Soc.* **1986**, *108*, 7430.

(52) A. W. Maverick, F. E. Klavetter *Inorg. Chem.* **1984**, *23*, 4129.

(53) M. Fujita, S. Nagao, M. Iida, K. Ogata, K. Ogura *J. Am. Chem. Soc.* **1993**, *115*, 1574.

(54) M. J. Hannon, C. L. Painting, W. Errington *Chem. Commun.* **1997**, 307.

(55) M. Fujita, O. Sasaki, T. Mitsuhashi, T. Fujita, J. Yazaki, K. Yamaguchi, K. Ogura *Chem. Commun.* **1996**, 1535.

(56) M. Fujita *Journal of Synthetic Organic Chemistry Japan* **1996**, *54*, 953.

(57) F. M. Romero, R. Ziessel, A. Dupont-Gervais, A. VanDorsselaer *Chem. Commun.* **1996**, 551.

(58) M. Fujita, J. Yazaki, K. Ogura *J. Am. Chem. Soc.* **1990**, *112*, 5645.

(59) F. A. Cotton, L. M. Daniels, C. Lin, C. A. Murillo *J. Am. Chem. Soc.* **1999**, *121*, 4538.

(60) P. J. Stang, D. H. Cao *J. Am. Chem. Soc.* **1994**, *116*, 4981.

(61) P. J. Stang, D. H. Cao, S. Saito, A. M. Arif *J. Am. Chem. Soc.* **1995**, *117*, 6273.

(62) R. V. Slone, J. T. Hupp, C. L. Stern, T. E. Albrecht-Schmitt *Inorg. Chem.* **1996**, *35*, 4096.

(63) P. J. Stang, J. A. Whiteford *Organometallics* **1994**, *13*, 3776.

(64) J. A. Whiteford, C. V. Lu, P. J. Stang *J. Am. Chem. Soc.* **1997**, *119*, 2524.

(65) P. J. Stang, N. E. Persky *Chem. Commun.* **1997**, 77.

(66) B. Hasenknopf, J. M. Lehn, B. O. Kneisel, G. Baum, D. Fenske *Angew. Chem., Int. Ed. Engl.* **1996**, *35*, 1838.

(67) R. W. Saalfrank, I. Bernt, E. Uller, F. Hampel *Angew. Chem., Int. Ed. Engl.* **1997**, *36*, 2482.

(68) O. Mamula, A. von Zelewsky, G. Bernardinelli *Angew. Chem., Int. Ed.* **1998**, *37*, 290.

(69) N. Matsumoto, Y. Motoda, T. Matsuo, T. Nakashima, N. Re, F. Dahan, J. P. Tuchagues *Inorg. Chem.* **1999**, *38*, 1165.

(70) B. Grossmann, J. Heinze, E. Herdtweck, F. H. Kohler, H. Noth, H. Schwenk, M. Spiegler, W. Wachter, B. Weber *Angew. Chem., Int. Ed. Engl.* **1997**, *36*, 387.

(71) P. L. Jones, K. J. Byrom, J. C. Jeffery, J. A. McCleverty, M. D. Ward *Chem. Commun.* **1997**, 1361.

(72) H. Jiang, W. B. Lin *J. Am. Chem. Soc.* **2003**, *125*, 8084.

(73) B. J. Holliday, C. A. Mirkin *Angew. Chem., Int. Ed.* **2001**, *40*, 2022.

(74) F. A. Cotton, C. Lin, C. A. Murillo *Proc. Natl. Acad. Sci. U. S. A.* **2002**, *99*, 4810.

(75) G. F. Swiegers, T. J. Malefetse *Coord. Chem. Rev.* **2002**, *225*, 91.

(76) G. F. Swiegers, T. J. Malefetse *Chem. Rev.* **2000**, *100*, 3483.

(77) C. Piguet, G. Bernardinelli, G. Hopfgartner *Chem. Rev.* **1997**, *97*, 2005.

(78) M. Albrecht *Chem. Rev.* **2001**, *101*, 3457.

(79) D. W. Johnson, K. N. Raymond *Supramolecular Chemistry* **2001**, *13*, 639.

(80) M. Fujita, S. Nagao, K. Ogura *J. Am. Chem. Soc.* **1995**, *117*, 1649.

(81) P. Baxter, J. M. Lehn, A. Decian, J. Fischer *Angew. Chem., Int. Ed. Engl.* **1993**, *32*, 69.

(82) R. W. Saalfrank, A. Stark, K. Peters, H. G. Vonschnering *Angew. Chem., Int. Ed. Engl.* **1988**, *27*, 851.

(83) R. W. Saalfrank, A. Stark, M. Bremer, H. U. Hummel *Angew. Chem., Int. Ed. Engl.* **1990**, *29*, 311.

(84) J. S. Fleming, K. L. V. Mann, C. A. Carraz, E. Psillakis, J. C. Jeffery, J. A. McCleverty, M. D. Ward *Angew. Chem., Int. Ed.* **1998**, *37*, 1279.

(85) E. J. Enemark, T. D. P. Stack *Angew. Chem., Int. Ed.* **1998**, *37*, 932.

(86) S. Mann, G. Huttner, L. Zsolnai, K. Heinze *Angew. Chem., Int. Ed. Engl.* **1996**, *35*, 2808.

(87) T. Beissel, R. E. Powers, K. N. Raymond *Angew. Chem., Int. Ed. Engl.* **1996**, *35*, 1084.

(88) R. W. Saalfrank, R. Burak, A. Breit, D. Stalke, R. Herbstirmer, J. Daub, M. Porsch, E. Bill, M. Muther, A. X. Trautwein *Angew. Chem., Int. Ed. Engl.* **1994**, *33*, 1621.

(89) R. W. Saalfrank, B. Horner, D. Stalke, J. Salbeck *Angew. Chem., Int. Ed. Engl.* **1993**, *32*, 1179.

(90) T. Beissel, R. E. Powers, T. N. Parac, K. N. Raymond *J. Am. Chem. Soc.* **1999**, *121*, 4200.

(91) D. L. Caulder, R. E. Powers, T. N. Parac, K. N. Raymond *Angew. Chem., Int. Ed.* **1998**, *37*, 1840.

(92) T. N. Parac, D. L. Caulder, K. N. Raymond *J. Am. Chem. Soc.* **1998**, *120*, 8003.

(93) H. Ito, T. Kusukawa, M. Fujita *Chem. Lett.* **2000**, 598.

(94) M. Yoshizawa, Y. Takeyama, T. Kusukawa, M. Fujita *Angew. Chem., Int. Ed.* **2002**, *41*, 1347.

(95) C. Bruckner, R. E. Powers, K. N. Raymond *Angew. Chem., Int. Ed.* **1998**, *37*, 1837.

(96) A. J. Amoroso, J. C. Jeffery, P. L. Jones, J. A. McCleverty, P. Thornton, M. D. Ward *Angew. Chem., Int. Ed. Engl.* **1995**, *34*, 1443.

(97) J. J. Sokol, M. P. Shores, J. R. Long *Angew. Chem., Int. Ed.* **2001**, *40*, 236.

(98) P. A. Berseth, J. J. Sokol, M. P. Shores, J. L. Heinrich, J. R. Long *J. Am. Chem. Soc.* **2000**, *122*, 9655.

(99) J. J. Sokol, M. P. Shores, J. R. Long *Inorg. Chem.* **2002**, *41*, 3052.

(100) M. P. Shores, J. J. Sokol, J. R. Long *J. Am. Chem. Soc.* **2002**, *124*, 2279.

(101) M. Ziegler, J. L. Brumaghim, K. N. Raymond *Angew. Chem., Int. Ed.* **2000**, *39*, 4119.

(102) B. Olenyuk, J. A. Whiteford, A. Fechtenkotter, P. J. Stang *Nature* **1999**, *398*, 796.

(103a) J. M. Lehn, A. Rigault, J. Siegel, J. Harrowfield, B. Chevrier, D. Moras *Proc. Natl. Acad. Sci. U. S. A.* **1987**, *84*, 2565.

(103b) A. D. Cutland-Van Noord, J. W. Kampf, V. L. Pecoraro *Angew. Chem., Int. Ed.* **2002**, *41*, 4667.

(103c) J. A. Johnson, J. W. Kampf, V. L. Pecoraro *Angew. Chem., Int. Ed.* **2003**, *42*, 546.

(104) R. E. Ernst, M. J. O'Connor, R. H. Holm *J. Am. Chem. Soc.* **1967**, *89*, 6104.

(105) E. L. Muetterties *J. Am. Chem. Soc.* **1968**, *90*, 5097.

(106) E. L. Muetterties *J. Am. Chem. Soc.* **1969**, *91*, 1636.

(107) R. S. Cahn, C. Ingold, V. Prelog *Angew. Chem., Int. Ed. Engl.* **1966**, *5*, 385.

(108) C. J. Cathey, E. C. Constable, M. J. Hannon, D. A. Tocher, M. D. Ward *J. Chem. Soc., Chem. Commun.* **1990**, 621.

(109) E. C. Constable, M. D. Ward, D. A. Tocher *J. Chem. Soc., Dalton Trans.* **1991**, 1675.

(110) E. C. Constable, M. D. Ward *J. Am. Chem. Soc.* **1990**, *112*, 1256.

(111) R. Kramer, J. M. Lehn, A. Marquisrigault *Proc. Natl. Acad. Sci. U. S. A.* **1993**, *90*, 5394.

(112) D. L. Caulder, K. N. Raymond *Angew. Chem., Int. Ed. Engl.* **1997**, *36*, 1440.

(113) S. R. Batten, R. Robson *Angew. Chem., Int. Ed.* **1998**, *37*, 1461.

(114) A. F. Wells *Three-Dimensional Nets and Polyhedra*; John Wiley&Sons: New York, **1977**.

(115) A. L. Pickering, L. Cronin *DNA as a Supramolecular Scaffold*; Dekker: New York, **2003**.

(116) M. Fujita, N. Fujita, K. Ogura, K. Yamaguchi *Nature* **1999**, *400*, 52.

(117) M. Fujita, Y. J. Kwon, O. Sasaki, K. Yamaguchi, K. Ogura *J. Am. Chem. Soc.* **1995**, *117*, 7287.

(118) B. F. Hoskins, R. Robson, D. A. Slizys *J. Am. Chem. Soc.* **1997**, *119*, 2952.

(119) S. R. Batten, B. F. Hoskins, R. Robson *New J. Chem.* **1998**, *22*, 173.

(120) J. Konnert, D. Britton *Inorg. Chem.* **1966**, *5*, 1193.

(121) L. R. Macgillivray, S. Subramanian, M. J. Zaworotko *J. Chem. Soc., Chem. Commun.* **1994**, 1325.

(122) A. F. Wells *Structural Inorganic Chemistry*; Oxford University Press: **1983**.

(123) K. Mereiter, J. Zemann, A. W. Hewat *Am. Mineral.* **1992**, *77*, 839.

(124) M. A. Brook, R. Faggiani, C. J. L. Lock, D. Seebach *Acta Crystallogr., Sect. C: Cryst. Struct. Commun.* **1988**, *44*, 1981.

(125) M. Yoshizawa, T. Kusukawa, M. Fujita, K. Yamaguchi *J. Am. Chem. Soc.* **2000**, *122*, 6311.

(126) M. Yoshizawa, T. Kusukawa, M. Fujita, S. Sakamoto, K. Yamaguchi *J. Am. Chem. Soc.* **2001**, *123*, 10454.

(127) S. A. Levi, P. Guatteri, F. C. J. M. van Veggel, G. J. Vancso, E. Dalcanale, D. N. Reinhoudt *Angew. Chem., Int. Ed.* **2001**, *40*, 1892.

(128) B. F. Abrahams, S. R. Batten, B. F. Hoskins, R. Robson *Inorg. Chem.* **2003**, *42*, 2654.

(129) S. L. Zheng, M. L. Tong, X. M. Chen, S. W. Ng *J. Chem. Soc., Dalton Trans.* **2002**, 360.

(130) L. Carlucci, G. Ciani, D. M. Proserpio, S. Rizzato *J. Solid State Chem.* **2000**, *152*, 211.

(131) J. Y. Yang, M. P. Shores, J. J. Sokol, J. R. Long *Inorg. Chem.* **2003**, *42*, 1403.

(132) G. Schwarzenbach, H. B. Burgi, W. P. Jensen, G. A. Lawrance, L. Monsted, A. M. Sargeson *Inorg. Chem.* **1983**, *22*, 4029.

(133) M. Ishii, M. Umehara, M. Nakahara *Bull. Chem. Soc. Jpn.* **1987**, *60*, 125.

(134) D. Kuppert, J. Sander, C. Roth, M. Worle, T. Weyhermuller, G. J. Reiss, U. Schilde, I. Muller, K. Hegetschweiler *Eur. J. Inorg. Chem.* **2001**, 2525.

(135) X. S. Tan, Y. Fujii, T. Sato, Y. Nakano, M. Yashiro *Chem. Commun.* **1999**, 881.

(136) J. Glerup, H. Weihe, P. A. Goodson, D. J. Hodgson *Inorg. Chim. Acta* **1993**, *212*, 281.

(137) Y. Fujii, T. Kiss, T. Gajda, X. S. Tan, T. Sato, Y. Nakano, Y. Hayashi, M. Yashiro *J. Biol. Inorg. Chem.* **2002**, *7*, 843.

(138) G. Park, E. Dadachova, A. Przyborowska, S. J. Lai, D. S. Ma, G. Broker, R. D. Rogers, R. P. Planalp, M. W. Brechbiel *Polyhedron* **2001**, *20*, 3155.

(139) G. Park, J. Shao, F. H. Lu, R. D. Rogers, N. D. Chasteen, M. W. Brechbiel, R. P. Planalp *Inorg. Chem.* **2001**, *40*, 4167.

(140) K. A. Deal, G. Park, J. Shao, N. D. Chasteen, M. W. Brechbiel, R. P. Planalp *Inorg. Chem.* **2001**, *40*, 4176.

(141) C. Sissi, F. Mancin, M. Palumbo, P. Scrimin, P. Tecilla, U. Tonellato *Nucleosid. Nucleotid.* **2000**, *19*, 1265.

(142) R. P. Planalp, G. S. Park, R. D. Rogers, M. W. Brechbiel *Abstracts of Papers of the American Chemical Society* **1999**, *218*, U868.

(143) K. Kamisawa, K. Matsumoto, S. Ooi, R. Saito, Y. Kidani *Bull. Chem. Soc. Jpn.* **1981**, *54*, 1072.

(144) R. E. Marsh, M. Kapon, S. Z. Hu, F. H. Herbstein *Acta Crystallogr., Sect. B: Struct. Sci.* **2002**, *58*, 62.

(145) K. Kamisawa, K. Matsumoto, S. Ooi, H. Kuroya, R. Saito, Y. Kidani *Bull. Chem. Soc. Jpn.* **1978**, *51*.

(146) S. T. Cham, C. I. Diakos, L. T. Ellis, R. R. Fenton, V. P. Munk, B. A. Messerle, T. W. Hambley *J. Chem. Soc., Dalton Trans.* **2001**, 2769.

(147) H. Manohar, D. Schwarzenbach, W. Iff, G. Schwarzenbach *J. Coord. Chem.* **1979**, *8*, 213.

(148) J. W. Pauly, J. Sander, D. Kuppert, M. Winter, G. J. Reiss, F. Zurcher, R. Hoffmann, T. F. Fassler, K. Hegetschweiler *Chem. Eur. J.* **2000**, *6*, 2830.

(149) L. Cronin, P. H. Walton *Chem. Commun.* **2003**, 1572.

(150) L. Cronin, S. P. Foxon, P. J. Lusby, P. H. Walton *J. Biol. Inorg. Chem.* **2001**, *6*, 367.

(151) L. Cronin, B. Greener, S. P. Foxon, S. L. Heath, P. H. Walton *Inorg. Chem.* **1997**, *36*, 2594.

(152) G. Park, A. M. Przyborowska, N. Ye, N. M. Tsoupas, C. B. Bauer, G. A. Broker, R. D. Rogers, M. W. Brechbiel, R. P. Planalp *J. Chem. Soc., Dalton Trans.* **2003**, 318.

(153) H. Stetter, J. Bremen *Chem. Ber.* **1973**, *106*, 2523.

(154) E. B. Fleischer, A. E. Gebala, A. Levey, P. A. Tasker *J. Org. Chem.* **1971**, *36*, 3043.

(155) T. Bowen, R. P. Planalp, M. W. Brechbiel *Bioorg. Med. Chem. Lett.* **1996**, *6*, 807.

(156) F. Lions, K. V. Martin *J. Am. Chem. Soc.* **1957**, *79*, 1572.

(157) A. Baeyer *Ber. Deutsch. Chem. Ges.* **1886**, *19*, 159.

(158) F. Urbach, J. E. Saneski, L. J. Turner, D. H. Bush *Inorg. Chem.* **1968**, *7*, 2169.

(159) Although Lions and Martin report a 57 % yield upon reduction of chtt, previous attempts have failed to reproduce such efficiency. Additionally, the formation of two isomers was not recognised.

(160) Picture taken from the Web Page of S. E. Bialkowski, Department of Chemistry and Biochemistry, Utah State University.

(161) R. de Levie *Aqueous Acid-Base Equilibria and Titrations*; Oxford University Press: New York, **1999**.

(162) J. L. Sudmeier, C. N. Reilley *Anal. Chem.* **1964**, *36*, 1698.

(163) P. Paoletti, M. Ciampolini, A. Vacca *J. Phys. Chem.* **1963**, *67*, 1065.

(164) G. Seeber, B. Kariuki, L. Cronin *Chem. Commun.* **2002**, 2912.

(165) J. H. Ammeter, H. B. Burgi, E. Gamp, V. Meyer-Sandrin, W. P. Jensen *Inorg. Chem.* **1979**, *18*, 733.

(166) Program PLATON - (a) A. L. Spek, *Acta Crystallogr.*, Sect A **1990**, C34, 46. (b) PLATON, A Multipurpose Crystallographic Tool, Utrecht University, Utrecht, The Netherlands, A. L. Spek, **1998**.

Analysis of potential hydrogen bonds and schemes with d(D...A) < {R(D)+R(A)+0.50}, d(H...A) < {R(H)+R(A)-0.12} Å., D-H...A > 100.0º. For analysis of hydrogen-bonded molecular aggregates, see *Acta Crystallogr.*, Sect. B **1980**, B36, 2113.

(167) A. W. Addison, T. N. Rao, J. Reedijk, J. Vanrijn, G. C. Verschoor *J. Chem. Soc., Dalton Trans.* **1984**, 1349.

(168) A. F. Hollemann, E. Wiberg *Lehrbuch der Anorganischen Chemie*; Walter de Gruyter: Berlin, **1995**.

(169) G. J. A. A. Koolhaas, W. L. Driessen, J. Reedijk, J. L. vanderPlas, R. A. G. deGraaff, D. Gatteschi, H. Kooijman, A. L. Spek *Inorg. Chem.* **1996**, *35*, 1509.

(170) M. Saburi, K. Miyamura, M. Morita, S. Yoshikawa, S. Tsuboyama, T. Sakurai, H. Yamazaki, K. Tsuboyama *Bull. Chem. Soc. Jpn.* **1987**, *60*, 2581.

(171) M. Saburi, K. Miyamura, M. Morita, Y. Mizoguchi, S. Yoshikawa, S. Tsuboyama, T. Sakurai, K. Tsuboyama *Bull. Chem. Soc. Jpn.* **1987**, *60*, 141.

(172) A. McAuley, S. Subramanian *Inorg. Chim. Acta* **2000**, *300*, 477.

(173) G. Kickelbick, T. Pintauer, K. Matyjaszewski *New J. Chem.* **2002**, *26*, 462.

(174) U. Suksangpanya, A. J. Blake, P. Hubberstey, D. J. Parker, S. J. Teat, C. Wilson *Crystengcomm* **2003**, 10.

(175) O. P. Gladkikh, N. F. Curtis *Acta Crystallogr., Sect. C: Cryst. Struct. Commun.* **1996**, *52*, 1418.

(176) R. Crescenzi, E. Solari, C. Floriani, A. Chiesi-Villa, C. Rizzoli *J. Am. Chem. Soc.* **1999**, *121*, 1695.

(177) M. H. Choi, B. J. Kim, I. C. Kim, S. H. Kim, Y. Kim, J. M. Harrowfield, M. K. Lee, M. Mocerino, E. Rukmini, B. W. Skelton, A. H. White *J. Chem. Soc., Dalton Trans.* **2001**, 707.

(178) P. S. Donnelly, J. M. Harrowfield, B. W. Skelton, A. H. White *Inorg. Chem.* **2000**, *39*, 5817.

(179) E. H. Alilou, M. Giorgi, M. Pierrot, M. Reglier *Acta Crystallogr., Sect. C: Cryst. Struct. Commun.* **1992**, *48*, 1612.

(180) V. Kolesnichenko, J. J. Luci, D. C. Swenson, L. Messerle *J. Am. Chem. Soc.* **1998**, *120*, 13260.

(181) F. Simon, K. Boubekeur, J. C. P. Gabriel, P. Batail *Chem. Commun.* **1998**, 845.

(182) P. A. Angaridis, P. Baran, R. Boca, F. Cervantes-Lee, W. Haase, G. Mezei, R. G. Raptis, R. Werner *Inorg. Chem.* **2002**, *41*, 2219.

(183) R. Patow, D. Fenske *Z. Anorg. Allg. Chem.* **2002**, *628*, 1279.

(184) P. Sobota, J. Utko, L. B. Jerzykiewicz *Inorg. Chem.* **1998**, *37*, 3428.

(185) X. Yang, C. B. Knobler, M. F. Hawthorne *Angew. Chem., Int. Ed. Engl.* **1991**, *30*, 1507.

(186) H. Lee, M. Diaz, C. B. Knobler, M. F. Hawthorne *Angew. Chem., Int. Ed.* **2000**, *39*, 776.

(187) P. A. Angaridis, P. Baran, R. Boca, F. Cervantes-Lee, W. Haase, G. Mezei, R. G. Raptis, R. Werner *Inorg. Chem.* **2002**, *41*, 2219.

(188) E. M. Holt, S. L. Holt, N. W. Alcock Acta Crystallogr., *Sect. C: Cryst. Struct. Commun.* **1982**, *11*, 505.

(189) W. Clegg, O. M. Lam, B. P. Straughan *Angew. Chem., Int. Ed. Engl.* **1984**, *23*, 434.

(190) B. F. Straub, F. Rominger, P. Hofmann *Inorg. Chem.* **2000**, *39*, 2113.

(191) S. Herold, S. J. Lippard *Inorg. Chem.* **1997**, *36*, 50.

(192) P. J. Steel, C. J. Sumby *Chem. Commun.* **2002**, 322.

(193) Crystallisations were carried out in plastic vials resulting in royal blue cubic crystals of **45**. Interestingly, crystallisation of identical reaction mixtures in glass vials resulted in the formation of the μ_2-chloro bridged dinuclear complex **41**. Possible explanation for the presence of chloride ions could be the contamination of the copper(II) fluoride starting material or dissolution of chloride ions from the crystallisation glass vials by hydrofluoric acid, which is indicated by the observation that no contamination of chloride ions was observed upon crystallisation from plastic vials. This observation is interesting as no 'free' hydrofluoric acid was expected in solution since the pH was adjusted to the slightly alkaline pH 7.7.

(194) J. C. Dyason, P. C. Healy, L. M. Engelhardt, C. Pakawatchai, V. A. Patrick, C. L. Raston, A. H. White *J. Chem. Soc., Dalton Trans.* **1985**, 831.

(195) A. Jouaiti, M. Geoffroy, G. Bernardinelli *J. Chem. Soc., Dalton Trans.* **1994**, 1685.

(196) G. A. Bowmaker, P. D. W. Boyd, C. E. F. Rickard, M. L. Scudder, I. G. Dance *Inorg. Chem.* **1999**, *38*, 5476.

(197) A. J. Blake, N. R. Brooks, N. R. Champness, M. Crew, A. Deveson, D. Fenske, D. H. Gregory, L. R. Hanton, P. Hubberstey, M. Schroder *Chem. Commun.* **2001**, 1432.

(198) H. Oshio, Y. Saito, T. Ito *Angew. Chem., Int. Ed.* **1997**, *36*, 2673.

(199) R. Wegner, M. Gottschaldt, H. Gorls, E. G. Jager, D. Klemm *Chem. Eur. J.* **2001**, *7*, 2143.

(200) X. M. Liu, A. C. McLaughlin, M. P. de Miranda, E. J. L. Mcinnes, C. A. Kilner, M. A. Halcrow *Chem. Commun.* **2002**, 2978.

(201) P. D. Newman, M. B. Hursthouse, K. M. A. Malik *J. Chem. Soc., Dalton Trans.* **1999**, 599.

(202) G. Codina, A. Caubet, C. Lopez, V. Moreno, E. Molins *Helv. Chim. Acta* **1999**, *82*, 1025.

(203) H. J. Callot, J. Fischer, R. Weiss *J. Am. Chem. Soc.* **1982**, *104*, 1272.

(204) T. N. Margulis, L. J. Zompa *Inorg. Chim. Acta* **1992**, *201*, 61.

(205) K. Kamisawa, K. Matsumoto, S. Ooi, Kuroya H., R. Saito, Y. Kidani *Bull. Chem. Soc. Jpn.* **1978**, *51*, 2330.

(206) R. Saito, Y. Kidani *Chem. Lett.* **1977**, 1141.

(207) G. Aullon, D. Bellamy, L. Brammer, E. A. Bruton, A. G. Orpen *Chem. Commun.* **1998**, 653.

(208) L. Brammer, D. Zhao, F. T. Ladipo, J. Braddockwilking *Acta Crystallogr., Sect. B: Struct. Sci.* **1995**, *51*, 632.

(209) Z. Qin, M. C. Jennings, R. J. Puddephatt *Inorg. Chem.* **2001**, *40*, 6220.

(210) M. C. Navarro-Ranninger, M. J. Camazon, A. Alvarezvaldes, J. R. Masaguer, S. Martinezcarrera, S. Garciablanco *Polyhedron* **1987**, *6*, 1059.

(211) R. R. Fenton, F. Huq, T. W. Hambley *Polyhedron* **1999**, *18*, 2149.

(212) G. Seeber, A. L. Pickering, D.-L. Long, L. Cronin *Chem. Commun.* **2003**, 2002.

(213) B. Greener, L. Cronin, G. D. Wilson, P. H. Walton *J. Chem. Soc., Dalton Trans.* **1996**, 401.

(214) M. Kanesato, F. N. Ngassapa, T. Yokoyama *Anal. Sci.* **2001**, *17*, 471.

(215) M. Figuet, M. T. Averbuch-Pouchot, A. D. d'Hardemare, O. Jarjayes *Eur. J. Inorg. Chem.* **2001**, 2089.

(216) J. Sanmartin, M. R. Bermejo, A. M. Garcia-Deibe, O. R. Nascimento, L. Lezama, T. Rojo *J. Chem. Soc., Dalton Trans.* **2002**, 1030.

(217) Y. Umezawa, S. Tsuboyama, K. Honda, J. Uzawa, M. Nishio *Bull. Chem. Soc. Jpn.* **1998**, *71*, 1207.

(218) Y. Umezawa, M. Nishio *Bioorganic & Medicinal Chemistry* **1998**, *6*, 493.

(219) The program ChemNMR Pro is implemented within the program ChemDraw Ultra V.7.0.1 in the ChemOffice 2002 package.

(220) R. A. D. Wentworth, P. S. Dahl, C. J. Huffman, W. O. Gillum, W. E. Streib, J. C. Huffman *Inorg. Chem.* **1982**, *21*, 3060.

(221) D. Z. Niu, B. W. Sun, Z. S. Lu, Z. M. Wang, C. H. Yan *Acta Crystallogr., Sect. E:Struct. Rep. Online* **2001**, *57*, M589-M590.

(222) E. B. Fleischer, A. E. Gebala, D. R. Swift, P. A. Tasker *Inorg. Chem.* **1972**, *11*, 2775.

(223) E. Colacio, J. M. Dominguez-Vera, M. Ghazi, R. Kivekas, J. M. Moreno, A. Pajunen *J. Chem. Soc., Dalton Trans.* **2000**, 505.

(224) P. Chaudhuri, M. Winter, U. Florke, H. J. Haupt *Inorg. Chim. Acta* **1995**, *232*, 125.

(225) Z. M. Xu, S. White, L. K. Thompson, D. O. Miller, M. Ohba, H. Okawa, C. Wilson, J. A. K. Howard *J. Chem. Soc., Dalton Trans.* **2000**, *11*, 1751.

(226) S. O. Sommerer, B. L. Westcott, A. J. Jircitano, K. A. Abboud *Inorg. Chim. Acta* **1995**, *238*, 149.

(227) A. Jantti, K. Rissanen, J. Valkonen *Acta Chem. Scand.* **1998**, *52*, 1010.

(228) C. M. Liu, R. G. Xiong, X. Z. You, Y. J. Liu, K. K. Cheung *Polyhedron* **1996**, *15*, 4565.

(229) M. Mikuriya, Y. Hatano, E. Asato *Bull. Chem. Soc. Jpn.* **1997**, *70*, 2495.

(230) D. Z. Niu, Z. S. Lu, H. J. Ma, B. W. Sun *Chin. J. Struct. Chem.* **2001**, *20*, 387.

(231) Further addition of zinc(II) chloride results in precipitation of a white solid. The ^{1}H-NMR spectrum of the remaining solution shows identical signals to the 1.0 equivalent spectrum with reduced intensities. This suggests that upon further addition of zinc(II) ions, higher nuclearity complexes are formed which are insoluble in deuterated methanol.

(232) K. Mochizuki, S. Miyashita *Chem. Lett.* **1996**, 899.

(233) A. Mangia, C. Pelizzi, G. Pellizi *Acta Crystallogr., Sect. B: Struct. Sci.* **1974**, *30*, 2146.

(234) M. R. Caira, L. R. Nassimbeni, P. R. Woolley *Acta Crystallogr., Sect. B: Struct. Sci.* **1975**, *31*, 1334.

(235) A. M. Atria, R. F. Baggio, N. Espinosa, M. T. Garland, J. Manzur, Y. Moreno, E. Spodine *Acta Crystallogr., Sect. C: Cryst. Struct. Commun.* **1994**, *50*, 1066.

(236) W. Kraus, G. Nolze *J. Appl. Crystallogr.* **1996**, *29*, 301.

(237) Programs for Crystal Structure Analysis (Release 97-2). G. M. Sheldrick, Institut für Anorganische Chemie der Universität Göttingen, Tammanstrasse 4, D-3400 Göttingen, Germany, 1998.

(238) A. Altomare, G. Cascarano, C. Giacovazzo, A. Guagliardi *J. Appl. Crystallogr.* **1993**, *26*, 343.

(239) L. J. Farrugia *J. Appl. Crystallogr.* **1999**, *32*, 837.